

*Characterisation of neurogenesis and  
neuronal subtypes in the embryonic zebrafish  
telencephalon*

Philippa Ruth Bayley

Submitted to the University of London in 2004 in partial  
fulfilment of the requirements for the award of

PhD



University College London

UMI Number: U602450

All rights reserved

INFORMATION TO ALL USERS

The quality of this reproduction is dependent upon the quality of the copy submitted.

In the unlikely event that the author did not send a complete manuscript and there are missing pages, these will be noted. Also, if material had to be removed, a note will indicate the deletion.



UMI U602450

Published by ProQuest LLC 2014. Copyright in the Dissertation held by the Author.  
Microform Edition © ProQuest LLC.

All rights reserved. This work is protected against  
unauthorized copying under Title 17, United States Code.



ProQuest LLC  
789 East Eisenhower Parkway  
P.O. Box 1346  
Ann Arbor, MI 48106-1346

# Abstract

The telencephalon is the embryonic structure that in mammals gives rise to the cerebral cortex and the basal ganglia. Despite the manifest differences in size, structure and function of telencephalic derivatives in different vertebrate species, the underlying patterning of the embryonic telencephalon is highly conserved.

Very little is known about the development of the zebrafish telencephalon beyond the earliest embryonic stages of neural induction and patterning. One major outstanding question is the mechanism underlying telencephalic eversion, a process that is peculiar to ray-finned fish and that results in the dorsal telencephalon folding out laterally rather than evaginating as it does in most other vertebrate species. I used a range of techniques to monitor proliferation, neurogenesis, and axon extension over the entire period of embryogenesis. This led me to propose a mechanism for an observed rearrangement within the telencephalon between 2 and 3 days post fertilisation (dpf) that may also underlie the eversion process.

To characterise the neuronal populations of the dorsal telencephalon I made a careful expression analysis of three LIM-homeobox (*Lhx*) genes, genes that are involved in neuronal subtype specification in a variety of systems. The *Lhx* genes *lhx1a*, *lhx1b* and *lhx5* are expressed in spatially co-ordinated overlapping domains in the dorsal telencephalon and some of these genes are later expressed in the telencephalon-derived olfactory bulb. This suggested a dorsal origin of some olfactory bulb neurons.

To further probe the morphogenetic movements and cell migrations that shape the zebrafish telencephalon I performed a fate map of the 1dpf telencephalon. I developed a cell labelling technique that uses the Kaede protein, a green fluorescent protein that is converted to a red fluorescent form on irradiation with UV light. By labelling small groups of cells in the 1dpf telencephalon and following them to their positions at 5dpf I established that the most posterior regions of the dorsal telencephalon contribute to the OB at 5dpf. In addition I identified two populations of migratory cells in the ventral telencephalon, contributing cells to the OB and the dorsal telencephalon respectively. These populations may reveal a previously unknown conservation between fish and tetrapods.

## Acknowledgments

Even as I come to write this section, (hopefully) one of the last in this thesis, I can't quite believe that my almost 5 years of PhD at UCL will soon be over. Although this project has been very much my own, there are many people who have helped me get to this point that I would like to thank.

My supervisor, Jon Clarke, has been very brave taking on the telencephalon to add to his repertoire of favourite brain areas, and I am very grateful for all his advice and encouragement throughout my time in his lab. Steve Wilson, my second supervisor, has also been an excellent source of ideas and constructive criticism. Marina Mione has been my number one source of information for all things telencephalic, helping me not only experimentally but also with advice and discussions. Similarly, Marika Kapsimali has always been ready to help me out, especially with impenetrable fish neuroanatomy!

The Clarke lab, both the old gang – Adam, Dave and Manuel - and our newer additions – Julie and Laurel - have been brilliant both scientifically and socially. Although if we're honest about it, visits to the Indian YMCA and Diwana's probably outweighed scientific discussions by about 10:1. The Martin lab members, now dispersed, were also great neighbours for the first four years. Roberta Weber was a stalwart PhD companion, and Mike Redd was always distractible for a few hours to talk about tricky scientific problems or more likely U.S. politics. Also thanks to the Wilson lab, the Wellcome gang, and to Tom Hawkins for making me a pinhole enthusiast.

The Tuebingen massive, especially their expatriate emissary Florian, opened my mind to the possibilities of zebrafish research and to the wonders of German beer, and Chris Klisa was not only a screening buddy but also a great host in Dresden. My friends, particularly Paula, Greg, Charlotte, Elle, Ben and Phil deserve special thanks for their care and patience, especially over these last few months of writing. Even if they all thought fish brains were a bit mad, they never showed it.

And of course my family, my parents Sabine and Peter and my sister Olivia, who have supported me wonderfully through this enterprise, taking care of me at home and dealing with my rants and raves when they arose. And to David, without whose honesty and unwavering encouragement, I wouldn't have made it this far.

## **Table of contents**

<b>Abstract</b>	<b>2</b>
<b>Acknowledgments</b>	<b>3</b>
<b>Table of contents</b>	<b>4</b>
<i>List of figures and tables</i>	<b>11</b>
<b>Chapter 1</b>	<b>13</b>
<b>Chapter 2</b>	<b>39</b>
<b>Chapter 3</b>	<b>48</b>
<b>Chapter 4</b>	<b>91</b>
<b>Chapter 5</b>	<b>138</b>
<b>Chapter 6</b>	<b>193</b>
<b>References</b>	<b>201</b>

<b>Chapter 1: General Introduction</b>	<b>13</b>
<i>The comparative anatomical approach</i>	13
<i>The zebrafish telencephalon develops by a process of eversion</i>	15
<i>Highly conserved genes reveal telencephalic subdivisions</i>	17
<i>Strengths of the zebrafish model</i>	18
<i>Early forebrain development in zebrafish</i>	19
<i>Dorso-ventral patterning within the telencephalon</i>	21
<i>The subpallium generates migratory interneurons that populate the pallium</i>	28
<i>Olfactory bulb interneurons migrate from the LGE</i>	29
<i>The structure and origins of the olfactory bulb</i>	30
<i>The LIM-HD family of transcription factors – structure and function</i>	32
<i>LIM-HD function requires multi-protein complexes</i>	33
<i>Transcriptional targets of LIM-HD proteins</i>	37
<i>Aims of the work</i>	37
<b>Chapter 2: Materials and Methods</b>	<b>39</b>
<i>2.1 Live embryo care</i>	39
<i>2.2 Agarose mounting of live embryos</i>	39
<i>2.3 DNA and RNA microinjection</i>	40
<i>2.4 Preparation of DNA</i>	40
<i>2.5 Preparation of synthetic mRNA</i>	40
<i>2.6 Preparation of probes for in situ hybridisation</i>	41
<i>2.7 In situ hybridisation</i>	42
<i>2.8 Double in situ hybridisation</i>	44
<i>2.9 In situ hybridisation followed by antibody labelling</i>	44
<i>2.10 Antibody labelling</i>	45
<i>2.11 BrdU pulse labelling</i>	46
<i>2.12 Detection of the BrdU signal</i>	46
<i>2.13 Image acquisition</i>	47
<i>2.14 Image processing</i>	47

<b>Chapter 3: General characterisation of the developing telencephalon</b>	<b>48</b>
<b>3.1: Aim and Introduction</b>	<b>48</b>
<i>Morphogenesis of the zebrafish telencephalon</i>	48
<i>Pallial and subpallial divisions within the zebrafish telencephalon</i>	49
<i>The zebrafish dorsal telencephalon is everted</i>	50
<i>Proliferation and differentiation in the zebrafish telencephalon</i>	50
<i>The early axon scaffold</i>	51
<i>Axon tracts coincide with domains of regulatory gene expression</i>	52
<i>Aim of this chapter</i>	53
<b>3.2: Materials and Methods</b>	<b>54</b>
<i>Fish lines</i>	54
<i>Bodipy labelling</i>	54
<i>DiI labelling of the olfactory projection</i>	54
<i>Kaede RNA injection</i>	55
<i>Immunolabelling</i>	55
<i>Imaging</i>	55
<b>3.3: Results</b>	<b>56</b>
<i>External morphology of the telencephalon</i>	56
<i>Early organisation of the neuroepithelium</i>	59
<i>Neurogenesis is precocious in the telencephalon</i>	62
<i>Neurogenesis and cell division</i>	62
<i>Summary of proliferation and differentiation studies</i>	70
<i>The axon scaffold provides landmarks in the telencephalon</i>	71
<i>Neuronal populations marked by the Tg(dlx4/6:GFP) line</i>	78
<b>3.4: Discussion</b>	<b>82</b>
<i>Major morphological changes between 2dpf and 3dpf</i>	82
<i>Eversion as a result of the morphogenetic rotation</i>	83
<i>Questions posed by the eversion model</i>	87

<i>Establishing axes within the telencephalon</i>	88
<i>Neurogenesis in the telencephalon</i>	89
<b>Chapter 4: LIM-homeobox genes in the developing telencephalon</b>	91
<b>4.1: Aim and Introduction</b>	91
<i>Lhx genes and neuronal subtype specification</i>	91
<i>The Lhx1/5 subgroup in mouse, Xenopus and zebrafish</i>	92
<i>Lhx1 and Lhx5 are expressed early in development</i>	92
<i>Lhx expression in the forebrain</i>	93
<i>Aim of this chapter</i>	94
<b>4.2: Materials and Methods</b>	95
<i>Fish lines</i>	95
<i>DNA constructs</i>	95
<i>Preparation of antisense probes</i>	95
<i>Double in situ hybridisation</i>	95
<i>Vibratome sectioning of double in situ labelled specimens</i>	96
<i>In situ hybridisation in GFP lines</i>	96
<i>Outline of unsuccessful projects – a transgenic lhx1a:GFP line</i>	97
<i>Antibodies to LIM-HD proteins</i>	97
<i>Morpholinos to lhx1a and lhx1b</i>	97
<b>4.3: Results</b>	99
<i>Expression of lhx1a in the telencephalon</i>	99
<i>Expression of lhx1a in other brain areas</i>	103
<i>Expression of lhx1b in the telencephalon</i>	103
<i>Expression of lhx1b in other brain areas</i>	106
<i>Expression of lhx5 in the telencephalon</i>	106
<i>Expression of lhx5 in other brain areas</i>	109

<i>lhx1a and lhx5 are expressed in the olfactory bulb</i>	109
<i>Expression of lhx1a, lhx1b and lhx5 in combination</i>	112
<i>lhx1a, lhx1b and lhx5 expression and neuronal phenotype</i>	118
<i>lhx1a, lhx1b and lhx5 expression and pallial markers</i>	118
<i>lhx1a, lhx1b and lhx5 expression and a subpallial marker</i>	124
<b>4.4: Discussion</b>	129
<i>Expression of lhx1a, lhx1b and lhx5 subdivides the dorsal telencephalon</i>	129
<i>Spatial relationships of Lhx expression domains are retained through development</i>	130
<i>Lhx-expressing cells are neurons with a pallial identity</i>	131
<i>lhx1a and lhx5 highlight olfactory bulb neurons</i>	132
<i>lhx1a and lhx1b are expressed in ventral telencephalic areas at 5dpf</i>	134
<i>Divergence of expression along the rostro-caudal axis</i>	135
<i>Comparison of expression domains between species</i>	135
<i>Future experiments – other Lhx genes in the telencephalon</i>	136
<i>Functional experiments with the Lhx genes</i>	136
<b>Chapter 5: Fate-mapping the telencephalon with a Kaede protein method</b>	138
<b>5.1: Aim and Introduction</b>	138
<i>Olfactory bulb structure and function</i>	138
<i>The embryonic origins of the olfactory bulb</i>	139
<i>The ganglionic eminences supply interneurons to cortical areas</i>	140
<i>Aim of this chapter</i>	141
<b>5.2: Materials and Methods</b>	142
<i>Properties of the Kaede protein</i>	142
<i>The Kaede construct</i>	142
<i>Expression of Kaede using DNA and RNA</i>	142
<i>Raising Kaede-injected embryos</i>	142

<i>Agarose mounting</i>	143
<i>Focal photoconversion of Kaede</i>	143
<i>Procedure for photoconversion of Kaede</i>	144
<i>Confocal imaging</i>	144
<i>Analysis</i>	145
<b>5.3: Results</b>	146
<i>Features of Kaede protein photoconversion</i>	146
<i>Designating regions within the telencephalon</i>	147
<i>Imaging photoconverted specimens</i>	150
<i>Cells labelled in T1</i>	153
<i>Cells labelled in the T1 roof</i>	156
<i>Cells labelled in T2</i>	159
<i>Cells labelled in T3</i>	159
<i>Cells labelled in T4, T5 and T6</i>	162
<i>Cells labelled in T7</i>	165
<i>Cells labelled in T8 and T9</i>	168
<i>Timing of T1/roof contribution to the OB</i>	171
<i>Summary</i>	171
<b>5.4: Discussion</b>	177
<i>Pallial areas T1, T2 and T3 contribute to the OB – a potential source of projection neurons?</i>	177
<i>Subpallial contribution to the OB – a potential source of interneurons?</i>	181
<i>Non-OB contributions of T1-T3 and T8-T9</i>	183
<i>T4, T5 and T6 – subpallial areas with a pallial contribution</i>	184
<i>T4, T5 and T6 may contribute striatal interneurons</i>	185
<i>Morphogenetic movement vs. migration</i>	185
<i>Guiding tangential migration within the telencephalon</i>	186
<i>Co-ordinating Kaede fate-mapping data with Lhx expression domains</i>	188
<i>What specifies the dorsal telencephalic contribution to the OB?</i>	189
<i>Post-embryonic development of the OB</i>	190

<i>Limitations of the method and further work</i>	191
<b>Chapter 6: General Discussion</b>	193
<i>Evidence points to a morphogenetic movement between 2 and 3dpf</i>	193
<i>What drives a morphogenetic movement?</i>	194
<i>The rostral movement may underlie eversion</i>	194
<i>Insights into the origin of the choroid tela</i>	195
<i>Testing the predictions of the eversion/choroid tela model</i>	198
<i>Evaluation of the work</i>	199
<i>Concluding remarks</i>	199
<b>References</b>	201

# List of Figures and Tables

## Chapter 1: General Introduction

Figure 1.1 A: Eversion and evagination	16
Figure 1.1 B: The vertebrate lineage	16
Figure 1.2 : Patterning and cell migration in the mammalian telencephalon	23
Figure 1.3: LIM-HD protein interactions	35

## Chapter 3: General characterisation of the developing telencephalon

Figure 3.1: Brain morphology 24hpf to 5dpf	58
Figure 3.2: Structure of the forebrain neuroepithelium	61
Figure 3.3: Early neurogenesis in the telencephalon	64
Figure 3.4: BrdU labelling in the <i>Tg(HuC:GFP)</i> line – 24hpf and 36hpf	67
Figure 3.5: BrdU labelling in the <i>Tg(HuC:GFP)</i> line – 44hpf to 5dpf	69
Figure 3.6: Telencephalic organisation from 24hpf to 5dpf labelled by anti-acetylated $\alpha$ -tubulin	73
Figure 3.7: Details of telencephalic projections 48hpf to 5dpf labelled by anti-acetylated $\alpha$ -tubulin	77
Figure 3.8: Cell populations labelled in the <i>Tg(dlx4/6:GFP)</i> line – 26hpf to 5dpf	80
Figure 3.9: Models of eversion	86

## Chapter 4: LIM-homeobox genes in the developing telencephalon

Figure 4.1: Cutting and mounting whole telencephalic sections	99
Figure 4.2: <i>lhx1a</i> expression – 19hpf to 5dpf	102
Figure 4.3: <i>lhx1b</i> expression – 14hpf to 5dpf	105
Figure 4.4: <i>lhx5</i> expression – 19hpf to 5dpf	108
Figure 4.5: <i>lhx1a</i> and <i>lhx5</i> in the olfactory bulb	111
Figure 4.6: <i>lhx1a</i> , <i>lhx1b</i> and <i>lhx5</i> in combination	114
Figure 4.7: Schematic representation of <i>lhx1a</i> , <i>lhx1b</i> and <i>lhx5</i> expression	117
Figure 4.8: <i>lhx1a</i> , <i>lhx1b</i> and <i>lhx5</i> in the <i>Tg(HuC:GFP)</i> line	120
Figure 4.9: <i>lhx1a</i> , <i>lhx1b</i> and <i>lhx5</i> with pallial markers	123
Figure 4.10: <i>lhx1a</i> , <i>lhx1b</i> and <i>lhx5</i> in the <i>Tg(dlx4/6:GFP)</i> line	127

## **Chapter 5: Fate-mapping the telencephalon with a Kaede protein method**

Figure 5.1: Photoconversion of Kaede protein	149
Figure 5.2: Fate-mapped regions within the telencephalon	152
Figure 5.3: Lateral activations in T1	155
Figure 5.4: Dorsal activations in T1/roof	158
Figure 5.5: Lateral activations in T2 and T3	161
Figure 5.6: Lateral activations in T4 and T5	164
Figure 5.7: Lateral activations in T6 and T7	167
Figure 5.8: Lateral activations in T8 and T9	170
Figure 5.9: Following cell movement from T1 into the olfactory bulb	173
Figure 5.10: Summary diagram showing contributions of regions T1-T9	175
Figure 5.11: Comparison of regions T1-T9 with known markers	179
Table 5.1: Summary of contributions of regions T1-T9	176

## **Chapter 6: General Discussion**

Figure 6.1: Model of eversion and choroid tela formation	197
--	-----

# Chapter 1: Introduction

The vertebrate nervous system has a complexity that is quite awe-inspiring. An extraordinary number of neuronal and glial cells are generated, organised and the neurons connected in functional circuits, controlling and co-ordinating almost all physiological functions. Understanding the origins of nervous system complexity is one of the major goals of neuroscience, and studying nervous system formation during the course of embryogenesis is currently one of the most exciting and productive approaches.

This focus of this thesis is the development of one area of the brain - the telencephalon. The telencephalon is an embryonic brain area that in mammals gives rise to the adult structures of the cerebral cortex and basal ganglia. In humans, these brain areas, particularly the cerebral cortex, are thought to be responsible for a plethora of higher functions, including consciousness, memory, language, cognition and emotion.

It may therefore seem a strange choice to study the telencephalon in a non-mammal such as the zebrafish *Danio rerio*. The telencephalon is indeed the most divergent area of the brain, and it is without question that the functions performed by this area vary widely between species. However, the study of telencephalic development has revealed a striking degree of conservation, particularly in terms of telencephalic subdivisions, across a wide range of vertebrate species (Bachy et al., 2002a; Fernandez et al., 1998; Puellas et al., 2000). This has led to the notion of a common telencephalic Bauplan, variations in which give rise to the manifest differences in size, complexity and function observed across vertebrates. One of the purposes, therefore, of studying zebrafish telencephalic development is to further establish the commonalities and divergences between zebrafish and better-studied species and examine how this relates to differences in adult structures and in function.

## *The comparative anatomical approach*

The field of developmental neuroscience is not more than 20 years old, but its foundations in neuroanatomy go back almost 200 years. Using a combination of histological methods including axon tract tracing, anatomists investigated the

structure and organisation of a huge variety of vertebrate telencephalons including those of tetrapod amphibians, reptiles, birds and mammals, and of a variety of fish species (Butler and Hodos, 1996; Striedter, 1997). By making comparisons between closely and distantly related species, the hope was that homologous and homoplastic structures could be deduced. This would therefore reveal telencephalic organisation in terms of highly conserved and more recently evolved structures.

The comparative anatomical approach identified one of the most fundamental conserved features of the telencephalon, its subdivision into the dorsally located pallium (roof of the telencephalon) and the ventrally located subpallium (floor of the telencephalon). In mammals, the subpallium consists of structures that bulge into the ventricular space called the ganglionic eminences. These structures give rise to components of the basal ganglia including the striatum and pallidum. The pallium, on the other hand, gives rise to cortical structures including the olfactory cortex and the hippocampus. However, anatomy alone was unable to determine the origins of several structures in the mammalian telencephalon, such as the amygdala, septum and olfactory bulb (Striedter, 1997).

One major shortfall of the comparative anatomical approach was that it rested heavily on morphology of telencephalic structures and connectivity between telencephalic and other brain areas. The telencephalon is the most divergent area of the brain and varies widely in its morphology and connectivity between species. Comparisons, therefore, even between quite closely related groups such as mammals and birds proved very problematic for comparative anatomists. For example, the avian telencephalon has cortical structures but also a massive thickening in the lateral telencephalic wall called the dorsoventricular ridge (DVR). Using morphological comparison, the DVR has greatest similarity to the mammalian ganglionic eminences, suggesting that it is part of the subpallium. In fact, as a result of subsequent more sophisticated examination the DVR is now known to be a pallial area, albeit one that looks radically different to the mammalian neocortex (Fernandez et al., 1998; Puelles et al., 2000; Striedter, 1997). Such confusions are widespread through the literature and are only now being unravelled.

Extending the comparative anatomical approach to the embryonic telencephalon already has many advantages over studying adult brain anatomy. Von Baer proposed that ontogeny recapitulates phylogeny, the idea being that an organism passes through its ancestral evolutionary states during the course of its

development. Although modern evolutionary and development theory firmly contradicts this idea, it is nonetheless true to say that more similarities exist earlier in development than later (Striedter, 1997). Studying early development therefore gives unique insights into the commonalities and divergences between different species in their telencephalic organisation.

*The zebrafish telencephalon develops by a process of eversion*

Comparative approaches to studying telencephalic organisation often exclude fish species such as zebrafish, restricting studies to tetrapod species (Marin et al., 1998; Striedter, 1997). This is not because of a lack of information about fish telencephalic anatomy, but because the adult zebrafish telencephalon is radically different in its morphology to that of tetrapods. The tetrapod telencephalon is evaginated, with the telencephalic vesicles enclosing two lateral ventricles. The zebrafish telencephalon, however, is everted, with dorsal telencephalic tissue turned out laterally, and the entire dorsal surface covered by a thin choroid tela or epithelium (Butler, 2000; Butler and Hodos, 1996).

A schematic diagram in Fig 1.1 A shows the proposed mechanisms of evagination and eversion, adapted from Butler (2000). The striking difference is that during the evagination process, dorso-medial structures in the neural tube remain medial with the telencephalic vesicles bulging out laterally i.e. evaginating. In contrast, during the eversion process, structures that were dorso-medial in the neural tube are displaced to lateral positions, resulting in a topographical rearrangement of telencephalic areas. A further consequence of eversion is that the proliferative ventricular zone, which in an evaginated telencephalon would line the ventricles, becomes located on the dorsal surface of the telencephalon.

The everted telencephalon is not restricted to zebrafish but is a property of the large group of actinopterygian or ray-finned fish, of which zebrafish is one species. Eversion is a peculiarity of actinopterygian fish, as other groups of fish such as the jawless agnathans (species such as the lamprey) and cartilaginous fish undergo an evagination process. Similarly, all tetrapod species, which diverged from the actinopterygian lineage some 420 million years ago, undergo telencephalic evagination. Figure 1.1 B shows the evolutionary relationships of these species. Actinopterygians, despite being the only group to undergo telencephalic eversion, still represents the vast majority of fish species including experimental species such

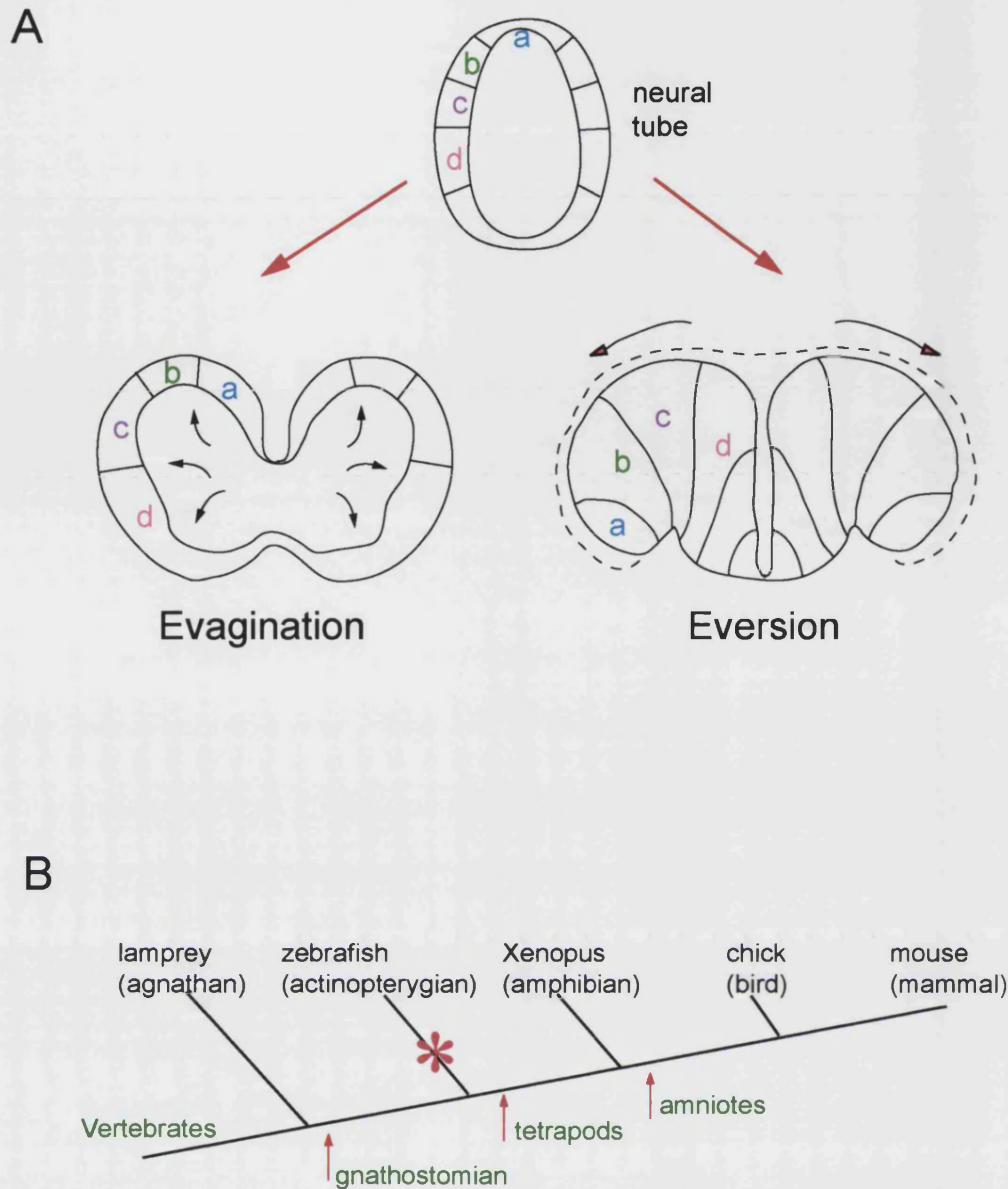


Figure 1.1

A shows the contrasting telencephalic evagination and eversion processes, adapted from Butler (2000). During evagination, the telencephalic vesicles bulge out laterally; in eversion, the dorsal parts of the neural tube turn out like flaps and the dorsal surface is covered with a choroid tela. Hypothetical regions within the neural tube (labelled a-d) are arranged differently in an evaginated versus an everted telencephalon.

B shows a basic evolutionary tree indicating some of the major transitions in the vertebrate lineage. Zebrafish are part of the actinopterygian fish group, which diverged from the tetrapod lineage 420 million years ago (adapted from Bachy et al., 2001). The hypothesised evolution of eversion is indicated by an asterisk.

as goldfish. It is therefore of interest to uncover how this alternative strategy evolved and why it was retained by single but species-rich group of fish.

The topological rearrangement of telencephalic areas in everted versus evaginated telencephalons poses a considerable and unresolved problem for fish neurobiologists. Distinct areas of the zebrafish pallium are evident anatomically (Wullimann and Rupp, 1996), but the general lack of functional data about these areas makes comparisons difficult. Areas such as those receiving olfactory input are located in the lateral pallium in both evaginated and everted species, casting doubt on simple topological eversion for all pallial areas (Wullimann and Rink, 2002). Other areas, however, inferred from lesion studies as the fish homologues of the mammalian hippocampus and amygdala, are topologically shifted as would be expected during eversion (Portavella et al., 2002; Salas et al., 2003). These results highlight the need to provide a comprehensive description of eversion, involving the location of many more functional areas of the everted dorsal telencephalon.

The eversion process is likely to be an embryonic event, setting the stage for subsequent adult proliferation and morphogenesis. To date, the only evidence of embryonic eversion has come from a study of proliferation in the zebrafish telencephalon. The authors report proliferating cells at the dorsal telencephalic surface from stages as early as 2 days post fertilisation (dpf) (Wullimann and Knipp, 2000). However, there have been no attempts to address the mechanism of telencephalic eversion during embryogenesis, and in general descriptions of this process are based on speculation rather than observation (Butler, 2000). It is therefore one of the main aims of this thesis to make observations of telencephalic development over the entire period of embryogenesis use this information to develop potential mechanisms for the eversion process.

#### Highly conserved genes reveal telencephalic subdivisions

The comparative anatomical approach has been revolutionised by the discovery of the genes that highlight telencephalic subdivisions. These genes are remarkably conserved between a wide range of vertebrate species (Fernandez et al., 1998; Puelles et al., 2000). For example, the expression of vertebrate orthologues of the *Drosophila empty spiracles (ems)* gene have now been compared in a range of tetrapod species including frog, turtle, chick and mouse, where they highlight similar pallial areas. Early patterns of *Emx* and of other highly conserved pallial genes have

therefore been able to resolve some of the issues that the comparative anatomical approach could not, such as the pallial nature of the DVR in birds (Fernandez et al., 1998; Puelles et al., 2000). Furthermore, the *Emx* genes are expressed in the dorsal telencephalon of evolutionarily distant groups, such as cartilaginous fish (Derobert et al., 2002) and may even perform a similar role in the specification of *Drosophila* dorsal neuronal identity (Weiss et al., 1998).

The striking conservation of telencephalic patterning mechanisms across all vertebrate species is facilitating rapid progress in understanding zebrafish telencephalic development. The difficulties inherent in the comparative anatomical approach, as outlined above, can now be somewhat overcome by following domains of gene expression through development. However, not many of these studies have yet been undertaken, and it is one of the aims of this thesis to further characterise the expression domains of genes within the dorsal telencephalon in order to extend the comparative analysis.

#### *Strengths of the zebrafish model*

The zebrafish has a number of attributes that make it an excellent model for studying brain development. Of prime importance is the genetic tractability of the organism. The zebrafish model is very amenable to large-scale mutagenesis screening, and mutants identified by this forward genetics method underpin much zebrafish developmental research. Mutants produced by insertional mutagenesis methods are easy to clone (Golling et al., 2002), and the cloning of those produced by ENU-mediated mutagenesis is facilitated by improved mapping techniques and the progressive sequencing of the zebrafish genome (Talbot and Hopkins, 2000). As the genome sequence becomes more comprehensive, techniques such as TILLING should enable specific mutants in any known gene to be generated (Wienholds et al., 2003). Gene expression can also be manipulated by the injection of DNA and RNA sequences, the external fertilisation of zebrafish oocytes giving access to the embryo from the 1-cell stage. Morpholino oligonucleotides are a further genetic tool, specifically disrupting the translation of a targeted RNA sequence (Heasman, 2002) and frequently phenocopying their respective mutant lines (e.g. Walshe and Mason, 2003).

Zebrafish are also amenable to the introduction of engineered transgenic sequences, and this has led to an explosion of transgenic lines bearing reporters such

as green fluorescent protein (GFP) under the control of specific regulatory sequences (Jessen et al., 1998). Transgenic GFP lines are particularly useful to zebrafish researchers because the transparency of the early embryo offers unrivalled opportunities for live DIC and fluorescence imaging (e.g. Koster and Fraser, 2001). This attribute of transparency, a result of the yolk being contained in a sac rather than distributed through the embryo (Kimmel et al., 1995), also enables detailed observation of stained wholemount preparations. This is an attribute I have fully exploited during the course of this thesis work.

Furthermore, the genome duplication event that occurred in the actinopterygian fish after they diverged from the tetrapod lineage gives insight into the evolutionary forces that have shaped the zebrafish brain (Amores et al., 1998; Postlethwait et al., 1998). For example, zebrafish seem to have retained a large proportion of their duplicated genes, and it has been suggested that many of these genes have undergone a process of subfunctionalisation whereby the ancestral expression pattern of a single gene becomes partitioned between the duplicates (Force et al., 1999). This process is still little understood, especially in terms of functional consequences for different brain areas, but it is clear that gene duplication events as also happened much earlier in the vertebrate lineage provided great scope for functional innovation, such as the evolution of jaws (Postlethwait et al., 1998).

### *Early forebrain development in zebrafish*

The numerous attributes of the zebrafish model, as described above, have made it one of the foremost models for studying early CNS development and patterning. In this section, I will outline some of the main events that underlie neural induction and the subsequent patterning of forebrain areas including the telencephalon. I will also describe some of the dramatic morphogenetic movements that shape the most rostral neural tissue and the implications of these movements for subsequent patterning events.

Neural induction is a complex process that occurs during gastrulation and involves the acquisition of neural identity by a subset of ectodermal cells. Numerous molecules are involved in neural induction, but I will only touch on some of the known key players here. Neural induction itself seems to rest primarily on the antagonism of anti-neuralising BMP signalling by molecules emanating from the embryonic organiser, the embryonic shield in zebrafish (reviewed in Wilson and

Houart, 2004). These molecules have mainly been isolated through work in *Xenopus*, and include molecules that bind directly to BMPs such as Noggin and Chordin. The neural fate is therefore somewhat the default state of the tissue, although work in other species suggests other factors such as Fgf signalling may be additionally required for neural induction (reviewed in Bally-Cuif and Hammerschmidt, 2003; Stern, 2002).

The activation-transformation model of Nieuwkoop (reviewed in Stern, 2002), infers that induced or “activated” neural tissue has anterior character that must be subsequently patterned by posteriorising or “transforming” signals. More recent evidence also suggests that posteriorising signals are responsible for imparting A-P pattern on neural tissue with otherwise anterior character. The candidate posteriorising signals are numerous, and in zebrafish include Wnts, Fgfs, Retinoic acid, Nodals and BMPs (reviewed in Wilson and Houart, 2004; Bally-Cuif and Hammerschmidt, 2003).

The induction of the telencephalon itself has been well-studied in zebrafish and relies on local signalling from a population of cells at the anterior border of the neural plate (ANB; Houart et al., 1998). Removing these cells at mid-gastrulation stages results in the loss of telencephalic markers, and transplanting them to more caudal levels of the neural tube induces ectopic telencephalic markers (Houart et al., 1998). The ANB is therefore a source of signals that promote telencephalic fates and recent work indicates that one signal emanating from the ANB is a locally-acting antagonist of prospective posteriorising factors. The ANB secretes *Tlc*, a Wnt antagonist, potentially interfering with a number of posteriorising Wnt signals emanating from more caudal levels of the neuraxis (Houart et al., 2002). The ANB, and the equivalent signalling centres in other species are likely to have more extensive roles than Wnt antagonism, possibly involving Fgf signalling (Shimamura and Rubenstein, 1997). The zebrafish ANB also expresses *fgf3* and *fgf8*, both of which affect the patterning of the telencephalon when misexpressed (Shanmugalingam et al., 2000; Walshe and Mason, 2003).

The forebrain comprises not only the telencephalon, but also the eyes and the diencephalon, including the hypothalamus. The early development of these structures involves both a host of patterning events as outlined above as well as dramatic morphogenetic movements. The prospective forebrain areas occupy the

most anterior part of the neural plate, but their arrangement gives little indication of how they will come to be organised in the brain. Thus, at early neural plate stages telencephalic precursors form the most anterior and lateral field, with prospective ventral telencephalon lying anterior to dorsal telencephalon (Whitlock and Westerfield, 2000) and the eye field and prospective diencephalon lying progressively more posteriorly. This organisation is dramatically rearranged as axial midline neural tissue (hypothalamic precursors) moves rostrally, splitting the eye field and coming to underlie the telencephalon (Varga et al., 1999). By the time the neural plate has converged to form a rod, the telencephalon occupies a dorsal rostral position, with the hypothalamus directly underlying it in a ventral rostral position (reviewed in Wilson and Houart, 2004). The mechanisms controlling this morphogenetic movement are unclear, but nodal signalling is required for the correct specification and subsequent migration of the hypothalamic precursors, without which the hypothalamus is absent and the retinal fields develop as a single cyclopic eye (Varga et al., 1999).

The early events in telencephalic induction and patterning, therefore, rely primarily on the sequential antagonism of factors that induce non-neural fates (BMPs) and caudal neural character (Wnts). However it is also clear that numerous other factors are at play during the complex interlinked processes of gastrulation, neural induction and patterning, and neurulation.

#### *Dorso-ventral patterning within the telencephalon*

As I have outlined, some of the key players in the early induction and patterning of the telencephalon have been identified through work in zebrafish. However, the subsequent patterning of the telencephalon that generates the progenitor domains of the subpallium and pallium is relatively little understood in fish. Most of this work has been carried out in the mouse, where elegant experiments predominantly using mutants have probed the mechanisms underlying patterning and neurogenesis within the telencephalon (Fig 1.2 A).

Substantial evidence points to the mechanisms involved in telencephalic patterning being highly conserved between vertebrate species (Fernandez et al., 1998; Puelles et al., 2000). Therefore, despite the lack of functional experiments addressing these issues in zebrafish, the progressive identification of fish orthologues of the mammalian genes involved in telencephalic patterning gives

substantial insight into these processes. The next major challenge for zebrafish researchers is to use the data generated from the mouse model to design functional experiments to probe zebrafish telencephalic patterning.

#### *Dorso-ventral patterning – the role of sonic hedgehog*

The secreted signalling protein Sonic hedgehog (Shh) plays a key role in dorso-ventral (D-V) patterning within the telencephalon, as it does at more caudal levels of the neural tube. In the spinal cord, a ventral source of this diffusible signal sets up a gradient imparting D-V positional information to different levels of the neural tube. Cells respond to this positional information by turning on a variety of mostly homeodomain-containing transcription factors, each with a defined D-V limit (Briscoe et al., 1999). The transcription factors work both in concert with each other and in mutually repressive interactions to specify discrete neural and glial progenitor domains that are both spatially and temporally regulated (reviewed in Jessell, 2000).

The parallels with the telencephalon are striking, with Shh signalling playing a vital role particularly in ventral telencephalon specification. Zebrafish *shh* mutants lack both ventral telencephalic and anterior diencephalic territories (Barth and Wilson, 1995; Rohr et al., 2001) and mutants in zebrafish *smoothened*, which codes for a protein required for Shh signal transduction show similar defects (Varga et al., 2001). *Shh* mutant mice also have a lack of ventral forebrain tissue and are cyclopic (Chiang et al., 1996), as are some humans with *Shh* mutations. The source of the Shh signal is unlikely to itself be telencephalic, as the small population of ventral telencephalic Shh-expressing cells appear too late during development to pattern this tissue. The presumptive telencephalon may be exposed to Shh signalling from the organiser during gastrulation (Gunhaga et al., 2000), or Shh signalling may emanate from ventral tissues such as the prechordal plate or the hypothalamus (reviewed in Wilson and Houart, 2004).

As at more caudal levels of the neuraxis, Shh activity is antagonised by signalling from the dorsal neural tube (Jacob and Briscoe, 2003). In mammals, the Shh antagonist *Gli3* is expressed in the most dorsal regions of the telencephalon. *Gli3* is essential for dorsal telencephalic fates (Kuschel et al., 2003; Theil et al., 1999; Tole et al., 2000) and the role of this transcription factor will be discussed in detail later. In the *Gli3* mutant, ventral markers are expanded at the expense of dorsal markers, and the reverse is seen in *Shh* mutants (Rallu et al., 2002). However,

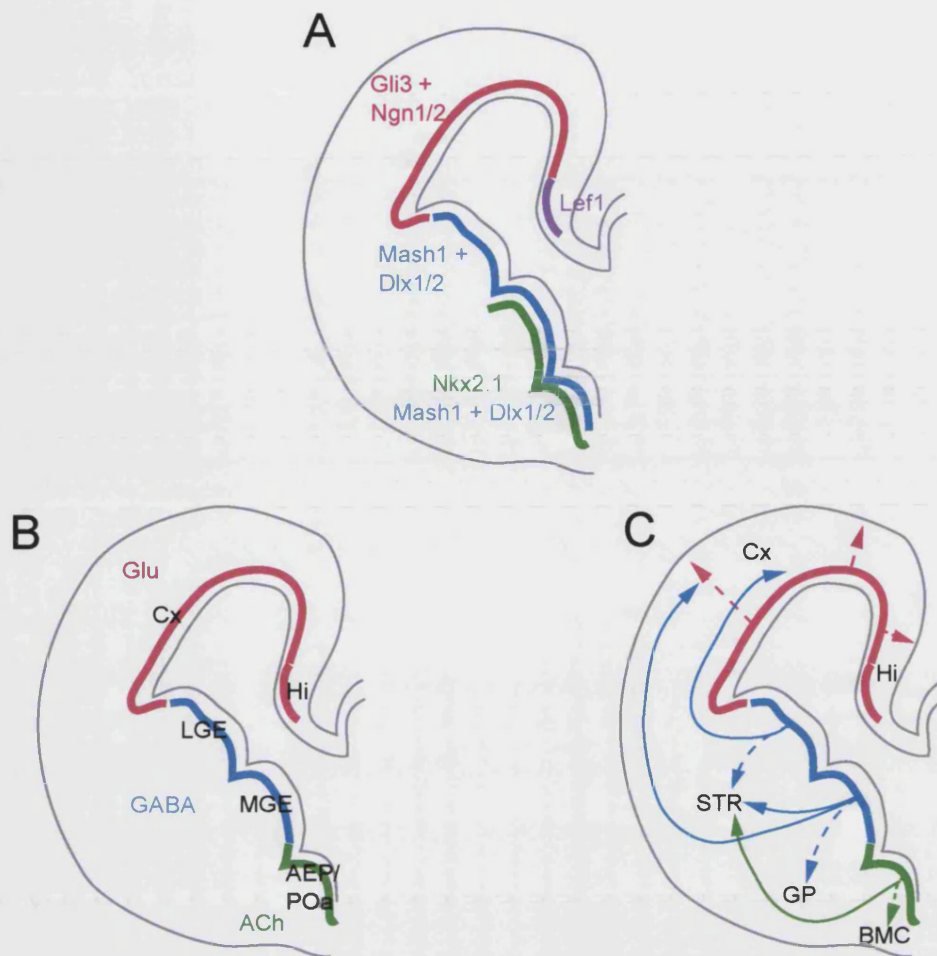


Figure 1.2: Patterns of neurogenesis and cell migration in the mouse telencephalon

A-C show schemas representing the right telencephalic hemisphere from an E14 mouse embryo (adapted from Wilson and Rubenstein, 2000). A shows different progenitor domains specified by combinations of transcription factors. B shows the major subdivisions of the subpallium (LGE, MGE and AEP/POa) and pallium (Cx and Hi), and the predominant neurotransmitter phenotypes of the neurons generated within these areas. C shows the migration pathways of neurons, using arrows to indicate their origins within different progenitor domains. Radial migrations are indicated with dotted lines, and tangential migrations by solid lines.

ACh - acetylcholine; AEP - anterior endopeduncular area; BMC - basal magnocellular cluster; Cx - cortex; GABA - gamma-amino-butyric-acid; Glu - glutamate; GP - globus pallidus; Hi - hippocampus; LGE - lateral ganglionic eminence; MGE - medial ganglionic eminence; POa - anterior preoptic area; STR - striatum.

the *Shh/Gli3* double mutant retains aspects of D-V patterning within the telencephalon (Rallu et al., 2002). This data strongly implicates other factors in the D-V patterning of the telencephalon and candidate molecules include Wnts, BMPs, nodals and Fgfs. In zebrafish, nodals are known to lie upstream of Shh signalling, and abrogation of nodal signalling results in very severe cyclopia and loss of ventral forebrain tissues as described above (Rohr et al., 2001; Varga et al., 1999).

#### *Ventral telencephalic patterning and neurogenesis*

Prominent features within the mammalian subpallium are the lateral and medial ganglionic eminences (LGE and MGE), two adjacent bulges in the ventral telencephalic wall (Figure 1.2 A and B). The LGE, which abuts the cortex, gives rise to the striatum, while the MGE gives rise to the pallidal component of the basal ganglia (reviewed in Wilson and Rubenstein, 2000). Shh has the ability to induce the expression of genes essential for LGE and MGE specification, namely *Gsh2* and *Nkx2.1*. *Gsh2*, which is expressed predominantly in the LGE, also has a vital function in D-V telencephalic patterning, because it cross-represses a dorsal telencephalic gene *Pax6*, forming the cortico-striatal boundary (Corbin et al., 2000; Stoykova et al., 2000; Toresson et al., 2000; Yun et al., 2001). The adjacent MGE is dependent on a different homeobox gene, *Nkx2.1*, which like *Gsh2* is induced by Shh signalling. In *Nkx2.1* mutants, the MGE acquires LGE character (Sussel et al., 1999), with no expansion of cortical markers. However *Nkx2.1* and *Gsh2* are not cross-repressive in their action, rather acting co-operatively to pattern the ventral telencephalon (Corbin et al., 2003).

In the zebrafish telencephalon, embryonic structures equating to the LGE and MGE have not yet been defined. Ventral telencephalic development is dependent on Shh signalling, with nodal signals acting upstream of *shh* (Rohr et al., 2001). Downstream of Shh signalling is *nk2.1b*, a zebrafish orthologue of the mammalian MGE-specific *Nkx2.1* gene (Rohr et al., 2001). Although zebrafish *nk2.1b* is expressed in a restricted region of the ventral telencephalon, the expression pattern alone is not enough to designate this area the zebrafish equivalent of the MGE. Further hampering the elucidation of zebrafish subpallial subdivisions is the lack of zebrafish orthologues of *Gsh1* and *Gsh2*, genes that would give insight into a possible equivalent of the LGE.

Comparative anatomical evidence from studies in adult actinopterygian species (particularly teleosts, the zebrafish group) indicates that there are likely to be subdivisions within the embryonic zebrafish subpallium that would correspond to the mammalian LGE, MGE and the septal region. Adult subpallial nuclei have been identified as either striatal (the dorsal tier of nuclei) or septal (the ventral tier) on the basis of neurotransmitter expression and connectivity (Wullimann and Rink, 2002). In particular, the striatal formation is uniquely Substance P immunoreactive, and receives ascending dopaminergic innervation from the ventral diencephalon. The septal formation, on the other hand, is uniquely cholinergic and as in amniotes has a massive descending output to the midline hypothalamus (Wullimann and Rink, 2002). The embryonic subpallium, therefore, is likely to be divided into different progenitor zones responsible for generating these different neuronal subtypes. Further experiments are needed to establish whether the genes responsible for this patterning in mammals play the same roles in zebrafish.

The genes controlling neurogenesis, as opposed to patterning, within the mammalian ventral telencephalon have clear zebrafish orthologues. The proneural gene *Mash1* plays an instructive role in subpallial neurogenesis (Casarosa et al., 1999), and its zebrafish orthologue, *zash1*, is also expressed exclusively in the ventral telencephalon (Wullimann and Mueller, 2002). Downstream of *Mash1* activity, the *Dlx* genes are involved in subpallial progenitor differentiation. *Dlx* genes are upregulated in the *Mash1* mutant, indicating premature differentiation of progenitors (Casarosa et al., 1999), and they negatively regulate Notch signalling thereby promoting neural progenitor differentiation (Yun et al., 2002).

*Dlx* genes are organised in pairs within the genome, a feature that is conserved between mammals and zebrafish (Ellies et al., 1997), and the *Dlx1/2* and *Dlx5/6* pairs are those most strongly implicated in subpallial neurogenesis (Anderson et al., 1997b; Eisenstat et al., 1999; Long et al., 2003; Stuhmer et al., 2002). *Dlx* function has not been well investigated in zebrafish, but a number of *dlx* genes have expression domains restricted to the subpallium (Akimenko et al., 1994; Zerucha et al., 2000). The recent generation of a GFP line under the control of the *dlx4/6* intergenic region (equivalent to *Dlx5/6* in mouse) provides a useful tool for further investigating the functions of these genes in subpallial neurogenesis (Zerucha et al., 2000).

### *Dorsal telencephalic patterning and neurogenesis*

The mammalian dorsal telencephalon, or pallium, comprises the cerebral cortex (neocortex), olfactory cortex, hippocampus and cortical hem (Grove et al., 1998). The most dorsal telencephalic neuroepithelium also gives rise to a monolayered secretory neuroepithelium called the choroid plexus (reviewed in Campbell, 2003). The molecules responsible for generating these structures are being rapidly elucidated in the mouse model, but very little is known about their roles in the zebrafish.

Development of the dorsal telencephalon is critically dependent on two signalling centres, the roofplate and the anterior neural border (ANB). One of the key molecules expressed in the roofplate is the Shh antagonist *Gli3*. In the roofplate, *Gli3* induces the expression of a variety of BMPs and Wnts, both of which have roles patterning the adjacent cortical tissue and both of which are absent in *Gli3* mutants (Kuschel et al., 2003; Theil et al., 1999; Tole et al., 2000). BMPs have a very local role specifying choroid plexus fates, with particularly clear roles for *Bmp2* and *Bmp4* (Hebert et al., 2002). Wnt signalling, on the other hand, is responsible for the growth and differentiation of the adjacent hippocampus, with a clear role for *Wnt3a* (Lee et al., 2000).

*Gli3* is also required for neocortical gene expression, with mutants showing a dorsal to ventral transformation of the telencephalon. This is because in *Gli3* mutants, where roofplate signalling molecules are absent, Fgf signalling from the ANB promotes rostro-ventral structures over dorso-medial ones (Kuschel et al., 2003). This fits well with the observation that *Gli3* is required for the expression of the dorsal telencephalic genes *Emx1* and *Emx2* (Theil et al., 1999), of which *Emx2* at least is expressed in a gradient highest caudally (Bishop et al., 2000; Mallamaci et al., 2000). The *Emx* genes play critical roles in dorsal telencephalic development, with *Emx2* mutants and *Emx1/2* double mutants showing particularly severe defects in many aspects of dorsal telencephalon development (Bishop et al., 2003; Mallamaci et al., 2000; Muzio et al., 2002; Muzio and Mallamaci, 2003; Shinozaki et al., 2004; Yoshida et al., 1997).

One of the major roles of *Emx2* is to repress Fgf signals emanating from the ANB, thereby regulating positional signalling within the cortex (Fukuchi-Shimogori and Grove, 2003). This has been most elegantly shown for the positioning of the

barrel cortex, a somatosensory field that receives input from the rodent whisker pad. By selectively increasing the levels of *Emx2* within the range of Fgf signals from the ANB, the position of the barrel cortex could be shifted rostrally. Local overexpression of *Fgf8* conversely shifted the barrel cortex to more caudal positions. The patterning of mid-cortical areas therefore relies on competition between signals in the roofplate and those emanating from the ANB (Fukuchi-Shimogori and Grove, 2003).

*Pax6* is another gene that plays a vital role in dorsal telencephalic patterning, interacting with the cortical patterning processes outlined above. At early embryonic stages the role of *Pax6* is predominantly mutual repression of *Gsh2*, thereby forming the cortico-striatal boundary (Corbin et al., 2000; Toresson et al., 2000; Yun et al., 2001). In the neocortex, *Pax6* may interact antagonistically with *Emx2* (Muzio and Mallamaci, 2003). The two genes are expressed in opposing gradients, with *Pax6* modulating the rostro-lateral cortex (Bishop et al., 2000; Bishop et al., 2002) whereas *Emx2* acts primarily in the caudal-medial cortex (Mallamaci et al., 2000).

Pallial patterning in the zebrafish is very little understood. This is partly because no roofplate-based signalling centre has been identified in the zebrafish. The other major signalling centre implicated in mammalian dorsal telencephalic patterning, the ANB, has been identified and relatively well characterised. Following its role as a source of anti-caudalising Wnt antagonists early in development (Houart et al., 2002), the ANB is a source of Fgf signals, and abrogation of this signalling results in multiple forebrain defects (Houart et al., 1998; Shanmugalingam et al., 2000; Walshe and Mason, 2003). It is unclear, however, to what extent dorsal telencephalic development is specifically affected. Further characterisation of this brain area and the markers expressed within it will help to clarify this issue.

The zebrafish pallium does however express many of the same genes as the vertebrate pallium, including three members of the Emx family – *emx1*, *emx2* and *emx3*. All three genes have very similar expression domains within the telencephalon (Kawahara and Dawid, 2002; Morita et al., 1995), with *emx2* at least being additionally expressed in the olfactory placodes as it is in mouse (Yoshida et al., 1997). The zebrafish pallium also expresses two members of the T-box family of transcription factors, *tbr1* and *eomesodermin* (Mione et al., 2001; Yonei-Tamura et al., 1999). In the mammalian pallium the T-box genes *Tbr1* and *Tbr2* play roles in

cortical neuron specification and differentiation (Bulfone et al., 1999; Bulfone et al., 1995; Bulfone et al., 1998), and their precise function in zebrafish is being investigated (M. Mione, personal communication).

Pax6 expression is less conserved between mammals and fish, with no pallial radial glia-associated expression evident in the zebrafish. Pax6 expression is however evident at the pallial-subpallial boundary (Wullimann and Rink, 2002), an expression domain that is conserved between amniotes (Puelles et al., 2000). Various pallial and subpallial identities for this region have been proposed, but one possibility is that Pax6 marks a ventral pallial region that contributes to the claustrum and amygdala (Puelles et al., 2000; Wullimann and Rink, 2002).

*The subpallium generates migratory interneurons that populate the pallium*

Until recently it was thought that the two main cortical neuronal subtypes, the glutamatergic projection neurons and GABAergic interneurons, were both generated in the cortical ventricular zone. However, the discovery of cortical cells expressing the ventral telencephalic marker *Dlx2*, and the continuity of these cells with subpallial *Dlx2*-expressing cells (reviewed in Marin and Rubenstein, 2001) opened the door on not only the tangential migration of GABAergic interneurons from the ganglionic eminences to the cortex, but a host of other tangential migrations (Figure 1.2 B and C). In rodents the ganglionic eminences are now known to supply not only the vast majority of GABAergic cortical interneurons (including those of the piriform cortex and hippocampus), but also interneurons to the olfactory bulbs and to components of the basal ganglia. The careful dissection of the genetics of ventral telencephalon specification, as outlined above, has revealed the distinct sources and phenotypes of these various migratory populations (reviewed in Marin and Rubenstein, 2001).

The notion that the tangentially migrating and GABAergic interneuron populations were one and the same came from pioneering work by Anderson et al. (1997). They showed that GABA-expressing cells could migrate in brain slices *in vitro* from subpallial to pallial areas (Anderson et al., 1997a). Furthermore, severing a cultured coronal brain slice at the cortical-striatal boundary lead to a massive decrease in GABAergic cortical cells, similar to the effect of knocking out the *Dlx1* and *Dlx2* genes, known to be essential for ventral telencephalic neuron differentiation (Anderson et al., 1997b). Subsequently, a variety of elegant

experiments from a number of groups identified the MGE rather than the LGE as the primary source of cortical interneurons. DiI application to the MGE labels tangentially migrating cells that express GABA (Lavdas et al., 1999) and cells from the MGE and LGE have quite different properties, with transplanted MGE cells readily migrating into the cortex both in slice culture and adult brain (Wichterle et al., 1999) and *in utero* (Wichterle et al., 2001). Genetic manipulations that specifically perturb the MGE, as in the *Nkx2.1* mutant, also dramatically reduce cortical interneuron numbers (Sussel et al., 1999).

The MGE and the ventrally adjacent anterior endopeduncular area / anterior preoptic area (AEP/Poa) are also the source of tangentially migrating GABAergic and cholinergic interneurons that populate the striatum, the basal ganglia derivative of the LGE. Again, mutants such as *Nkx2.1*, *Mash1* and *Dlx1/2* affect this population, with *Mash1* and *Dlx1/2* mutants affecting predominantly the early- and late-born interneurons respectively (Marin et al., 2000). The AEP is also thought to be the source of telencephalic oligodendrocytes, a lineage that is also controlled by Shh-signalling (Nery et al., 2001)

#### Olfactory bulb interneurons migrate from the LGE

The LGE is the predominant source of quite a different population of tangentially migrating cells, supplying the olfactory bulb (OB) with its juxtglomerular and granule cell interneuron populations. This migration has been known for much longer than tangential migrations from the MGE, because the continual supply of interneurons to the OB into adulthood was highlighted in studies of adult proliferation (reviewed in Alvarez-Buylla, 1997; Marin and Rubenstein, 2001).

In transplantation studies, the cells of the embryonic LGE show distinct migratory behaviours to those of the MGE, with very few cells migrating to the cortex and instead migrating to the OB (Wichterle et al., 1999; Wichterle et al., 2001). Studies of ventral telencephalon patterning mutants also reveal OB phenotypes; the *Gsh2* *-/-* mouse has a massive reduction in OB interneurons at mid-embryonic stages (Corbin et al., 2000; Yun et al., 2001), suggesting that the dorsal LGE is the primary origin of these neurons. The dorsal LGE also expresses *Pax6* (Corbin et al., 2000; Yun et al., 2001), and *Er81* (Stenman et al., 2003), both of which mark OB neurons, while *Islet1*, which is found in other areas of the LGE, is not expressed in the OB (Stenman et al., 2003). *Mash1* *-/-* and *Dlx1/2* *-/-* mice also

show defects in the OB interneuron population, predominantly affecting early and late-born populations respectively (reviewed in Marin and Rubenstein, 2001).

Interneurons specified in the LGE migrate from an area just underlying the embryonic proliferative ventricular zone called the sub-ventricular zone (SVZ). Cells from the LGE SVZ converge to form a continuous stream of migratory cells known as the rostral migratory stream (RMS; reviewed in Alvarez-Buylla, 1997), which enters the OB and seeds the OB SVZ with progenitor cells (Wichterle et al., 2001). The RMS persists from early embryonic stages to adulthood, when the entire lateral wall of the lateral ventricle seems to contribute to the RMS (reviewed in Alvarez-Buylla, 1997). Cells in the postnatal RMS migrate in chains, expressing high levels of the cell adhesion molecule PSA-NCAM and surrounded by a sheath of astrocytes that seem to serve as a conduit for the migrating cells (Figure 2 in Alvarez-Buylla, 1997)(Chazal et al., 2000). Despite expressing neuronal markers such as TuJ1, cells in the RMS continue to divide during migration, indicating that they are indeed a progenitor population (Pencea and Luskin, 2003).

#### *The structure and origins of the olfactory bulb*

The OB is a derivative of the telencephalon and is the primary olfactory centre for odorant-sensing neurons in the olfactory epithelium. In mouse, the OB protrudes from the rostral tip of the pallium, close to the pallial-subpallial border. Evagination of the OB from the pallium is an Fgf-dependent process and may involve regulation of cell proliferation (Hebert et al., 2003). This initially evaginating OB structure is formed by the bulb projection neurons and is later invaded by subpallial-derived interneurons (reviewed in Alvarez-Buylla, 1997).

The projection neurons of the bulb, the mitral and tufted cells, are primarily glutamatergic and express pallial markers such as *Reelin*, *Tbr1* and *Emx2*. Mitral cell expression of these pallial markers has been sufficient to infer their pallial origins in *Xenopus* (Moreno et al., 2003), but this has only recently been confirmed by cell labelling experiments in the rat telencephalon (Nomura and Osumi, 2004). The development of the OB, then, has many parallels with that of the cortex, with projection neurons and interneurons having segregated embryonic origins.

As I have outlined above, mouse mutants where the LGE is affected also show defects in OB interneuron populations. Similarly, mutations targeting dorsal telencephalic markers, such as *Tbr1* and *Emx2*, show defects in the mitral cell

population as well as in the cortical projection neurons (Bulfone et al., 1998; Yoshida et al., 1997). What is very surprising is the seeming independence of the OB and the structure that innervates it, the olfactory epithelium (OE). Even in mouse mutants with severely compromised bulb structures, such as the *Tbr1* and *Dlx1/Dlx2* knockouts, olfactory sensory neurons from the OE still project axons to their stereotyped positions within the bulb (Bulfone et al., 1998). Conversely, mutations that affect the development of the OE do not prevent development of the bulb. For example, both *Mash1* (Casarosa et al., 1999) and *Dlx5* (Long et al., 2003) mutants still form an OB, albeit one that lacks some interneurons (due to the actions of these genes in the ventral telencephalon) and despite an absence of innervation from the OE.

#### *Cell migration within the zebrafish telencephalon*

The tangential migration of interneurons from the MGE to the cortex is now a very well-described phenomenon that is conserved between rodents and birds (Cobos et al., 2001a). Similarly, the tangential migration of OB interneurons from the LGE has been observed in primates (Kornack and Rakic, 2001; Pencea et al., 2001) and in birds (Cobos et al., 2001a). This type of migration obviously has the possibility of increasing neuronal diversity within a given brain area and may therefore be a mechanism conserved beyond tetrapod vertebrates.

Such migrations have yet to be described in zebrafish, but some indication that these migrations occur is provided by the expression of subpallial genes in the pallium and OB. For example, single *dlx*-expressing cells are seen in the dorsal telencephalon and OB from late embryonic stages (M.Mione, personal communication). This possibility needs to be further investigated and it is one of the main aims of my thesis to chart cell movements in the telencephalon throughout the period of embryogenesis to establish the origins and patterns of migratory cell populations.

#### *Neuronal subtype specification within the dorsal telencephalon*

The generation of multiple neuronal subtypes is fundamental to the formation of functional, interacting neuronal circuits within any brain area. Populations of neurons must therefore be endowed with different phenotypes, whether it is in terms of their pathfinding capabilities and axonal projections, or their neurotransmitter and

receptor repertoire. As I have outlined, the telencephalon uses the spatial segregation of different progenitor domains to specify neurons with different neurotransmitter phenotypes. Cell migration then serves to increase neuronal diversity within any given area, particularly in the dorsal telencephalon (reviewed in Marin and Rubenstein, 2001).

Many of the genes that are involved in the specification of pallial neurons, such as those of the *Emx* and *Tbr* families are expressed in broad domains over extended periods of embryogenesis. This absence of refined spatial and temporal regulation of gene expression raises the question of whether these genes are solely responsible for the observed incredible arealisation and specialisation of the mammalian cortex (Monuki and Walsh, 2001). The zebrafish dorsal telencephalon does not share the complexity of the mammalian cortex, but functional areas are proposed and have been identified in closely related species such as the goldfish (e.g. Portavella et al., 2002). It is therefore of prime importance to address the mechanisms that may specify neuronal subtypes within the dorsal telencephalon.

### *The LIM-HD family of transcription factors*

#### *LIM-HD structure and function*

Some of the prime candidates for controlling neuronal subtype specification are members of the LIM-homeodomain (LIM-HD) family of transcription factors, factors highly conserved in organisms as diverse as *Drosophila*, *C. elegans* and humans. These proteins form subset of the homeodomain (HD) superfamily, a superfamily whose members are involved in almost every aspect of embryonic patterning, polarity and differentiation. The distinguishing feature of the LIM-HD proteins is that they contain not only a DNA-binding homeodomain, but also two protein-interacting LIM domains. This is in contrast to other members of the HD superfamily that contain at most either a short protein-interaction motif (HOX proteins) or DNA binding domains (POU-HD or PAX proteins) in addition to the homeodomain (reviewed in Hobert, 2000; Bach 2000). Another feature of the LIM-HD proteins is that they are widely, although not exclusively, involved in the development of the nervous system (Dawid and Chitnis, 2001), and in vertebrates particularly in the more subtle aspects of neuronal phenotype such as axon extension and neurotransmitter profile.

LIM-HD proteins play instructive roles in neuronal subtype specification within the zebrafish CNS, especially in the spinal cord (Appel et al., 1995; Kikuchi et al., 1997; Segawa et al., 2001). However, almost nothing is known about the roles of LIM-HD proteins at more rostral levels of the CNS such as the telencephalon. A number of Lhx genes are expressed in the zebrafish telencephalon, including the genes *lhx1a*, *lhx1b* and *lhx5* (Toyama et al., 1995; Toyama and Dawid, 1997). Their expression patterns at early embryonic stages have been somewhat described, and may indicate a role in organiser function (Shawlot and Behringer, 1995; Taira et al., 1994; Watanabe et al., 2002). However, the later embryonic and postembryonic expression domains of these genes are as yet poorly characterised and it is unknown whether they highlight specific subpopulations of neurons within the telencephalon. It is one of the primary aims of my work to characterise the expression patterns of these genes in order to be able to infer a role for them in telencephalic neuronal specification.

LIM-HD proteins in other species are strongly implicated in the specification of forebrain neuronal subtypes. For example, mouse Lhx5 seems to have a specific role in the morphogenesis and differentiation of the hippocampus (Zhao et al., 1999). A further study has postulated that combinations of LIM-HD proteins and their cofactors may delineate many mammalian cortical regions, although functional evidence for this is currently lacking (Bulchand et al., 2003). Furthermore, combinations of transcription factors, including members of the LIM-HD family, mark specific nuclei in complex brain areas from embryonic to postnatal (or postembryonic) stages. For example, five Lhx genes (*Isl1*, *Lhx1*, *Lhx2*, *Lhx5* and *Lhx9*) and three other genes parcellate the developing thalamus, highlighting specific nuclei from embryonic to postembryonic stages (Nakagawa and O'Leary, 2001). A similar situation exists in *Xenopus*, where the same patterns of Lhx gene expression are seen to mark functional subdivisions within the forebrain at embryonic, larval and adult stages (Bachy et al., 2001; Moreno et al., 2004; N. Moreno, personal communication).

#### *LIM-HD function requires multi-protein complexes*

The key to understanding the mechanism of LIM-HD function lies within the structure of the protein. LIM-HD proteins can bind directly to other factors such as POU-HD proteins, but the majority of LIM-HD interactions are via the cofactor

family of Ldb proteins (also called NLI/CLIM/Chip; reviewed in Bach, 2000; Figure 1.3 A). Zebrafish have four Ldb proteins, all of which are widely expressed during development, especially in the forebrain (Toyama et al., 1998). Ldb proteins have intrinsic dimerising capacity, separate from their LIM domain binding sites (Jurata and Gill, 1997; Jurata et al., 1998), and are therefore able to mediate interactions between LIM-HD proteins including the formation of homomeric and heteromeric complexes (reviewed in Bach, 2000). Since cells often express more than one LIM-HD protein, the exact combination being critical for appropriate cell subtype specification (e.g. Appel et al., 1995; Thaler et al., 2002), it has been proposed that heteromeric LIM-HD complexes may underlie the so-called LIM combinatorial code. Recent persuasive evidence, reviewed below, indicates that this may indeed be the case.

LIM-HD proteins do not only form transcription-activating complexes. Via Ldb, they can also bind a class of LIM-domain only proteins (LMO). Complexes with LMO may cause transcriptional repression because of the absence of the DNA-binding homeodomain in LMO proteins (reviewed in Bach et al., 2000; Figure 1.3 B). Similar to LMO, transcriptional repression may also be caused by the binding (via Ldb) of a LIM-HD protein with an alternatively spliced form of the same protein that lacks a functional homeodomain (Failli et al., 2000). Failli et al. postulate that this could be a method both to spatio-temporally regulate the transcriptional effects of Lhx9 and to add another level of refinement to the LIM-HD code. Finally LIM-HD proteins can form repressive complexes by binding to RLIM, which in turn recruits the Sin3A/histone acetylase transcriptional repressor complex (Bach et al., 1999).

The huge variety of potential binding partners for LIM-HD proteins, and their ability to act in both transcriptional activation and repression complexes, highlights the difficulties of pinning down LIM-HD function in any given cell type. However, a number of researchers have been able to assess LIM-HD function in a variety of systems, and I will review some of the work most relevant to zebrafish below.

The instructive and combinatorial action of LIM-HD proteins was first implied by experiments in the zebrafish spinal cord. Different primary motorneuron subtypes express different combinations of the LIM-HD proteins Islet1, Islet2 and Lhx3 (Appel et al., 1995). It had already been shown that the fate of the three primary motorneuron subtypes, which have different axon trajectories, could be

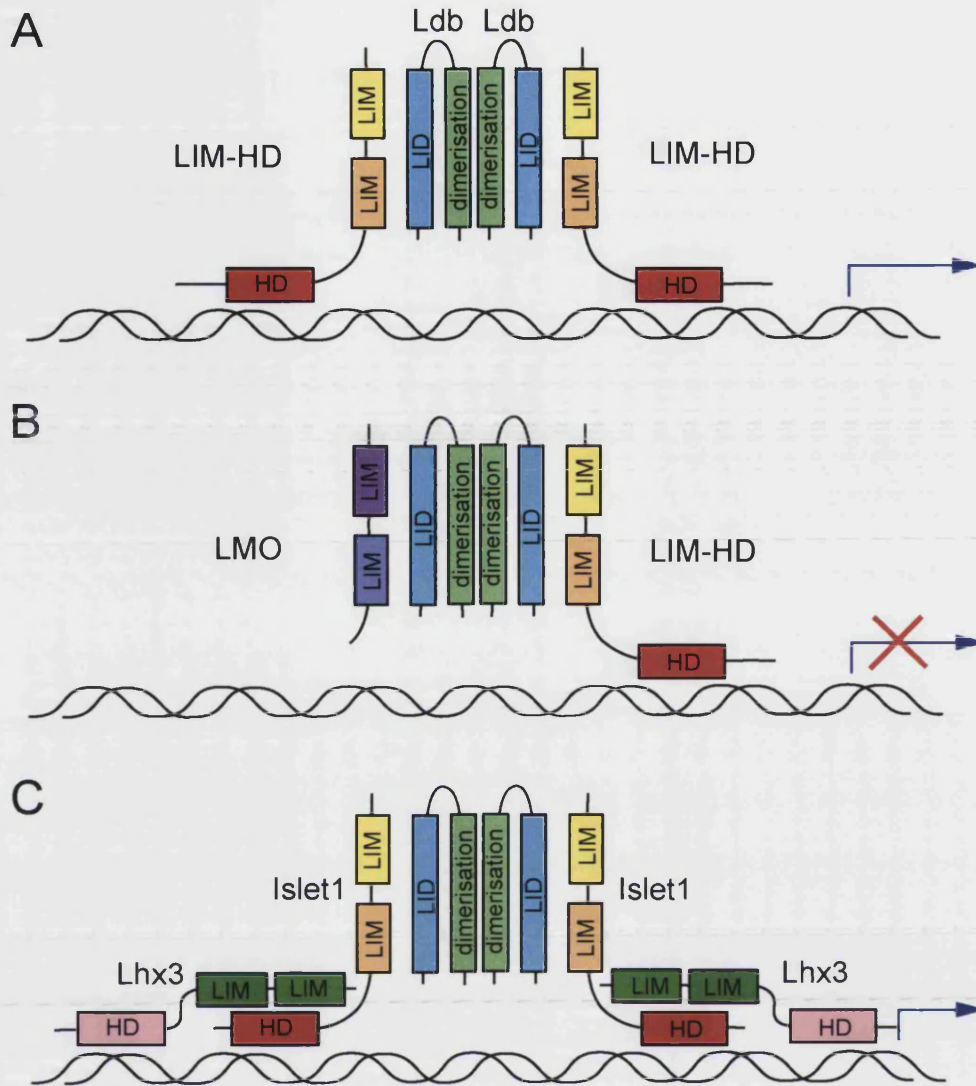


Figure 1.3

Schematic diagrams showing LIM-HD protein interactions.

A shows two LIM-HD proteins in a complex with an Ldb dimer. This transcription activating complex can involve two identical or two different LIM-HD proteins.

B shows how the binding of a LIM-domain only (LMO) protein in place of a LIM-HD protein can inhibit transcription.

C shows the hexameric protein complex involved in spinal cord motor neuron determination as proposed by Thaler et al., 2002. Lhx3 binds to sites near the homeodomain of Islet1 rather than in a heteromeric complex with Ldb and Islet1.

Diagrams adapted from Hobert and Westphal, 2000 and Thaler et al., 2002.

changed by transplantation until just before axonogenesis (Eisen, 1991). Appel et al. (1995) then showed that this fate change was accompanied by a change in *islet1* mRNA expression, appropriate for the new position of the transplanted motoneuron. Thus the MiP motoneuron, which would normally express *islet1*, could be induced to express *islet2*, a characteristic of the CaP/VaP neurons, and extend a CaP/VaP axon if transplanted to the more caudal position at least 2 hours before axonogenesis (Appel et al., 1995). This result indicated not only the importance of specific LIM-HD expression for cell subtype specification, but also the finely grained positional information that must exist within the spinal cord to control Lhx gene expression.

Work by members of Hitoshi Okamoto's group investigated more closely the roles of the LIM-HD Islet factors in neuronal subtype specification (Kikuchi et al., 1997; Segawa et al., 2001). They disrupted the action of Isl2 and Isl3 by overexpressing only the LIM domains of these two proteins, which then acted as dominant negative constructs. The LIM<sup>Isl2</sup> and LIM<sup>Isl3</sup> constructs overlapped in their effects, both affecting cell types where either Isl2 or Isl3 is expressed, including the primary motoneurons. However, a surprising result was that the rescue was much more specific, Isl2 rescuing only Isl2-expressing cell types and the same for Isl3. A further surprise was that overexpressing the LIM-interacting domain of Ldb, which should also act as a dominant negative but bind the LIM domains of all LIM-HD proteins, produced the same phenotype as the expression of LIM<sup>Isl2</sup> and LIM<sup>Isl3</sup> (Segawa et al., 2001). These results highlight the surprising specificity of LIM-HD interactions despite extensive sequence similarities between closely-related members, and suggest that there may be yet more factors involved that regulate these processes (Dawid and Chitnis, 2001; Segawa et al., 2001).

The confirmation that heteromeric complexes of LIM-HD proteins are directly responsible for cell type specification was recently shown by Thaler et al., (2002). In the chick ventral spinal cord, postmitotic neurons choose between V2 interneuron (V2 IN) and motoneuron (MN) cell fates. V2 IN's express Lhx3 and Ldb, whereas MN's express Lhx3, Ldb and Islet1 (Isl1). Using a variety of engineered fusions that brought together the functional domains of Lhx3, Ldb and Isl1 in single molecules rather than as protein complexes, the authors demonstrated that a 2 Ldb: 2 Lhx3 tetramer is responsible for V2 IN specification, while MN's are specified by a novel 2 Ldb: 2 Isl1: 2 Lhx3 hexamer (Figure 1.3 C). In the MN-specific hexameric complex, Isl1 displaces Lhx3 because of its greater affinity for

Ldb, but Lhx3 still binds in the complex via its LIM domains to sites in Isl1. Surprisingly, the authors found no role for homomeric or heteromeric tetramers of Isl1 or Lhx3 in MN specification, and this raises interesting questions about the structure and function of heteromeric complexes in other systems.

#### *Transcriptional targets of LIM-HD proteins*

LIM-HD proteins clearly play roles in neuronal subtype specification, as outlined in the many examples above. However their transcriptional targets remain largely unknown. Recent evidence suggests LIM-HD and Ldb proteins may regulate the expression of F3, a cell recognition molecule expressed on axons and glia, in a subset of zebrafish neurons (Gimnopoulos et al., 2002). This is consistent with a role for LIM-HD proteins in regulating axon outgrowth and pathfinding. Other recent evidence suggests that downstream targets of LIM-HD proteins in spinal motor neurons may include the *Eph/ephrin* family of genes (Kania and Jessell, 2003), a family with wide-ranging roles in cell migration and axon pathfinding, including in the guidance of thalamocortical axons (Bishop et al., 2003).

#### *Aims of the work*

In the course of this introduction I have outlined the present level of knowledge with respect to the development of the zebrafish telencephalon. Beyond the early induction and patterning of this brain area, very little is known about the morphogenesis or cell movements that shape the mature telencephalic structure. The process of dorsal telencephalic eversion remains particularly unexplored, yet a thorough description of this process is central to any comparative approach involving zebrafish. Furthermore, little is known about the specification of neuronal subtypes within the telencephalon. The broad conservation of patterning mechanisms gives some insight into these processes, but the specification of telencephalic derivatives such as the olfactory bulb has yet to be investigated.

My work therefore has three main aims:

1. To provide a detailed description of the basic processes that shape the zebrafish telencephalon over the entire period of embryogenesis, including morphogenesis, proliferation, neurogenesis and axon tract formation, and to use these observations to gain insight into the eversion process.

2. To investigate the potential roles of Lhx genes in telencephalic subtype specification, particularly focussing on the specification of olfactory bulb cell types.
3. To use cell labelling techniques to build a picture of the morphogenetic movements and migrations that shape the telencephalon, with a particular focus on the spatial origins of the olfactory bulb.

## Chapter 2: Materials and Methods

Many of the methods described in this chapter were used throughout the practical work of this project; those methods are described in detail here. General zebrafish methods can also be found in the Zebrafish Book (Westerfield, 2000). Methods that apply specifically to the work of one chapter are described in the respective “Materials and Methods” section of the appropriate chapter.

### *2.1 Live embryo care*

Embryos were staged according to Kimmel et al., (1995) and cared for according to standard protocols described in the Zebrafish Book (Westerfield, 2000). Embryos were grown at 28.5°C in either system water with a small amount of methylene blue to offset infection or in embryo medium (Zebrafish Book). To prevent pigment formation, 0.003% w/v Phenylthiocarbamide (PTU, Sigma) was added to the embryo medium from 24hpf.

Wild type embryos were generally provided by communal stocks of fish from a mixture of genetic backgrounds, kept on a 14h/10h light/dark cycle. Spawning was natural and embryos were collected in mesh-lined boxes. I also used the *Tg(HuC:GFP)* line (Park et al., 2000) and the *Tg(dlx4/6:GFP)* line (Zerucha et al., 2000). Embryos were dechorionated using sharpened watchmaker’s forceps.

### *2.2 Agarose mounting of live embryos*

For all mounting, dechorionated embryos were anaesthetised according to the Zebrafish Book using tricaine (3-amino benzoic acid ethylester, Sigma) in embryo medium. Embryos were mounted in 1.5% low melting-point agarose (Sigma) that had been previously dissolved in embryo medium. Embryos for mounting were pipetted singly into a glass bijou bottle containing molten agarose at approximately 37°C. They were then drawn up into a fire-polished glass pipette with excess agarose and expelled onto a slide or coverslip. Precise orientation of the embryos was performed within 30 seconds using a blunt tungsten needle.

For imaging procedures, live embryos were usually mounted in agarose on a coverslip and surrounded by either a ring of silicone grease (RS, Oxford) or a glass

ring (Fisher). The well was then filled with embryo medium/tricaine into which water immersion lenses were directly dipped.

### *2.3 DNA and RNA microinjection*

Embryos from natural spawnings were collected and injected from the 1- to 4-cell stage according to guidelines in the Zebrafish Book. Briefly, micropipettes were pulled from borosilicate glass capillaries (with filament) on a horizontal Flaming/Brown micropipette puller (model P-87, Sutter Instrument Co.), producing micropipettes with a long, fine, sealed tip. Micropipettes were backfilled with 1-2 $\mu$ l DNA or RNA solution, made up in Danieau buffer (Zebrafish Book), and the very tip of the micropipette was broken off such that a short (< 0.5 second) puff from the Picospritzer (General Valve Corporation) would dispense a drop approximately 100 $\mu$ m in diameter.

Embryos were laid, in their chorions, along the edge of a glass slide glued to the inside of a petri dish lid. Excess liquid was removed so that the meniscus held the embryos along the slide. Embryos were then injected through the chorion, directly into a single blastomere with minimum disruption to the underlying yolk. Following injection, embryos were transferred to embryo medium and grown at 28.5°C.

### *2.4 Preparation of DNA*

Plasmid DNA was introduced into XL1-blue/ DH5 $\alpha$  strains of E.coli using a 30 second heat shock at 42°C. After overnight growth at 37°C on LB Agar plates with 100 $\mu$ g/ml ampicillin (Sigma), single colonies were picked and inoculated into mini cultures of 2-3ml of LB with 100 $\mu$ g/ml ampicillin and grown overnight. Plasmid DNA was prepared from individual cultures using Qiagen miniprep kits (Qiagen), and eluted from the column with 10mM Tris-Cl, pH 8.5.

Larger scale midi- and maxipreps of plasmid DNA were performed using Promega kits with standard protocols (Promega). The final concentration of plasmid DNA was established by spectrophotometry at 260/280nm and adjusted to 1 $\mu$ g/ $\mu$ l with ultrapure H<sub>2</sub>O, before being stored at -20°C.

### *2.5 Preparation of synthetic mRNA*

All solutions and tips should be DNase/RNase-free

1. Linearise construct with appropriate enzyme to include polyA sequence in the transcript
2. Purify linearised DNA using Qiagen Quickspin columns. Elute in 30µl 10mM Tris-Cl, pH 8.5
3. Using Mmessage machine kit (SP6; Ambion), make up transcription reaction with 1µg DNA, 2µl 10x buffer, 10µl 2x dNTP's, 2µl enzyme in a total volume of 20µl
4. Incubate at 37°C for 2 hours; add 2µl DNase and incubate for a further 30'
5. Add 30µl H<sub>2</sub>O to the reaction
6. Add 50µl phenol-chloroform; mix, spin at 13K rpm for 2'; remove and save top layer
7. Prepare Sephadex G50 column by vortexing and then spinning for 1' at 2K rpm; load top layer onto top of column and spin for 2' at 2K rpm
8. Add 50µl 5M NH<sub>4</sub>OAc to column eluate
9. Add 200µl 100% EtOH; vortex; leave at -20°C for at least 2 hours
10. Spin at 13K rpm for 30' to pellet RNA
11. Wash pellet with 70% EtOH and spin at 13K rpm for 10'
12. Remove all liquid and air-dry pellet; resuspend in 20µl RNase-free H<sub>2</sub>O

### *2.6 Preparation of probes for in situ hybridisation*

1. Linearise construct with the appropriate enzyme for making antisense probe. Digest mix is 10µl DNA at 1µg/µl, 1.5µl enzyme, 4µl 10x enzyme buffer in a total volume of 40µl. All enzymes from Promega
2. Digest DNA for 2 hours at 37°C
3. Purify linearised DNA using a Quickspin purification column (Qiagen). Elute in 30µl 10mM Tris-Cl, pH 8.5.
4. Make up probe synthesis/labelling mix: 11.5µl H<sub>2</sub>O, 3µl linearised DNA template, 5µl 5x polymerisation buffer, 1µl 0.1M DTT, 0.5µl RNasin (Promega), 2µl DIG or FITC labelling mix (Roche), 2µl polymerase (T7 or T3; Promega).
5. Run reaction for 2h at 37°C. Add 2µl DNase and incubate for a further 30 minutes

6. Spin a Mini Quick Spin RNA purification column (Roche) for 2 minutes at 2K rpm. Load entire reaction mixture onto column matrix and spin for 4 minutes at 4K rpm.
7. Add 40µl deionised formamide (Sigma) to the eluate and freeze at -80°C.
8. Run a small aliquot on gel to verify probe size and quality

### *2.7 In situ hybridisation*

Clean solutions are DNase/RNase free.

Hybridisation solution (all reagents from Sigma): 25ml Formamide, 3.25ml 20xSSC pH 5.0 with citric acid, 0.5ml 0.5M EDTA pH 8.0, 25µl Torula yeast RNA 100µg/ml, 1ml 10% Tween-20, 100µl Heparin (sodium salt) 50µg/ml, made up to 50ml with RNase-free water.

1. Fix in 4% PFA made up in clean PBS overnight at 4°C
2. Wash embryos in clean PBS
3. Dehydrate embryos through 25%/50%/75% MetOH/PBS and store at -20°C for up to one month.
4. Rehydrate embryos through 75%/50%/25% MetOH/PBS; 5 mins each step
5. Wash embryos 2 x 5 mins in clean PBTw (PBS+0.5% Tween-20)
6. Digest embryos with 10 µg/ml Proteinase K (Roche) in PBTw (10 µg/ml is 1x concentration; stock is usually 10-15 mg/ml). Times can vary from 2 minutes in 1x ProK (24hpf) to 1hour in 10x ProK (5dpf); each batch of enzyme should be tested
7. Wash embryos briefly in PBTw
8. Post-fix for 20 mins in 4% PFA at room temperature
9. Rinse and wash once with PBTw
10. Rinse once with 50% PBTw/50% Hyb mix. Let embryos settle
11. Incubate in 100% Hyb mix at 65°C for at least 1 hour
12. Add pre-warmed probe in fresh Hyb solution to embryos and incubate overnight at 65°C. Amount of probe needed varies widely, but is usually 1µg per tube (400µl hyb).

All hyb and SSC washes should be at 65°C; heat solutions in the waterbath

13. Rinse twice with pre-warmed Hyb solution
14. Wash 2 x 30 mins with Hyb solution

15. Wash in 75%Hyb, 25% 2xSSC, 50%Hyb, 50% 2xSSC, 25%Hyb, 75% 2xSSC; 5 mins each.
16. Wash 10 mins in 2xSSC
17. Wash 30 mins 0.2xSSC
18. Wash in 10mM PIPES 0.5M NaCl for 5 mins
19. RNase treatment (if necessary): 10 µg/ml RNase A (Sigma), 1µl RNase T1 (Sigma) in 5ml PIPES/NaCl
20. Wash in PIPES/NaCl
21. Wash in MAB for 5 mins
22. Incubate in MAB + 2% Boehringer Block reagent for at least 1hr
23. Incubate overnight at 4°C in fresh MAB+block with appropriate antibody - anti-DIG AP (Roche) 1:5000; anti-FLU AP (Roche) 1:2500
24. Wash in MAB for 6 x 30 mins
25. Wash 3 x 5 mins in buffer for appropriate colour reaction, and perform colour reaction

NBT/BCIP (blue/purple):

Tris-HCl, pH9.5	2.5ml of 2M
MgCl <sub>2</sub>	2.5ml of 1M
NaCl	1ml of 5M
Tween-20	0.5ml of 10%
Make up to 50ml with P water	

FastRed (pink/red; also fluorescent)

Tris-HCl, pH8.2–8.5	2.5ml of 2M
MgCl <sub>2</sub>	2.5ml of 1M
NaCl	1ml of 5M
Tween-20	0.5ml of 10%
Make up to 50ml with P water	

Colour reaction: 5ml AP buffer + 15µl NBT (75mg/ml) + 17.5µl BCIP (50mg/ml)

Colour reaction: 2ml AP buffer + 1 FastRed tablet (Roche). Filter with 0.2µm syringe filter before use

26. Wash in PBTw, and add 1 drop 0.5M EDTA to stop reaction. Do not do this for double in situ.
27. Dehydrate in MetOH: 25%/50%/75% and rehydrate. This may intensify staining and reduce background, especially in the yolk
28. Post-fix in 4% PFA for 20 mins at room temperature
29. Dehydrate into 70% glycerol with PBS and store at 4°C

### *2.8 Double in situ hybridisation*

Localising two transcripts simultaneously involves labelling two different probes with DIG and FITC respectively. These are hybridised at the same time but then detected separately, both with alkaline phosphatase-conjugated antibodies with different coloured substrates - NBT/BCIP (blue) and Fast red (red/pink). The stronger probe is usually labelled with FITC and detected with Fast Red substrate, but this can be varied.

The double in situ hybridisation protocol is carried out as detailed in the protocol above, except that both probes (DIG and FITC-labelled) are hybridised at the same time (step 12). Then following the first colour reaction (step 25):

1. Rinse in PBT but DO NOT add EDTA
2. Inactivate the AP in 0.1M glycine pH 2.2 in PBS for 10 minutes – no longer
3. Rinse 5 x 5 mins in PBT. It is very important to remove all of the glycine
4. Incubate 15 mins in 2% Boehringer block in MAB
5. Incubate overnight with second antibody diluted appropriately in 2% block in MAB
6. Follow steps 24-29 from above protocol.

### *2.9 In situ hybridisation followed by antibody labelling*

For *in situ* hybridisation followed by antibody labelling, follow single *in situ* hybridisation procedure to step 25. Then:

1. Following *in situ* revelation step, rinse well in PBTw. Do not add any EDTA if secondary antibody to be used is an enzyme conjugate (e.g. -HRP, -AP)
2. Refix in 4% PFA for at least 20 minutes
3. Incubate in blocking solution of 10% NGS (Sigma) in PBTw for 1 hour
4. Incubate in primary antibody in 1% NGS/PBTw overnight at 4°C
5. Wash 6 x 20 minutes in PBTw
6. Incubate in secondary antibody in 1% NGS/PBTw overnight at 4°C
7. Wash 6x20 minutes in PBTw. For fluorescent secondary antibodies the protocol is finished.
8. For DAB staining, follow antibody labelling protocol (below) from step 12
9. Postfix embryos in 4% PFA, wash and store in PBS

### 2.10 Antibody labelling

A standard antibody labelling protocol was used for all antibodies apart from anti-BrdU, described in the next section. All washes and incubations were either in 1.5ml microtubes (Merck), 4- or 24-well plates (Nunclon) or 7ml plastic universal tubes.

1. Fix embryos in 4% Paraformaldehyde (PFA, Sigma) in 1x PBS (phosphate-buffered saline) overnight at 4°C if younger than 48hpf

Fix embryos in 2% Trichloroacetic acid (TCA, Sigma) for 3 hours at RT if 48hpf or older

2. Wash 3 x 5 minutes in PBTr (PBS + 1% Triton X-100 (Sigma))

3. Permeabilise embryos if older than 24hpf. Prechill trypsin solution on ice (0.25% trypsin (Sigma) in PBS).

Incubate the embryos in this solution on ice for 5-10 minutes. Older embryos may need longer time and time of incubation also depends on sensitivity of the antibody. Each batch of trypsin can be different so titration is often necessary upon first use.

4. Wash 5 x 5 minutes in PBTr.

5. Wash in 10% normal goat serum (NGS; Sigma) in PBTr for 1 hour at room temperature.

6. Incubate embryos in primary antibody + 1% NGS in PBTr overnight at 4°C.

The concentration of primary antibody depends on the individual antibody.

7. Wash 4-5 x 20 minutes with PBTr.

8. Block endogenous peroxidase if using a peroxidase-conjugated secondary antibody:

Wash 1 x 5 minutes in 50% methanol/PBS

Wash 1 x 10 minutes in 100% methanol

Incubate in methanol/peroxide for 10 minutes at room temperature, (1ml methanol/ 50µl 6% H<sub>2</sub>O<sub>2</sub>).

Wash 5 minutes 50% methanol/PBS.

9. Wash 5 minutes in PBTr.

10. Incubate in secondary antibody + 1% normal goat serum in PBTr overnight at 4°C or for 4 hours at room temperature.

11. Wash for 6-8 x 15 minutes in PBTr.

If using fluorescent secondary this is the end of the procedure.

12. If developing embryos with Diaminobenzoic acid (DAB; Sigma) then prepare a dilute potassium permanganate solution and keep to one side in case of spillages of DAB.
13. Develop embryos in DAB (1 tablet (10mg;) per 12ml PBS). Incubate embryos in this for 10 minutes.
14. Start reaction by adding 1-2 $\mu$ l 6% H<sub>2</sub>O<sub>2</sub> per 3 ml of DAB solution. Monitor reaction under dissecting microscope.
15. End reaction by transferring embryos back to PBS.
16. Refix embryos in 4% PFA for 20 minutes.
17. Store in either PBS or 30% glycerol until imaging.

### *2.11 BrdU pulse labelling*

1. Make up BrdU at a working concentration of 1-2mg/ml in embryo medium with 15% dimethyl sulfoxide (DMSO, Sigma).
2. Take embryos through washes of 5%, 10% and 15% DMSO in embryo medium, allowing the embryos to equilibrate at each step (approximately 3 minutes).
3. Place embryos in the petri dish with the solution containing BrdU and place dish on ice for 20minutes.
4. Wash embryos back into embryo medium until fixation or further manipulation.

### *Detection of the BrdU signal*

1. Fix in 4% Paraformaldehyde (PFA) for at least 24h at 4°C
2. Wash in PBS
3. Dehydrate embryos through a methanol series into 100% MeOH for at least 1hr at -20°C. Embryos can be stored like this for several weeks.
4. Rehydrate embryos through PBS/MeOH series back into PBS.
5. Wash in PBS 2 x 5 minutes.
6. Permeabilise embryos in 10  $\mu$ g/ml proteinase K (Roche) for 20-40 minutes if older than 10 hpf.
7. Rinse in 2 mg/ml glycine (Sigma)/ PBS 2-3 times.
8. Rinse in PBS 3-4 times.
9. Re-fix in 4%PFA for 30-60 minutes.
10. Rinse in H<sub>2</sub>O 3-4 times.

11. Incubate in 2N HCl for 1hr (8.6ml stock/50ml dH<sub>2</sub>O) at room temperature. It is important to make this 2N solution up fresh each time.
12. Wash in PBTr 3-4 x 5 minutes
13. Block in 2% normal goat serum in PBTr for 1 hr at room temperature
14. Incubate in primary antibody (anti-BrdU, 1:200, Sigma) at least overnight at 4°C.
15. Wash in PBTr 6-8 x 15minutes
16. Incubate in secondary antibody overnight.
17. Wash off secondary antibody by 6-8 x 15 minutes PBTr. If revealing secondary antibody using DAB then follow antibody labelling protocol from step 12.
18. Refix for about 24 hrs prior to dissection.

### *2.13 Image acquisition*

A variety of microscope systems were used during the course of this project. DIC images of non-fluorescent *in situ* hybridised and immunolabelled specimens were taken on an upright Nikon microscope, with a Micropublisher digital camera (Q imaging) run by Openlab 3.1.4 software (Improvision, UK). Epifluorescence and DIC imaging of live specimens was carried out on a Zeiss Axioplan 2 microscope, with water immersion lenses. Images were captured with a Hamamatsu Orca-ER digital camera run by Openlab 3.1.4 software (Improvision, UK). Confocal imaging of fluorescent specimens was carried out on Leica microscopes running Leica software.

### *2.14 Image processing*

Fluorescence images from confocal microscopy were processed using the freely-available NIH image v1.63 software (<http://rsb.info.nih.gov/nih-image/Default.html>) to assemble and project stacks of images. ImageJ v1.32 software (<http://rsb.info.nih.gov/ij/>) was used to create red/green overlays. Adobe Photoshop 7 was used to create fluorescence/DIC overlays, and for general image adjustment. Figures were prepared in Adobe Illustrator 10.

### 3.1: Aim and Introduction

The zebrafish brain is a relatively little-studied structure compared to that of the mouse and chick. The telencephalon, the area of the brain that in mammals gives rise to the cerebral cortex and basal ganglia, is among those structures that remain to be explored. We have substantial insight into the induction and early patterning of this brain region (reviewed in Wilson and Houart, 2004), and also some information about the structure and connectivity of the adult brain e.g. (Rink and Wullimann, 2001; Wullimann and Rink, 2002). However, particularly lacking is a study of how basic characteristics of the telencephalon such as proliferation, differentiation and connectivity change over the period of embryogenesis. This information is essential for developing a comprehensive model of telencephalic development and will provide the basis for more functional experiments in the future.

#### *Morphogenesis of the zebrafish telencephalon*

The morphogenesis of the forebrain is a complex process (reviewed in (Wilson and Houart, 2004)). During the patterning of the neural plate at gastrulation stages, the telencephalon is the most rostrally-located of all the forebrain subdivisions, with ventral telencephalic precursors lying anterior to dorsal telencephalic precursors (Whitlock and Westerfield, 2000). However, as hypothalamic precursors move anteriorly, splitting the eye fields, and under the telencephalic anlage (Varga et al., 1999), the telencephalon becomes a dorsal rather than rostral structure in the neural tube. A variety of fate-mapping experiments indicate this is the case for species as diverse as *Xenopus*, turtle, chick and mouse, leading Fernandez et al. to conclude that the telencephalic vesicle derives from the dorsal aspect of the prosencephalic (forebrain) vesicle (Fernandez et al., 1998). This distinguishes the telencephalon from more caudal brain areas, which are formed as transverse segments of the neural tube, and has implications for the patterning and morphogenesis of this brain area.

The early morphogenesis of the telencephalon has been somewhat described (Wilson et al., 1990). The optic recess (OR) is the point from where the optic cups evaginate from the rest of the forebrain, and is taken to be the anterior-ventral limit between the telencephalon and the hypothalamus. The ventricular space that leads into the OR, strictly the third ventricle, then becomes the structure delimiting the

telencephalon from the diencephalon (Wilson et al., 1990). The ventricular space is continuous between the telencephalon and diencephalon. A feature also evident between 1dpf and 2dpf is the ventral flexure in the brain, caudal to the hypothalamus and rostral to the midbrain (Ross et al., 1992; Wilson et al., 1990). Subsequent studies have shown that the ventral flexure causes a kink in the longitudinal axis of the brain eventually reorienting forebrain expression domains almost 90° relative to the original brain axis (Hauptmann and Gerster, 2000; Hauptmann et al., 2002).

#### *Pallial and subpallial divisions within the zebrafish telencephalon*

The prosomere theory proposes that subdivisions analogous to the well-characterised hindbrain segments (Lumsden and Keynes, 1989) are present in the forebrain and can be defined by gene expression domains. At its inception, the prosomere theory was applied to all forebrain regions including the telencephalon (Puelles and Rubenstein, 1993), but the recently revised model proposes only three diencephalic prosomeres – the pretectum, thalamus and prethalamus (Puelles and Rubenstein, 2003). However, the telencephalon is not without its subdivisions; a highly conserved feature of the telencephalon across species is its division into subpallial (ventral) and pallial (dorsal) regions (Fernandez et al., 1998; Puelles et al., 2000). These divisions have functional relevance, the subpallium giving rise to the basal ganglia and the pallium to the cerebral cortex and other associated structures in mammals.

The zebrafish telencephalon can also be divided into pallial and subpallial regions, based primarily on the expression of conserved genes such as *emx* (Kawahara and Dawid, 2002; Morita et al., 1995), *tbr1* and *eomesodermin* (Mione et al., 2001) and *reelin* (Costagli et al., 2002) in the pallium, and the *dlx* genes (Akimenko et al., 1994; Zerucha et al., 2000) and *nk2.1b* (Rohr et al., 2001) in the subpallium. However, unlike the morphologically evident ganglionic eminences that mark the subpallium in mammals (for review see Wilson and Rubenstein, 2000), there are no obvious morphological subdivisions between pallial and subpallial areas in zebrafish. Some researchers use cell morphology to infer the subdivisions (e.g. (Wullmann and Rink, 2002)), but this has not been extensively backed up by gene expression analysis. In fact, a rigorous analysis of zebrafish pallial and subpallial areas over the entire period of embryogenesis is not present in the literature.

### *The zebrafish dorsal telencephalon is everted*

The actinopterygian (ray-finned) fish-specific process of eversion further hampers understanding of zebrafish telencephalic development. Eversion is contrasted with the much more widely-employed evagination of the telencephalic vesicles. In an evaginated telencephalon, dorso-medial structures in the neural tube remain dorso-medial following evagination, while the telencephalic vesicles bulge out laterally (Butler, 2000; Butler and Hodos, 1996). In contrast, in an everted telencephalon, dorso-medial structures in the neural tube become relocated to lateral positions. The right and left sides of the dorsal telencephalon therefore form laterally turned out “flaps”, with the proliferative VZ on the dorsal surface.

Eversion is thought to occur during embryogenesis, but almost no description of this process exists beyond some proliferation data discussed below (Wullimann and Knipp, 2000). Models such as the one in Figure 1.1 A, and Butler (2000) are instead derived from adult telencephalic morphology, interpolating between the starting point of the neural tube and the end point of the adult telencephalon. The events that occur in between are currently purely speculative.

Addressing the issue of eversion is therefore critical for any comparative approach to studying telencephalic development. Recent evidence suggests that functional areas of the zebrafish telencephalon are quite conserved between everted and non-everted species (Wullimann and Rink, 2002), suggesting the dramatic topological eversion illustrated in Fig 1.1 A may not present an accurate picture of eversion. However, until there is a more detailed study of the eversion process this issue will remain unresolved.

### *Proliferation and differentiation in the zebrafish telencephalon*

Patterns of proliferation through and beyond embryogenesis have been partially described in work by Mario Wullimann. He used PCNA, a relatively crude marker of proliferating cells because of its persistence in postmitotic cells, to look at proliferation between 1 and 5dpf (Wullimann and Knipp, 2000; Wullimann and Puelles, 1999). Unfortunately, with only limited data presented for each timepoint, it is difficult to establish a complete picture of proliferation in this complex and dynamic 3-dimensional brain area. But broadly speaking, proliferation is restricted to the ventricular zone (VZ) and he defines further pallial and subpallial areas where proliferation is particularly focussed (Wullimann and Knipp, 2000). In addition,

Wullimann reports that an everted dorsal telencephalon is apparent by 48hpf, as evidenced by PCNA +ve profiles on what he labels as the dorsal surface of the telencephalon (Wullimann and Knipp, 2000). Certainly by 5dpf, PCNA +ve profiles are evident over the entire medio-lateral surface of the dorsal telencephalon, indicating an everted telencephalon (Wullimann and Puelles, 1999).

Neurogenesis in the zebrafish telencephalon has also been somewhat described although mostly at early embryonic stages. The first neurons to form in the telencephalon are in the ventral telencephalon and are called the dorsorostral cluster (drc; to distinguish them from the ventrorostral cluster in the anterior diencephalon; Easter et al., 1992; Ross et al., 1992). The neurons of the drc are marked at 16hpf by immunoreactivity for acetylcholine esterase (Ross et al., 1992) and HNK-1 (Macdonald et al., 1994), and by 17hpf they extend axons that cross the boundary between the telencephalon and diencephalon, pioneering the supraoptic tract (Chitnis and Kuwada, 1990).

#### *The early axon scaffold*

In conjunction with studying neurogenesis, members of the Easter and Kuwada labs characterised the early axon tracts and commissures of the zebrafish brain to further investigate its development and connectivity (Chitnis and Kuwada, 1990; Wilson et al., 1990). Overall the 24hpf brain contains a very simple scaffold of tracts and commissures, with the telencephalon containing only two tracts and one commissure. The commissure is the anterior commissure (AC) that lies just anterior to the optic recess and the tract of the anterior commissure (TAC) is the fasciculated bundle of telencephalic axons that feeds into it. The other telencephalic tract is the supraoptic tract that crosses from the telencephalon to the diencephalon, initially carrying only telencephalic efferents including the first axons of the drc neurons (Chitnis and Kuwada, 1990; Wilson et al., 1990).

At 24hpf, axons are also seen invading the dorsal telencephalon from the olfactory placode (Chitnis and Kuwada, 1990; Wilson et al., 1990). These are the axons of pioneer neurons in the placode, pathfinding for the axons of olfactory sensory neurons that enter the telencephalon at around 48hpf (Whitlock and Westerfield, 1998). The area of the telencephalon innervated by the olfactory neurons is or will become the olfactory bulb (OB), the primary receptive field for olfactory information. By 48hpf, axons labelled from the olfactory epithelium

terminate in distinctive glomeruli within the telencephalon (Wilson et al., 1990), suggesting the beginnings of a differentiated OB. Indeed, more recent studies show that by 3.5dpf, a nascent form of the stereotyped glomerular map found in the adult OB is apparent (Dynes and Ngai, 1998). Although the OB forms within the telencephalon, by adult stages the bulbs are located at the rostral tip of the brain, segregated from the rest of the telencephalon (Wullimann and Rupp, 1996). The development of this brain area will be addressed in detail in Chapter 5.

#### *Axon tracts coincide with domains of regulatory gene expression*

The forebrain can be divided into longitudinal and transverse domains according to the expression patterns of a variety of genes, but this is much more apparent in the diencephalon than in the telencephalon (Hauptmann and Gerster, 2000; Hauptmann et al., 2002). Furthermore, axon tracts and commissures and the neuronal populations that pioneer them are often aligned with domains of regulatory gene expression (Hjorth and Key, 2001; Macdonald et al., 1994; Wilson et al., 1997). Especially well studied is the commissure region of the anterior telencephalon and diencephalon. The optic recess is flanked by the AC on the telencephalic side and the postoptic commissure (POC) on the diencephalic side, and local activity of regulatory gene expression in domains flanking the commissures is required for their formation. The regulatory genes include members of the *Eph/ephrin* family, *netrin1* and *netrin2*, *pax2.1* and *shh* (reviewed in Wilson et al., 1997) and *robo2* (Hutson and Chien, 2002).

The requirement of these regulatory genes for commissure formation is supported by the identification of a number of loss-of-function mutants with forebrain commissure defects. The *noi* (*pax2.1*) mutant shows aberrant crossing of commissural axons between the AC and POC as well as retinal axon pathfinding defects (Macdonald et al., 1997). The *ace* (*fgf8*) mutant also shows severe commissure defects, with AC and POC axons wandering between the two commissures in the optic stalk territory (Shanmugalingam et al., 2000). Optic axons are also severely affected in *ace* where they cross the midline at the optic chiasm. These phenotypes may be attributable to the loss or mis-specification of midline cells, as evidenced by the disruption of many midline gene expression domains in *ace* (*fgf8*) (Shanmugalingam et al., 2000). Finally the *astray*(*robo2*) mutant shows pathfinding and error correction defects particularly in retinal axons navigating the

optic chiasm (Hutson and Chien, 2002). The Robo ligands Slit2 and Slit3 are expressed in tissue flanking the chiasm, and the inability of *astray* axons to sense this signal seems to be the origin of their pathfinding defects.

*Aim of this chapter*

The aim of this chapter is to broadly characterise the development of the telencephalon in terms of its morphogenesis, regionalisation, proliferation, differentiation and connectivity over the entire period of embryogenesis. Covering the period from early embryonic (1dpf) to early postembryonic (5dpf) stages allows me to follow the dynamics of telencephalic development and leads me to propose a new model for the eversion process.

## 3.2: Materials and Methods

### *Fish lines*

In addition to various wildtype strains, the *Tg(HuC:GFP)* (Park et al., 2000) and *Tg(dlx4/6:GFP)* (Zerucha et al., 2000) transgenic lines were used in the experiments in this chapter.

### *Bodipy labelling*

Bodipy 505/515 is a simple fluorophore that permeates cell membranes and binds to yolk platelets in the cell cytoplasm of zebrafish embryos (Cooper et al., 1999). The fluorophore stains the cytoplasm selectively when imaged on the confocal microscope giving contrast between the stained cytoplasm and unstained nuclei and interstitial space.

All Bodipy dyes were made up in 100% DMSO at a concentration of 100  $\mu$ M and stored at  $-20^{\circ}\text{C}$ . Embryos were labelled in their chorions from the tailbud (10hpf) stage at a final concentration of 5  $\mu$ M of the Bodipy dyes in embryo medium.

Embryos were washed 2-3 times in embryo medium before being imaged. Bodipy dyes are not fixable and hence can only be used on live tissue.

### *DiI labelling of the olfactory projection*

Projections from the olfactory epithelium were labelled in live zebrafish at 5dpf following the method of Dynes and Ngai (1998). Briefly, a solution of 2mg/ml DiI (Molecular Probes) in 95% ethanol, 5% dimethyl formamide (Sigma) was diluted 1:1000 in embryo medium (Zebrafish Book). Embryos were incubated in this solution for 20 minutes at  $28.5^{\circ}\text{C}$  followed by several rinses in embryo medium.

Embryos were left for 1 hour for the DiI to label the projections, before being fixed and dissected for epifluorescence imaging on a Zeiss Axioplan2 microscope with a x40 water immersion objective.

### *Kaede RNA injection*

Kaede is a green fluorescent protein derived from a stony coral species (Ando et al., 2002). Kaede RNA was synthesised as described in section 2.5 from a pCS2-Kaede construct kindly provided by Dr Atsushi Miyawaki and amplified using conventional maxiprep methods (section 2.4). A NotI site was used to linearise the construct for *in vitro* transcription with SP7 polymerase (section 2.5). Synthesised RNA was purified by phenol chloroform extraction and precipitation (section 2.5), and the pellet resuspended in Danieau buffer (The Zebrafish Book) to give a working concentration of 50ng/μl for microinjection.

Embros were injected at the 2-8-cell stage to give chimeric labelling as described in section 2.3.

### *Immunolabelling*

Immunolabelling was performed as described in section 2.10. The following antibodies were used – anti-acetylated  $\alpha$ -tubulin (Sigma) followed by anti-mouse IgG Alexa 488 (Molecular Probes), and anti-GFP (Upstate Biotech) followed by anti-rabbit IgG Alexa 488 (Molecular Probes). BrdU labelling was performed as described in section 2.11 and detected as described in section 2.12. The primary anti-BrdU antibody (Sigma) was followed by an anti-mouse IgG Alexa 568 secondary antibody (Molecular Probes). The HuC:GFP signal was imaged without any antibody labelling.

### *Imaging*

Fixed and stained embryos were dissected using fine watchmaker's forceps and microsurgical blades (John Weiss), and the skin was removed where possible. Dissected specimens were mounted on slides, coverslipped and the slides sealed with nail varnish before imaging. Image acquisition and image processing were carried out as described in sections 2.13 and 2.14.

### 3.3: Results

#### *External morphology of the telencephalon*

My investigations into the telencephalon began with simple observations of brain structure at a variety of stages from 24hpf to 5dpf (Fig 3.1), extending previous work by Wilson et al., (1990). One of the most obvious features of the telencephalon is its boundary with the diencephalon, marked initially by the optic recess (OR). The ventricle leading into the OR highlights the entire ventral and medial surface of the telencephalon. This ventricle, which begins to form at 16hpf, is expanded and more clearly seen at 24 and 36hpf (Fig 3.1 A and B). At 48hpf, the ventricle continues to delimit the telencephalon, particularly at the dorso-posterior border with the diencephalon (Fig 3.1 C). Beyond 48hpf the ventricle becomes less evident, and at 3 and 5dpf, a morphological boundary within the brain tissue itself seems to indicate the border between telencephalon and diencephalon (Fig 3.1 D and E).

Another feature that is immediately obvious, and is central to understanding anatomical descriptions, is the previously described ventral flexure of the brain (Wilson et al., 1990; Hauptmann and Gerster, 2000; Fig 3.1). This flexure takes place between late somitogenesis stages (19hpf) and 36hpf, and distorts the alar-basal boundary of the neural tube so that it is no longer horizontal (Hauptmann and Gerster, 2000). The telencephalon, first recognisable morphologically as a dorsally-located structure in the neural tube becomes a rostrally-located structure. Consequently, the telencephalon becomes reoriented almost 90° with respect to the longitudinal axis of the rest of the brain. Surfaces of the telencephalon that were dorsal, become anterior (rostral) relative to the rest of the brain. However, the point of flexure lies outside the telencephalon, between the expanding hypothalamus on the ventral side and the expanding midbrain (especially the optic tectum) on the dorsal side. It is therefore logical to maintain the dorso-ventral and antero-posterior axes consistent with their positions at somitogenesis stages (Hauptmann and Gerster, 2000, 2002). The axes are indicated in Fig 3.1 for stages up to 48hpf; beyond this point orientation within the telencephalon is not discernable without further labelling.

**Figure 3.1: Brain morphology 24hpf to 5dpf**

A-E are DIC images of fixed, fully dissected specimens at the stages indicated; A'-E' are outlines of the same specimens. All scale bars represent 100µm. In A' and B' red arrowheads indicate the point of ventral flexure and in A'-C' blue arrowheads indicate the position of the telencephalic roof.

Anterior-posterior and dorso-ventral axes are indicated as compass points, but refer only to the orientation of the telencephalon.

F is an outline drawing of an adult zebrafish brain taken from Wulliman (1996).

AC – anterior commissure

E – epiphysis

hy – hypothalamus

OB – olfactory bulb

t/tel – telencephalon

v - ventricle

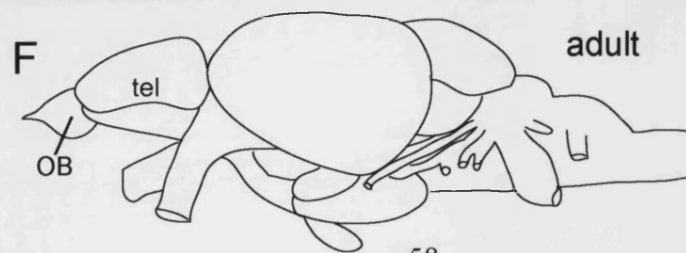
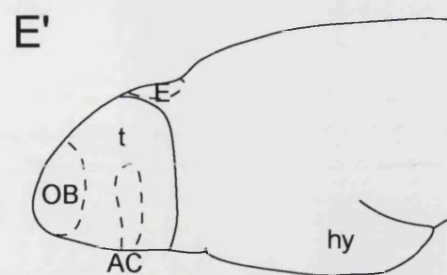
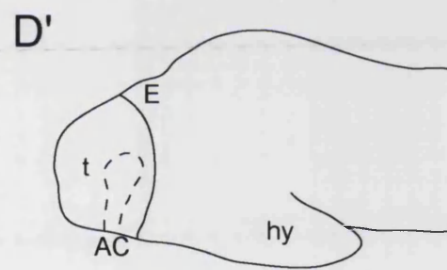
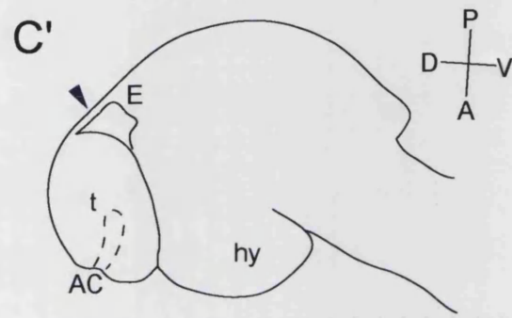
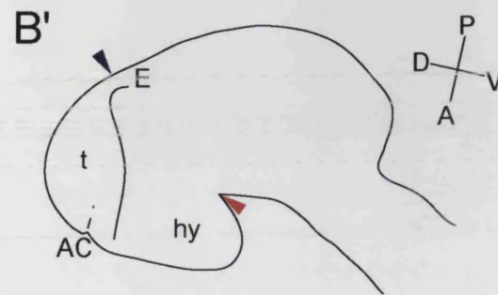
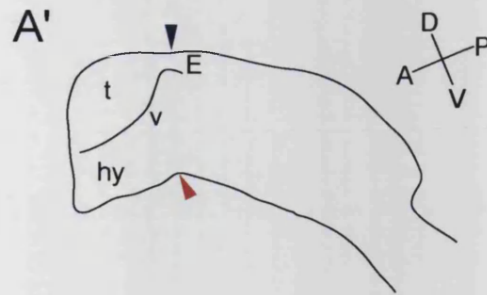


Figure 3.1

A final observation that can be made from unstained fixed tissue is the position of the olfactory bulb (OB) at 5dpf (Fig 3.1 E). This structure lies within the telencephalon at 5dpf and is telencephalically derived. However, by adult stages, the paired olfactory bulbs lie outside the telencephalon, forming the most rostral part of the CNS (Fig 3.1 F). The embryonic development of the OB will be addressed in detail in Chapter 5.

#### *Early organisation of the neuroepithelium*

I used confocal microscopy to analyse the structure of the telencephalic neuroepithelium. Cells in living embryos were visualised either with the fluorescent protein Kaede (see Chapter 5; Ando et al., 2002) or with the vital dye Bodipy 505/515 that labels the cytoplasm of all cells (e.g. Cooper et al., 1999). These techniques enabled examination of both individual cell morphology and at morphology of the tissue as a whole.

At 16hpf the CNS has the form of a solid neural rod, in contrast to other vertebrates where primary neurulation directly generates a neural tube enclosing ventricular space. The neural rod is devoid of ventricular space and is comprised of cells with an elongated neuroepithelial morphology (Lyons, 2003; Fig 3.2 A and B). As in all vertebrates (and as at other levels of the zebrafish neuraxis), cell division is restricted to the ventricular surface that in the neural rod equates with the midline seam. Neuroepithelial cells therefore undergo interkinetic nuclear migration between the midline and pial surfaces (data not shown). At about 16hpf, the first signs of a border between the telencephalon and diencephalon are visible as the OR and ventricular space begin to form. This is more evident ventrally (Fig 3.2 B) than dorsally (Fig 3.2 A).

Between 16hpf and 24hpf the ventricle opens up substantially, with the border of the telencephalon and diencephalon positioned at the point where the ventricle is most expansive. Also at 24hpf, the right and left sides of the telencephalon become separated as the ventricle enlarges, remaining closely apposed only in dorsal areas (Fig 3.2 C and D). However, the telencephalic and diencephalic neuroepithelium are still continuous. At this stage neurons become visible at the pial surface of the telencephalon, forming a distinct mantle layer. The axons of these neurons, although not visible in these figures, will extend over the lateral surface of the brain in the neuropil of the marginal zone. The mantle zone is more extensive at

### Figure 3.2: Structure of the forebrain neuroepithelium

All figures show single confocal sections; A-D and F show horizontal sections, anterior to the bottom, E a sagittal section. All figures except E show embryos mosaically expressing *Kaede* RNA; E shows an embryo labelled with BODIPY 505/515. All scale bars are 50µm.

A and B show two horizontal sections through the same 15ss (16hpf) embryo; A is more dorsal than B. In A, elongated neuroepithelial (NE) cells span the width of the neural tube. In contrast, cells at the most anterior tip of the neural tube have a pyramidal morphology (arrowheads in A and B). In B, the ventricular space is starting to form (arrow).

C and D are sections through different 24hpf embryos. C shows neurons, identifiable by their morphology in the mantle layer (white arrowheads) and a cell dividing perpendicular to the ventricular surface (red line). A white arrow indicates the border between the telencephalon and diencephalon in C and D. In D, pyramidal cells in the anterior neuroepithelium are visible (arrowhead).

E shows a parasagittal section close to the midline of a 19hpf embryo. A distinct layer of regularly arranged cells is visible at the dorsal surface of the telencephalon, extending into the “roof” (arrowhead).

F shows a further horizontal section at 30hpf. Red arrowheads and the dotted line indicate a distinct mantle layer; the transition between telencephalon and diencephalon is indicated by a white arrow.

di - diencephalon

ey – eye

hy – hypothalamus

OP – olfactory placode

tel - telencephalon

v – ventricle

VZ – ventricular zone

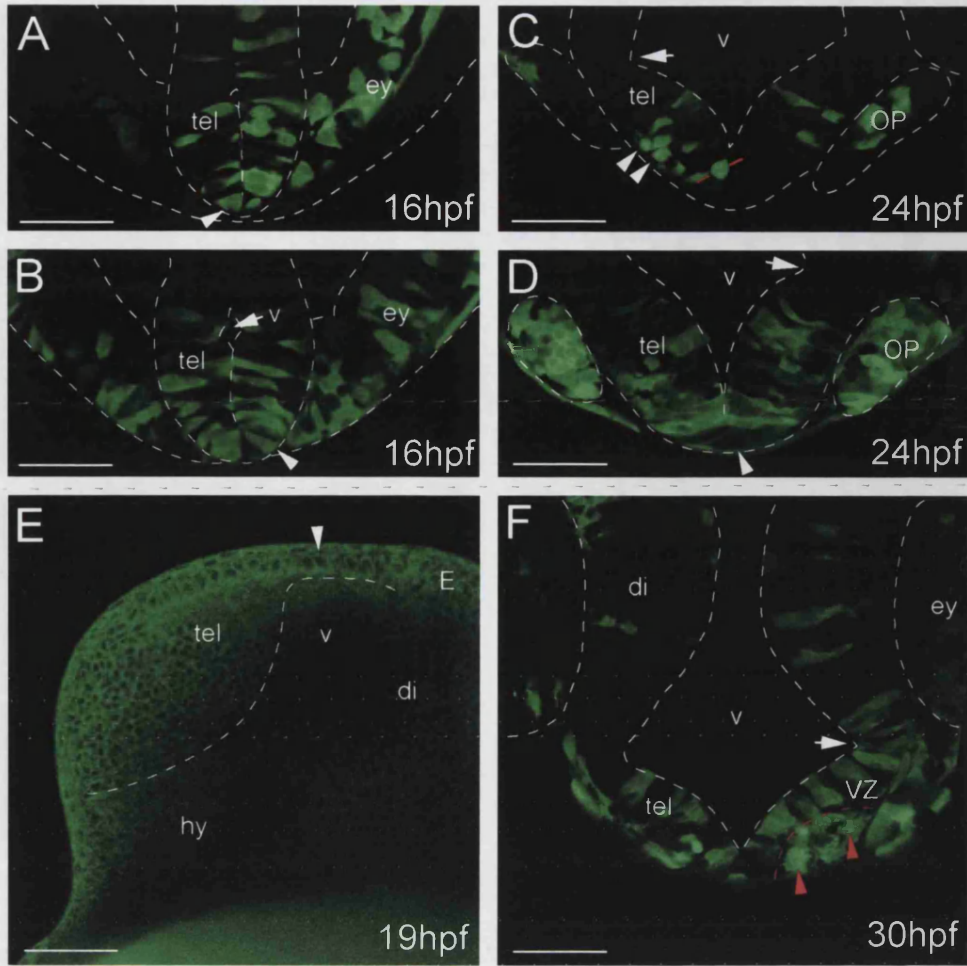


Figure 3.2

30hpf (Fig 3.2 F) and is clearly distinct from the proliferative ventricular zone, where the nuclei of neuroepithelial cells are located.

Examining embryos from the lateral aspect at 19hpf highlights the tissue that connects the dorsal posterior telencephalon to the dorsal diencephalon; tissue I call the roof. In 19hpf specimens labelled with Bodipy 505/515, this tissue is seen as a continuation of the dorsal telencephalic neuroepithelium, comprising a single layer of regularly arranged cuboidal cells of uniform size (arrowhead in Fig 3.2E).

#### *Neurogenesis is precocious in the telencephalon*

The telencephalon contains some of the earliest differentiating neurons in the CNS, and is accelerated in its neurogenesis compared to the adjacent diencephalon. I used the *Tg(HuC:GFP)* line, a pan-neuronal line expressing GFP in all postmitotic neurons (Park et al., 2000), to observe this rapid neurogenesis. The first neurons appear in the presumptive telencephalon at about 13hpf (Fig 3.3 A and B). These are neurons of the dorsorostral cluster (drc; Easter et al., 1992; Ross et al., 1992). The drc is surprisingly extensive, even at 13hpf (Fig 3.3 A), with the brightest neurons lying very laterally in the telencephalon (Fig 3.3 B). At 19hpf, the drc is more substantial with additional GFP +ve cells in the posterior telencephalon (Fig 3.3 C and D). A similar pattern of GFP labelling was seen using anti-GFP antibody labelling in the *Tg(HuC:GFP)* line (Fig 3.3 E-F), and included the labelled axons of drc neurons pioneering the SOT (Chitnis and Kuwada, 1990; Fig 3.3 F).

By 26hpf, a substantial population of GFP-expressing neurons exists in the telencephalon (Fig 3.3 G and H). This is in marked contrast to the anterior diencephalon where only a small group of neurons lie ventral to the OR. At this stage, and a little later at 30hpf (Fig 3.3 I and J), the telencephalic neuronal population extends into the roof. This observation, as well as confirming the roof as a continuation of the neuroepithelium, also has interesting implications for the origins of some dorsal telencephalic neurons that will be explored further in Chapter 5.

#### *Neurogenesis and cell division*

In order to mark proliferating and differentiated cells simultaneously and thus describe the organisation of ventricular zones and mantle layers, I pulsed *Tg(HuC:GFP)* embryos

### Figure 3.3: Early neurogenesis in the telencephalon

A-D and G-J show images of live *Tg(HuC:GFP)* embryos at the stages indicated. A-D are single confocal sections, G and I are projections of multiple parasagittal sections to the midline; H and J are projections of sections taken as indicated in G and I. E and F are single sections through *Tg(HuC:GFP)* embryos labelled with anti-GFP antibody. All scale bars are 50µm

A and B show the first telencephalic neurons of the dorsorostral cluster (drc; white arrowheads) at 14hpf (10ss) in a lateral (A) and a horizontal (B) section.

C and D show an expanded drc at 19hpf (arrowheads and arrow in C) in a sagittal (C) and a horizontal (D) section.

E and F show single sagittal sections in embryos labelled with a fluorescently-conjugated anti-GFP antibody. White arrowheads indicate neurons of the drc, which by 19hpf are extending axons into the supraoptic tract (SOT; arrowheads in F). Immunostaining is also visible in posterior areas of the 16hpf telencephalon (white arrow in E).

G and H show the neuronal population of the telencephalon at 24hpf; neurons are present in the roof (white arrow in G).

I and J show the neuronal population at 30hpf in the telencephalon and anterior diencephalon. Neurons are visible in the telencephalic roof (arrow in I) and GFP +ve axons are visible in the anterior commissure (arrowhead in J).

E – epiphysis

di – diencephalon

OP – olfactory placode

tel – telencephalon

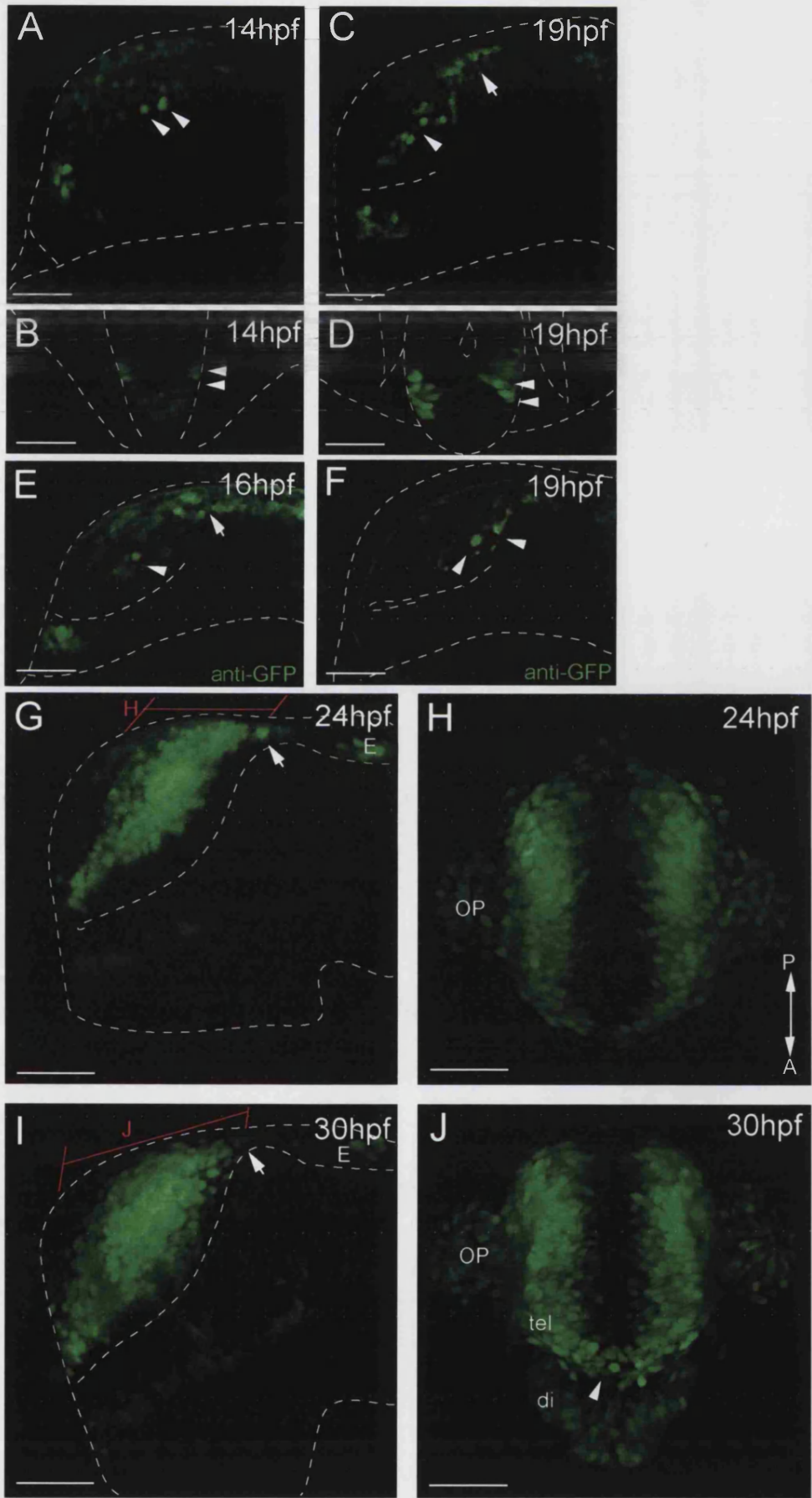


Figure 3.3

with BrdU. I used short pulses of BrdU (15-30 minutes) with minimal survival times to label cells undergoing DNA replication in S-phase. This population should be mutually exclusive of GFP- expressing neurons. S-phase occurs away from the ventricular surface, where cells return to divide (e.g. Lyons, 2003), so BrdU labelling should highlight the maximum width of the VZ at any given stage.

I performed BrdU pulse experiments at stages from 24hpf to 5dpf, fixing the specimens immediately after the pulse. Two main themes emerge from this data. The first is that as cavitation separates the right and left sides of the telencephalon, the VZ forms as a convex medial surface. The second important observation is that the eversion process happens between 2 and 3dpf and results in an everted VZ on the dorsal surface of the telencephalon.

At 24hpf and 36hpf, the VZ is a continuously curved surface (Fig 3.4). Dorsally and anteriorly, the right and left sides are closely apposed, but more ventrally and posteriorly they are separated by ventricular space (Fig 3.4 C, F, G). A broad area of proliferation is evident anteriorly (arrowheads in Fig 3.4 B and E). The telencephalic VZ is also continuous with the diencephalic VZ, as indicated by the dotted white lines in all panels. A further interesting observation is that BrdU +ve profiles are present at most levels in the VZ, including at the ventricular surface in some cases (arrow in Fig 3.4 C). This observation suggests that, unlike in the hindbrain (Lyons, 2003), S-phase is not restricted to the basal VZ. At 24hpf and 36hpf, there is no evidence of a dorsally everted VZ. BrdU profiles seen on the dorsal surface of the telencephalon are in fact skin cells, evident from their flattened morphology and from comparison with DIC images (Fig 3.4 A and D).

48hpf is the stage at which other researchers have reported a dorsally-everted VZ using either a marker of mitosis (Shanmugalingam, 1999), or the broad proliferating cell marker PCNA (Wullimann and Knipp, 2000; their Figure 2A). The critical difference between their data and my data is that the surface they define as dorsal VZ, I define as posterior VZ, taking into account the ventral flexure as illustrated in Fig 3.1 C. What I see at 48hpf (Fig 3.5 B and C) and at slightly earlier stages (Fig 3.5 A), using the presence of BrdU profiles as the defining criterion for the VZ, is a very similar situation to that seen at 24 and 36hpf. Namely, the VZ is still a continuously curved surface covered in proliferating cells. Critically, dividing cells are evident up to the posterior border of the telencephalon with the diencephalon, but the VZ does not extend over the dorsal surface of the

**Figure 3.4: BrdU labelling in the *Tg(HuC:GFP)* line – 24hpf and 36hpf**

All figures show single confocal sections at the levels shown in the right-hand panel of line drawings. All scale bars are 50µm; line drawings are not to scale. In all panels white dotted lines indicate continuity of the telencephalic and diencephalic VZ.

A and B show parasagittal sections through the 24hpf telencephalon. BrdU +ve cells line the ventricle at all levels (white dotted lines); BrdU +ve cells on the dorsal surface of the telencephalon in A are skin cells. In the midline, the VZ is broader anteriorly and ventrally (arrowhead in B). In C, a horizontal section shows the continuously curved surface of the VZ; BrdU +ve profiles appear very close to the ventricular surface (arrow).

D and E show parasagittal sections through the 36hpf telencephalon. In D, the VZ lines the ventricle (white dotted lines), including the preoptic area (arrow) and the telencephalic roof (blue arrowhead). More medially, in E, the anterior proliferation zone is prominent (arrowhead), as it is in F (arrowhead). F and G are two sections at the levels shown in the right-hand panel. The continuity of the telencephalic and diencephalic VZ is indicated by white dotted lines

di - diencephalon

E – epiphysis

hy – hypothalamus

OP – olfactory placode

POa – preoptic area

skin – skin cells on surface of the brain

t/tel – telencephalon

v – ventricle

HuC/BrdU

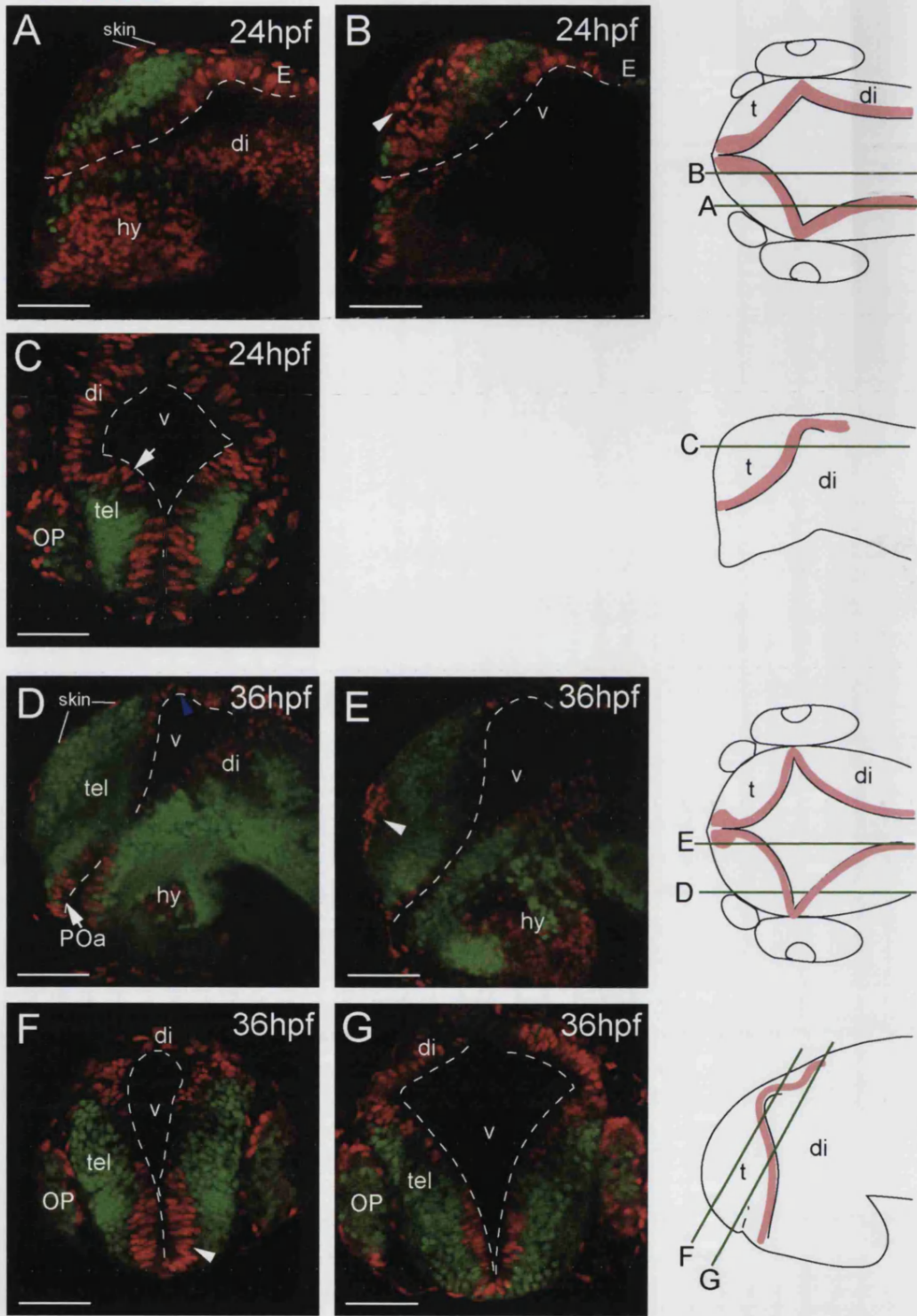


Figure 3.4

**Figure 3.5: BrdU labelling in the *Tg(HuC:GFP)* line – 44hpf to 5dpf**

All figures show either parasagittal confocal sections with anterior to the left (A, B, D and G) or as shown in the drawings at the bottom of the page (C, E-F, H). All scale bars are 50  $\mu\text{m}$ ; drawings are not to scale.

A shows a projection of sagittal sections at 44hpf. BrdU profiles line the ventricle, from the preoptic area (POa) to the posterior border with the diencephalon (blue arrowhead).

B shows a single section from a specimen at 48hpf, showing the same pattern of proliferation in the preoptic area (POa) and posterior telencephalon (blue arrowhead). No BrdU profiles are evident on the dorsal surface of the telencephalon. C shows a section through the telencephalon and dorsal diencephalon; the anterior proliferation zone is broad and continuous with the remaining VZ (arrows).

D shows BrdU profiles on the dorsal telencephalic surface, with a rostral limit indicated by the blue arrowhead. BrdU profiles are also evident in the posterior VZ (arrowhead) and the preoptic area (POa).

Dorsally everted BrdU profiles are seen in a transverse section in E (blue arrowheads), and the anterior proliferation zone is evident (white arrowhead). More posteriorly in the telencephalon, F shows BrdU profiles intercalated with neurons in the midline VZ (arrow).

G shows that at 5dpf, BrdU profiles are present in the dorsal surface of the telencephalon with their rostral limit at the olfactory bulb (blue arrowhead). BrdU profiles are absent from the posterior ventricular surface in this section (dotted white line), but are present in the preoptic area (POa)

In a horizontal section (H), the dorsal surface of the telencephalon is dotted with BrdU +ve profiles (white arrowheads) in marked contrast to the adjacent habenulae (Ha). A projection of all BrdU profiles in a different specimen (I) shows the mediolateral extent of the everted VZ and the absence of everted profiles in the OB. The anterior proliferation zone is evident (arrow), as are elongated blood vessels that are also BrdU positive (arrowhead). Dark shadows are caused by pigment cells on the brain surface.

AC – anterior commissure

E – epiphysis

Ha – habenula (dorsal diencephalon)

hy – hypothalamus

OB – olfactory bulb

OE – olfactory epithelium

POa – preoptic area

HuC/BrdU

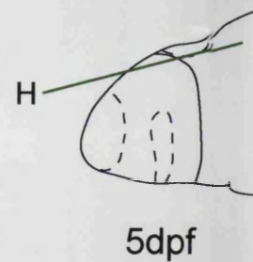
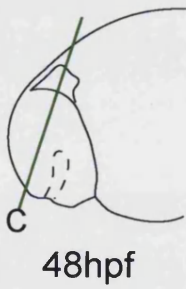
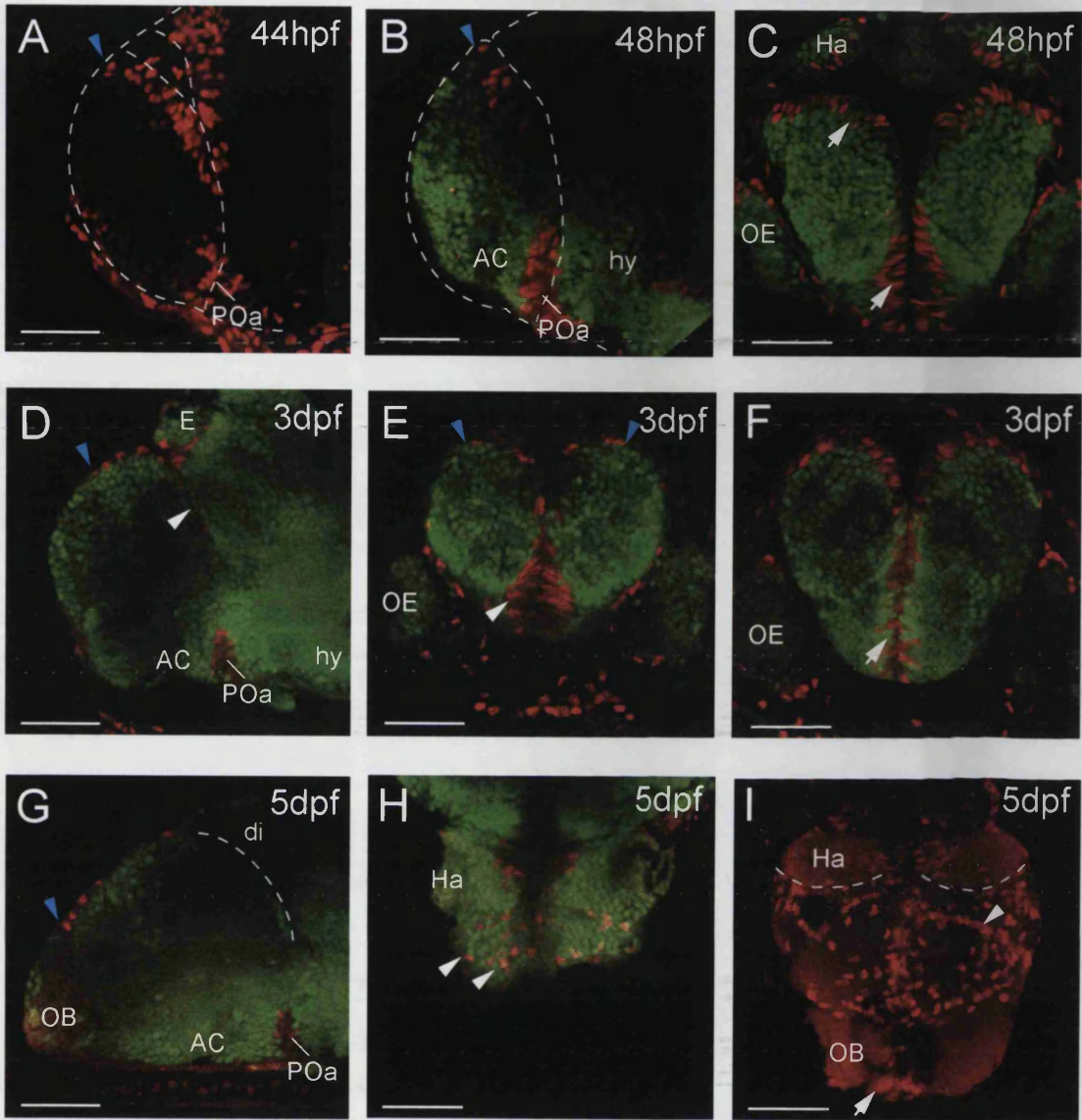


Figure 3.5

telencephalon (blue arrowheads in Fig 3.5 A and B). This is true for all timepoints up to and including 48hpf, and is constant despite the changing morphology of the ventricle and the telencephalic tissue.

At 3dpf, a markedly different situation is apparent with respect to the telencephalic VZ. For the first time, BrdU +ve profiles are evident within the dorsal surface of the telencephalon as defined in Fig 3.1 D (Fig 3.5 D); the removal of the skin prior to imaging ensures that these are not dividing skin cells. The dorsal VZ may extend as far as the olfactory bulb, although without an additional marker this is uncertain. In the mediolateral axis BrdU profiles do not extend to the lateral limits of the telencephalon (blue arrowheads in Fig 3.5 E). BrdU profiles are also still evident on the posterior surface of the telencephalon, although these are relatively sparse in my specimens probably due to the short BrdU pulse times. Despite the altered situation in the dorsal telencephalon, the proliferation zones in the midline (Fig 3.5 F), anterior telencephalon (Fig 3.5 E) and preoptic area (Fig 3.5 D) remain constant.

At 5dpf the eversion of the telencephalon is more extensive. BrdU +ve profiles are located in the dorsal surface of the brain, with a clear rostral limit at the border with the olfactory bulb (Fig 3.5 G and I). Horizontal sections reveal BrdU +ve profiles over the entire rostro-caudal and medio-lateral surface of the dorsal telencephalon, in contrast to the adjacent habenulae where no dorsally-located BrdU +ve profiles are seen (Fig 3.5 H and I). Dividing cells are also present in the midline VZ, especially in the anterior proliferation zone, and there are a few BrdU profiles at the posterior ventricular surface (data not shown). The preoptic area continues to show strong proliferation ventral to the level of the supraoptic tract (Fig 3.5 G).

#### *Summary of proliferation and differentiation studies*

In summary, neurogenesis in the telencephalon is precocious with respect to adjacent brain areas, such that at 24hpf the telencephalon already contains a substantial neuronal population (Fig 3.3). Proliferation is continuous over all ventricular surfaces of the telencephalon, but there are also zones of enhanced proliferation in the anterior telencephalon and in the preoptic area as identified by others (Shanmugalingam, 1999; Wullimann and Knipp, 2000). A key finding is that a dorsal, everted proliferative area becomes evident between 2dpf and 3dpf, and by 5dpf covers the dorsal surface of the telencephalon (Fig 3.5). This everted VZ

covers the entire rostro-caudal and medio-lateral extents of the dorsal surface of the telencephalon, except the rostrally-located olfactory bulb.

*The axon scaffold provides landmarks in the telencephalon*

In order to gain a more thorough understanding of telencephalic morphogenesis, I used an antibody to acetylated  $\alpha$ -tubulin to label all axon tracts and commissures at a variety of stages. Axon tracts and commissures have the advantage that their positions are usually stable relative to one another. Therefore, any movement of these tracts may indicate a morphogenetic movement of the surrounding tissue. Secondly, careful analysis of acetylated  $\alpha$ -tubulin-labelled specimens provides interesting information about the connectivity of different telencephalic areas, much of which has been relatively poorly described, especially at stages beyond 48hpf.

Morphogenetic movements are most evident by comparing lateral views of embryos from 24hpf to 5dpf. Firstly, between 24 and 36hpf, the ventral flexure clearly alters the orientation of the telencephalic tract of the anterior commissure (TAC) and the anterior commissure (AC) with respect to the longitudinal axis of the brain (Fig 3.6 A and B). However, as previously observed, the ventral flexure does not seem to cause any internal reorganisation within the telencephalon, as the AC, SOT and POC retain their orientation with respect to one another. This is in contrast to the tract of the postoptic commissure (TPOC), which goes from being relatively straight at 24hpf to making a right-angled bend in the ventral diencephalon at 36hpf (Ross et al., 1992); Fig 3.6 B). This confirms previous results and indicates that acetylated tubulin labelling is a possible readout of morphogenetic tissue movement.

Major changes within the telencephalon itself happen between 48hpf and 3dpf. At 48hpf, the TAC and AC are much more robust than at 36hpf and in addition, the first clear evidence of OB neuropil is visible (Fig 3.6 C). The OB has a glomerular structure, formed by the multiple contacts between axon terminals of incoming olfactory sensory neurons (OSN) and the dendrites of bulb neurons. This gives the OB an appearance distinct from the rest of the telencephalic neuropil and locates it in the most posterior dorsal area of the telencephalon, almost adjacent to the border with the diencephalon.

At 3dpf, the OB neuropil is not only much more substantial, but is now located at the rostral tip of the telencephalon, at some distance from the diencephalic

Figure 3.6: Telencephalic organisation from 24hpf to 5dpf labelled by anti-acetylated  $\alpha$ -tubulin.

A-E show projections of confocal sagittal sections to the midline in each specimen. Tracts and commissures are marked and the brain morphology outlined at each stage. Scale bars are 50 $\mu$ m in all figures.

A shows the simple axon scaffold of the 24hpf forebrain. Fibres are just reaching the midline in the AC (arrow); the SOT has formed.

B shows the forebrain at 36hpf; all axon tracts and commissures are much thicker than at 24hpf

C shows the 48hpf forebrain. The olfactory bulb (OB) neuropil is visible, with its posterior limit (indicated by red arrowhead) close to the border with the diencephalon. The stria medullaris projection is evident, leading to the habenular commissure (white arrow).

D shows a 3dpf embryo; the OB is rostrally-located, with its posterior border at some distance from the diencephalon (red arrowhead). The incoming olfactory nerve (ON) is substantial but has been severed in this preparation. The stria medullaris has two components in this specimen (white arrowheads), but other embryos show a single tract.

E shows the rostral position of the OB at 5dpf (red arrowhead indicates limit); again the ON has been severed. A branch of the ON looks to be bypassing the OB (white arrow). The stria medullaris consists of a single fasciculated tract (arrowhead).

AC – anterior commissure  
DVDT – dorsoventral diencephalic tract  
Ha – habenula  
OB – olfactory bulb  
OC – optic chiasm  
ON – olfactory nerve  
PC – posterior commissure  
POC – postoptic commissure  
SOT – supraoptic tract  
TAC – tract of the anterior commissure  
TPC – tract of the posterior commissure  
TPOC – tract of the postoptic commissure

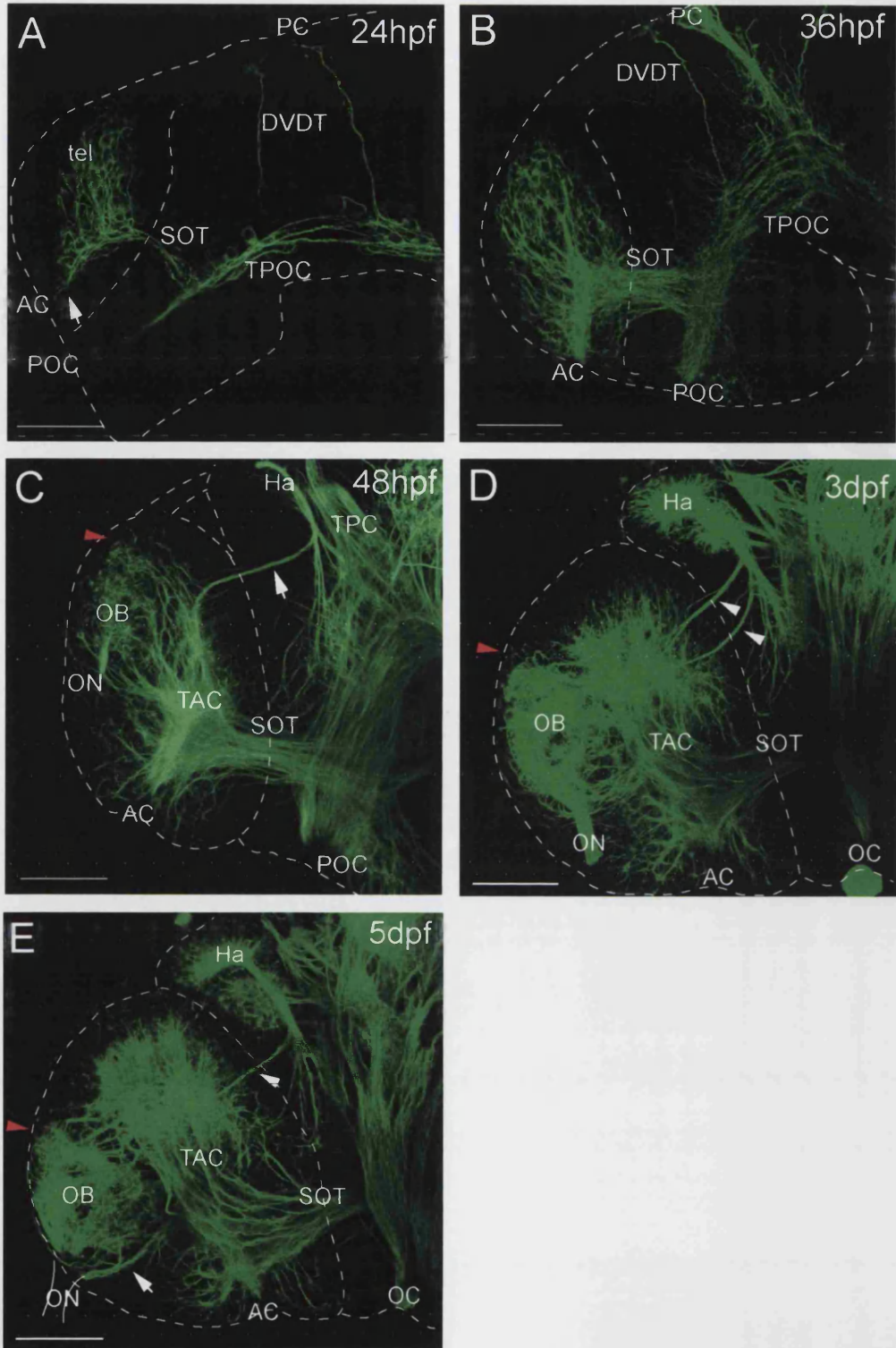


Figure 3.6

border (Fig 3.6 D). This striking change in dorsal telencephalic organisation is paralleled somewhat by a change in ventral telencephalic areas. Thus, the AC becomes “tucked in” on the underside of the telencephalon, close to the diencephalic border. The SOT retains its position but the angle between the AC and SOT is decreased.

At 5dpf, this situation is more marked. The OB is now located right at the rostral tip of the telencephalon, more than 100µm from the posterior border with the diencephalon (Fig 3.6 E) where the OB was situated at 48hpf. The OB neuropil is slightly more extensive and segregated from the rest of the telencephalon than at 3dpf, and lies more basally within the telencephalon. The AC and SOT retain very similar positions to those at 3dpf.

In conclusion, tracking the position of the OB from 48hpf to 5dpf seems to indicate a morphogenetic movement within the telencephalon that brings the OB from a dorsal-posterior position close to the border with the diencephalon to a rostral location. This “rotation” is paralleled somewhat by changes in the organisation of the ventrally-located AC and SOT.

Secondarily, acetylated tubulin labelling revealed a number of tracts and commissures that have been as yet poorly described in the zebrafish brain. These features, although their functions are presently unknown, nonetheless provide a more complete picture of telencephalic connectivity:

*1) stria medullaris*

The stria medullaris forms part of a system that connects telencephalic and thalamic efferents to the habenulae, and then on to the interpeduncular nucleus via the fasciculus retroflexus (e.g. Yanez and Anadon, 1994). A component of the stria medullaris is evident at 48hpf leading from the telencephalon to the habenular commissure (Fig 3.6 C; there are no known reciprocal connections from the habenulae to the telencephalon). At 3dpf these tracts are still evident, appearing as two parallel tracts in some specimens but more frequently as a single fasciculated tract (Fig 3.6 D). The tract has a similar appearance at 5dpf (Fig 3.6 E). Although the stria medullaris appears to originate in the mid-telencephalon, at 48hpf there may be a component that originates in the OB (arrowheads in Fig 3.7 A). This observation would need to be substantiated by more detailed tract tracing, especially at later stages when connections from the bulb are much more complex.

## *2) olfactory tracts*

The olfactory tracts are present in the adult as the medial and lateral olfactory tracts (MOT and LOT), and carry secondary olfactory fibres from the bulb to the telencephalon. In the 3dpf embryo, there are multiple connections between the OB and telencephalon, especially dorsally where the secondary olfactory fibres are hardly fasciculated (Fig 3.7 D). By 5dpf these connections are much more fasciculated, forming the two main tracts with other minor connections between the OB and telencephalon (Fig 3.7 E-G). The two main tracts are presumed to correspond to the adult LOT and MOT, with the LOT more dorsal and lateral (Fig 3.7 E) and the MOT more medial and ventral (Fig 3.7 F).

## *3) olfactory epithelium projections into the TAC*

Examination of the olfactory tracts lead to the identification of a projection from the olfactory epithelium (OE) that rather than terminating in the bulb projects directly into the TAC of the telencephalon (Fig 3.7 G). This projection was robust and was also labelled by the application of DiI to the OE (Fig 3.7 H). OE projections labelled in this way were variable, with some projecting contralaterally via the AC and others ipsilaterally. This projection bears strong similarity to projections from OE cells described by Dynes and Ngai (1998) at 3.5dpf. In their study, the neurons extending these axons were unipolar as opposed to the bipolar olfactory sensory neurons.

## *4) intra-olfactory bulb commissure*

A further observation revealed that that the right and left olfactory bulbs are connected by a fine, relatively defasciculated commissure. This commissure is evident at 3dpf (Fig 3.7 C) and 5dpf (Fig 3.7 E) and connects the bulbs in their most dorsal region. It is not known, and would be interesting to establish, whether this commissure persists into adulthood.

Figure 3.7: Details of telencephalic projections 48hpf-5dpf labelled by anti-acetylated  $\alpha$ -tubulin.

A-G show single confocal sections with the orientations indicated in the bottom panel; H shows an epifluorescence image.

A shows a confocal section through the fore- and midbrain at 48hpf. Part of the stria medullaris tract is indicated by arrowheads; a component of this projection may originate in the OB.

B shows the massive extent of the 3dpf anterior commissure (AC) compared to the habenular commissure (HaC).

C shows the intra-OB commissure at 3dpf (arrow) and the glomerular structure of the OB.

D shows multiple unfasciculated projections from the dorsal OB to the telencephalon at 3dpf (arrows).

E and F show sections at different D-V levels through the lateral (E) and medial (F) olfactory tracts at 5dpf. The intra-OB commissure is also visible in E (arrowhead).

G shows projections into the tract of the anterior commissure (TAC) – one from the OB (arrowhead) and one from the olfactory epithelium (OE) that bypasses the bulb (arrow).

H shows that labelling the OE with DiI indeed labels both the ON and projections direct to the AC. In this specimen, growth cone-tipped axons are seen in the AC at 5dpf (red arrows).

AC – anterior commissure

HaC – habenular commissure

LOT – lateral olfactory tract

MOT – medial olfactory tract

OB – olfactory bulb

OE – olfactory epithelium

ON – olfactory nerve

SOT – supraoptic tract

TAC – tract of the anterior commissure

tec – tectum

tel - telencephalon

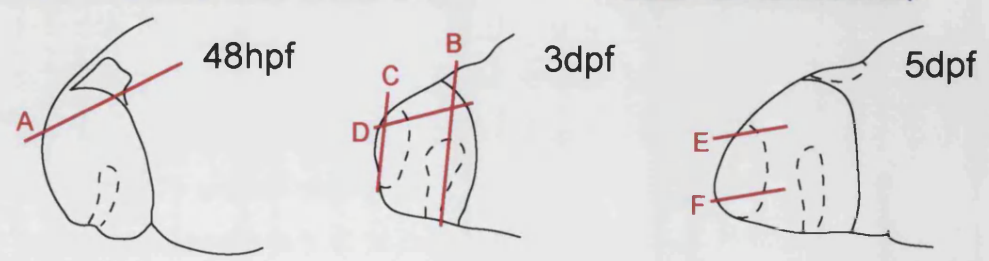
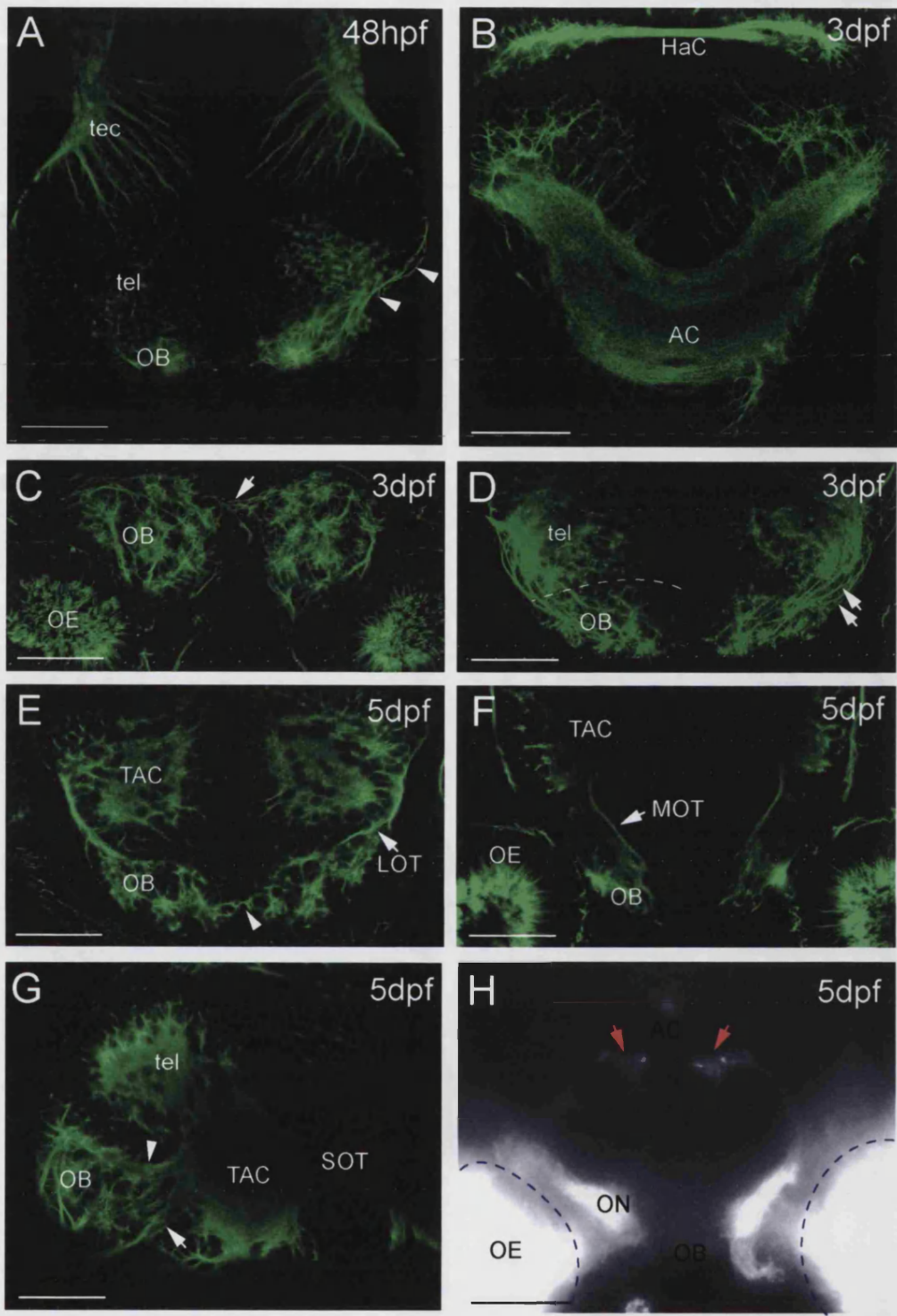


Figure 3.7

### *Neuronal populations marked by the Tg(dlx4/6:GFP) line*

The experiments presented so far have addressed global telencephalic neuronal populations and their projections. However, one of the major issues that remains unresolved is how the pallial and subpallial areas of the zebrafish telencephalon develop. Pallial gene expression patterns have been reported at various stages (Kawahara and Dawid, 2002; Mione et al., 2001), but subpallial gene expression patterns remain little reported (Akimenko et al., 1994; Zerucha et al., 2000). The generation of a transgenic GFP line under the control of the *dlx4/dlx6* intergenic region provides an ideal tool to follow subpallial neurons over time (Zerucha et al., 2000). The *dlx4* and *dlx6* genes are well-characterised markers of the subpallium in many species including mouse (where *dlx4* is *Dlx5*), chick and zebrafish (Akimenko et al., 1994; Fernandez et al., 1998; Puelles et al., 2000), and the *Tg(dlx4/6:GFP)* line accurately replicates the endogenous expression of both these genes (Zerucha et al., 2000).

The most striking feature highlighted by this line is the vast extent of the subpallium, especially at later embryonic stages (Fig 3.8). Expression of the transgene at 26hpf highlights a broad band in the ventral telencephalon that corresponds well to the D-V division postulated in Fig 3.1 A (Fig 3.8 A). *dlx4/6* expression is parallel to but stops several cell diameters from the ventral ventricular surface, indicating that the transgene is not expressed in proliferating cells of the VZ. At 36hpf, expression of *dlx4/6* is slightly more condensed but nonetheless restricted to the ventral telencephalon (Fig 3.8 B). GFP +ve fibres are seen in the SOT but are considerably less frequent in the AC (data not shown).

At 2dpf, *dlx4/6* expression is broader than at 36hpf, and extends into more rostral parts of the telencephalon; the same is true at 3dpf and 5dpf as the *dlx4/6* population continues to expand (Fig 3.8 C-E). Horizontal sections reveal that the bulk of *dlx4/6* expression is very medial in the telencephalon – lateral areas are generally *dlx4/6* negative (Fig 3.8 F). Labelled axons, which appear primarily in the SOT at 2dpf, appear additionally in the AC at 3dpf and 5dpf, indicating a large population of commissural neurons in the ventral telencephalon.

This transgenic line also highlights two other groups of neurons in addition to those located in the ventral telencephalon. Scattered *dlx4/6*-expressing cells are seen in the dorsal telencephalon, the first cells appearing there at 48hpf (arrowheads in Fig 3.8 C-E). These are single, isolated cells and confocal imaging from the dorsal

Figure 3.8: Cell populations labelled in the *Tg(dlx4/6:GFP)* line – 26hpf to 5dpf

A-E show projections of sagittal sections to the midline in *Tg(dlx4/6:GFP)* embryos; F shows a projection of sections as indicated in E. G and H are 20µm sagittal (G) and transverse (H) sections with *tbr1* expression in blue and Dlx-expression in brown, kindly provided by M. Mione. All scale bars are 50µm except where indicated.

A shows *dlx4/6* expression in a live 26hpf embryo. *dlx4/6* is expressed broadly in the ventral telencephalon, several cell diameters from the ventricular surface. This expression is matched by a similar domain in the diencephalon.

B shows a fixed embryo at 36hpf. *dlx4/6* is again expressed ventrally, around the AC, with GFP +ve fibres present in the SOT (arrowhead).

By 2dpf (C), *dlx4/6*-expressing cells are not only present in the ventral telencephalon, but also as single cells in the posterior dorsal telencephalon (arrowhead in C).

D shows a 3dpf embryo; *dlx4/6*-expressing cells are present in the OB (arrow), dorsal telencephalon (arrowhead) and throughout the ventral telencephalon.

E shows an embryo at 5dpf; the OB cells have an elaborate morphology characteristic of interneurons (arrow). Single cells in the dorsal telencephalon (arrowheads in E and F) also have an elaborate morphology (inset E'; scale bar = 5µm).

F shows the interface of DiI-labelled olfactory sensory neuron axon terminals and OB interneurons (arrow). At higher magnification in a single section (F'; scale bar = 5µm), the two populations make multiple contacts within a glomerulus. Also evident in F is the restriction of *dlx4/6* expression to midline regions in the telencephalon.

G shows Dlx-expressing cells in the ventral telencephalon around the AC. *tbr1* expression is evident in dorsal areas, as well as in the OB (asterisk) and just rostral to the AC, overlapping with but not coexpressing with Dlx (arrowhead).

H shows a section at the level indicated in G. Dorsal and lateral *tbr1* expression surrounds medial Dlx-expressing cells, again overlapping with Dlx in an area just rostral to the AC (arrowhead).

AC – anterior commissure  
OB – olfactory bulb  
OC – optic chiasm  
OE – olfactory epithelium  
SOT – supraoptic tract  
tel – telencephalon

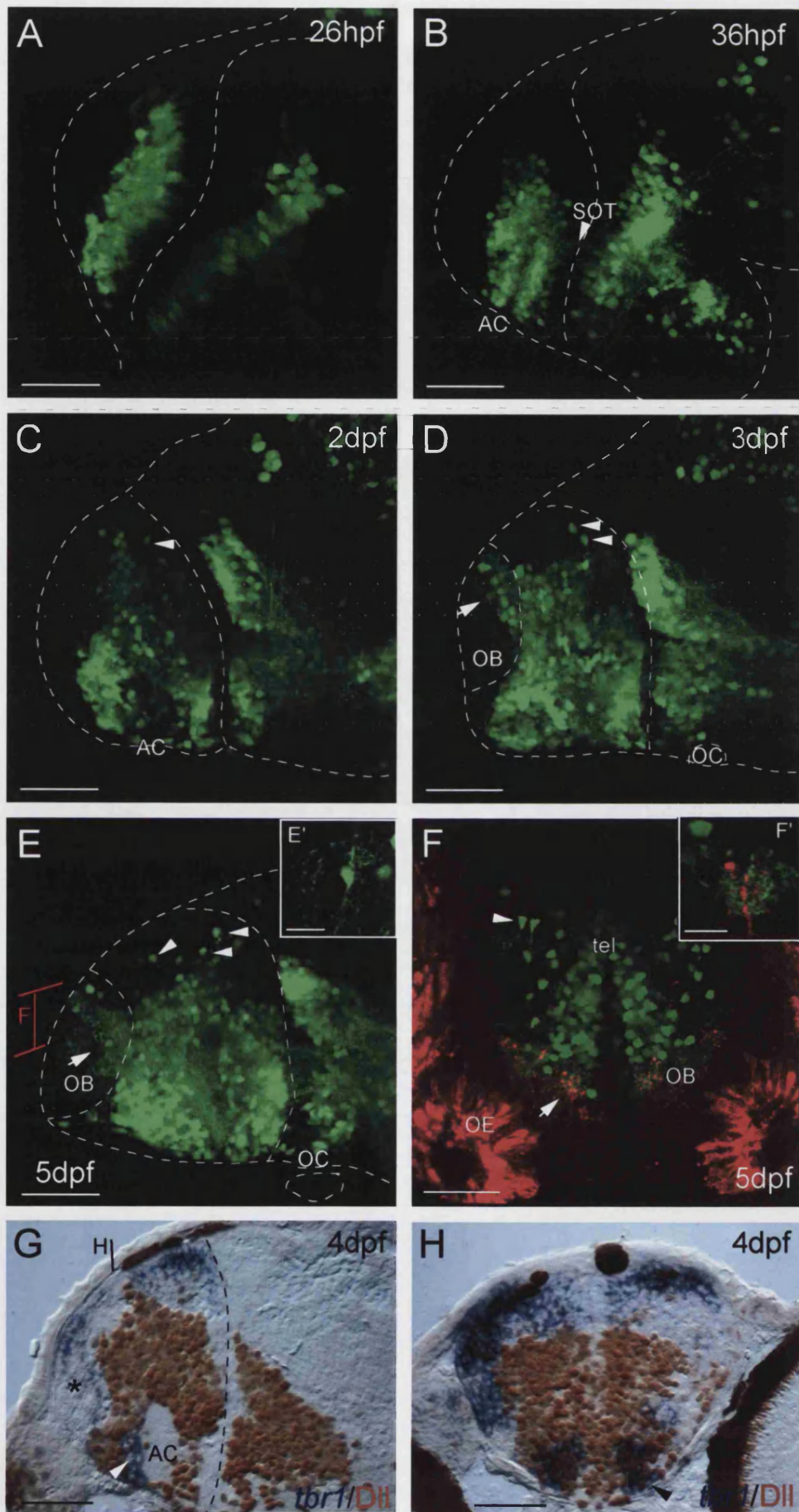


Figure 3.8

aspect reveals extensive processes characteristic of interneuron morphology (Fig 3.8 E'). Indeed, these cells may well represent the ventral to dorsal migration of telencephalic interneurons seen in higher vertebrates such as chick and mouse (Cobos et al., 2001a; reviewed in Marin and Rubenstein, 2001)

The second group of neurons highlighted are interneurons within the OB (M. Mione, work in progress; Long et al., 2003). These cells are visible in the OB from 3dpf (Fig 3.8 D-F). They again have a characteristic morphology with extremely elaborate dendritic arbours, and do not project outside the bulb as confirmed by the absence of GFP fibres in the olfactory tracts (Fig 3.8 F and data not shown). The interneuron arbours are intimately connected with incoming OSN axon terminals; labelling the OSNs with DiI reveals the close apposition of these two populations (Fig 3.8 F and F'). The interneuron cell bodies themselves also occupy a distinctive position within the bulb, lying in the posterior OB at 3 and 5dpf (Fig 3.8 D-F).

To further investigate the pallial and subpallial subdivisions of the zebrafish telencephalon I analysed specimens prepared by M. Mione that highlight both of these populations. Sections were labelled both with the anti-Dlx antibody (which labels all Dlx-expressing cells) and hybridised with *tbr1* (a pallial marker; Mione et al., 2001). *tbr1* expression is evident in dorsal areas, but also extends into the olfactory bulb (asterisk in Fig 3.8 G), where it highlights projection neurons (Mione et al., 2001). The transverse section also shows *tbr1* expression extending from dorsal into lateral telencephalic areas, lateral to Dlx expression (Fig 3.8 H).

A further domain of *tbr1* expression is evident very ventrally in the telencephalon, just anterior to the AC (arrowheads in Fig 3.8 G and H). High magnification examination of this domain indicates it overlaps with but does not coexpress with Dlx. Although this *tbr1* expression domain is very ventral, it is nonetheless continuous with the other expression domains described above. The subpallial or pallial nature of this domain is unclear.

In summary, the pallial-subpallial division in the 4dpf zebrafish telencephalon is both a dorso-ventral and a medio-lateral division. That is the pallium in dorsal and lateral areas seems to envelop a core of ventral and medial subpallial cells, in a small way not dissimilar to "the overarching ambition" of the mammalian cortex.

### 3.4: Discussion

The aim of this chapter was to make a broad characterisation of the telencephalon, in terms of its morphology, proliferation, differentiation and connectivity over the entire period of embryogenesis. This information is generally missing from the literature, with most studies either focussing on multiple features at a single time point or a single feature through time. Furthermore, the zebrafish telencephalon is morphologically so different to that of mouse or even *Xenopus*, that it was impossible to use data from these species as the groundwork for my studies. I therefore felt this work was necessary background in order to perform further investigations into how the telencephalon develops, and after speaking to other zebrafish researchers and struggling to make comparisons with their data I realised the importance of making observations at multiple time points. In addition, even these simple observations have led to novel insights into the morphogenetic movements that shape the telencephalon, movements that may underlie the actinopterygian-specific process of telencephalic eversion.

#### *Major morphological changes between 2dpf and 3dpf*

The description of a morphogenetic movement that results in major adjustments within the telencephalon is the major finding of this chapter. This morphogenetic movement, which occurs between 2 and 3dpf, is distinct from the previously reported ventral flexure that occurs earlier in development and brings the telencephalon to the rostral pole of the brain (Hauptmann and Gerster, 2000; Hauptmann et al., 2002; Ross et al., 1992). The ventral flexure, as judged by acetylated tubulin labelling of mature axons, does not result in any discernable reorganisation within the telencephalon.

In contrast, the morphogenetic movement between 2 and 3dpf causes quite major adjustments within the telencephalon. Most notably, the olfactory bulb (OB) moves from a very dorsal-posterior position (close to the border with the diencephalon) at 2dpf to a rostral position at 3dpf, even more pronounced at 5dpf (Fig 3.6 C-E). This striking movement is paralleled by some minor changes in the ventral telencephalon, with the AC moving closer to the ventral border with the diencephalon.

The observed morphogenetic movement is also apparent looking at changes in the VZ as highlighted by BrdU incorporation into proliferating cells. At stages up to and including 2dpf, BrdU profiles are continuous over the ventricular surface of the telencephalon, and are evident in the roof of the telencephalon and diencephalon (Fig 3.4). At 2dpf, BrdU profiles are apparent up to the posterior border of the telencephalon with the diencephalon (Fig 3.5 A and B). However, at 3dpf, BrdU profiles are evident for the first time on the dorsal surface of the telencephalon, an area that was not previously ventricular (Fig 3.5 D). This pattern of dividing cells is more enhanced at 5dpf, where BrdU profiles are seen covering the entire dorsal surface of the telencephalon except for the OB (Fig 3.5 G-I).

These two lines of evidence therefore strongly point towards a “rotatory” morphogenetic movement that brings the OB to a rostral position and the VZ to the dorsal surface. These two processes appear to be coordinated, in that the OB and VZ are adjacent to each other both at 48hpf and at 3dpf. In other words, the VZ never covers the OB, suggesting the altered position of the two structures at 3dpf is the result of the same underlying movement. The “rotation” does not however seem to affect the ventral telencephalon as much as the dorsal, as evidenced by the persistence of the preoptic area proliferation zone and the position of the SOT.

#### *Eversion as a result of the morphogenetic rotation*

One of the major implications of my BrdU data is that an everted telencephalon could be a direct result of the morphogenetic movement described above. Eversion is the actinopterygian-specific process by which the dorsal ventricular surface apparently becomes “turned out” in a medio-lateral direction, as illustrated in Figure 3.9 B. Thus it has been proposed that structures that are originally medial and dorsal in the neural tube later become lateral and more ventral, with the whole dorsally-everted surface covered by a thin choroid tela (Butler, 2000; Butler and Hodos, 1996). The mechanism by which the eversion process takes place has remained elusive, although understanding it is key to comparative uses of the zebrafish telencephalon.

In my model (Fig 3.9 A), key event would be the separation of the right and left sides of the telencephalon that occurs during ventricle formation at about 16hpf. From this point onwards, the posterior-ventral surfaces lose contact with each other, forming the continuously curved surface seen in the medio-lateral axis of my

specimens. The subsequent rotatory morphogenetic movement between 48hpf and 3dpf then brings an already parted VZ from the posterior to the dorsal surface of the telencephalon. In this model there is no need for the VZ to undergo extensive medio-lateral spreading, because the entire medio-lateral surface is already VZ and has been since the ventricle first formed. Once proliferative cells are present on the dorsal surface, subsequent proliferation would elaborate the pallial telencephalon, producing the enlarged and obviously everted structure seen in the adult (Wullimann and Rupp, 1996).

The lack of a substantial literature means it is in fact difficult to know what the “current model” of eversion is and therefore how my model compares. Much of the work on eversion has rested on an analysis of the adult telencephalon (Butler, 2000; reviewed in Butler and Hodos, 1996), the end-point of the eversion process, with no examination of intermediate time points. Although the adult telencephalon has strong similarities with the organisation at 5dpf, there are also major differences. Simply in terms of size, the embryonic telencephalon is not more than 250  $\mu\text{m}$  in any dimension, while even at 1 month post fertilisation the telencephalon is approximately 1 millimetre in all dimensions. Therefore the huge cell proliferation that occurs during this period, and into adult stages, could dramatically alter telencephalic morphology and mask the underlying morphological arrangements. Furthermore, the methods used to assess eversion have been very indirect, relying on features such as blood vessels in the sulci of the brain (Butler, 2000).

Mario Wullimann is one of the few zebrafish researchers who has addressed eversion at embryonic stages. Using the proliferating cell marker PCNA, he observed a dorsally everted pallial proliferation zone already at 2dpf (Wullimann and Knipp, 2000). Aside from the drawbacks of using PCNA, a marker known to persist beyond final mitosis (Wullimann and Puelles, 1999), the data he presents broadly agrees with my observations. The key difference is that the surface he labels as dorsal, I label as posterior. It is also clear that the region of proliferation he observes, even though he labels it as the dorsal surface, does not extend beyond what would be the posterior border of the telencephalon with the diencephalon. The exact timing of the appearance of a dorsally-everted telencephalon is not as important as the mechanism by which it gets there. Unfortunately, on this topic Wullimann makes little comment.

### Figure 3.9: Models of eversion

A shows a model of eversion based on a morphogenetic rotation between 2dpf and 3dpf. The VZ is indicated by thick red lines; dotted lines indicate places where proliferation may be very sparse. Blue arrowhead indicates the roof at early stages and the choroid tela at 5dpf. Light blue ovals represent the olfactory bulb. In the transverse section of the 5dpf telencephalon, the full medio-lateral extent of the VZ is indicated.

B shows the conventional model of eversion and evagination, adapted from Butler (2000)

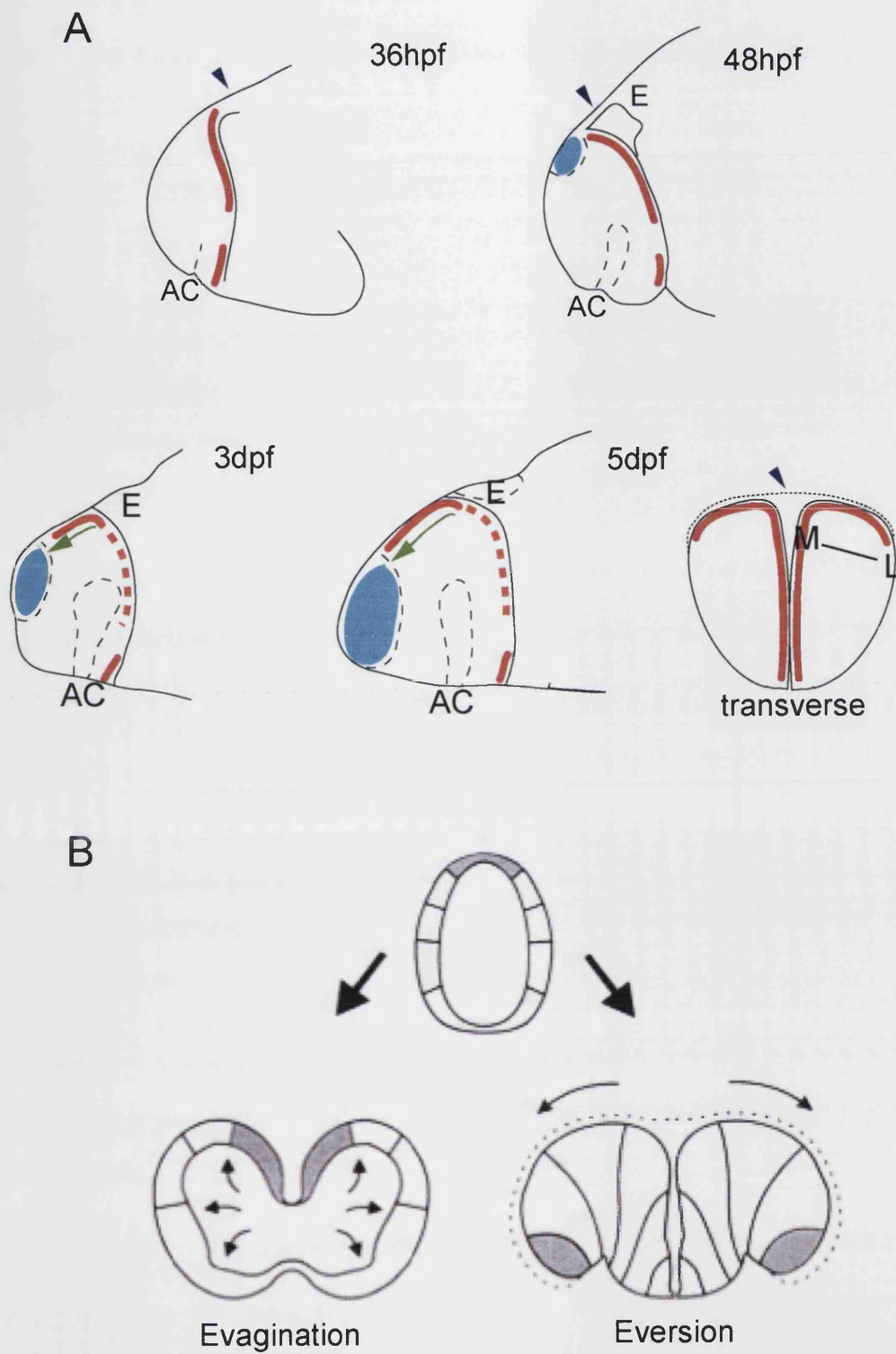


Figure 3.9

There are limited mechanisms by which a new area of VZ can form. Importantly, the new area must come from existing proliferative cells. The model suggested by the simplified schematic drawings in many anatomical texts (e.g. (Butler and Hodos, 1996) involves an opening out of the right and left sides at the midline dorsal surface (Figure 3.9 B). This model also uses as its starting point a neural tube with ventricular space. Unfortunately this is far from an accurate starting point for the zebrafish telencephalon, which is a dorsal compartment of the uncavitated neural rod. However, extrapolating from this schematic model to the zebrafish would mean the dorsal midline VZ would separate and turn out laterally. This does not seem to be what my data shows, but it would certainly be worth exploring this possibility with further experiments.

#### *Questions posed by the eversion model*

My model is not intended to explain the entire eversion mechanism, merely to suggest that it may be the posterior VZ rather than the midline VZ that is the origin of dorsally-everted VZ. Obviously many questions remain, and are indeed posed by this model. For example, how is the movement of the VZ driven and orchestrated? Are all areas of the posterior VZ recruited to the dorsal surface? Do progenitors in the VZ already have pallial or subpallial identities and how are these reconciled with the morphogenetic movement? Future experiments, initially focussing on making a more detailed description of the changing VZ with closely-spaced time points, but extending to cell labelling in transgenic lines will hopefully begin to address these questions.

A further question to consider is to what extent the adult zebrafish telencephalon is everted, morphologically or in terms of functional areas. Across the teleost group (a subgroup of the actinopterygians, of which zebrafish and goldfish are members), eversion seems to be morphologically simple, i.e. a lateral folding out of the dorsal telencephalon that is not further complicated by secondary migration of cell masses (Butler, 2000). However, functional evidence is not so clear-cut. Behavioural experiments involving lesion studies have identified putative areas within the goldfish that correspond to the hippocampus and amygdala, on the basis of their selective roles in spatial and emotional learning respectively (Portavella et al., 2002). The amygdala is medially located in goldfish, while the hippocampus is laterally located. A simple rearrangement of functional areas in the everted

telencephalon is therefore evident, as the amygdala and hippocampus occupy lateral and medial locations respectively in the evaginated telencephalon. However, the major olfactory input to the teleost telencephalon is laterally and posteriorly located, as it is in tetrapods (Wullimann and Rink, 2002). The question is, therefore, whether the eversion process affects all areas of the dorsal telencephalon.

The identification of markers for areas such as the amygdala and hippocampus at embryonic stages would help to clarify this issue. The movements of functional areas could then be tracked throughout the eversion process. Although I have not followed the movements of any functional areas during eversion, my model would support more dramatic rearrangements for some pallial areas than for others, thus an incomplete eversion as suggested in Wullimann and Rink (2002).

#### *Establishing axes within the telencephalon*

Establishing dorso-ventral and anterior-posterior axes within the telencephalon is not a trivial matter. A-P usually equates with rostro-caudal, with D-V perpendicular to this axis. However, as in other species the telencephalon is a derivative of the dorsal neural tube/rod (Fernandez et al., 1998), and only comes to be located at the rostral pole of the zebrafish brain through the subsequent morphogenetic movement of the ventral flexure (Wilson et al., 1990; Hauptmann and Gerster, 2000; discussed above). It is therefore not appropriate to treat the telencephalon as a transverse segment of the neural tube, and A-P and D-V axes have to be adjusted accordingly.

Also somewhat problematic is the notion that in the telencephalon, dorsal and ventral should equate with pallial and subpallial regions. The zebrafish telencephalon, as this chapter suggests, is lacking a rigorous characterisation of pallial and subpallial areas. Markers have been established for the two regions - *emx* genes (Kawahara and Dawid, 2002; Morita et al., 1995), *tbr1* and *eomesodermin* (Mione et al., 2001) for the pallium; *dlx* genes for the subpallium (Akimenko et al., 1994)) but these have not been characterised over the entire period of embryogenesis. Nor have I addressed this issue comprehensively in this chapter. However, using the *Tg(dlx4/6:GFP)* line (Zerucha et al., 2000) as a marker of subpallial neurons has given some interesting insights into the extent and position of the subpallium at various stages (Fig 3.8). Namely, *dlx4/6* expression is restricted to topographically ventral telencephalic areas at early stages (Fig 3.8 A and B), but extends progressively more rostrally up to 5dpf (Fig 3.8 C-E). *dlx4/6* expression is

predominantly medial, particularly from 2dpf onwards (Fig 3.8 F), but is excluded from the VZ itself at all stages. Pallial gene expression, as assessed in specimens prepared and kindly donated by M. Mione, compliments *Dlx* expression, covering dorsal and lateral areas of the telencephalon (Fig 3.8 G and H). The pallial and subpallial populations are exclusive of each other, although there is an area anterior to the AC where *Dlx* and *tbr1* expression are strongly intermingled but not coexpressing. This ventral *tbr1*-positive region may be associated with one of the olfactory tracts (M. Mione, personal communication), and this will be discussed further in subsequent chapters.

How does this assessment of pallial and subpallial areas therefore match with the axes described in Fig 3.1? Initially, *dlx4/6* expression fits broadly within the ventral portion of the telencephalon. But at progressively later stages, *dlx4/6* expression extends into regions that would be dorsal according to the D-V axis at 3 and 5dpf (Fig 3.1 D' and E'). Ultimately, having a system of axes is important in order to be able to describe expression domains and the relative positions of different structures. However, it is not imperative that dorsal and ventral should equate absolutely with pallial and subpallial areas. It would certainly be convenient to have such a system, even if just to ease the task of anatomists, but since zebrafish pallial and subpallial areas are so extensively overlapping in the medio-lateral axis (Fig 3.8 G and H) this is not possible. Instead, a major focus of future work should be to provide a rigorous characterisation of pallial vs. subpallial areas at a variety of stages, to enable anatomists to fit their descriptions within functionally relevant subdivisions of the telencephalon rather than topographic positions.

### *Neurogenesis in the telencephalon*

The telencephalon is precocious in its neurogenesis compared to the adjacent diencephalon. I used the *Tg(HuC:GFP)* line (Park et al., 2000) to assess the telencephalic neuronal population over time, and found that between 13hpf and 24hpf the population grows dramatically.

Neurogenesis from 24hpf onwards was monitored using the *Tg(HuC:GFP)* line in conjunction with BrdU labelling (Fig 3.4 and Fig 3.5). These experiments, with short BrdU pulses followed by immediate fixation, highlighted two mutually exclusive populations of cells. In comparison to previous studies analysing proliferation and differentiation (Wullmann and Knipp, 2000), the combination of

the HuC-GFP line with BrdU gave a much more detailed picture. For example, PCNA levels can remain at 30-40% of their maximum for about 24hours after division (Wullimann and Puelles, 1999), leading to an inaccurate picture of the 24hpf telencephalon as entirely proliferative. PCNA also labels such large numbers of cells, especially at early stages, that the analysis of subtle changes in the VZ is very difficult. In contrast, my results show that in many cases, BrdU incorporation is not restricted to cells in the basal VZ but takes place at all levels in the VZ. I also saw that in areas where proliferation was very sparse, BrdU profiles and HuC positive neurons were found side by side at the ventricular surface (Fig 3.5 F). These results suggest that proliferation within the telencephalon may be regulated somewhat differently to other areas, and may warrant further investigation.

## 4.1 Aim and Introduction

The mechanisms that underlie the specification of neuronal subtypes are of great interest to developmental neurobiologists. Functional neuronal circuitry within and between brain areas relies on the ability to generate neurons with a variety of axonal projection patterns, neurotransmitter and receptor profiles. The mammalian dorsal telencephalon, which gives rise to the cerebral cortex, is a brain area with numerous specialisations including visual, auditory, olfactory, somatosensory and motor areas. The zebrafish dorsal telencephalon, although not as elaborate as its mammalian equivalent, also shows specialisations especially in terms of its connectivity, suggesting it too has functional specialisations (Wullimann and Rink, 2002). However, the molecular mechanisms underlying the specification of different neuronal subtypes in the zebrafish, and especially within the telencephalon, remain elusive.

### *Lhx genes and neuronal subtype specification*

The LIM-homeobox (Lhx) genes encode a large family of transcription factors, the LIM-HD proteins, that are known to be involved in the specification of neuronal subtypes in a wide variety of species (Bach, 2000; Dawid and Chitnis, 2001; Hobert and Westphal, 2000). The feature that sets LIM-HD proteins apart from other transcription factors in the homeodomain superfamily is their ability to bind both DNA via the homeodomain and other proteins via their LIM domains. This means that LIM-HD proteins can form both homomeric and heteromeric complexes involving other LIM-HD proteins or other classes of transcription factor (Bach, 2000; Dawid and Chitnis, 2001; Hobert and Westphal, 2000). In many systems studied to date, it seems that specific combinations of LIM-HD factors are responsible for the specification of neuronal subtypes. For example, in the zebrafish spinal cord, motoneuron subtypes are specified by different combinations of the LIM-HD proteins Islet1, Islet2 and Lhx3 (Appel et al., 1995; Segawa et al., 2001). The combinatorial expression of LIM-HD proteins suggests that LIM-HD heteromeric complexes may underlie the function of these proteins, but biochemical evidence for this is somewhat lacking and the exact composition of transcriptional complexes may vary between systems (e.g. Thaler et al., 2002).

### *The Lhx1/5 subgroup in mouse, Xenopus and zebrafish*

Mammals have thirteen known LIM-HD proteins, *Drosophila* five and *C. elegans* seven, and these proteins can be grouped into six subgroups each containing LIM-HD proteins with sequences conserved across species (Hobert and Westphal, 2000). My work addressing LIM-HD proteins in zebrafish has focussed on members of the LIN-11 subgroup of LIM-HD proteins. This group, named after the *C. elegans* founding members *lin-11* and *mec-3*, contains the vertebrate Lhx genes *Lhx1* and *Lhx5* (Hobert and Westphal, 2000). Zebrafish, as a result of an ancient genome duplication (Postlethwait et al., 1998), has three members. Originally called *lim1*, *lim5* and *lim6* (Toyama et al., 1995; Toyama and Dawid, 1997), these genes have recently been renamed *lhx1a* (*lim1*), *lhx1b* (*lim6*) and *lhx5* (*lim5*) to fit with standard nomenclature (ZFIN).

### *Lhx1 and Lhx5 are expressed early in development*

The vertebrate *Lhx1* and *Lhx5* genes are somewhat different from the other LIM-HD subgroups because although they are expressed in neurons in the CNS, *Lhx1* at least seems to have a highly conserved role much earlier in development. Gain-of-function experiments in *Xenopus* show that *x-Lhx1* has a role in neural induction (Taira et al., 1994), dependent upon activation by activin/nodal signals (Watanabe et al., 2002). In mouse, knocking out the *Lhx1* gene results in severe truncation of head structures anterior to the otic vesicle (Shawlot and Behringer, 1995) and the gene is required in both primitive streak-derived tissues and visceral endoderm for proper head formation (Shawlot et al., 1999). Later roles of *Lhx1* have therefore been difficult to dissect because of the drastic effects of interfering with early organiser function. *Lhx5* is also expressed early in development in mouse (Sheng et al., 1997) and *Xenopus* (Toyama et al., 1995), but misexpression experiments have yet to reveal the role of *Lhx5* in early development. In fact, the mouse knockout of *Lhx5* has relatively specific effects on the development of the hippocampus, interfering particularly with the differentiation and migration of cells that contribute to Ammon's horn and the dentate gyrus (Zhao et al., 1999).

The function of the zebrafish orthologues of *Lhx1* and *Lhx5* - *lhx1a*, *lhx1b* and *lhx5* has been little studied, but their expression patterns have been briefly described (Toyama et al., 1995; Toyama and Dawid, 1997). *Lhx1a* and *Lhx1b*,

proteins sharing 81% amino acid identity, are both predominantly expressed in the shield (zebrafish organiser) at gastrulation stages (Toyama and Dawid, 1997). Conservation of activin/nodal response elements between *Xenopus Lhx1* and zebrafish *lhx1a* suggests similar regulation of early expression (Watanabe et al., 2002), and a possible conservation of function. Indeed, experiments I attempted injecting *lhx1a* mRNA lead to massively expanded head tissue at the expense of trunk tissue (data not shown). This potential role of *lhx1a* in the head organiser of zebrafish was not investigated further. Zebrafish *Lhx5*, sharing 69% amino acid identity with *Lhx1b*, also has an early expression pattern but one which is distinct from *lhx1a* or *lhx1b* expression. *lhx5* is expressed in the entire blastoderm of the gastrulating embryo, except at the margin where mesoderm is forming (Toyama and Dawid, 1997).

#### *Lhx expression in the forebrain*

Expression analysis of *lhx1a*, *lhx1b* and *lhx5* at post-gastrulation stages shows widespread expression in the CNS. *lhx1a* and *lhx1b* are expressed in discrete groups of cells in the forebrain, midbrain and hindbrain from early somitogenesis stages (13hpf) onwards (Toyama and Dawid, 1997). *lhx5* is similarly expressed in many regions of the neuraxis, with a particularly strong expression domain in the presumptive diencephalon from 13hpf onwards (Toyama et al., 1995). All three genes have distinct expression domains in the telencephalon, and a detailed study of these expression domains is the focus of my work in this chapter.

Bachy et al., (2001) have already undertaken a detailed analysis of the forebrain expression of *xLhx1* and *xLhx5*, as well as other members of the LIM-HD family, in *Xenopus*, and compared the expression to mouse. They find very strong conservation of expression patterns of *Lhx1* and *Lhx5* between the two species in the diencephalon, but more divergent patterns in the telencephalon (Bachy et al., 2001). While mouse *Lhx1* is expressed in the pallium, *xLhx1* is only expressed in the subpallium. *Lhx5* is more similar, with both species showing broad pallial expression domains. *Xenopus* forebrain expression of these genes has been analysed further at larval and adult stages, where they are found to mark the same subdivisions through time (Moreno et al., 2004). Both genes have restricted expression domains within pallial and subpallial subdivisions, with *xLhx5* being

notably expressed in the mitral cells of the olfactory bulb, suggesting a pallial origin for these cells (Moreno et al., 2003; Moreno et al., 2004).

This relative wealth of data from other species gives a good grounding for making a comparative study with zebrafish. The retained duplication of the *Lhx1* gene in zebrafish makes the comparison particularly interesting, because the combined expression patterns of zebrafish duplicates have often been found to replicate the expression patterns seen in other species (Force et al., 1999).

#### *Aim of this chapter*

The main aim of this chapter is to make a detailed characterisation of the telencephalic domains of *lhx1a*, *lhx1b* and *lhx5*, with a view to identifying telencephalic subdivisions. Analysing the expression of these genes in combination with each other and with other markers highlights the relationship of different telencephalic domains over the period of embryogenesis. It also gives some insight into morphogenetic movements that may be important in generating the mature telencephalic structure.

## 4.2: Materials and Methods

### *Fish lines*

In addition to wildtype strains of zebrafish, I also used the *Tg(HuC:GFP)* line (Park et al., 2000) and the *Tg(dlx4/6:GFP)* line (Zerucha et al., 2000).

### *DNA constructs*

The DNA constructs used during the course of this chapter were *lim1 (lhx1a)* and *lim6 (lhx1b)* (Toyama and Dawid, 1997), *lim5 (lhx5)* (Toyama et al., 1995), *shh* (Krauss et al., 1993), *mitfb* (Lister et al., 2001), *emx3* (originally named *emx1*) (Morita et al., 1995), *tbr1* (Mione et al., 2001).

### *Preparation of antisense probes*

DNA constructs were amplified using conventional midi- and maxiprep methods (section 2.4). Antisense probes were made from linearised DNA according to conventional methods (section 2.6), and with the following enzymes: *lhx1a*, *lhx1b* and *lhx5* – linearise with BamHI, transcribe with T7; *shh* – linearise with HindIII, transcribe with T7; *mitfb* – linearise with NotI, transcribe with T3; *emx3* – linearise with BamHI, transcribe with T3; *tbr1* – linearise with Sall, transcribe with SP6.

### *Double in situ hybridisation*

Double *in situ* hybridisation was performed as described in section 2.8 to simultaneously visualise the expression patterns of two different genes. This involved using both dioxygenin (DIG) and fluorescein (FITC)-labelled probes. The two substrates used for alkaline-phosphatase conjugated antibodies were NBT/BCIP (Boehringer Mannheim) and Fast Red (Roche). The Fast Red colour reaction was always performed first, to avoid the NBT/BCIP signal overwhelming the weaker Fast Red signal. The stronger probe was usually labelled with FITC and detected with Fast Red, the weaker probe was therefore usually labelled with DIG and detected second. However, in as many cases as possible I tried different combinations of probe-labelling and AP substrate, to control for any possible differences between probes.

All *in situ* hybridised specimens were photographed on a Nikon microscope with a Micropublisher digital camera (Q imaging), controlled through Openlab 3.1.4 software (Improvision, UK).

#### *Vibratome sectioning of double in situ labelled specimens*

Double *in situ* hybridisation was performed as described in section 2.8 to simultaneously visualise the expression patterns of two different genes. In some cases, vibratome sections of these specimens were made, in order to more closely examine expression domains. At the end of the double *in situ* protocol, specimens for sectioning were left in PBS rather than being transferred to 70% glycerol.

1. Prepare solutions with 0.375g gelatin (Sigma) in 25ml PBS (heat to dissolve) and 20g egg albumin (Sigma) in 50ml PBS (do not heat).
2. Mix the gelatin and albumin solutions together and add 15g sucrose (Sigma).
3. Put 2ml gelatin/albumin in a small mould, add 200µl 25% glutaraldehyde and the embryo and orient immediately before the block sets.
4. Trim the block, mount it with superglue on a vibratome chuck and cut 35-50µm sections.
5. Mount the sections in PBS on a slide for imaging

These specimens were imaged on a Nikon microscope with a Micropublisher digital camera (Q imaging) and Openlab 3.1.4 software (Improvision, UK).

#### *In situ hybridisation in GFP lines*

The embryos used for these experiments were from the *Tg(HuC:GFP)* and *Tg(dlx4/6:GFP)* lines. *In situ* hybridisation was performed for *lhx1a*, *lhx1b* and *lhx5* as described in sections 2.7 and 2.9, using DIG-labelled probes and the fluorescent Fast Red AP substrate. GFP was then detected using the anti-GFP primary antibody (Upstate Biotech), and an Alexa 488 conjugated anti-rabbit IgG secondary antibody (Molecular Probes).

## Outline of unsuccessful projects

### *A transgenic *lhx1a*:GFP line*

With our interest in cell tracing and live imaging, I tried to develop a transgenic GFP line under the control of sequences that regulate *lhx1a* expression. Constructs containing either 9kb or 3kb of genomic sequence, including the first exon, first intron and part of the second exon of the *lhx1a* gene as well as upstream sequences were developed and kindly donated by Dr N. Takahashi in the laboratory of Dr I. Dawid (NIH, Bethesda MD). Injection of either the short or long construct, linearised or circular, did not result in discernable GFP expression in any of the injected embryos. Nonetheless, injected embryos were grown to adulthood and in-crossed, but no fluorescent progeny were obtained. The first intron has been shown to be essential for early embryonic expression (Watanabe et al., 2002), raising the possibility that other intron sequences that were absent from the genomic constructs are required for later CNS expression.

### *Antibodies to LIM-HD proteins*

I also tried to develop an antibody specific to Lhx1a. Because of the extensive homology between Lhx1a and Lhx1b (81% amino acid identity), I used very short (100-150bp) regions from the more variable 3' regions of the gene and fused them to the 3' end of the sequence for glutathione-S-transferase (GST; pGEX-2T vector donated by M. Redd). Following purification of these GST fusion proteins by glutathione columns, the proteins were injected into rabbits to generate polyclonal antibodies (Cambridge Biosciences). Unfortunately, I did not detect any specific binding of the resulting antisera to either whole protein extracts from wildtype or *lhx1a*-overexpressing embryos in Western blots or in wholemounts. Other groups have also generated antibodies to LIM-HD proteins including to Lhx1. However, no specific staining in wholemount was observed either with an antibody to *Xenopus* Lim1 (xLhx1; Karavanov et al., 1996; sold by Chemicon International) or an antibody to rat Lim2 that also cross-reacts with chick, rat and mouse Lim1 and Lim2 (4F2; Developmental Studies Hybridoma Bank, Iowa).

### *Morpholinos to *lhx1a* and *lhx1b**

A further attempt to probe *Lhx* gene function involved generating morpholino oligonucleotides to disrupt the translation of *lhx1a* and *lhx1b* mRNA. 25mer sequences were designed to the 5' UTR of the *lhx1a* and *lhx1b* genes, as these regions share little sequence similarity. Specific effects on neurogenesis or Lhx-expressing populations were not observed, although high doses of morpholino resulted in gastrulation defects that may be related to the early expression of these genes (Toyama and Dawid, 1997).

## 4.3: Results

I have undertaken a detailed study of the expression of three zebrafish LIM-homeobox (Lhx) genes, *lhx1a*, *lhx1b* and *lhx5* over the first five days of development. I have also analysed the expression of these genes with respect to other markers in the telencephalon, including those that define pallial and subpallial territories. Through this analysis I have been able to extensively characterise the Lhx-expressing populations, and gain clues about their possible functions in the developing telencephalon.

I started my expression analysis at late somitogenesis stages and continued through to beyond the end of embryogenesis, 5dpf. By 5dpf, the telencephalon has much in common with the adult telencephalon in terms of neuronal organisation, the presence of tracts and commissures and the location of proliferative regions (Wullmann and Puelles, 1999). My primary interest, therefore, was to analyse telencephalic domains of Lhx expression and to relate them to the processes that shape the telencephalon during embryogenesis. To aid in the imaging and interpretation of telencephalic expression domains I made use of “whole telencephalic sections”, which involved cutting off the telencephalon and mounting it on its flat side for imaging, as shown below.

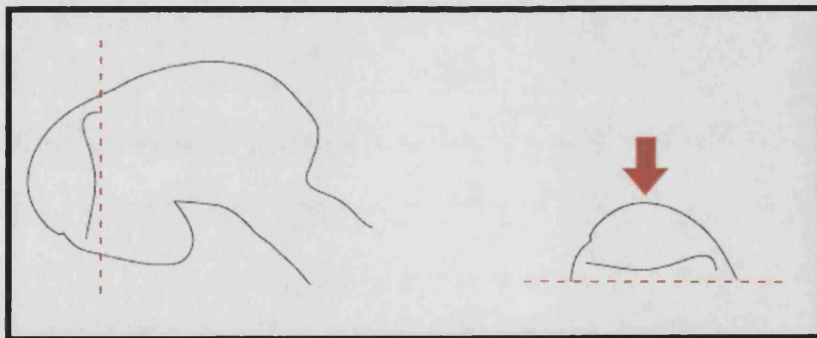


Figure 4.1: Cutting and mounting of whole telencephalic sections from wholmount stained specimens.

### *Expression of lhx1a in the telencephalon*

Expression of *lhx1a* in the CNS begins at approximately 8ss (13hpf) in cells throughout the neuraxis, mostly in the presumptive hindbrain and spinal cord but with single cells in the presumptive telencephalon (Toyama and Dawid, 1997; data not shown). At 20ss, when the boundary of the telencephalon is clearly visible,

*lhx1a* is expressed in a group of posteriorly-located dorsal telencephalic cells (Fig 4.2 A and B). Looking from the rostral aspect at the telencephalon, the *lhx1a*-expressing cells form bilateral stripes close to the midline (Fig 4.2 C). In a number of cases, cells expressing *lhx1a* were observed still in contact with the prospective ventricular surface, suggesting that a few of these cells may still be proliferative or had just undergone their final mitosis (data not shown). At later stages *lhx1a*-expressing cells are not seen in obviously proliferative areas (data not shown).

At 24hpf, *lhx1a* expression in the telencephalon appears as two bilateral domains separated by 4-5 cell diameters of non *lhx1a*-expressing tissue (Fig 4.2 D-F). I have designated the more dorso-posterior domain as *lhx1a* domain 1 and the more dorso-anterior domain as *lhx1a* domain 2, to simplify their identification within the telencephalon. The two domains have slightly different sizes (Fig 4.2F) and domain 1 lies very close to the posterior border with the diencephalon (Fig 4.2D). These telencephalic expression domains remain similar at 32hpf and 48hpf, although the distance between domain 1 and 2 increases, and domain 2 becomes progressively further from the midline (Fig 4.2 G, I, J and L). In addition, between 32hpf and 48hpf, domain 1, while remaining juxtaposed to the posterior telencephalic border, expands dramatically in the mediolateral axis (Fig 4.2 K and L). Examination of stages between 32hpf and 48hpf reveals this mediolateral expansion begins laterally as a thin stream of *lhx1a*-expressing cells and becomes more robust up to 48hpf (data not shown).

At 3dpf, the expression of *lhx1a* in the telencephalon looks surprisingly different to the pattern at 48hpf. Two domains of *lhx1a* expression are still present, but domain 1 now lies far from the posterior border of the telencephalon (Fig 4.2M), within the olfactory bulb (OB; Fig 4.2N). The OB has a structure distinct from the rest of the telencephalon because of its glomeruli (see Chapter 3), and can therefore be identified in fixed tissue under high power magnification (data not shown). Domain 2 lies just anterior to the AC (Fig 4.2M). From 3dpf onwards the expression of *lhx1a* in the telencephalon changes little – at 5dpf *lhx1a* continues to be expressed in both the OB and adjacent to the AC (Fig 4.2 O and P). This is confirmed by *in situ* hybridisation on cryostat sections from this region (data not shown).

Figure 4.2: *lhx1a* expression 19hpf to 5dpf

Figure shows expression of *lhx1a* in lateral wholemounts (A, D, G, J, M, O; scale bars=100µm), dorsal wholemounts (B, E, H, K; scale bars=100µm) and whole telencephalic sections (C, F, I, L, N, P; scale bars=50µm) at 19hpf (A-C), 24hpf (D-F), 32hpf (G-I), 48hpf (J-L), 3dpf (M-N) and 5dpf (O-P). Q and R show *shh* expression in lateral (Q) and dorsal (R) wholemounts at 36hpf; blue arrowheads mark the *zona limitans intrathalamica* (*zli*)

In lateral wholemounts, white dotted lines demarcate the telencephalon, and green spots mark the anterior commissure where appropriate. Black arrowheads mark the posterior border of the telencephalon with the diencephalon.

At 19hpf (20-somite stage), *lhx1a* is expressed in a single posterior-dorsal telencephalic domain (blue arrowheads in A and B and bracket in C), close to the border with the diencephalon (black arrowhead in A). Additional expression is seen in the anterior hypothalamus, ventral midbrain, and in the hindbrain rhombomeres.

At 24hpf, *lhx1a* is expressed in two bilaterally symmetrical domains in the telencephalon, domain 1 adjacent to the border with the diencephalon (blue arrowhead in D and F) and domain 2 more anteriorly (blue arrow in D, E and F). *Lhx1a* expression in the ventral thalamus, midbrain and hindbrain rhombomeres is broader than at 19hpf (D and E).

By 32hpf, *lhx1a* expression is strengthened in all areas (G and H), especially in the thalamus both dorsal and ventral to the *zli* (compare G and Q). In the telencephalon, domain 1 (blue arrowhead in G, H and I) lies close to the border with the diencephalon (black arrowhead in G), while domain 2 lies close to the anterior commissure (AC; blue arrow in G and I).

At 48hpf, *lhx1a* expression persists in the hypothalamus, ventral and dorsal thalamus and tectum, and a new expression domain appears in the optic tectum (J and K). In the telencephalon, domain 1 (blue arrowhead in J) still lies close to the border with the diencephalon (black arrowhead in J), but the domain is spread in the mediolateral axis (brackets in K and L). Domain 2 (blue arrow in J and L) remains close to the AC.

In the 3dpf telencephalon, domain 1 (blue arrowhead in M and N) lies anteriorly within the OB, at some distance from the border with the diencephalon (black arrowhead in M). Domain 2 (blue arrow in M and N) is located just anterior to the AC. The cut made to produce the section in N is shown by a black dotted line in M.

At 5dpf, *lhx1a* expression persists in the dorsal OB (blue arrowhead in O and P) and adjacent to the AC (blue arrow in P). The cut made to produce the section in P is shown by a black dotted line in O.

di – diencephalon  
t – telencephalon

mb – midbrain  
hb – hindbrain

d1 – domain 1 of *lhx1a*  
d2 – domain 2 of *lhx1a*

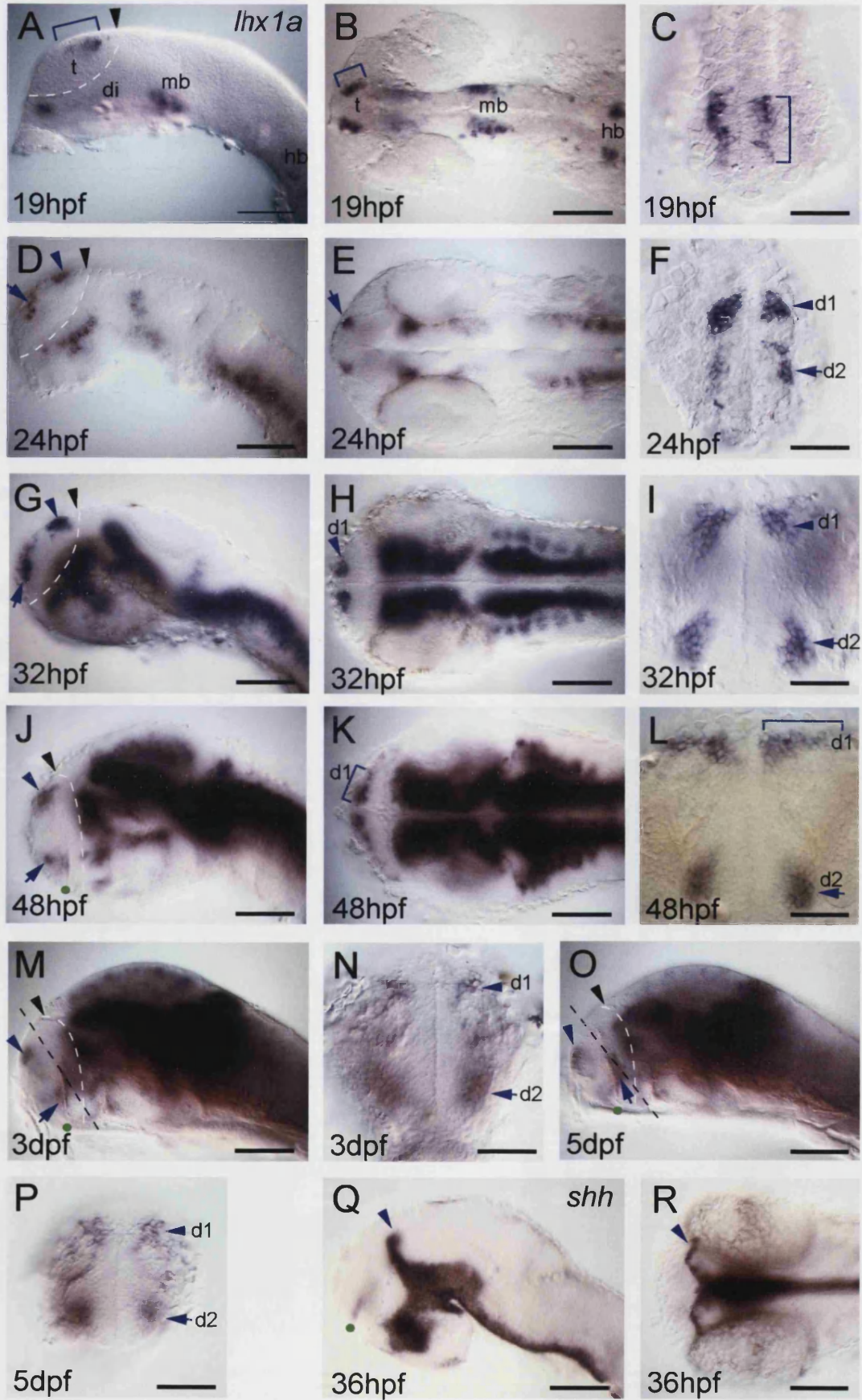


Figure 4.2

#### *Expression of *lhx1a* in other brain areas*

Outside the telencephalon, *lhx1a* expression begins in small clusters of cells in the anterior hypothalamus, ventral midbrain and hindbrain rhombomeres (Fig 4.2 A and B). These expression domains expand during the 5 days of embryogenesis examined, with a new expression domain appearing in the optic tectum at 48hpf (Fig 4.2J). The expression of *shh* at 36hpf identifies the *zona limitans intrathalamica* (zli), a boundary between the dorsal and ventral thalamus (Fig 4.2 Q and R) and comparison with *lhx1a* suggests that *lhx1a* expression flanks the zli but is not expressed within it (compare Fig 4.2 G and Q). The *lhx1a* hindbrain expression is also worth noting - a distinctive rhombomeric pattern with stripes of expression adjacent to rhombomere boundaries and “loops” of *lhx1a*-expressing cells in the lateral part of each hindbrain segment (Fig 4.2 H and K).

#### *Expression of *lhx1b* in the telencephalon*

The expression of *lhx1b*, a gene unique to zebrafish and highly homologous to *lhx1a*, also shows complex patterns in the telencephalon throughout development. At 10ss (14hpf), *lhx1b* is already expressed in single cells in the presumptive telencephalon (Fig 4.3A). By 20ss (19hpf) this telencephalic domain is much broader and dorsally located within the posterior telencephalon, adjacent to the border with the diencephalon (Fig 4.3B). From the rostral aspect, the *lhx1b*-expressing cells appear as bilateral stripes, 2-3 cell diameters from the midline (Fig 4.3C). As with *lhx1a* expression at this stage I sometimes observed *lhx1b*-expressing cells in contact with the midline, perhaps indicating that they were about to or had recently undergone their final mitosis (data not shown).

From 24hpf to 48hpf, the bilateral stripes of *lhx1b* expression in the telencephalon remain relatively constant in size and shape (Fig 4.3 F, I and L) but are located progressively more anteriorly with respect to the posterior border of the telencephalon and therefore closer to the anterior commissure (Fig 4.3 D, G and J). A second expression domain appears in the telencephalon at 36hpf, between the AC and the ventral border of the telencephalon (Fig 4.3 G and I), in a region known as the preoptic area (Wullmann and Knipp, 2000). This domain is visible but much weaker at 48hpf (Fig 4.3 J and L).

In the 3dpf telencephalon, *lhx1b* expression directly abuts the AC, which now lies on the ventral side of the brain (Fig 4.3 M and N). No expression between

Figure 4.3: *lhx1b* expression 14hpf to 5dpf

Figure shows *lhx1b* expression in lateral wholemounts (A, B, D, G, J, M, O; scale bars=100µm), dorsal wholemounts (E, H, K; scale bars=100µm), whole telencephalic sections (C, F, I, L; scale bars=50µm) and ventral wholemounts (N and P; scale bars=50µm) at 14hpf (A), 19hpf (B and C), 24hpf (D-F), 36hpf (G-I), 48hpf (J-L), 3dpf (M-N) and 5dpf (O-P). Black arrowheads indicate the posterior telencephalic/diencephalic border, white dotted lines demarcate the telencephalon, and green spots mark the anterior commissure where appropriate.

At 14hpf (10 somite stage) *lhx1b* is expressed in discrete cells in the telencephalon (A), and in isolated cells in the diencephalon.

By 20ss, telencephalic *lhx1b* expression consists of a broad dorsal domain (dotted line in B), which comprises bilateral stripes of expression (C). *lhx1b* is also expressed in the posterior hypothalamus and ventral midbrain, as well as in the hindbrain rhombomeres (B).

24hpf expression of *lhx1b* shows expansion of all previously existing expression domains (D and E). Telencephalic expression (dotted line in D) abuts the border with the diencephalon (black arrowhead in D). Bilateral stripes in the telencephalon are slightly reoriented to form an inverted “V” shape (F).

At 36hpf, an additional expression domain appears in the ventral telencephalon, in the preoptic area (blue arrow in G and I). A further expression domain appears in the diencephalon, just anterior to the postoptic commissure (black arrow in G). Expression in the hypothalamus, ventral thalamus and tegmentum are expanded (G and H). Rhombomeric expression is highly organised, with each hindbrain segment displaying a stereotyped pattern of *lhx1b*-expressing cells (black arrows in H).

At 48hpf expression in the telencephalon is weaker than at earlier stages but both the bilateral stripes (dotted line in J; bracket in L) and expression in the preoptic area (blue arrow in J and L) remain. In the diencephalic preoptic area, *lhx1b* expression is very strong (black arrow in J and L). In the hindbrain, the stereotyped pattern of *lhx1b* expression remains (black arrows in K).

At 3dpf, the bilateral stripes of *lhx1b* expression lie on the ventral side of the brain, abutting the AC (blue arrowhead in M, a specimen dissected before *in situ* hybridisation). Cells in the diencephalic preoptic area also continue to express *lhx1b* (black arrows in M and N).

5dpf expression patterns show bilateral domains adjacent to the AC (blue arrowheads in O and P) and diencephalic preoptic area expression (black arrow in O).

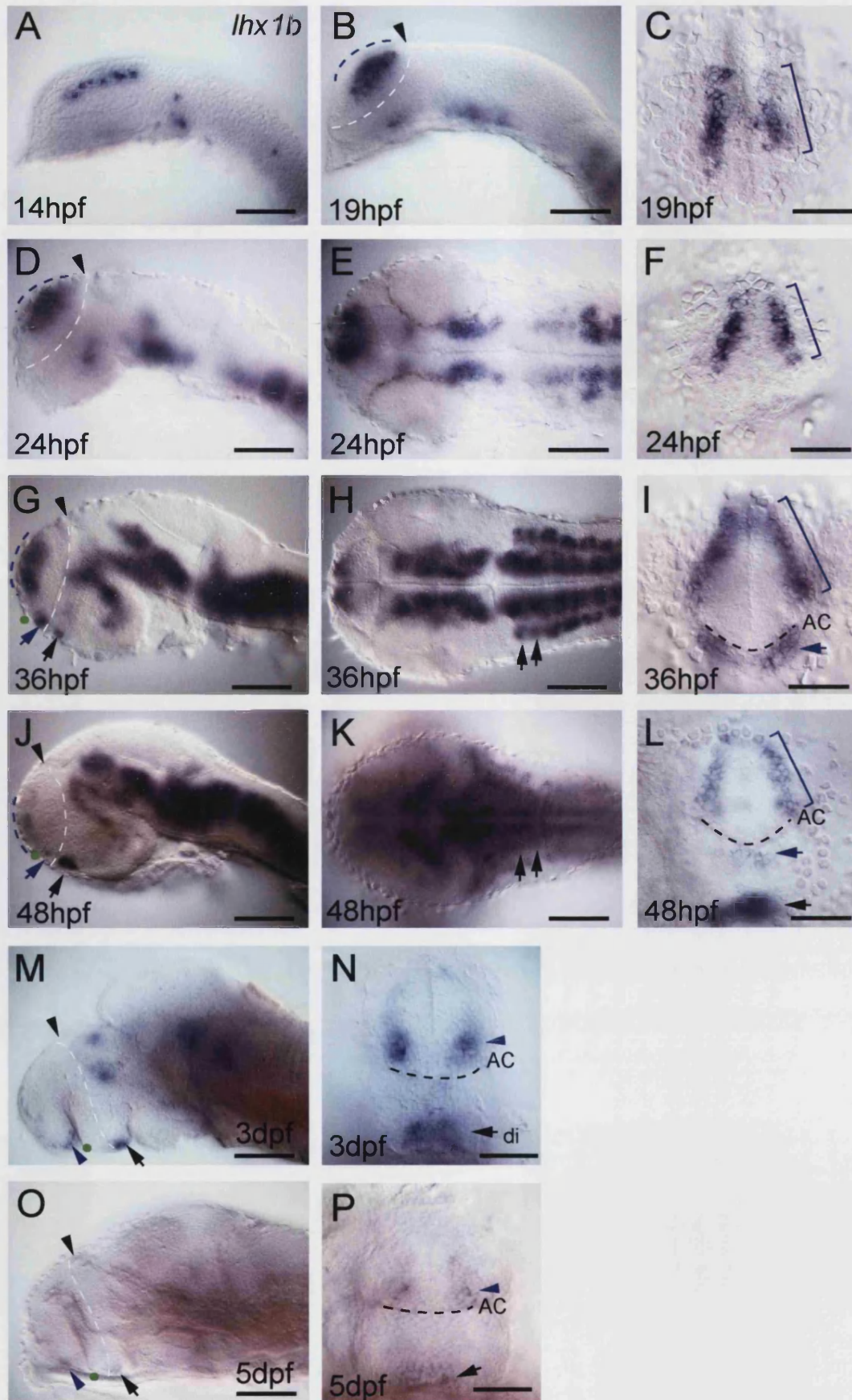


Figure 4.3

the AC and ventral telencephalic border is detected, suggesting that the domain seen at 36 and 48hpf is only transient. Similarly at 5dpf, bilateral weak domains of *lhx1b* adjacent to the AC are the only domains present in the telencephalon (Fig 4.3 O and P).

#### *Expression of lhx1b in other brain areas*

Outside the telencephalon, *lhx1b* is expressed in the ventral thalamus, dorsal thalamus, ventral midbrain and hindbrain rhombomeres from 19hpf onwards. At 36hpf, a new expression domain appears between the optic recess and the postoptic commissure (Fig 4.3G) and remains until at least 5dpf (Fig 4.3O). These cells may form part of the preoptic area (Wullmann and Knipp, 2000). In the hindbrain, the expression of *lhx1b* is very similar to expression of *lhx1a*, with each rhombomere containing two stripes of *lhx1b*-expressing cells adjacent to the boundaries and a “loop” of cells more laterally (Fig 4.3 H and K).

#### *Expression of lhx5 in the telencephalon*

In contrast to *lhx1a* and *lhx1b* expression, *lhx5* does not begin to be expressed in the telencephalon until 19hpf (20ss), where it appears as a faint domain in the dorsal telencephalon adjacent to the diencephalic border (Fig 4.4 A and B). By 24hpf, expression in the dorsal telencephalon is much more robust (Fig 4.4 C and D), and when viewed rostrally comprises broad bilateral domains which begin approximately 2-3 cell diameters from the midline (Fig 4.4E). At 24hpf, an additional expression domain appears in the ventral telencephalon (blue arrow in Fig 4.4C), which becomes stronger at 36hpf (Fig 4.4 F). This posterior domain is visible, deep from the tissue surface, in a rostral view at 36hpf, as is the now broadened, more superficial expression of *lhx5* in the dorsal telencephalon (Fig 4.4H), which appears as two inverted triangle-shaped domains. Noticeably, *lhx5* expression is much closer to the midline posteriorly than it is more anteriorly. At 48hpf, the triangular domains of *lhx5* in the dorsal telencephalon closely resemble those at 36hpf. However *lhx5* is not evenly expressed throughout the domain, being stronger in the most posterior part (Fig 4.4K). In general, *lhx5* expression in the telencephalon seems weaker than at 36hpf, although this may be due to technical reasons.

Figure 4.4: *lhx5* expression 19hpf to 5dpf

Figure shows *lhx5* expression in lateral wholemount (A, C, F, I, L, N; scale bars=100µm), dorsal wholemount (B, D, G, J; scale bars=100µm) and whole telencephalic sections (E, H, K, M, O; scale bars=50µm) at 19hpf (A-B), 24hpf (C-E), 36hpf (F-H), 48hpf (I-K), 3dpf (L-M) and 5dpf (N-O).

The telencephalon is demarcated by white dotted lines, the posterior border of the telencephalon indicated by a black arrowhead and the AC indicated with a green spot where appropriate.

At 20ss, *lhx5* expression is strongest in a broad dorso-ventral band through the diencephalon. Faint expression is also seen in the dorsal telencephalon (blue arrowheads in A and B), close to the diencephalic border (black arrowhead in A) and in the anterior hypothalamus.

By 24hpf *lhx5* is broadly expressed in the dorsal telencephalon (blue arrowheads in C and D; E) and in a small domain in the ventral telencephalon (blue arrow in C). *lhx5* continues to be expressed in a broad band of the diencephalon and in the anterior hypothalamus (C).

At 36hpf, the broad dorsal expression domain in the telencephalon (blue arrowhead in G; H) remains adjacent to the border with the diencephalon (black arrowhead in F). The ventral telencephalic expression domain is strengthened (blue arrow in F and deep out of focus in H). Additional strong expression is observed through the diencephalon and midbrain (F), as well as in the hindbrain rhombomeres (G).

48hpf expression of *lhx5* (I-K) is very similar to the expression at 36hpf. However, expression in the telencephalon is not uniform, with posterior cells expressing the highest level of *lhx5* (bracket in K).

Expression of *lhx5* in the 3dpf telencephalon is found in an anterior domain in the OB (blue arrowhead in L; bracket in M), far from the border with the diencephalon (black arrowhead in L). The ventral telencephalic domain lies between the tract of the anterior commissure and the telencephalic/diencephalic boundary (blue arrow in L).

Similarly at 5dpf (N-O), *lhx5* telencephalic expression is seen in the OB (blue arrowhead in N; bracket in O) and through a broad region of the ventral telencephalon (blue arrow in N).

OB – olfactory bulb  
di - diencephalon

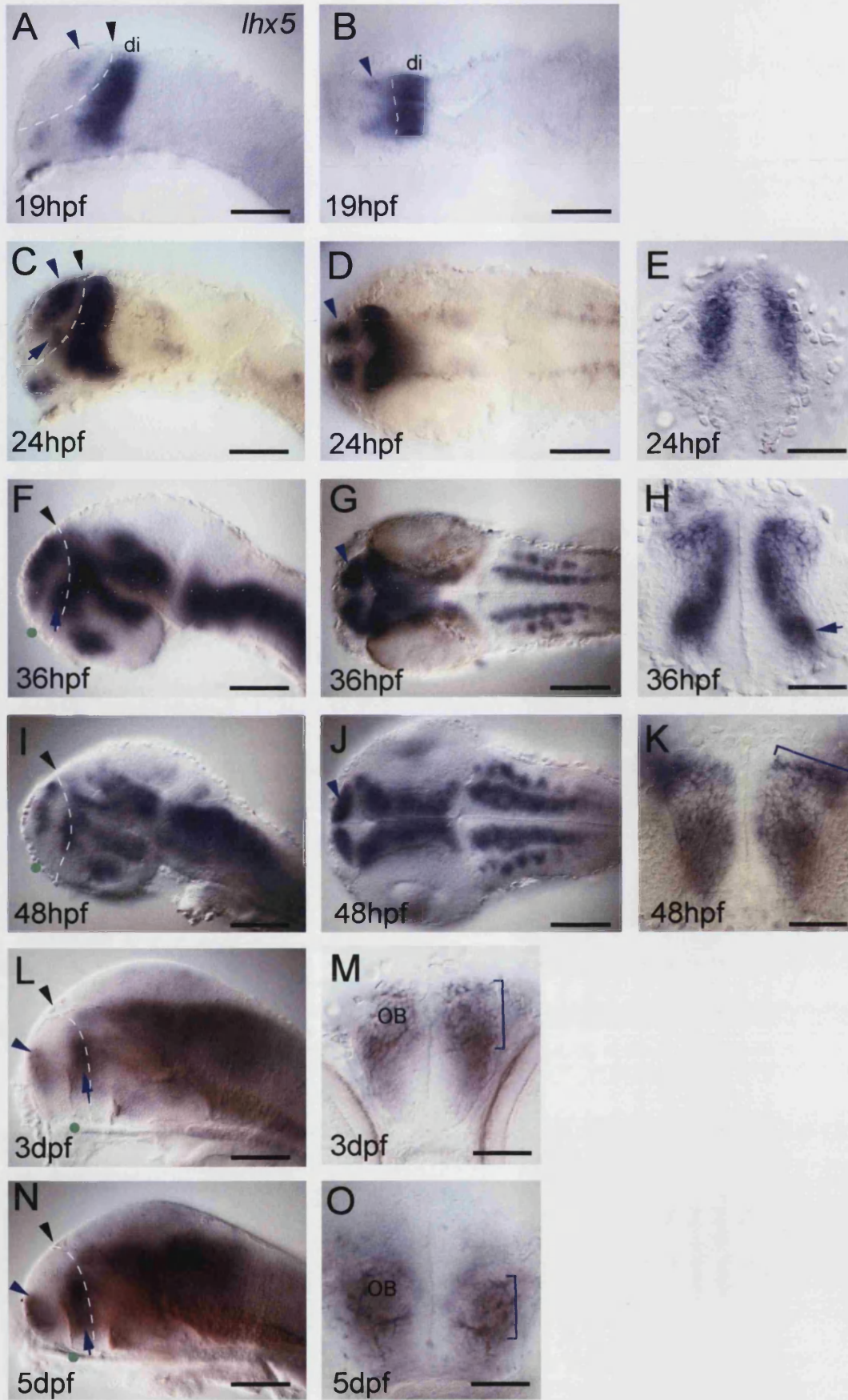


Figure 4.4

In the 3dpf telencephalon, *lhx5* expression occupies quite different positions than at 48hpf, with a strong expression domain in the OB and another caudal to the AC (Fig 4.4L). Looking at the OB shows that *lhx5* is expressed broadly in this region (Fig 4.4M), in contrast to *lhx1a*, which is restricted to the dorsal OB at this stage (Fig 4.4N). At 5dpf, the telencephalic expression domains remain similar to those at 3dpf, although all expression domains lie a little more basally within the brain (Fig 4.4 N and O).

#### *Expression of lhx5 in other brain areas*

Outside the telencephalon, *lhx5* is expressed in a broad band in the diencephalon (Fig 4.4 A and B). This expression domain appears much earlier than any telencephalic expression, around 5ss (12hpf) (Toyama et al., 1995; data not shown). An additional diencephalic expression domain appears in the anterior hypothalamus at 24hpf (Fig 4.4 C) and persists as the hypothalamus grows until at least 48hpf (Fig 4.4 F and I). *lhx5* expression elsewhere in the brain is difficult to classify without further markers, but is probably also expressed in the ventral thalamus, dorsal thalamus, the pretectum and the tegmentum, and in the hindbrain rhombomeres (Fig 4.4 F, G, I and J). In the hindbrain, *lhx5* expression bears strong resemblance to *lhx1a* expression, with lateral “loops” of expression in each rhombomere (Fig 4.4G).

#### *lhx1a and lhx5 are expressed in the olfactory bulb*

My analysis of the expression of *lhx1a* and *lhx5* shows that both genes are expressed in the olfactory bulb (OB), a telencephalon-derived structure, at 3dpf and 5dpf. To further investigate the relationship between *lhx1a* and *lhx5* and the OB, I performed *in situ* hybridisations for *mitfb*, a gene expressed in the OB (Lister et al., 2001) at a variety of stages. Without two-colour *in situ* hybridisation it is impossible to say that the genes are expressed in precisely the same domain, but *lhx1a* and *lhx5* do share similar dorsal limits of expression with *mitfb* at 48hpf (Fig 4.5 A-E) and the same dorsal limit at 3dpf (Fig 4.5 F-I). Performing a double *in situ* with *lhx1a* and *mitfb* in the same colour also suggests at least a partial overlap of the two genes at 48hpf (Fig 4.5 D). This fits well with my previous observation that *lhx1a* and *lhx5* are expressed in the OB from 3dpf, if not before.

To see whether *lhx1a* and *lhx5* expression persists in the OB beyond embryonic stages I analysed *in situ* hybridisations on cryostat sections for these

Figure 4.5: *lhx1a* and *lhx5* in the OB

A-C and G-I show lateral wholemounts, rostral to the left, scale bars=100µm. D-F show whole telencephalic sections, dorsal to the top, scale bars=50µm. The telencephalon is demarcated by white dotted lines and the AC indicated by a green spot where appropriate.

A shows the telencephalic expression of *mitfb* at 48hpf (blue arrowhead) which occupies a similar position to domain 1 of *lhx1a* (black arrowhead in B) and dorsal telencephalic expression of *lhx5* (black arrowhead in C).

D shows *mitfb* expression in a whole telencephalic section at 48hpf (blue arrowhead in D). In E, *lhx1a* (black arrowheads) and *mitfb* expression (blue arrowhead) are somewhat overlapping. F shows *mitfb* expression at 3dpf.

G-I show the similar position of *mitfb* (blue arrowhead in G), *lhx1a* (black arrowhead in H) and *lhx5* (black arrowhead in I) expression at 3dpf.

J shows *lhx1a* expression in isolated cells (black arrowhead) in the olfactory bulbs at 1 month post fertilisation. Scale bar=100µm

K shows *lhx5* expression in isolated cells (black arrowhead) and in the bulb periphery (black arrow) at 1 month post fertilisation. Scale bar=100µm

OB – olfactory bulb

tel – telencephalon

d1 – domain 1 of *lhx1a* expression

d2 – domain 2 of *lhx1a* expression

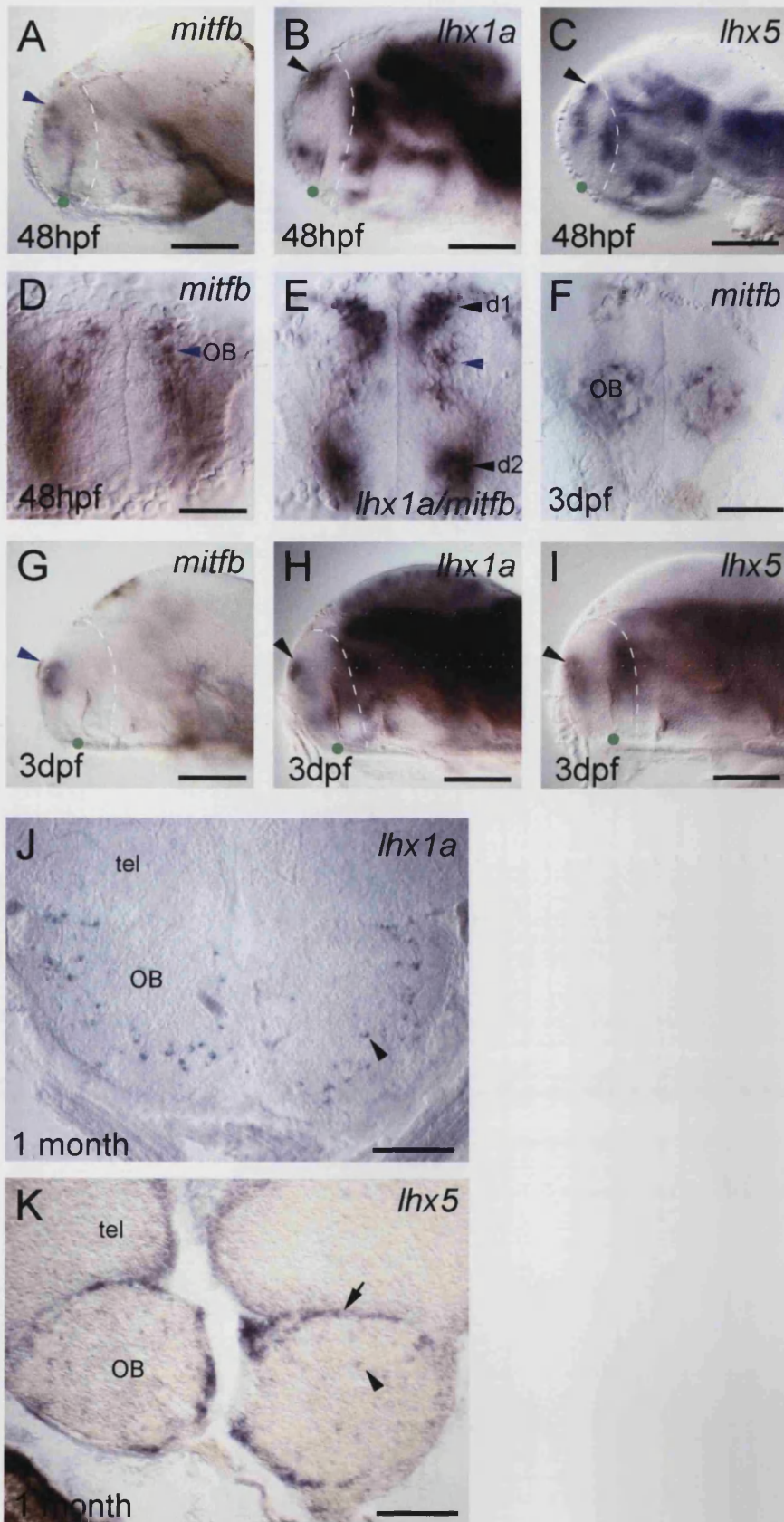


Figure 4.5

genes at 1 month post fertilisation in specimens prepared by M. Mione and C. Kwong. *Lhx* gene expression is known to persist in telencephalic regions until adult stages (Moreno et al., 2004) and indeed in juvenile zebrafish *lhx1a* and *lhx5* continue to be expressed in a subset of cells in the OB. *lhx1a* is expressed in scattered cells in an outer lamina of the bulb, in the position of mitral cells (Fig 4.5 J; Mione et al., 2001 and M. Mione, personal communication). *lhx5* is expressed strongly in the periphery of the bulb, probably in the olfactory nerve layer, and also in scattered cells within the bulb (Fig 4.5 K). Further expression analysis to establish whether *lhx1a*- and *lhx5*-expressing populations overlap was attempted but was unsuccessful.

#### *Expression of lhx1a, lhx1b and lhx5 in combination*

Observations of the expression patterns of single *Lhx* genes through development led to the question of whether the domains of *lhx1a*, *lhx5* and *lhx1b* are overlapping in the CNS, especially within the telencephalon. To address this question I used two-colour double *in situ* hybridisation techniques to label pairs of genes simultaneously, and performed these experiments at 24hpf when the *Lhx* expression patterns are relatively simple and at 32hpf, when they are more complex. Technical difficulties hindered attempts to perform these experiments at later stages.

#### *lhx1a and lhx1b*

In the telencephalon, *lhx1a* and *lhx1b* are expressed in strikingly co-ordinated domains with respect to each other (Fig 4.6 A, B, C and E). Of the two *lhx1a* domains, domain 1 is exclusive of *lhx1b* expression (Fig 4.6 B and B'), while domain 2 overlaps completely with the *lhx1b*-expressing domain (Fig 4.6 B and B''). The *lhx1b* domain extends posteriorly from *lhx1a* domain 2 towards the midline. The co-ordinated expression of these two genes is very similar at both 24hpf and 32hpf (Fig 4.6 B and E).

Elsewhere in the brain, *lhx1a* and *lhx1b* have almost completely overlapping expression domains at 24hpf, although *lhx1a* is slightly more broadly expressed in the ventral diencephalon (Fig 4.6 A). Similarly, at 32hpf, expression of the two genes in the midbrain and hindbrain is completely overlapping (Fig 4.6 C and D). Only one region of the dorsal hypothalamus expresses *lhx1a* exclusive of *lhx1b* (Fig 4.6 C).

Figure 4.6: *lhx1a*, *lhx1b* and *lhx5* in combination

Figures show double *in situ* hybridisations for *lhx1a* with *lhx1b* (A-E), *lhx1a* with *lhx5* (F-J) and *lhx5* with *lhx1b* (K-P). Specimens are shown at 24hpf (A-B, F-G, K-M) and 32hpf (C-E, H-J, N-P). Scale bars represent 100µm in lateral and dorsal wholemounts, 50µm in whole telencephalic and vibratome sections, and 5µm in the highly magnified images in B', B'', G' and G''. A white dotted line demarcates the telencephalon in lateral wholemounts.

*lhx1a* and *lhx1b* are expressed in extensively overlapping domains at both 24hpf and 32hpf (A, C and D), except in the ventral thalamus at 32hpf where they are expressed in adjacent domains (black arrowhead in C). In the telencephalon, *lhx1b* expression overlaps with domain 2 of *lhx1a* at both 24hpf (red arrow in A, B, and region shown magnified in B'') and at 32hpf (red arrow in C and E). However *lhx1b* expression does not overlap with *lhx1a* domain 1 at either stage (red arrowhead in A, B, C and E; region shown magnified in B').

*lhx1a* and *lhx5* expression also overlaps extensively at 24hpf (black arrowhead in F), and at 32hpf (black arrowheads in H; I) although *lhx1a* is expressed alone in the midbrain (H). In the telencephalon, *lhx5* is expressed in a broad domain of the dorsal telencephalon which encompasses *lhx1a* domain 1 (blue arrowhead in F, G, H and J; region shown magnified in G'). Domain 2 of *lhx1a* expression, however, lies just ventral to the *lhx5* expression domain at both 24hpf and 32hpf (blue arrow in F, G, H and J; region shown magnified in G'').

*lhx5* and *lhx1b* expression overlaps somewhat at 24hpf (K and L), most strikingly in the ventral thalamus (black arrowhead in K). At 32hpf, expression is still overlapping in the ventral thalamus (black arrowhead in N) but *lhx1b* is expressed alone in the midbrain (N). In the telencephalon, *lhx1b* expression lies medial to the broad domain of *lhx5* expression at 24hpf (M). At 32hpf, a similar pattern is evident, although *lhx1b* expression is not level with the dorso-posterior border of *lhx5* (arrows in O). A horizontal 50µm vibratome section through the telencephalon at the level shown in N confirms the more medial expression of *lhx1b* (blue arrowhead in P), with a possible zone of overlap of the two genes (black bracket in P).

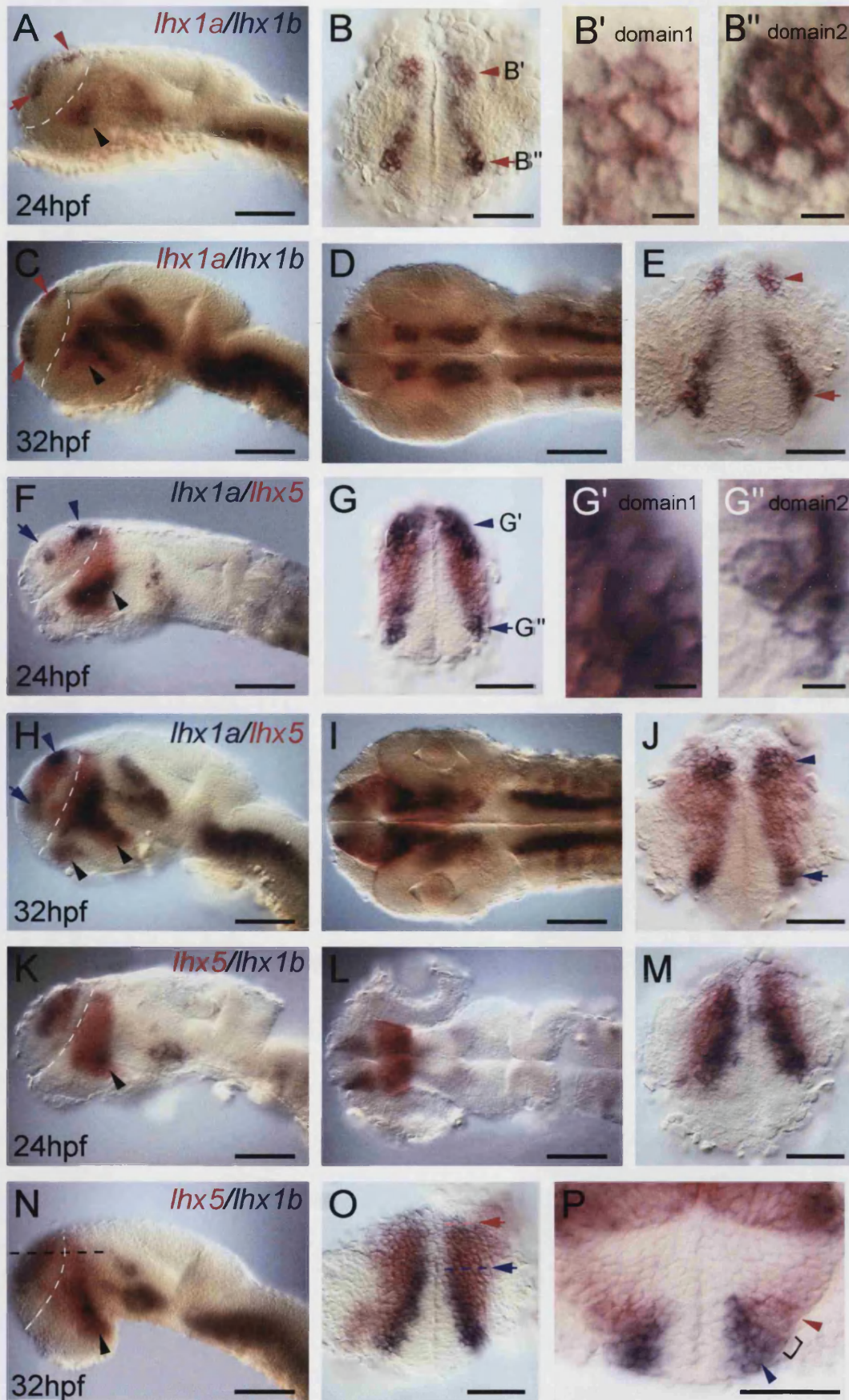


Figure 4.6

### *lhx1a and lhx5*

In the telencephalon, *lhx1a* and *lhx5* also show strikingly co-ordinated expression domains with respect to each other (Fig 4.6 F, G, H and J). Both at 24hpf and 32hpf, *lhx1a* domain 1 falls completely within the *lhx5* domain (Fig 4.6 G, G' and J). However, the same is not true for *lhx1a* domain 2, which lies juxtaposed to, but not within, the *lhx5* domain (Fig 4.6 G, G'' and J). Assessment of this was made by high power light microscopy and confirmed by lateral wholemount views that show domain 2 of *lhx1a* lying just dorsal to *lhx5* expression (Fig 4.6 F and H). At 48hpf, the relationship between these two domains is even clearer, with *lhx1a* domain 2 positioned below the anterior limit of *lhx5* expression (data not shown).

Outside the telencephalon, the *lhx5* expression domains in the diencephalon encompass all diencephalic *lhx1a*-expressing regions and extend more broadly, both at 24hpf and 32hpf (Fig 4.6 F and H). The two genes also overlap completely in the hindbrain at 32hpf (Fig 4.6I); at 24hpf *lhx5* is not highly expressed in the hindbrain. The midbrain is the only region where the two genes are not overlapping – here *lhx1a* is expressed alone at both 24hpf and 32hpf (Fig 4.6 F and H).

### *lhx5 and lhx1b*

Again the telencephalon shows an interesting co-ordination of the expression domains of *lhx5* and *lhx1b*. At 24hpf, *lhx1b* expression lies along the medial edge of *lhx5* expression, probably overlapping to some extent (Fig 4.6 M). The A-P limits of the two genes are very similar at 24hpf, but at 32hpf, *lhx1b* expression has shifted anteriorly with respect to *lhx5* (Fig 4.6 O). This is confirmed by vibratome sections cut through the telencephalon of stained specimens – dorsal-posterior sections contain only *lhx5*-expressing cells and ventral-anterior sections only *lhx1b*-expressing cells. A mid-telencephalic vibratome section contains both populations with a possible zone of overlap between them (Fig 4.6P).

Outside the telencephalon, the expression of *lhx5* and *lhx1b* is very similar to the expression of *lhx1a* and *lhx1b*. In the diencephalon and hindbrain the two genes are overlapping; the midbrain is the only area to express *lhx1b* alone (Fig 4.6 K, L and N).

### *Summary*

Comparison of the expression domains of *lhx1a*, *lhx1b* and *lhx5* using double *in situ* hybridisation techniques reveal precise spatial co-ordination of Lhx-expressing domains in the telencephalon. Combining the results for the three genes (summarised in Fig 4.7) indicates that domain 1 of *lhx1a* overlaps completely with *lhx5* expression, but is exclusive of *lhx1b*. Domain 2 of *lhx1a*, however, is the other way round, overlapping completely with *lhx1b* expression but exclusive of *lhx5*. *lhx1b*, which forms bilateral stripes in an inverted V-shape, lies just medial to *lhx5* expression, possibly overlapping slightly at both 24hpf and 32hpf. Between these two timepoints, *lhx1b* expression shifts relative to *lhx5*, moving slightly more anteriorly. However, all other relationships between the gene expression domains remain constant between 24hpf and 32hpf.

Outside the telencephalon, the Lhx genes studied here are frequently found in overlapping expression domains. This is especially true for *lhx1a* and *lhx1b* that are particularly closely overlapping throughout the brain, except for in a region of the ventral thalamus. *lhx5* has a more restricted expression pattern than *lhx1a* or *lhx1b*, but in the diencephalon *lhx1a* and *lhx1b* fall completely within the *lhx5* domain. In the hindbrain, all three genes are expressed in indistinguishable domains.

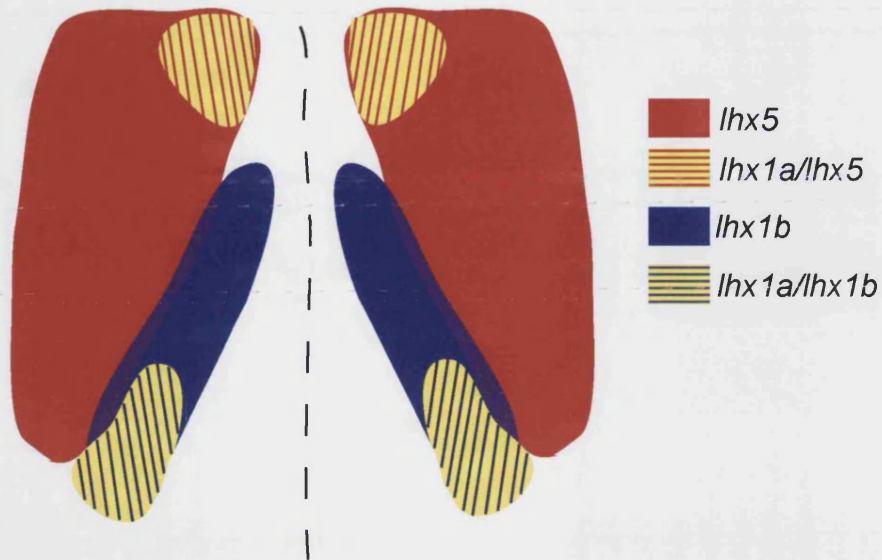


Figure 4.7: co-ordinated expression of *lhx1a*, *lhx1b* and *lhx5* in the telencephalon

Schematic diagram showing an anterior view of the whole telencephalon at 32hpf. Domain 1 of *lhx1a* expression overlaps with *lhx5* (yellow and red stripes), domain 2 overlaps with *lhx1b* (yellow and blue stripes). *lhx5* (red) and *lhx1b* (blue) expression domains are adjacent but almost entirely non-overlapping.

### *lhx1a, lhx1b and lhx5 expression and neuronal phenotype*

Current evidence suggests that Lhx genes are switched on in neuronal progenitor cells at or around the time of their final mitosis (reviewed in Shirasaki and Pfaff, 2002), i.e. when they become differentiated neurons. Rather than assume that this was the case for the telencephalic populations of *lhx1a*, *lhx1b* and *lhx5*, I wanted to test this directly using the pan-neuronal *Tg(HuC:GFP)* line (Park et al., 2000). This line of fish expresses GFP under the control of the HuC promoter sequences in all postmitotic neurons with an approximate lag time of 4h (Lyons et al., 2003). By performing *in situ* hybridisation for the Lhx genes using a red fluorescent substrate, and combining this with immunostaining for GFP, I was able to analyse coexpression in detail with confocal microscopy. These experiments were performed at both 24h and 36hpf; the data presented is only for the later time point to reduce the possibility that the time lag between cells becoming neurons and switching on GFP would be responsible for the results.

In general the results indicate that telencephalic Lhx gene expression domains coexpress HuC at 36hpf. This is shown for domains 1 and 2 of *lhx1a* (Fig 4.8 A), for *lhx1b* (Fig 4.8 B) and for the dorsal domain of *lhx5* (Fig 4.8 C). Interestingly, the ventral domain of *lhx5* expression in the telencephalon does not coexpress HuC (Fig 4.8 F). This may reflect a later birth of these cells compared to those in the dorsal telencephalon (see Fig 4.4 C).

In the diencephalon, the relationship between Lhx genes and HuC is more complex. All genes show regions of coexpression with HuC and regions of exclusivity. *lhx1a* and *lhx1b* largely coexpress HuC (Fig 4.8 D and E) while *lhx5* is largely exclusive of HuC in the caudal diencephalon (Fig 4.8 G).

### *lhx1a, lhx1b and lhx5 expression and pallial markers*

Having characterised the expression domains of *lhx1a*, *lhx5* and *lhx1b* both individually and in combination with each other, I wanted to know how expression in the telencephalon relates to markers of the dorsal telencephalon or pallium. The subdivision of the telencephalon into pallial (dorsal) and subpallial (ventral) regions has not only anatomical but also functional relevance since the pallium gives rise to neocortical structures (in mammals) and the subpallium to the basal ganglia (reviewed in Wilson and Rubenstein, 2000). Understanding these subdivisions in

Figure 4.8: *lhx1a*, *lhx1b* and *lhx5* in the *Tg(HuC:GFP)* line

All figures show single, transverse, confocal sections through 36hpf specimens double-labelled by anti-GFP antibody (green) and *in situ* hybridisation (red) for either *lhx1a* (A and D), *lhx1b* (B and E) or *lhx5* (C, F and G). Single sections through the telencephalon with red and green channels superimposed are presented in the first column (A-C), followed by the red (A', B' and C') and green channels alone (A'', B'' and C'') in adjacent panels. D to G show further sections from the same specimens as in A-C through more caudal regions of the telencephalon (F) or the diencephalon (D, E and G).

A shows extensive coexpression of *lhx1a* and HuC in a single section through the telencephalon of a 36hpf embryo. Domain 1 of *lhx1a* (white arrowhead) is more prominent in this section than domain 2 (white arrow); a few of these cells express little or no HuC:GFP.

B shows that *lhx1b* expression (B') lies at the medial edge of HuC (B'') expression.

C shows extensive coexpression of *lhx5* (C') and HuC (C'') in a single section through the telencephalon.

D and E show coexpression of *lhx1a* (D) or *lhx1b* (E) and HuC in single sections through the diencephalon.

F shows the HuC-negative ventral telencephalic domain of *lhx5* (white arrow); in addition medial cells in the posterior dorsal telencephalon express little HuC (white arrowhead). In G, a section through the diencephalon reveals further *lhx5* expression exclusive of HuC (white arrow in G).

d1 – domain 1 of *lhx1a* expression

d2 – domain 2 of *lhx1a* expression

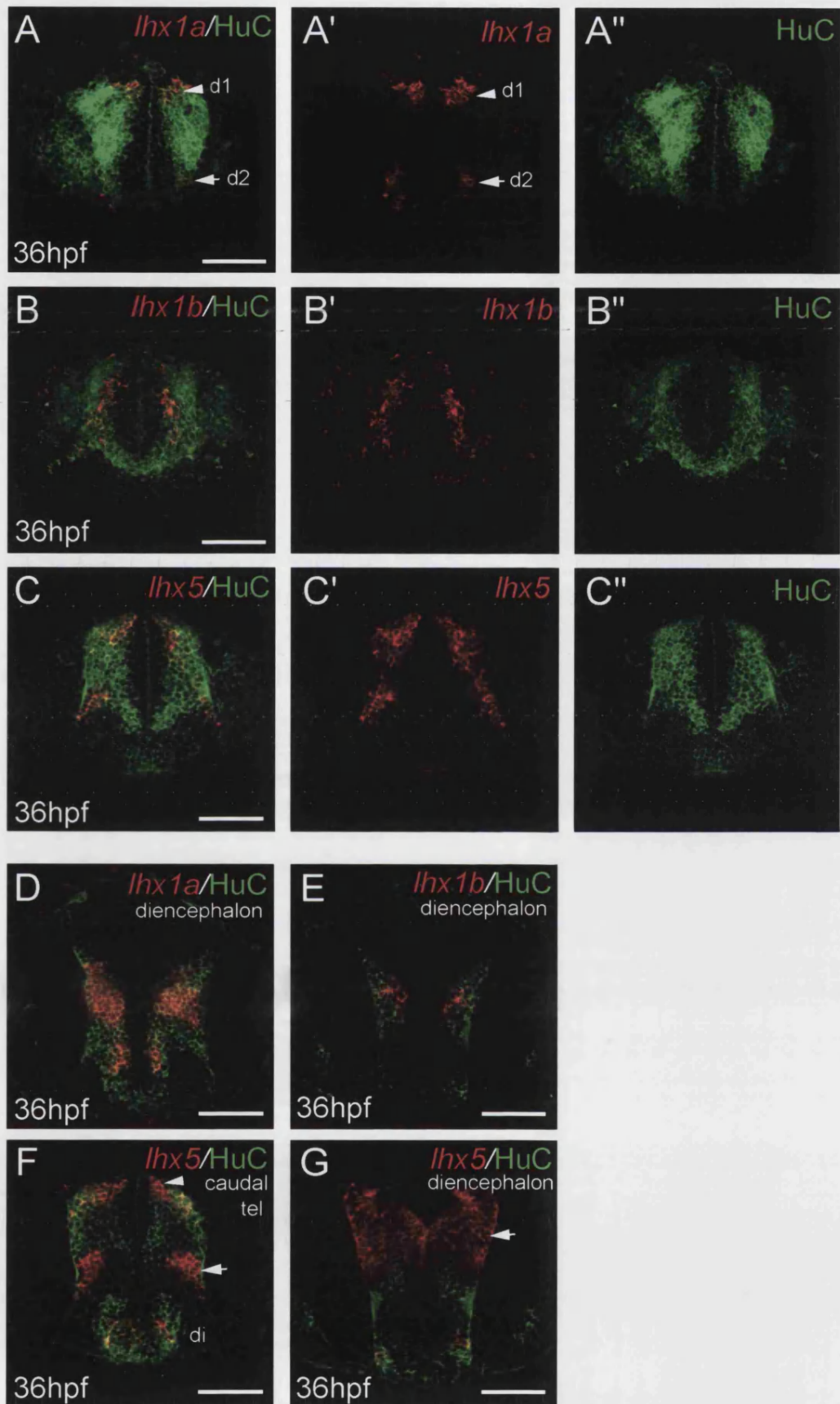


Figure 4.8

zebrafish, and how the Lhx genes are expressed with respect to them is essential background for any work addressing Lhx gene function.

I performed double *in situ* hybridisation at 24hpf and 36hpf for the Lhx genes with two dorsal telencephalic markers, *emx3* (Kawahara and Dawid, 2002; Morita et al., 1995), and *tbr1* (Mione et al., 2001; Yonei-Tamura et al., 1999). *Emx1* and *Tbr1* are largely overlapping but have slightly different pallial expression domains in both chick and mouse (Puelles et al., 2000). Zebrafish *emx3* was originally designated *emx1*, but subsequent identification of a gene more similar to mouse *Emx1* lead to its reclassification. No *emx3* group members are known in mammals (Derobert et al., 2002), but telencephalic expression patterns for zebrafish *emx1*, *emx2* and *emx3* are very similar (Kawahara and Dawid, 2002). Again, technical difficulties prevented these experiments from being performed at later stages but even between these two close timepoints differences were observed in the relative positions of *lhx1a*, *lhx5* and *lhx1b* and the dorsal telencephalic markers.

#### *Double labelling with emx3*

The *Emx* genes are well-characterised and consistent markers of the pallium in many vertebrate species (Fernandez et al., 1998; Puelles et al., 2000). At 24hpf and 36hpf, *emx3* is expressed in the zebrafish posterior dorsal telencephalon (Fig 4.9 A and C) in bilateral domains a few cell diameters from the midline (Fig 4.9 B and D).

Looking anteriorly, *emx3* also appears to be expressed in presumed ventricular zone cells, but at much lower levels.

In double labelling with *lhx1a* at 24hpf, *lhx1a* domain 1 lies within the most posterior part of the *emx3* domain. *lhx1a* domain 2 also partially overlaps with the *emx3* domain but extends slightly more anteriorly (Fig 4.9 E and F). At 36hpf *lhx1a* domain 2 lies completely outside the *emx3* domain. *lhx1a* domain 1, however, continues to occupy the same position in the most posterior part of the *emx3* domain (Fig 4.9 G and H).

A similar pattern is found with double labelling for *emx3* and *lhx1b*. *lhx1b* expression extends slightly beyond the anterior limits of *emx3* at 24hpf (Fig 4.9 I and J). However, by 36hpf, approximately two thirds of the *lhx1b* expression domain lies anterior to the *emx3* domain (Fig 4.9 K and L).

With *lhx5*, the expression domains are more difficult to distinguish because *lhx5* and *emx3* both occupy a large area of the dorsal telencephalon. At 24hpf, *lhx5*

Figure 4.9: *lhx1a*, *lhx1b* and *lhx5* with pallial markers

Figures show *in situ* hybridisation for the pallial markers *emx3* (A-D) and *tbr1* (S-T) and double *in situ* hybridisations for *emx3* with *lhx1a* (E-H), *lhx1b* (I-L) and *lhx5* (M-R) and for *tbr1* with *lhx1a* (U and V). Specimens are shown at 24hpf (A-B, E-F, I-J, M-N, Q) and 36hpf (C-D, G-H, K-L, O-P, R-V). Scale bars represent 100µm in lateral views, and 50µm in whole telencephalic and vibratome sections. In all lateral wholemounds anterior is to the left, in telencephalic sections to the top and in vibratome sections to the bottom. White dotted lines demarcate the telencephalon in lateral wholemounds.

Figures A-D show expression of *emx3* in the dorsal telencephalon in lateral wholemounds (A and C) and whole telencephalic sections (B and D), at 24hpf (A and B) and 36hpf (C and D). The position of the anterior commissure (AC) is indicated in C.

Figures E-H show expression of *emx3* (red) with *lhx1a* (blue) in lateral wholemounds (E and G) and whole telencephalic sections (F and H). (E-F) At 24hpf, *lhx1a* domain 1 (blue arrowhead) and domain 2 (blue arrow) lie within the *emx3* domain (red arrow shows anterior limit). (G-H) At 36hpf *lhx1a* domain 2 (blue arrow) lies anterior to the *emx3* domain (red arrow shows limit); *lhx1a* domain 1 (blue arrowhead) lies within the *emx3* domain.

Figures I-L show expression of *emx3* (red) with *lhx1b* (blue) in lateral wholemounds (I and K) and whole telencephalic sections (J and L). (I-J) At 24hpf, the anterior limit of *lhx1b* (blue arrow) extends just beyond that of *emx3* (red arrow). (K-L) At 36hpf, *lhx1b* expression (blue arrow) extends far beyond the limit of *emx3* expression (red arrow).

Figures M-R show expression of *emx3* (red) and *lhx5* (blue) in lateral wholemounds (M and O), whole telencephalic sections (N and P) and 35µm vibratome sections (Q and R). (M-N) At 24hpf, *emx3* and *lhx5* are almost entirely coincident in the telencephalon. A vibratome section at the level shown by the black dotted line in M shows the coincident expression domains (Q). (O-P) At 32hpf, the anterior limit of *lhx5* expression (blue arrow) extends beyond the limit of *emx3* expression (red arrow). A vibratome section at the level shown by the black dotted line in O shows a region of overlap (R).

Figures S-T show expression of *tbr1* in the 36hpf telencephalon; expression extends to the AC (labelled in S) and into the eminentia thalami (black arrowhead in S).

Figures U-V show expression of *tbr1* (red) with *lhx1a* (blue) in lateral wholemound (U) and telencephalic section (V). Domain 1 (blue arrowhead) domain 2 (blue arrow) of *lhx1a* lie within the *tbr1* domain at 36hpf.

d1 – domain 1 of *lhx1a* expression

d2 – domain 2 of *lhx1a* expression

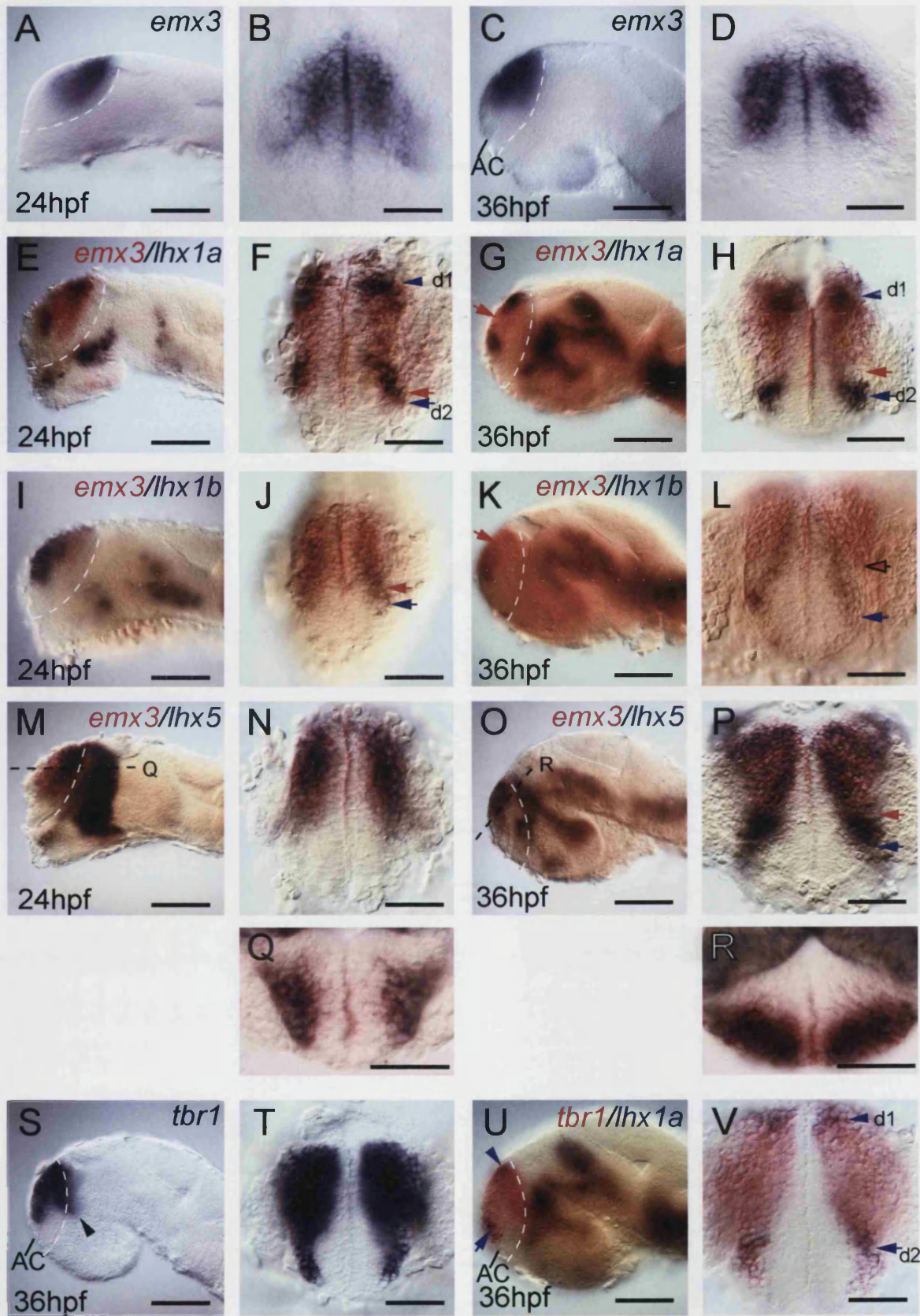


Figure 4.9

and *emx3* seem to be completely overlapping (Fig 4.9 M and N); vibratome sections through this region show that the genes have similar A-P and D-V extents in the telencephalon (Fig 4.9 Q and data not shown). At 36hpf, *lhx5* expression remains largely overlapping with *emx3*, but extends slightly beyond the anterior limit of *emx3* expression (Fig 4.9 O and P). Vibratome sections confirm these observations (Fig 4.9 R and data not shown). The ventral domain of *lhx5* expression, as seen deep from the tissue surface in Fig. 4.9 P, lies outside the *emx3* domain at all stages.

#### *Double labelling with tbr1*

*tbr1* is another pallial marker expressed in a variety of species including zebrafish (Mione et al., 2001; Puelles et al., 2000; Yonei-Tamura et al., 1999). As in chick and mouse, *tbr1* expression in zebrafish is broader than *emx3*, extending in the mantle layer of the anterior telencephalon almost to the level of the anterior commissure (Fig 4.9 S and T). Consequently, in double labelling experiments with *lhx1a*, both *lhx1a* domains lie within the *tbr1* expression domain (Fig 4.9 U and V). This is consistently seen up to 48hpf (data not shown). Following from observations of *lhx1a* with *tbr1*, the dorsal telencephalic domains of *lhx5* and *lhx1b* would be inferred to lie within the *tbr1* domain at 24, 36 and 48hpf. This is because neither *lhx1b* or *lhx5* extends more anteriorly than *lhx1a* at these stages.

#### *Summary of Lhx genes with pallial markers*

Examination of the Lhx genes with *emx3* and *tbr1* reveals differences in the areas covered by the two pallial markers, with implications for the pallial nature of Lhx expression domains. *emx3* has a smaller expression domain than *tbr1*, and double labelling with Lhx genes reveals that although the dorsal domains of *lhx1a*, *lhx1b* and *lhx5* mostly overlap with *emx3* at 24hpf, they all extend beyond its anterior limit at 36hpf. This is in marked contrast to results with *tbr1*, where *lhx1a* is and *lhx1b* and *lhx5* would be encompassed within the *tbr1* expression domain at all stages up to 48hpf. It therefore seems likely that all of the primary expression domains of *lhx1a*, *lhx1b* and *lhx5* lie within the pallium.

#### *lhx1a, lhx1b and lhx5 expression and a subpallial marker*

Having made a detailed examination of the relationship between *lhx1a*, *lhx1b* and *lhx5* and the dorsal telencephalic markers *emx1* and *tbr1*, I wanted to look at how the

same genes relate to a ventral telencephalic or subpallial marker. Although the primary Lhx expression domains lie within the pallium, as described above, I wanted to further investigate the relationship between pallial and subpallial areas. As a marker I used the *Tg(dlx4/6:GFP)* line, which expresses GFP under the control of the *dlx4/6* promoter. A more detailed characterisation of this line is presented in chapter 3, but the *dlx4/6* pair of genes are well-characterised markers of the subpallium and GFP expression in this line replicates their endogenous telencephalic expression (Zerucha et al., 2000). I used a combination of *in situ* hybridisation with a fluorescent substrate for either *lhx1a*, *lhx1b* or *lhx5* with immunohistochemistry for GFP to look at how these two cell populations relate to each other at 24hpf and 36hpf.

At 24hpf, no coexpression of *lhx1a* and *dlx4/6* is seen in the telencephalon. Both *lhx1a* domains lie dorsal to the *dlx4/6*-expressing cells with domain 2 adjacent to the *dlx4/6* expression (Fig 4.10C). Coexpression (as indicated by yellow in a red/green overlay) is however seen more caudally in the diencephalon in a group of approximately ten cells (data not shown). At 36hpf, *lhx1a* domain 1 still lies posterior to any GFP expression, whereas domain 2 overlaps with *dlx4/6*-expressing cells (Fig 4.10D). Strikingly, there is no discernable coexpression of *lhx1a* and *dlx4/6* in this region, with the two markers seemingly restricted to separate but intermingled cell populations. More caudally in the diencephalon, a small population of cells coexpress *lhx1a* and *dlx4/6*, but the majority of cells express either one marker or the other (Fig 4.10E).

*lhx1b* is very much like domain 2 of *lhx1a* in its relation to *dlx4/6* expression. At 24hpf, *lhx1b* is always found posterior, but directly adjacent, to *dlx4/6* expression (Fig 4.10I). However, by 36hpf, *dlx4/6*-expressing and *lhx1b*-expressing cells are in the same region with no coexpression evident (Fig 4.10J). More caudally, in the diencephalon, *dlx4/6* and *lhx1b* remain mutually exclusive, appearing in adjacent but non-overlapping domains (Fig 4.10K). The transient expression domain of *lhx1b* in the preoptic area is not visible in these specimens.

*lhx5* shows similar patterns with respect to *dlx4/6* expression. At 24hpf, *lhx5* expression within the telencephalon lies lateral to *dlx4/6* expression, with no coexpression of the two genes (Fig 4.10F). In the diencephalon, *dlx4/6* and *lhx5* are again mutually exclusive with a small group of *dlx4/6*-expressing cells lying within the broad domain of diencephalic *lhx5* expression (data not shown). At 36hpf, the

Figure 4.10: *lhx1a*, *lhx5* and *lhx1b* in the *Tg(dlx4/6:GFP)* line

A and B show lateral wholemount views of an *in situ* hybridisation for *dlx2* at 24hpf (A) and the expression of GFP in the at 32hpf (B). Scale bars=100µm

Figures show *in situ* hybridisation for *lhx1a* (C-E), *lhx5* (F-H) or *lhx1b* (I-K) combined with immunohistochemistry for GFP in the *Tg(dlx4/6:GFP)* line. All figures show single transverse confocal sections; scalebar in C represents 100µm in C-K.

*lhx1a* expression (arrowhead in C) lies posterior to *dlx4/6* expression (arrow in C) in the 24hpf telencephalon. At 36hpf, the two cell populations are mixing but not coexpressing (arrow in D). In the 36hpf diencephalon, *lhx1a* (arrowhead) and *dlx4/6* (arrow in E) may have a small region of coexpression.

*lhx5* expression in the 24hpf telencephalon (arrowhead in F) lies lateral to *dlx4/6* expression (arrow in F). At 36hpf, the two cell populations are overlapping and mixing but not coexpressing (arrow in G). The posterior domain of *lhx5* in the telencephalon (arrowhead in H) is also exclusive of, and lies lateral to, *dlx4/6* expression (arrow in H).

*lhx1b* expression in the 24hpf telencephalon (arrowhead in I) lies posterior to *dlx4/6* expression (arrow in I). At 36hpf, the two cell populations are found in the same region but there is no coexpression (arrow in J). More caudally in the diencephalon, *lhx1b*-expressing (arrowheads) and *dlx4/6*-expressing (arrows) cells lie in adjacent non-overlapping domains.

tel – telencephalon

di – diencephalon

d2 – domain 2 of *lhx1a* expression

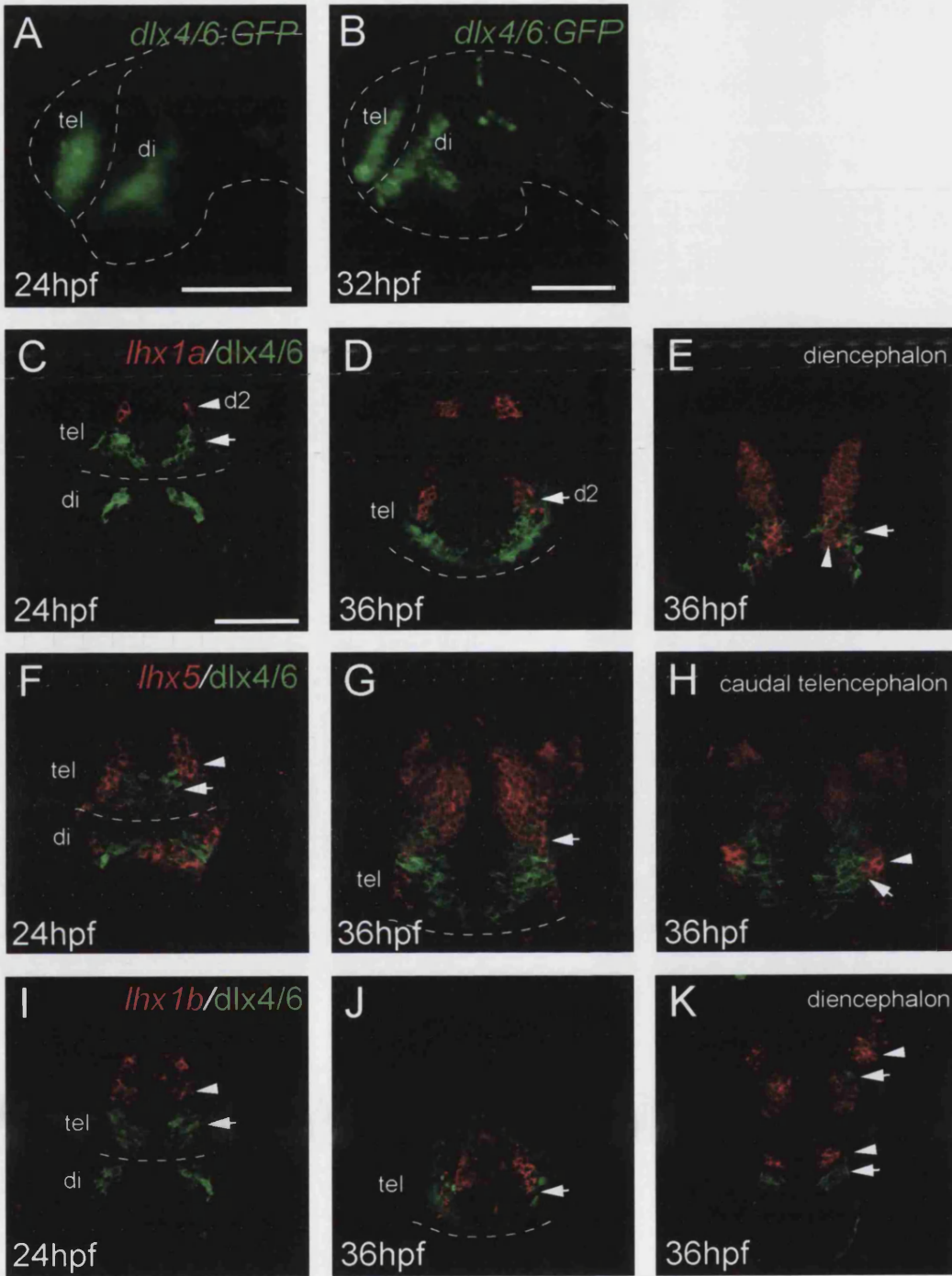


Figure 4.10

telencephalic populations of *lhx5* and *dlx4/6* are intermingled, but as with *lhx1a* and *lhx1b* no coexpression is evident (Fig 4.10G). In addition, the ventral telencephalic domain of *lhx5* expression is exclusive of and lies lateral to *dlx4/6* expression (Fig 4.10H).

*Summary of Lhx relationship to a subpallial marker*

The striking feature of Lhx expression in the *Tg(dlx4/6:GFP)* line is how rarely any coexpression of *lhx1a*, *lhx5* or *lhx1b* with *dlx4/6* is seen. In the telencephalon, there is no evidence of coexpression at either 24 or 36hpf. However, Lhx-expressing and *dlx4/6*-expressing cell populations are intermingled at 36hpf, and this has interesting implications for the separation of pallial and subpallial neurons in the mantle zone. Evidence from the diencephalon indicates a similar lack of coexpression; only in one part of the ventral diencephalon is there a small region where *lhx1a* and *dlx4/6* are coexpressed.

## 4.4 Discussion

I have performed a detailed analysis of the expression of three Lhx genes – *lhx1a*, *lhx1b* and *lhx5* – in the zebrafish telencephalon from early embryonic to postembryonic stages. By analysing expression of these Lhx genes singly, in combination with each other and in combination with markers for differentiated neurons as well as for pallial and subpallial regions of the telencephalon, I have gleaned information about the development of the telencephalon and the regions within it. Although totally descriptive at this stage, this information provides the necessary background for any experiments probing the functions of these genes.

### *Expression of lhx1a, lhx1b and lhx5 subdivides the dorsal telencephalon*

In the course of this expression analysis, I have mainly considered the domains of *lhx1a*, *lhx1b* and *lhx5* that persist through the entire period of embryogenesis. These are all dorsal telencephalic domains and consist of two *lhx1a* domains (domain 1 that is initially close to the posterior border with the diencephalon, and domain 2 that lies more anteriorly), a broad *lhx5* domain and an inverted V-shaped *lhx1b* domain.

Double *in situ* hybridisation analysis indicates that the dorsal telencephalon is subdivided at 24hpf and 32hpf by spatially co-ordinated and overlapping regions of expression of these Lhx genes (Fig 4.7). Thus domain 1 of *lhx1a* overlaps with the posterior part of *lhx5* expression, while domain 2 of *lhx1a* overlaps with the anterior part of *lhx1b* expression. *lhx5* and *lhx1b* are largely mutually exclusive, but may overlap slightly at the medial edge of *lhx5* expression. The dorsal telencephalon is therefore subdivided into four molecularly distinct regions – a *lhx1a/lhx5* region, a *lhx1a/lhx1b* region, a *lhx5*-only region and a *lhx1b*-only region.

Coexpression of multiple LIM-HD proteins within a single cell is thought to underlie the combinatorial specification of cell fate (Dawid and Chitnis, 2001; Hobert and Westphal, 2000). However, two-colour wholemount *in situ* hybridisation analysis with non-fluorescent substrates is not precise enough to detect coexpression at the single cell level. It would therefore be exciting to extend the analysis I have performed here by using two colour fluorescent *in situ* hybridisation techniques (Denkers et al., 2004) or by using specific antibodies to the LIM-HD proteins. Unfortunately, no such antibodies are currently available, but an

alternative strategy would be to develop a transgenic GFP line for one of the Lhx genes and combine this with fluorescent in situ hybridisation techniques as I have used in this chapter.

Nonetheless the subdivision of the zebrafish dorsal telencephalon into molecularly distinct domains may reveal a LIM-HD combinatorial code in the vertebrate forebrain. This has certainly been postulated by other workers for the mammalian cortex (Bulchand et al., 2003), thalamus (Nakagawa and O'Leary, 2001) and *Xenopus* forebrain (Bachy et al., 2002b; Bachy et al., 2001; Moreno et al., 2004), but functional experiments are lacking. It would therefore be of great interest to undertake these experiments in zebrafish and the possible strategies for this will be discussed later.

#### *Spatial relationships of Lhx expression domains are retained through development*

The striking subdivision of the dorsal telencephalon into four molecularly distinct regions of Lhx gene expression at 24hpf and 32hpf was a feature I wanted to explore at later stages of development. Unfortunately technical difficulties associated with performing two-colour in situ hybridisation in sections prevented this. Nonetheless, analysis of the Lhx genes by single in situ hybridisation in wholemount indicates that the spatial relationships of *lhx1a*, *lhx1b* and *lhx5* are retained through development. For example, domain 1 of *lhx1a* overlaps completely with the dorsal *lhx5* domain at 24hpf and 32hpf; both of these genes are expressed in the OB at 3 and 5dpf. Domain 2 of *lhx1a* overlaps with *lhx1b* expression, and both of these genes are expressed adjacent to the anterior commissure at 3 and 5dpf. *lhx5* and *lhx1b*, which only overlap slightly at the interface of their two domains, but which move relative to each other between 24hpf and 32hpf, have completely different locations at 5dpf.

The analysis of Lhx gene expression at multiple closely-spaced time points by no means guarantees the labelling of the same cell populations over time. However, I was unsuccessful in generating a GFP line for *lhx1a* which would have been a much more reliable tool for tracking *lhx1a*-expressing cells (work performed in collaboration with N. Takahashi and I. Dawid). Thus, in the absence of GFP lines for any of the Lhx genes (and indeed for any pallial markers at the time these experiments), expression analysis by *in situ* hybridisation was the only option.

The use of *in situ* hybridisation is not without precedent for following populations of Lhx-expressing cells. The Retaux laboratory, analysing Lhx genes in *Xenopus*, have frequently used expression of these genes to track populations of Lhx-expressing cells. In fact, in their most recent paper they follow the same populations from embryonic to post embryonic stages, leading them to suggest that Lhx genes can be used as reliable markers of the same cell populations (Moreno et al., 2003; Moreno et al., 2004). This suggests that Lhx gene expression is not only critical for the specification of neuronal subtypes but also for the maintenance of particular neuronal characteristics.

If my *in situ* hybridisation analysis does indeed track the same populations of neurons over time then it seems the populations move quite considerably. Particularly between 2dpf and 3dpf, domain 1 of *lhx1a* and the dorsal domain of *lhx5* both move rostrally to appear in the OB at 3dpf. More anteriorly-located domains such as domain 2 of *lhx1a* and the *lhx1b* expression domains seem to move to the ventral side of the brain where at 5dpf they lie adjacent to the anterior commissure (Fig 4.2 and 4.3 J and M). These movements are compounded by the major morphological changes that the telencephalon undergoes, particularly between 2dpf and 3dpf. In fact these morphogenetic movements may underlie the movements of Lhx-expressing domains, and this will be discussed further in Chapter 6.

#### *Lhx-expressing cells are neurons with a pallial identity*

It is widely accepted in the literature that Lhx gene expression in cells of the nervous system coincides with the adoption of a neuronal fate (Jessell, 2000; Shirasaki and Pfaff, 2002). In the zebrafish telencephalon, Lhx gene expression indeed predominantly coincides with a postmitotic neuronal marker. However, my data suggests that the time-lag between turning on *lhx1a*, *lhx1b* or *lhx5* and adopting a neuronal fate as assayed by HuC:GFP expression could be 12 hours or longer. For example, the second domain of *lhx5* expression, which appears in the ventral telencephalon, is visible at 24hpf (Fig 4.4 C), but at 36hpf remains HuC negative (Fig 4.8 F). This is also true in the diencephalon where expression domains visible from late somitogenesis stages (before 24hpf; Fig 4.4 A) are still HuC negative at 36hpf (Fig 4.8 G). Even allowing for the approximate 4-hour lag time between final mitosis and the appearance of detectable GFP expression (Lyons et al., 2003), Lhx expression must precede terminal differentiation by some time.

Nonetheless, the Lhx expression domains in the dorsal telencephalon are postmitotic by 32hpf and also overlap with the expression of the pallial marker *tbr1*. Domain 1 of *lhx1a* and *lhx5* expression additionally overlap with *emx3*, a further pallial marker, but domain 2 of *lhx1a* and *lhx1b* expression lie outside the *emx3* domain by 36hpf. In chick and mouse, *Emx1* labels a smaller area of the pallium than does *Tbr1* (Puelles et al., 2000). The pallial domain that is *Emx1*-negative but *Tbr1*-positive is proposed to identify the ventral pallium, a region which gives rise to the claustrum and amygdala (Puelles et al., 2000). At present it is not known whether the same ventral pallial region exists in zebrafish, but it is proposed to express Pax6 (Wullimann and Rink, 2002) and so double labelling with this marker would go some way to clarify the issue.

One small caveat with using *emx3* is that no known mammalian orthologues of this gene (Derobert et al., 2002; Kawahara and Dawid, 2002). It would therefore be wise to repeat these experiments with the newly-designated zebrafish *emx1*, whose orthologue *Emx1* has been much better characterised in tetrapod species (Fernandez et al., 1998; Puelles et al., 2000).

In agreement with a pallial nature for the dorsal Lhx domains, no coexpression of *lhx1a*, *lhx1b* or *lhx5* was ever seen with the subpallial marker *Dlx4/6*. The intermingling of the pallial Lhx and subpallial *Dlx*-expressing cells at 36hpf confirms the postmitotic nature of both populations, as boundaries between the pallium and subpallium are only strictly maintained in the VZ, not in the mantle layer (Wilson and Rubenstein, 2000).

A further domain of *lhx5* expression appears in the ventral telencephalon at 24hpf. This domain does not overlap with *emx3* expression, nor does it coexpress with *Dlx4/6*. The position of this domain and its gene expression profile suggest it may be part of the eminentia thalami (Wullimann and Mueller, 2004). The eminentia thalami also express *tbr1* (Mione et al., 2001; Puelles et al., 2000), so double in situ hybridisation for *lhx5* and *tbr1* would easily confirm this.

#### *lhx1a* and *lhx5* highlight olfactory bulb neurons

From 3dpf until at least 1 month post fertilisation, *lhx1a* and *lhx5* are expressed in the olfactory bulb (OB). These genes are expressed in neurons that are pallium-derived, and it is therefore possible they highlight the projection neurons of the olfactory bulb, the mitral cells. A pallial origin of mitral cells has been shown in

mammals by both mutant analyses (Bulfone et al., 1998; Yoshida et al., 1997) and cell tracing experiments (Nomura and Osumi, 2004). Moreover, *Xenopus Lhx5* also highlights both pallial areas early in development (Bachy et al., 2001) and mitral cells of the OB at later stages (Moreno et al., 2003; Moreno et al., 2004). Finally, the positions of the isolated *lhx1a* and *lhx5*-labelled cells in the OB at 1 month post fertilisation agrees well with the known position of the mitral cell layer (Byrd and Brunjes, 1995; Edwards and Michel, 2002; Mione et al., 2001).

A key future experiment would be to establish whether *lhx1a* and *lhx5* are coexpressed in individual neurons. The early expression domains of these two genes suggest that *lhx1a* is only expressed in a subset of the *lhx5* domain. However, at 1 month post fertilisation the two genes are expressed in similar numbers of cells in the putative mitral cell layer. The broader early expression domain of *lhx5* may be reflected in the additional expression of this gene in the bulb periphery. However, the periphery is characterised as the cell-sparse olfactory nerve layer (Byrd and Brunjes, 1995; Edwards and Michel, 2002) and therefore the cell population highlighted by this expression requires further characterisation.

Lhx genes are widely implicated in the regulation of neuronal attributes such as neurotransmitter phenotype and axon pathfinding (Appel et al., 1995; Segawa et al., 2001). Mitral cells are glutamatergic (Edwards and Michel, 2002), and therefore not obviously different from pallial projection neurons in this aspect of their phenotype, although they may additionally express other as yet unidentified neurotransmitters. However, the axonal projection of mitral cells, into the telencephalon via the olfactory tracts, is an attribute not shared by any resident telencephalic neurons. Furthermore, zebrafish mitral cell axons have two potential routes to the telencephalon, the lateral or the medial olfactory tracts (LOT and MOT), and nothing is known about the factors intrinsic to the neurons that regulate this choice. Formation of the LOT in mammals is regulated at least in part by the chemorepulsive molecules Slit1 and Slit2 that are secreted by the medially-located septum (Nguyen-Ba-Charvet et al., 2002). Mitral cells express one of the Slit receptors, Robo2, that may mediate this guidance (Nguyen Ba-Charvet et al., 1999). Guidance of mitral cell axons in the LOT may also involve semaphorin/neuropilin interactions, as mitral cells express neuropilin1 and show both repulsive and attractive reactions to different semaphorin subtypes (de Castro et al., 1999). Future functional experiments with *lhx1a* and *lhx5* might be able to investigate the possible

regulation of guidance molecule expression in mitral cells by LIM-HD proteins as well as the factors that may regulate the choice of projection via the LOT or MOT.

*lhx1a and lhx1b are expressed in ventral telencephalic areas at 5dpf*

Domain 2 of *lhx1a* and the *lhx1b* expression domain are seen in ventral telencephalic regions from 3dpf, despite their established pallial origin. This is reminiscent of *tbr1* expression, which is exclusively pallial at early stages but by 4dpf is seen in a domain in the ventral telencephalon. In fact, the expression of *lhx1a* domain 2, and presumably *lhx1b*, in the anterior tip of *tbr1* expression at 36hpf suggests these cells may have similar or adjacent destinations.

The identity of the ventrally-located *tbr1* expressing cells is unclear but they may be aligned along one of the olfactory tracts (M. Mione, personal communication). There is precedent for this in mammals, where cells originating in the pallium migrate tangentially and ventrally to align themselves along the course of the future LOT (Tomioka et al., 2000). These so-called LOT cells are identified by the Lot1 antibody, but the antibody does not recognise any specific cell population in the zebrafish telencephalon (T. Hirata, personal communication). The expression domains of *tbr1*, *lhx1a* and *lhx1b* in the ventral telencephalon suggest that if they are associated with an olfactory tract it is more likely to be the MOT than the LOT, on the basis of their ventral positions. This possibility should be further investigated by double labelling with axon markers and *in situ* hybridisation for *lhx1a* and *lhx1b*. It is also interesting to consider that genes downstream of Lhx genes such as cell adhesion molecules (Gimnopoulos et al., 2002) and members of the Eph/ephrin family (Kania and Jessell, 2003) have the potential to both cell autonomously regulate processes such as cell migration and axon pathfinding, but also to provide contact-dependent guidance signals for the axons of other neurons, as might occur in the formation of the olfactory tracts.

A further explanation for the ventral destinations of *lhx1a* and *lhx1b*-expressing cells is that they represent a dorsal to ventral migration. Such a migration is undertaken by the LOT cells discussed above, but actual invasion of the subpallial basal ganglia has been very rarely described. A lineage tracing experiment using permanent marking of *Emx1*-expressing cells reported a population of presumed pallial-derived neurons in the subpallium (Gorski et al., 2002), but no assessment

was made of their migratory path, phenotype or function. Nonetheless, this would be an interesting possibility to address with subsequent experiments in the zebrafish.

#### *Divergence of expression along the rostro-caudal axis*

A comparison of the expression domains of *lhx1a*, *lhx1b* and *lhx5* along the neuraxis indicates that the telencephalon is the region where greatest divergence in Lhx gene expression is seen. Even the paralogues *lhx1a* and *lhx1b*, resulting from a duplication of the ancestral *Lhx1* gene, have somewhat different expression domains (discussed above). This indicates that the promoter elements controlling *lhx1a* and *lhx1b* expression have diverged sufficiently from each other to establish at least some unique expression domains (Force et al., 1999). The telencephalon (or the prosencephalon as a whole), being one of the most recent additions to the vertebrate brain, is also a region where innovative use of existing genes can have major implications for the complexity and connectivity of the brain area (Bachy et al., 2001).

#### *Comparison of expression domains between species*

The telencephalon is also the most divergent brain area between vertebrate species. Innovations in telencephalic connectivity and subtype specification probably underlie the evolution of this brain area (Bachy et al., 2001). It might therefore be expected that few commonalities would exist between species with respect to telencephalic Lhx gene expression. In addition to this, *lhx1b* is a gene unique to zebrafish, making comparisons with other species more difficult. However, the combined expression of the two paralogues may reflect more closely the ancestral expression pattern, as is the case for *nk2.1a* and *nk2.1b* (Rohr et al., 2001).

In fact a comparison of Lhx gene expression with other species yields some evidence of conserved expression domains. Mouse *Lhx5* is a pallial marker, as well as being expressed in the hypothalamus, ventral thalamus, zli, pretectum and tectum (Bachy et al., 2001; Sheng et al., 1997). *Xenopus Lhx5* is also expressed in a large band of the pallium, juxtaposed to the *x-dll3*-defined subpallium and consequently with its border at the pallial-subpallial border (Bachy et al., 2001). As well as being a pallial marker, *x-Lhx5* is also expressed in the olfactory bulb at later stages, specifically in the mitral cell population (Moreno et al., 2003), as discussed above.

Less conservation exists for expression of *lhx1a/Lhx1*. Murine *Lhx1* is also a pallial marker, overlapping considerably in its expression with *Lhx5* (Bachy et al., 2001; Sheng et al., 1997). However, in the *Xenopus* telencephalon *x-Lhx1* is expressed only in a small area within the *x-Lhx9* positive subpallium (Bachy et al., 2001). There is therefore little conservation between the pallial domains of *lhx1a* and *lhx1b* in zebrafish and the subpallial domain of *x-Lhx1* in *Xenopus*.

### Future experiments

#### *Other Lhx genes in the telencephalon*

This investigation has also been limited in the number of Lhx genes studied. Members of other groups of the Lhx family are expressed in the telencephalon, including the recently identified *lhx2a* and *lhx2b* (M. Mione and K. Kwong, personal communication; received from H. Okamoto) and *islet1* (Higashijima et al., 2000). There may well be others, including zebrafish orthologues of *Lhx7* and *Lhx9* (Bachy et al., 2001). In a more comprehensive analysis it would be interesting to see how these other members of the Lhx family compare with the *lhx1a*, *lhx1b* and *lhx5* examined here.

#### *Functional experiments with the Lhx genes*

My initial aim after having characterised the expression domains of the three Lhx genes was to carry out functional experiments. However, morpholino oligonucleotides designed to the 5' UTR of *lhx1a* and *lhx1b* showed no specific CNS phenotype. This was compounded by a lack of good assays for Lhx gene function in the telencephalon, including failed attempts to raise antibodies specific to zebrafish Lhx1a. High doses of morpholino also affected organiser function, suggesting they were interfering with the early expression of *lhx1a* and *lhx1b* during gastrulation stages.

A possible way to circumvent the problems of interfering with early expression of Lhx genes would be to use dominant negative Lhx gene constructs under the control of a heatshock promoter. The dominant negative construct would consist of only the protein binding LIM domain of any given Lhx gene (Kikuchi et al., 1997; Segawa et al., 2001), while the heatshock promoter would allow expression of this construct to be controlled by treating an injected embryo with a brief period at elevated temperature. H. Segawa has already kindly provided LIM-

domain only constructs for *lhx1a*, so these experiments would be a priority for the future.

One caveat to bear in mind for performing functional experiments with LIM-HD proteins is the range of binding partners they have, such as the Ldb and LMO proteins. The presence or absence of these factors, and even their respective concentrations modulate LIM-HD function (Bach, 2000; Segawa et al., 2001; Thaler et al., 2002). *ldb* gene expression seems to be ubiquitous in the zebrafish telencephalon (Toyama et al., 1998), but the expression of Lmo proteins and the possibility of differentially spliced forms of the Lhx genes, as suggested by Failli et al (2000) to modulate Lhx9 function, should also be investigated.

## 5.1 Aim and Introduction

Many of the primary observations made in the previous two chapters indicate that cell and tissue movements play a significant role in shaping the developing telencephalon. I was particularly struck by the appearance of domains of Lhx gene expression in the olfactory bulb at 3dpf, and wanted to directly test whether these Lhx-expressing cells had their origins in the posterior dorsal telencephalon as their expression patterns suggest. I therefore developed and used a cell labelling technique to mark populations of telencephalic cells at 1dpf and follow them to their positions at 5dpf. I was particularly interested in the areas of the telencephalon that contribute cells to the olfactory bulb, because this is a defined structure within the telencephalon and is also the region where the Lhx genes *lhx1a* and *lhx5* are expressed.

### *OB structure and function*

The OB is a specialised structure that, although derived from the telencephalon, protrudes from the rostral tip of the brain and comes to lie outside the main bulk of telencephalic structures at adult stages in many, if not all vertebrates. The OB is the primary olfactory centre, receiving its sole input directly from the sensory neurons (OSN) of the olfactory epithelium (OE). The olfactory sensory neurons express one of a repertoire of olfactory receptor genes - 100 in zebrafish (Barth et al., 1996; Ngai et al., 1993); 1000 in mouse (Reed, 2004) giving them odorant specificity, and project to a specific glomerular location in the OB where other OSNs expressing the same odorant receptor converge (Mombaerts et al., 1996). The glomerulus is the interface of OSN axons with bulb neurons and the pattern of glomeruli is invariant between individuals of the same species (Baier and Korsching, 1994; Friedrich and Korsching, 1997).

The zebrafish olfactory bulb is gaining strength as a model for investigating olfaction (e.g. Edwards and Michel, 2002), but relatively little is known about its development. The first axons to reach the telencephalon from the olfactory placode (the precursor of the olfactory epithelium) reach and invade the prospective bulb region between 24 and 38hpf (Chitnis and Kuwada, 1990; Whitlock and Westerfield, 1998; Wilson et al., 1990). These are the axons of pioneer neurons and are

subsequently followed by the axons of the olfactory sensory neurons themselves from 2dpf onwards, which form distinctive glomeruli within the bulb (Dynes and Ngai, 1998; Whitlock and Westerfield, 1998). By 2dpf, a nascent form of the glomerular map is evident in the olfactory bulb, and by 3.5dpf approximately 15 glomeruli can be consistently identified (Dynes and Ngai, 1998). In the adult zebrafish olfactory bulb, approximately 100 glomeruli are evident (Baier and Korsching, 1994).

The OB contains two main neuronal subtypes – projection neurons and interneurons. The projection neurons, the mitral cells, are excitatory glutamatergic neurons (Edwards and Michel, 2002) that project to the olfactory areas of the telencephalon via the olfactory tracts. It is onto the dendrites of these neurons that OSN axons synapse in the glomeruli (Byrd and Brunjes, 1995). The interneuron population falls into two groups – glomerular interneurons and granule cell interneurons. Both populations are GABAergic and inhibitory (Edwards and Michel, 2002); the glomerular interneurons form local connections within the glomerulus while the granule cells mediate inhibitory interactions between mitral cells (Reed, 2004). Neither interneuron class projects outside the bulb. In both the zebrafish and mouse adult olfactory bulb, these cell types are segregated in different laminae, with the glomerular interneurons and mitral cells situated more peripherally in the bulb, and the granule cells more centrally (Byrd and Brunjes, 1995; Wullimann and Rupp, 1996).

#### *The embryonic origins of the olfactory bulb*

The embryonic origins of the mammalian OB are telencephalic and, as for the cerebral cortex, both pallial and subpallial areas contribute neurons to the bulb. The projection neurons, mitral and tufted cells, are glutamatergic and are thought to be pallial in origin. Mitral cells express pallial markers such as *Tbr1* and *Emx2* and mouse mutants targeting these genes lack mitral cells in the OB (Bulfone et al., 1998; Yoshida et al., 1997). Cell labelling experiments have also identified the pallium as the origin of bulb projection neurons, and they come from the rostral tissue directly underlying the point where the bulb will evaginate (Nomura and Osumi, 2004). In non-mammalian species, including zebrafish and *Xenopus*, mitral cells also express pallial markers such as *Eomesodermin*, *Tbr1* and *xLhx5*, and these

markers have been used to infer a pallial origin for mitral cells (Mione et al., 2001; Moreno et al., 2003).

The OB interneurons are, like the interneurons of the cortex, subpallium-derived. In mammals, the subventricular zone of the lateral ganglionic eminence (LGE) is the predominant source of OB interneurons during embryonic stages (Wichterle et al., 1999; Wichterle et al., 2001). Mutations that disrupt the patterning of the LGE or the neurogenesis within it, also affect the OB interneuron population (Bulfone et al., 1998; Corbin et al., 2000; Long et al., 2003; Stenman et al., 2003; Yun et al., 2001). Particularly strongly implicated in the generation of OB interneurons are the *Dlx* genes, genes that are expressed broadly in the subpallium. Both *Dlx1/Dlx2* and *Dlx5* mutants show massively reduced OB interneuron populations (Bulfone et al., 1998; Long et al., 2003), and a recent paper has shown that a subpopulation of *Dlx5*-expressing cells, also expressing the transcription factor *Er81* gives rise to the majority of OB interneurons (Stenman et al., 2003).

In zebrafish, the *dlx* genes are also widely expressed in the subpallium (Akimenko et al., 1994), and a GFP transgenic line driven by the *dlx4/dlx6* promoter (Zerucha et al., 2000; *Dlx5/Dlx6* in mouse) highlights interneurons within the OB (M.Mione, personal communication and Fig 3.8). It therefore seems likely that zebrafish OB interneurons also have a subpallial origin, but this has never been directly demonstrated.

#### *The ganglionic eminences supply interneurons to cortical areas*

In addition to the migration of interneurons from the LGE to the OB, the ganglionic eminences are also the source of migratory interneurons that come to reside in pallial structures such as the cortex and hippocampus. This tangentially-migrating population of cells has been identified in both mammals and chick, and at least at early embryonic stages its source is the MGE rather than the LGE (Cobos et al., 2001a; Wichterle et al., 1999; Wichterle et al., 2001). Again the *Dlx* genes are strongly implicated in the generation of these neurons, because in *Dlx1/Dlx2* mutants, tangential migration into the dorsal telencephalon is much reduced (Anderson et al., 1999; Anderson et al., 1997a). The zebrafish *dlx4/dlx6* GFP line also highlights some individual cells in the dorsal telencephalon (M. Mione, personal communication and Fig 3.8), but the spatial origin of these cells is unknown.

*Aim of this chapter*

The aim of these experiments was to label small groups of telencephalic cells at 1dpf and follow them to their positions at 5dpf, primarily to establish the origins of the OB. I found that OB cells are derived from a number of dorsally and posteriorly-located telencephalic areas; very ventral areas make no contribution to the OB. I also found that cells in different telencephalic regions show characteristic and consistent patterns of cell movement over the four days of embryogenesis examined, allowing me to build a picture of the migrations and morphogenetic movements that generate the telencephalon over this period.

## 5.2 Materials and Methods

### *Properties of the Kaede protein*

The Kaede protein is a recently discovered photoconvertible protein native to a coral species (Ando et al., 2002). The protein exists in two forms - a longer green fluorescent form and a shorter red fluorescent form. The red fluorescent protein is produced from the longer green Kaede protein by a UV-light dependent photolysis (Mizuno et al., 2003). Both forms of the protein are stable in living cells.

### *The Kaede construct*

The pCS2-Kaede construct, containing the full 1.8kb of Kaede cDNA was generously donated by Dr Atsushi Miyawaki and was amplified using conventional maxiprep methods (section 2.4). A NotI site was used to linearise the construct for *in vitro* transcription with SP7 polymerase (section 2.5). Synthesised RNA was purified by phenol chloroform extraction and precipitation (section 2.5), and the pellet resuspended in Danieau buffer (The Zebrafish Book) to give a working concentration of 50ng/ul for microinjection.

### *Expression of Kaede using DNA and RNA*

I tried two methods to express Kaede protein in zebrafish embryos – injection of DNA and injection of synthetic mRNA. DNA injections of the circular construct resulted in extremely chimeric embryos, frequently having only a handful of albeit brightly expressing cells. RNA injection gave much more uniform expression of green Kaede that persisted until at least 6dpf. For photoconversion experiments, injections of Kaede RNA were made into one blastomere of the 2- or 4-cell embryo, resulting in chimeric expression of Kaede protein. Chimeric embryos were more suitable for photoconverting small numbers of cells because they gave a greater possibility of specific activations with defined limits.

### *Raising Kaede-injected embryos*

Kaede-injected embryos were raised at 28.5°C in the dark, and from 24hpf in PTU to prevent pigment formation. At 24hpf, embryos were dechorionated and the brightest embryos selected using an FITC filter on a fluorescence dissecting microscope

(Leica). During all subsequent procedures, embryos were exposed to minimal light to prevent the possibility of non-specific photoconversion of Kaede protein. This involved keeping the embryos covered to prevent exposure to ambient light and also reducing the intensity of and exposure to white light during imaging.

### *Agarose mounting*

For all photoconversion procedures and subsequent imaging, embryos were anaesthetised in MS-222 and mounted individually in drops of 1.5% low melting point agarose. For all laterally-mounted embryos, the alignment of the eyes was used to orient the embryos; for other orientations, the midline was used. 3dpf and 5dpf embryos were almost always mounted dorsally, to avoid having to image through the eyes. In some cases, one eye was removed from 5dpf embryos before confocal imaging, in order that the specimen could be imaged from the lateral aspect.

### *Focal photoconversion of Kaede*

I tried four different methods to generate a focussed and restricted beam of UV-wavelength light to perform the photoconversions:

1. Using a Zeiss Axioplan2 microscope with water immersion objectives, I reduced the aperture in the fluorescence light path to its minimum size while using the DAPI filter set to generate UV-wavelength light. This gave a focussed beam, but the aperture size was too great, allowing too much UV light to pass and resulting in excessively large numbers of cells being red Kaede-labelled.
2. Again using a Zeiss Axioplan2 microscope with a x63 water immersion objective, I placed a 0.2mm brass pinhole (made by T. Hawkins) in the fluorescence light path, using the DAPI filter set to generate UV-wavelength light. The pinhole was inserted into the slider that holds the fluorescence aperture diaphragm, and thus could be easily removed for all other imaging procedures. Activations performed with this method resulted in discrete labellings of between 2-20 cells, ideal for my purposes. This method was most successful in my hands and was employed in all the experiments in this chapter.
3. I used a UV Micropoint laser on a Zeiss Axioplan2 microscope, which provided a very restricted beam of a single UV wavelength. This method was unable to give robust photoconversion of green to red Kaede, possibly because of insufficient laser power.

4. I tried multiphoton confocal microscopy, which offers the possibility of activating fluorophores only at the focal plane of the beam. Unfortunately, we were unable to establish the appropriate wavelength for the photoconversion and/or the laser was insufficiently powerful to trigger the photolysis reaction. Therefore I was unable to label any cells using this method.

#### *Procedure for photoconversion of Kaede*

To perform the focal photoconversion, chimeric Kaede-injected embryos at 26-30hpf were agarose-mounted as described. Embryos were viewed using a x63 water immersion objective and an FITC filter set (the GFP filter set was unsuitable as it allowed UV wavelengths to pass). The pinhole beam was carefully positioned over this site chosen for photoconversion, and the embryo was exposed to UV light for between 30 and 45 seconds.

Following photoconversion, DIC and red fluorescent images were captured of the embryo. Every specimen was then re-mounted in agarose to view the activation from a different aspect; again DIC and red fluorescent images were captured.

Embryos were then raised in the dark with PTU and re-imaged at 3dpf, mostly from the dorsal aspect. DIC and red fluorescent images were captured, often at a number of different focal planes, to record the positions of all labelled cells.

#### *Confocal imaging*

At 5dpf I made final observations of the embryos labelled at 1dpf, by laser scanning confocal microscopy (LCSM). Embryos were anaesthetised and individually mounted in agarose. In the majority of cases, embryos were mounted dorsally, angled slightly to reduce the imaging depth required to sample the entire telencephalon. In a few cases, embryos were imaged from the lateral aspect involving the removal of one eye. Both red and green Kaede signals were imaged, along with transmitted light, in confocal sections 3 $\mu$ m apart. The green Kaede signal gave an excellent cellular background against which the photoconverted red cells could be located, as it enabled easy identification of the olfactory bulb (OB), and all of the telencephalic tracts and commissures.

### *Analysis*

Analysis of the Kaede specimens involved recording the position and approximate number of all red-labelled cells and axons in each specimen. The presence of red-labelled cells in the OB was recorded, along with particularly distinctive cell morphologies such as extensive dendritic arbours. The presence of labelled axons in the olfactory tracts was also recorded, although no distinction was made between the medial and lateral olfactory tracts (MOT/LOT). In the rest of the telencephalon, the positions of red-labelled cells were described as dorsal, mid- or ventral telencephalon according to whether they were present dorsal to the fasciculated tract of the anterior commissure (TAC – dorsal), at the same levels as the TAC (mid-) or at the level of the AC itself (ventral) in horizontal sections. This classification is shown in Figure 5.2 F-I. The designation was not intended to reflect any pallial/subpallial divisions and was merely to aid in the description of the labelling. In addition to the location of cell bodies, the presence of axons in the TAC, AC or supraoptic tract (SOT, which leads from the telencephalon to the diencephalon) was recorded. Finally, a short summary of the positions of labelled cells was recorded for each specimen.

## 5.3 Results

In this set of experiments, I primarily sought to establish the spatial origins of the neurons of the zebrafish olfactory bulb (OB). The OB, although morphologically separated from the rest of the telencephalon in the adult brain, forms within the telencephalon during embryogenesis. The OB is therefore derived entirely from telencephalic cells and I restricted my study of its origin to this brain region. I labelled small groups of cells in the telencephalon at an early stage (1dpf), before the OB has formed, and followed the cells to their positions at 5dpf, when the OB has a structure distinct from the rest of the telencephalon. Using this approach I was able to assess which telencephalic regions make contributions to the OB, and also whether there are stereotyped patterns of cell movements characteristic of certain telencephalic areas.

### *Features of Kaede protein photoconversion*

In order to label small groups of cells in the embryonic telencephalon I developed a novel use for the recently discovered photoconvertible protein, Kaede (Ando et al., 2002). Native green fluorescent Kaede can be irreversibly cleaved by UV light to give a shorter red fluorescent form (Mizuno et al., 2003), making it an ideal tool for cell labelling experiments. The two proteins also have a number of excellent optical properties; the red and green forms are of similar brightness and the two proteins are excited by, and emit at, largely non-overlapping wavelengths. Experiments on Kaede-expressing cells in culture (Ando et al., 2002) have revealed other attributes that are essential for any live embryo applications. Namely, both forms of the protein are non-toxic and stable under normal cellular conditions, and both forms of the protein are distributed throughout the cytoplasm including in cell processes such as axons. Diffusion of the protein is also rapid; if green Kaede protein is photoconverted by a restricted UV beam directed to a cell body, all cellular processes are rapidly labelled with red Kaede protein (Ando et al., 2002). These properties of the Kaede protein made it a potentially ideal method for labelling and following cells with complex morphologies, such as neurons, in a live embryo.

Our novel application of the Kaede protein involved expressing it in zebrafish embryos and using its photoconvertible properties to non-invasively label

cells and follow them during development. I expressed Kaede protein in zebrafish embryos by injecting synthetic Kaede mRNA at the 1 to 4-cell stage. This results in embryos expressing green Kaede protein, with variable mosaicism, in all cell types including those of the nervous system (see Fig 3.2 and 5.1 A). Before exposure to UV light, background levels of red fluorescence are very low in a Kaede-expressing embryo (Fig. 5.1 B). However, following a 2 minute exposure to UV-light via a DAPI filter set, red fluorescence increases dramatically while green fluorescence concomitantly decreases (Fig. 5.1 C and D).

Having confirmed that I could express and photoconvert Kaede protein in a non-invasive manner in live embryos, I established a method to restrict the green-to-red photoconversion to a much smaller number of cells. By placing a 0.2mm pinhole in the fluorescence light path, I generated a small and focussed beam of UV light that could be directed on specific regions of the telencephalon. Exposure to 30 seconds of UV light via this method allowed me to perform discrete photoactivations of approximately 2-20 cells.

To check the extent and quality of the labelling I confocal imaged a number of specimens immediately following photoconversion. Figure 5.1 E-H shows one such specimen, imaged by epifluorescence microscopy from lateral and anterior aspects (Fig 5.1 E and F resp.) and then by confocal microscopy from the anterior aspect (Fig 5.1 G and H). The confocal images show a very similar pattern of photoconversion to the epifluorescence images (compare 5.1 F and H), although the confocal projection shows slightly more labelled cells than the epifluorescence image. This is probably attributable to the labelled cells not all being present in the same focal plane. Examining the photoconversion in single confocal sections (Fig 5.1G) shows that the labelled cells consist of both red and yellow (i.e. red and green) cells. Red cells, where complete conversion of Kaede has taken place, are at the focus of the beam, whereas yellow cells, where conversion of Kaede is incomplete, are more peripheral. In total, this photoconversion or “activation” has a diameter of approximately 30µm and has resulted in approximately 15 red-labelled cells.

#### *Designating regions within the telencephalon*

The aim of my experiments was to establish which regions of the telencephalon contribute to the OB. I chose not to randomly sample the entire telencephalon with Kaede activations, instead focussing on making multiple labellings in restricted,

### Figure 5.1: Activation of Kaede protein

Scale bars are 50 $\mu$ m in all figures. In all lateral views, anterior is to the left. In all dorsal views anterior is to the bottom. In all rostral views dorsal is to the top.

A and B show green (A) and red (B) Kaede signal in the brain of a chimeric 30hpf embryo, before any exposure to UV light. C and D show green (C) and red (D) Kaede signal after a 2-minute exposure to UV light. The red Kaede signal increases dramatically and there is concomittant loss of the green Kaede signal. All pictures are taken with the same exposure.

E, F, G and H show the same embryo immediately after a 0.2 mm pinhole activation at 28hpf in the mid-telencephalon. E and F are epifluorescence images overlaid on DIC images, G is a single confocal section and H is a maximum projection of all confocal sections overlaid on a transmitted light image. E shows cells labelled by the activation (blue arrowhead) from the lateral aspect; inset shows orientation for all subsequent panels. F shows the same embryo from the anterior aspect; the blue arrowhead indicates the focus of the activation. In G, a single confocal section reveals both red- (arrowheads) and yellow- (arrow) labelled cells. The projection (H) reveals all labelled cells and out-of-focus activation in the olfactory placode and contralateral telencephalon.

AC – anterior commissure  
di – diencephalon  
E – epiphysis  
ey – eye  
OB – olfactory bulb  
OE – olfactory epithelium  
OP – olfactory placode  
SOT – supraoptic tract  
TAC – tract of the anterior commissure  
tel – telencephalon  
v - ventricle

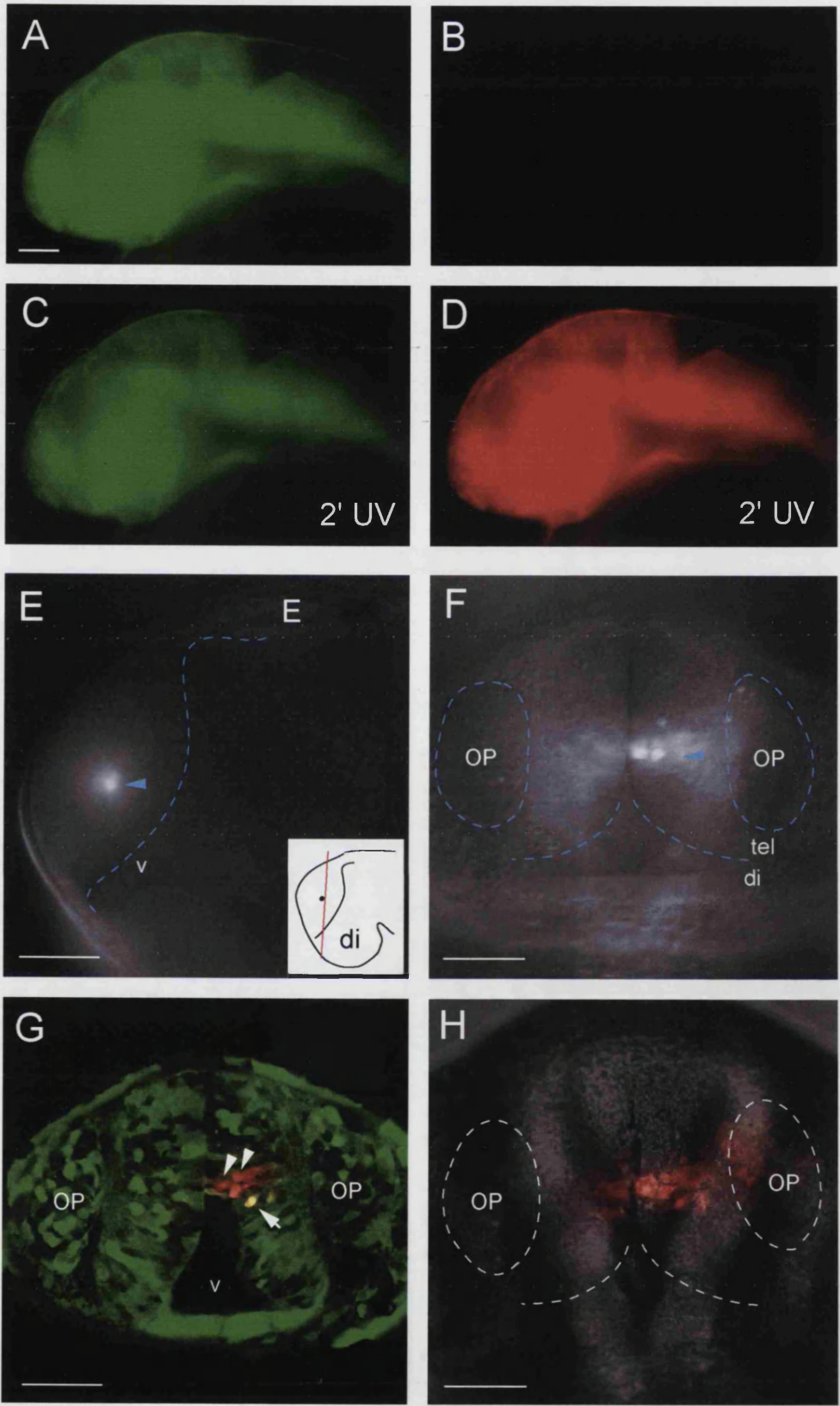


Figure 5.1

defined regions (designated T1 to T9). The arrangement and spacing of these regions are depicted schematically in Fig 5.2 A. In defining the regions, I primarily chose areas that could be easily and reproducibly located in the 1dpf telencephalon. T1 to T8 are therefore located along the borders of the telencephalon, either anteriorly (T1 to T5) or posteriorly along the ventricular surface (v; T6 to T8). A further consideration was that both pallial and subpallial areas of the telencephalon should be sampled, including the areas where the *Lhx* genes *lhx1a*, *lhx1b* and *lhx5* are expressed (Fig 5.2 B-D)

### *Imaging photoconverted specimens*

Immediately following photoconversion in a specific region at 1dpf, I imaged red fluorescence in each specimen from two aspects to establish the extent of the labelled cells. I also imaged each specimen at 3dpf, 2d after the activation, to observe the positions of labelled cells in a more mature telencephalon. I made final observations of the labelled cells at 5dpf by laser scanning confocal microscopy (LSCM). Both green and red Kaede signals (as well as transmitted light) were imaged through the entire telencephalon. The green Kaede signal, although distributed throughout the brain, provided an excellent cellular background against which to observe the red-labelled cells. For example, the distinctive structure of the OB, with its glomeruli, was easily identifiable.

Outside the OB I used landmarks provided by green Kaede expressing fibres in horizontal confocal sections to define broad dorsal, mid- and ventral telencephalic regions. These were not intended to reflect pallial/subpallial subdivisions within the telencephalon but simply aided in the location of red-labelled cells. Dorsal telencephalon was classified as being the area dorsal to the fasciculated bundle of ascending and descending fibres in the tract of the anterior commissure (TAC), mid-telencephalon was classified as being the region in which TAC fibres were present and ventral telencephalon was classified as the area in which commissural fibres of the anterior commissure (AC) were present (Fig 5.2 H). Representative horizontal sections through the telencephalon at dorsal, mid- and ventral levels are shown in Figure 5.2 F, G and H. with the bundles of TAC fibres highlighted in the mid-telencephalic section.

The green Kaede signal also enabled identification of axon tracts and commissures such as the lateral and medial olfactory tracts (LOT and MOT carrying

**Figure 5.2: Fate-mapped regions within the telencephalon**

A shows the positions of regions T1 to T9 in a lateral view schematic diagram of the 28hpf telencephalon. The anterior commissure, ventricle and epiphysis are marked. B, C, D and E show lateral views of subpallial and pallial gene expression patterns for comparison with A. Expression patterns of *Tg(dlx4/6:GFP)* (B; subpallial), *emx3* (pallial), *lhx1a* and *lhx5* are shown at the stages marked. F, G and H show the classification of the 5dpf telencephalon in to dorsal, mid- and ventral areas. Single confocal sections (scale bars=50µm) at representative positions are shown in a schematic diagram (I) to indicate relative positions of sections. The dorsal telencephalic area (F) is characterised by the absence of a fasciculated TAC, the mid-telencephalon by the presence of a fasciculated TAC (G) and the ventral telencephalon by the presence of the AC (H) in any given section.

AC – anterior commissure  
di – diencephalon  
E – epiphysis  
ey – eye  
OB – olfactory bulb  
OE – olfactory epithelium  
OP – olfactory placode  
SOT – supraoptic tract  
TAC – tract of the anterior commissure  
tel – telencephalon  
v - ventricle

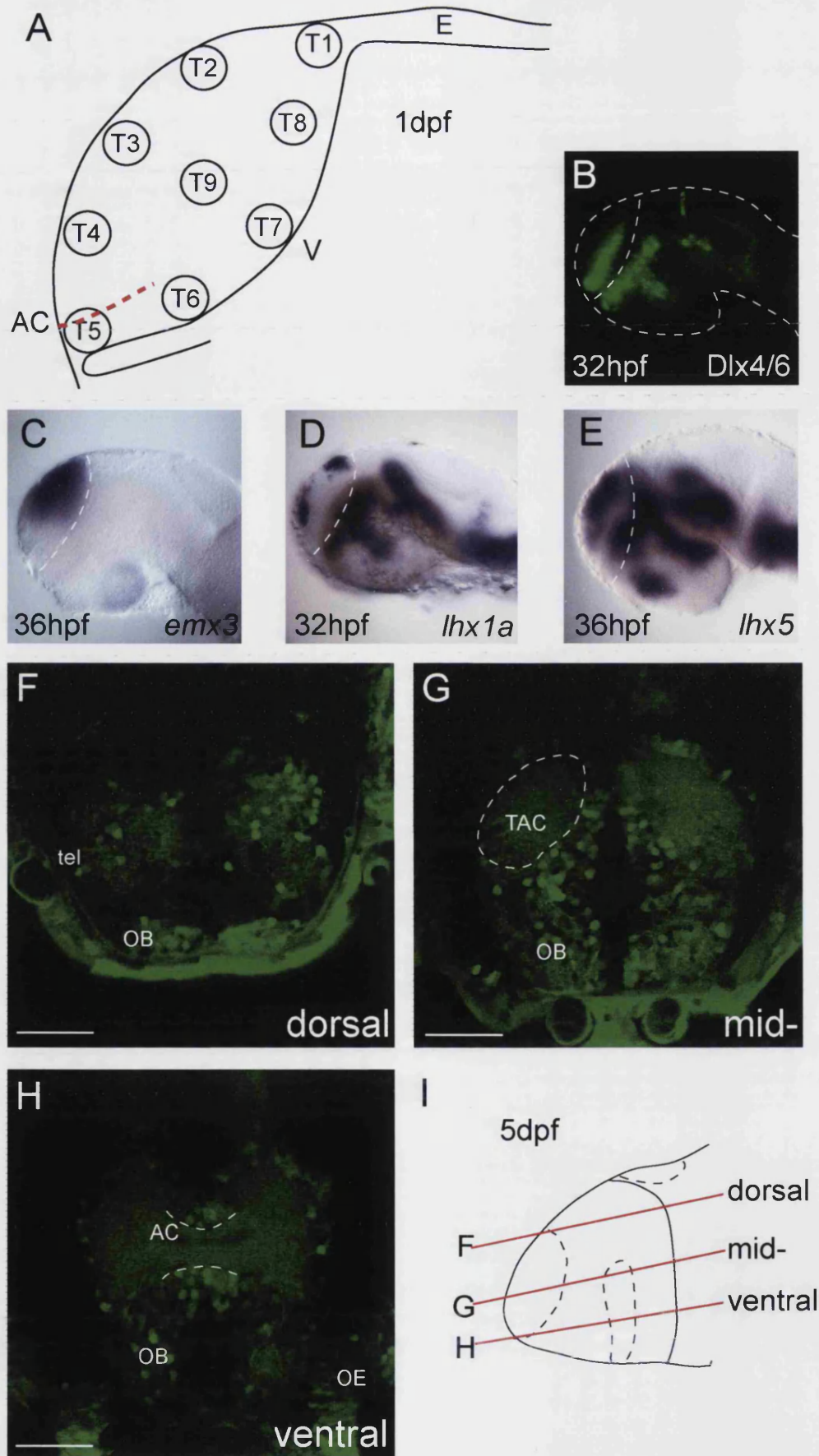


Figure 5.2

efferent fibres from the OB), as well as the TAC, the AC, and the supraoptic tract (SOT), which connects the telencephalon and diencephalon. Therefore, red-labelled fibres that appeared in these tracts and commissures could be recorded, giving added information about the axonal projections of labelled cells.

### *Cells labelled in T1*

I focussed my labellings on the region designated T1, in the most posterior dorsal telencephalon. This region is expected to lie within the pallium as defined by *emx3* and *tbr1* expression and close to the dorsal domain of *lhx1a* expression (Fig 5.2 C and D). Having made the observation that *lhx1a* is expressed in progressively more rostrally-located cells and by 3dpf is in the OB, I wanted to see if this reflected a real movement of cells in the telencephalon.

I performed a total of 31 activations in this area, approaching T1 most frequently from the lateral aspect (Fig 5.3) but also from the dorsal aspect (Fig 5.4). Lateral activations tended to result in a broader medio-lateral distribution of red-labelled cells whereas dorsal activations were restricted in the medio-lateral axis but extended in the dorso-ventral axis; this was as a result of the orientation of the UV-light beam. The exceptions to this were activations targeted to the neuroepithelial “roof”, the most posterior dorsal area at 1dpf, which although small in area has little tissue directly underlying it (see Fig 3.2 E). Therefore activations in this region generally resulted in a very restricted number of superficial cells being strongly labelled (e.g. Fig 5.4 D-F).

In all 31 activations in T1, red-labelled cells were observed in the OB at 5dpf (Fig 5.3 C and E). The labelled cells were found in all regions of the OB, with the number of cells present being dependent on the size of the original activation. The presence of cells in the OB was detectable before 5dpf, often by 3dpf (Fig 5.3 D). In addition to cell bodies being present in the OB in every 5dpf T1 specimen examined, fibres projecting to the telencephalon from the OB via the LOT/MOT were observed in 7/31 cases (Fig 5.3F). This strongly suggested that at least some of the red-labelled OB cells were mitral (projection) cells, the output neurons of the OB. Interneurons, the other major cell type of the OB, do not extend axons outside the bulb.

In many specimens activated in T1, (21/31), labelled cells were present in other telencephalic areas in addition to the OB (Fig 5.3 C). These cell profiles were

### Figure 5.3: Lateral activations in T1

All scale bars are 50µm

A, B and C show the same embryo. A is a DIC/fluorescent overlay of a lateral view of a 28hpf forebrain, with a Kaede activation in T1 (blue arrowhead). The posterior limit of the telencephalon is marked with a blue dotted line. B shows the same embryo from the dorsal aspect; the focus of the activation (blue arrowhead) is on the left-hand side. C shows the fate of all labelled cells at 5dpf (projection overlaid on a transmitted light image of the telencephalon); most labelled cells are in the OB with a few cells present in the anterior left telencephalon (white arrowhead).

D, E and F show results from a second embryo also activated in the same T1 position. D shows a 3dpf dorsal view of an activation in R1 at 28hpf; labelled cells are present bilaterally in the OB. E and F show single confocal sections at 5dpf at the levels shown in G; red cells are present in the OB (arrowheads in E) and red fibres (arrowheads in F) are present in the LOT/MOT (arrow in F), tAC and AC, indicating that some T1 cells become OB projection neurons.

AC – anterior commissure  
di – diencephalon  
E – epiphysis  
ey – eye  
MOT – medial olfactory tract  
OB – olfactory bulb  
OE – olfactory epithelium  
OP – olfactory placode  
SOT – supraoptic tract  
TAC – tract of the anterior commissure  
tel – telencephalon  
v - ventricle

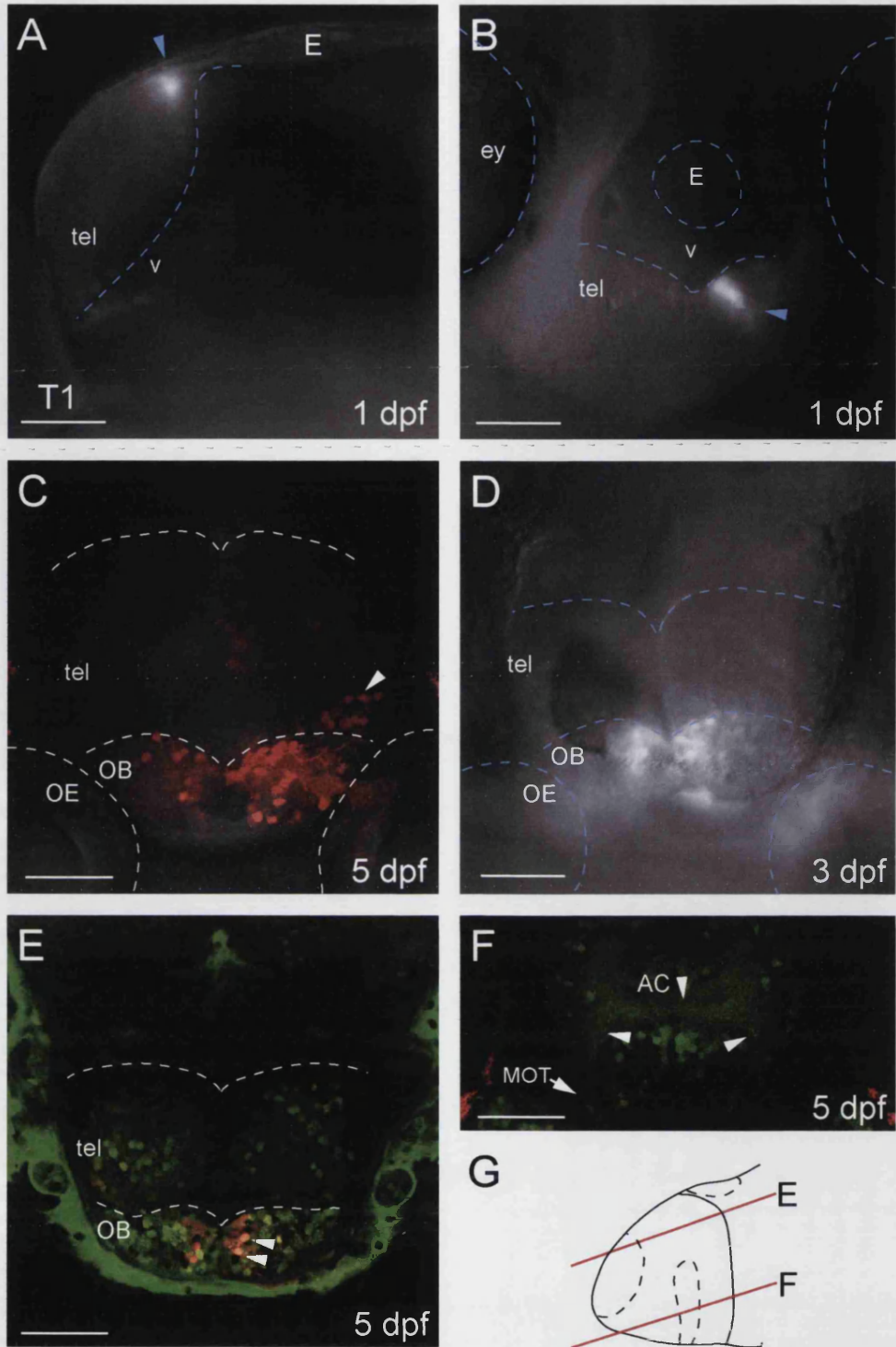


Figure 5.3

sometimes much fainter than those observed in the OB, possibly suggesting that they had not been at the focus of the activation. However, in many cases robust labelling was seen in the mid- and dorsal regions of the telencephalon, with cell bodies generally located anteriorly rather than posteriorly (white arrowhead in Fig 5.3 C). Labelled cells were never seen in the ventral telencephalon, around the anterior commissure, suggesting that dorsal telencephalic region T1 does not contribute cells to ventral telencephalic areas.

Cells labelled in T1 also contributed fibres to the tracts and commissures of the telencephalon. 27/31 specimens showed labelling in the TAC, and 16/31 in the AC itself (Fig 5.3F). A subset of these specimens had labelled cells exclusively in the OB, which reveals that mitral cell axons form part of the TAC and may be commissural. A specimen with unilateral labelling in the OB, where labelled fibres appeared in the contralateral TAC, confirmed the commissural nature of at least some mitral cell axons. In addition, 5/31 specimens showed labelling in the SOT that connects the telencephalon and diencephalon. These fibres were only evident in specimens that had both OB and telencephalic labelling, as would be expected given the telencephalic origins of the SOT (Wilson et al., 1990).

9/31 specimens showed labelling of a component of the stria medullaris (see Chapter 3 and data not shown), a tract that projects from the telencephalon to the dorsal diencephalic habenulae. Analysis of these specimens did not establish whether the labelled axons in this tract originated in the OB or telencephalon, but the stria medullaris is known to contain efferents from both areas in other fish species e.g. (Riedel and Krug, 1997).

#### *Cells labelled in the T1 roof*

A subclass of activations in T1 (7/31) was aimed directly at the cells of the telencephalic “roof”, a medial part of the neuroepithelium that lies just rostral to the border of the diencephalon and medially to the bulk of the telencephalic tissue (Fig 5.4 A and D and Fig 3.2 E). The roof itself is maybe only one cell diameter thick, and forms part of the telencephalic neuroepithelium. Activations in this region were carried out from the dorsal aspect and usually resulted in very few labelled cells with processes that extended laterally towards the pial surface (Fig 5.4D and data not shown). Examining these specimens at 3dpf gave an indication that labelled cells had moved rostrally (Fig 5.4B), relative to the posterior border of the telencephalon,

Figure 5.4: Dorsal activations in T1/roof

A-C show one embryo and D-F a second; all scale bars are 50µm

A shows an activation in T1 from the dorsal aspect at 28hpf (blue arrowhead); the position of the epiphysis is indicated. B shows a lateral view of the same embryo at 3dpf. The tel/di border is indicated by a white arrowhead, the position of the labelled cells by a blue arrowhead. C is a single parasagittal confocal section through the telencephalon; labelled cells are present in the outlined OB, far from the tel/di border (white arrowhead).

D and E show dorsal (D) and lateral (E) views of another activation in T1 from the dorsal aspect at 28hpf (blue arrowheads in D and E). At 5dpf, two labelled cells are visible lying within the OB (white arrowheads in F); other red labelling is within the skin.

AC – anterior commissure

di – diencephalon

E – epiphysis

ey – eye

OB – olfactory bulb

OE – olfactory epithelium

OP – olfactory placode

SOT – supraoptic tract

TAC – tract of the anterior commissure

tel – telencephalon

v - ventricle

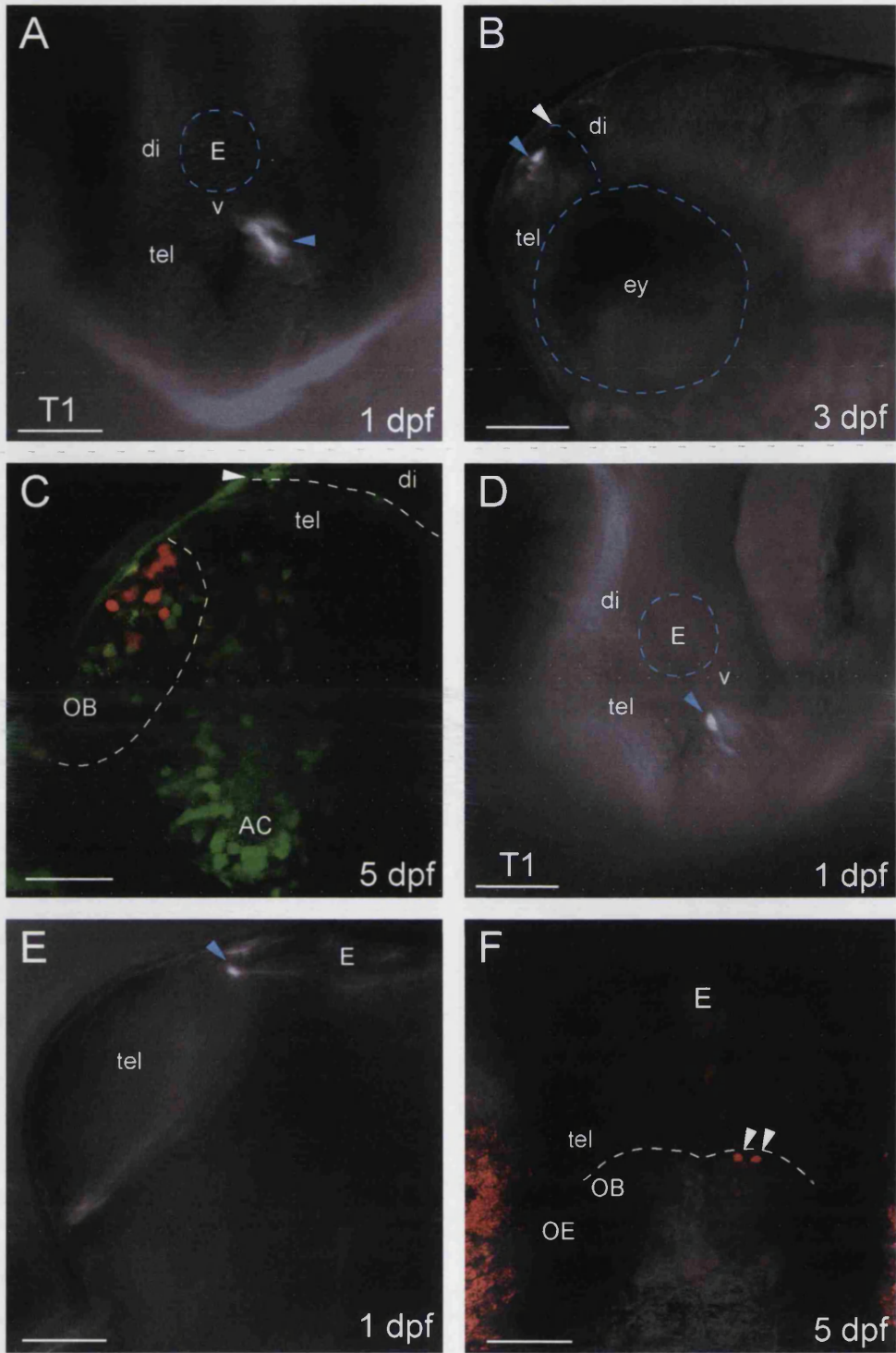


Figure 5.4

towards the position of the OB. Indeed, at 5dpf, all “roof” activations had labelled cells in the OB and in 6/7 cases the OB was the exclusive destination of all of the strongly labelled red cells (Fig 5.4F). This striking result showed that the most posterior dorsal cells in the telencephalon contribute exclusively to the OB, and have a neuronal fate.

### *Cells labelled in T2*

Moving more rostrally along the border of the telencephalon, I made 12 activations in T2, all from the lateral aspect (Fig 5.5 A and B). At 3dpf, many specimens had labelled cells in the OB (data not shown) and by 5dpf all 12 T2 specimens showed labelling in the OB (Fig 5.5 C). In fact, similar to activations in T1, 5/12 specimens had labelled cells restricted solely to the OB, with no other telencephalic labelling. In specimens with both OB and other telencephalic labelling, cells were found in mid- and ventral telencephalic areas, always anterior to the AC. In contrast to T1 cells, T2 cells were never seen in dorsal telencephalic areas, but this fits well with T2 being located more anterior and ventral than T1.

Labelled fibres were also visible in samples activated in T2. In 4/12 cases, fibres were seen in the olfactory tracts (Fig 5.5 D), again suggesting the presence of labelled mitral cells. Fibres were also clearly present in the TAC in 4/12 samples, and in the AC itself in a similar number of samples. No fibres were observed in the SOT, but this may be attributable to the limitations of imaging which was all done from the dorsal aspect. From this aspect, the SOT lies extremely deep in the tissue, and single labelled fibres may not be discernable.

### *Cells labelled in T3*

Further anterior and ventral to T2, 12 activations were made in T3. From comparisons with the expression pattern of *emx3* at this stage (Fig 5.2 C), T3 would be predicted to lie close to the pallial/subpallial border. Activations were mainly from the lateral aspect (Fig 5.5E) but 4/12 were from the anterior aspect; no difference in the distribution of labelled cells was seen between these two groups. Out of 12 activations in T3, 9 embryos had some labelling in the OB at 5dpf; the remaining 3 did not. However, in none of these specimens were labelled fibres seen in the LOT/MOT, although this does not rule out the labelled cells being projection neurons. Outside the OB, labelled cells were found in lower mid- and ventral

Figure 5.5: Lateral activations in T2 and T3

All scale bars are 50µm

A-D show a single embryo, activated in T2. A and B show lateral (A) and anterior (B) views of an activation in T2 at 30hpf (blue arrowheads in A and B). C shows the same embryo at 5dpf from the dorsal aspect; labelled cells are mainly present in the OB. In D, a confocal section at the level shown in H shows labelled fibres in the LOT/MOT (arrowhead) and labelled cells bilaterally in the OB.

E and F show an embryo activated in T3; G shows a second embryo. E shows a lateral view of an activation in T3 at 30hpf. At 5dpf, a single confocal section (F) shows labelled cells throughout the OB (arrowheads in F). G shows a confocal maximum projection of a T3 activated specimen, imaged at 5dpf from the lateral aspect. Cell bodies in the OB (arrow) and ventral telencephalon (arrowheads) are labelled, as well as fibres in the SOT and TAC.

AC – anterior commissure  
di – diencephalon  
E – epiphysis  
ey – eye  
MOT – medial olfactory tract  
OB – olfactory bulb  
OE – olfactory epithelium  
OP – olfactory placode  
SOT – supraoptic tract  
TAC – tract of the anterior commissure  
tel – telencephalon  
v - ventricle

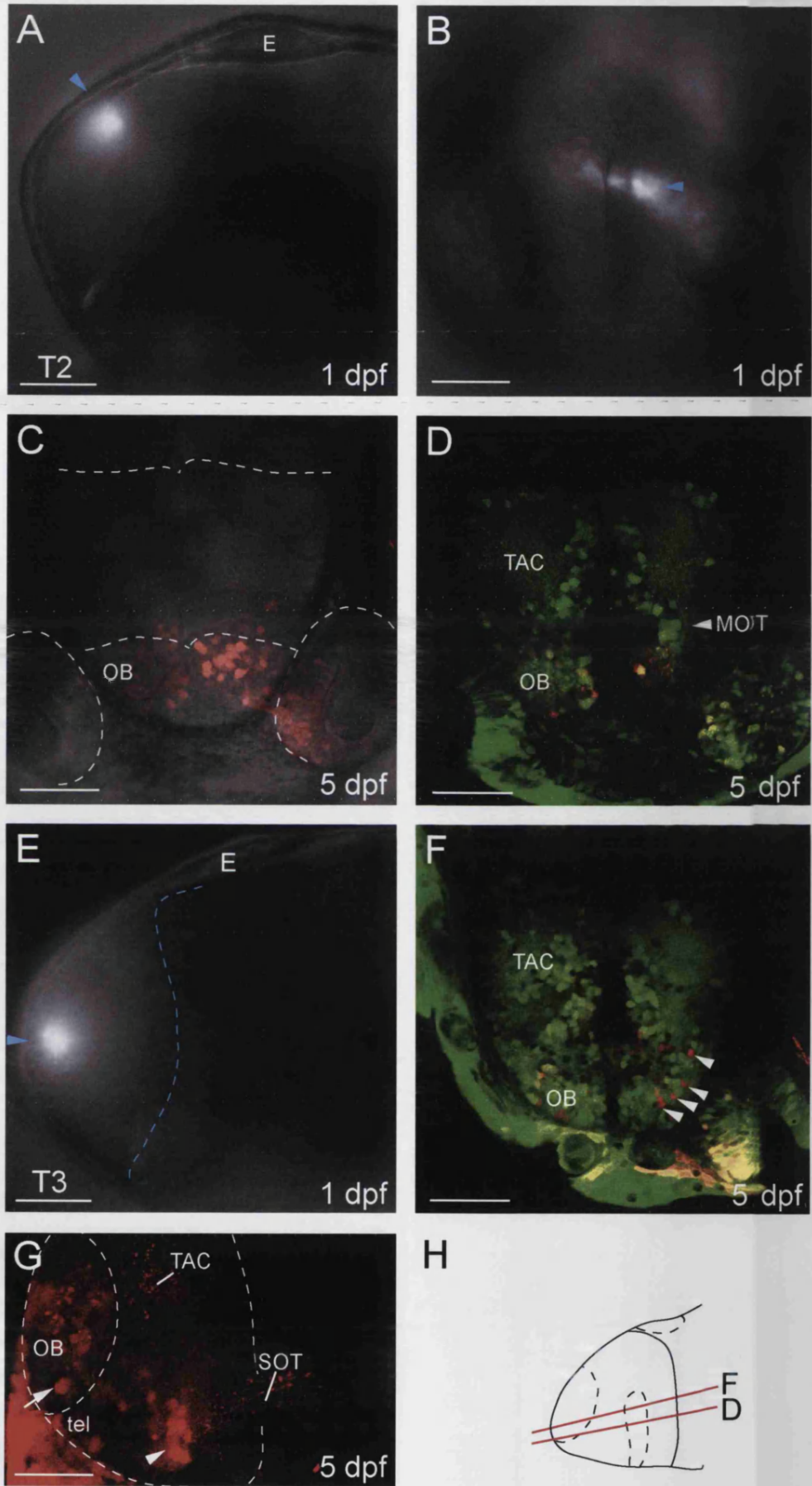


Figure 5.5

telencephalic areas. As with activations in T2, cells were always located anterior to the AC (Fig 5.5F).

Activations in T3 also resulted in labelled fibres in telencephalic tracts and commissures. In 4/12 specimens, axons were seen in the TAC, and in 2/12 specimens in the SOT (where specimens were imaged from the lateral aspect; Fig 5.5G). This indicated that at least some of the cells labelled in T3 activations send projections out of the telencephalon to more caudal brain areas.

#### *Cells labelled in T4, T5 and T6*

Labelling of cells in the regions designated T4, T5 and T6, in the most ventral-anterior part of the telencephalon, gave very consistent but remarkably different results to activations in the dorsal telencephalon (T1-T3). Out of a total of 33 activations in these three regions, no labelling was ever seen in the OB at 5dpf. Nor were there ever any labelled fibres in the olfactory tracts, which correlated well with the absence of labelled OB cells. The only labelling visible in the OB came from the terminals of olfactory sensory neurons (OSNs), which were unavoidably labelled in the olfactory placode during the activations in these ventral regions.

Outside the OB, labelled cells from activations in T4, T5 and T6 were present in ventral, mid- and dorsal telencephalic areas. The 5dpf patterns of labelling were quite consistent between the three areas, with some informative differences. Generally, labelled cells were present both clustered around the AC in the ventral telencephalon and also distributed singly throughout the mid- and dorsal telencephalon. Specifically, in T4, 9/11 specimens showed clustering of cells around the AC with scattered single cells present in the mid- and dorsal telencephalon (Fig 5.6 A-D); 2/11 specimens showed only the ventral telencephalic labelling. The distributed cells reached the most dorsal levels of the telencephalon, classified as such by the absence of fasciculated TAC fibres in this region (Fig 5.6 C). In the ventral telencephalon, labelled cells were mostly located anterior to the AC at both 3dpf and 5dpf (Fig 5.6B and D). This seemed to correlate with the position of T4 just dorsal to the AC at 1dpf (Fig 5.6A). Cells labelled in T4 at 1dpf also contributed to tracts and commissures in the telencephalon, with 4/11 specimens showing labelled fibres in the TAC, and 5/11 in the AC (Fig 5.6D). No specimens were seen with labelling in the SOT.

Figure 5.6: Lateral activations in T4 (A-D) and T5 (E-F).

A, C and D show the same embryo, E and F show another embryo; all scale bars are 50µm

A shows a lateral view of an activation in T4 at 26hpf (blue arrowhead); the border of the telencephalon and position of the AC are indicated. B shows a similarly-activated embryo from the dorsal aspect at 3dpf; labelled cells lie anterior to the AC. Confocal sections (C and D) at 5dpf at the positions indicated in G reveal isolated labelled cells in the dorsal telencephalon (arrowheads in C; note the absence of labelled cells from the OB) and clustered labelled cells in the ventral telencephalon, anterior to the AC (D). A labelled neuron has an axon extending into the AC (arrowhead in D).

E shows a lateral view of an activation in T5 at 26hpf (blue arrowhead), with the position of the AC indicated. At 3dpf, a lateral view of the same embryo reveals labelled cells in mid- and dorsal telencephalic areas (F, blue arrowheads); no cells are present in the OB. Labelled cells clustered around the AC in this specimen are present at a different focal plane.

AC – anterior commissure  
di – diencephalon  
E – epiphysis  
ey – eye  
OB – olfactory bulb  
OE – olfactory epithelium  
OP – olfactory placode  
SOT – supraoptic tract  
TAC – tract of the anterior commissure  
tel – telencephalon  
v - ventricle

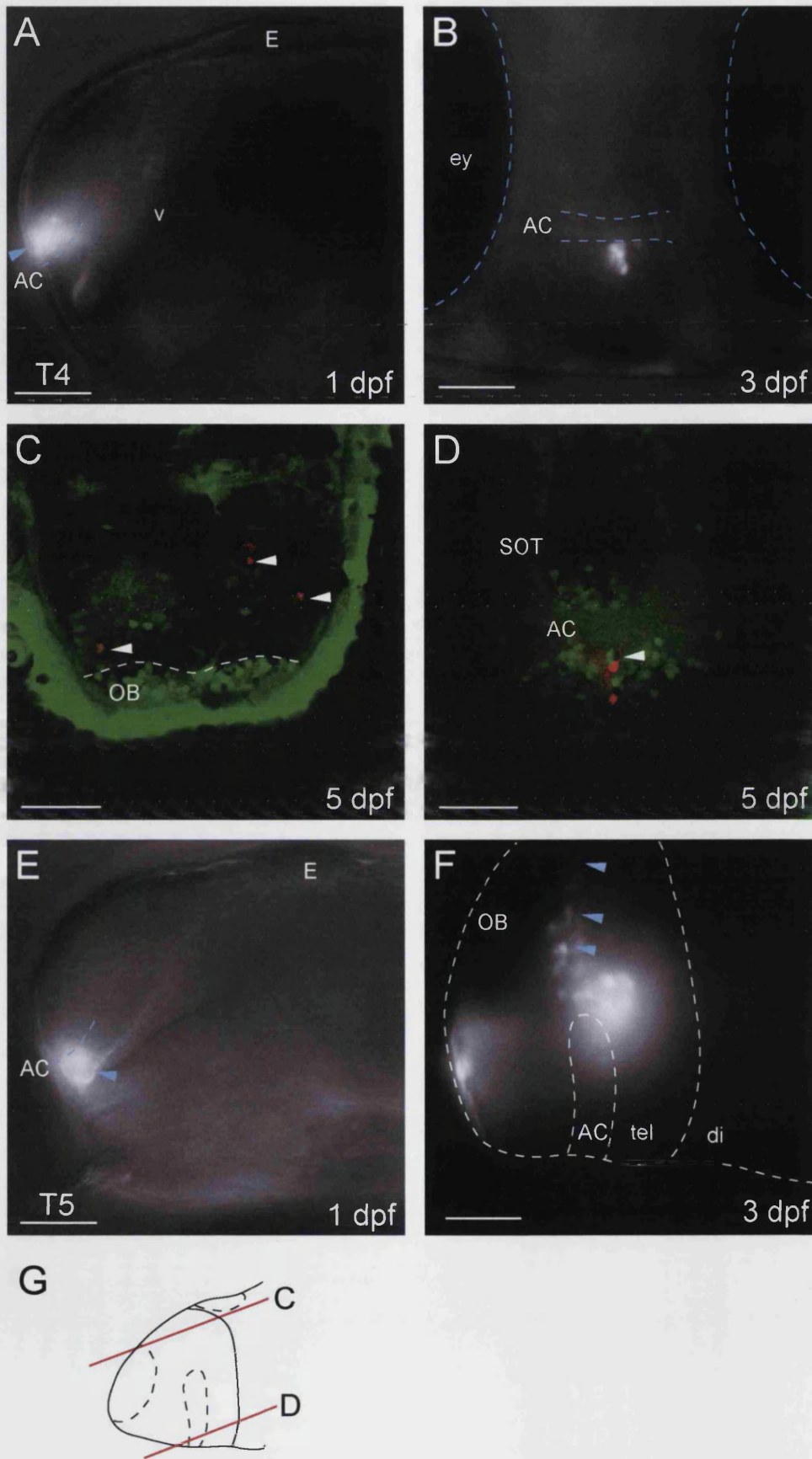


Figure 5.6

As with activations in T4, activations in T5 showed the same distinctive pattern of labelled cells, with 15/16 specimens showing clustering of cells around the AC and a mid- and dorsal distribution of single cells. In these specimens, labelled cells were present both anterior and posterior to the AC, fitting with the relative positions of T5 and the AC at 1dpf (Fig 5.6 E). By 3dpf, this distinctive pattern of labelled cells was already apparent, with labelled cells appearing both around the AC (data not shown) and in a “stream” through mid- and dorsal telencephalic areas (Fig 5.6 F). Similar patterns were seen when specimens were imaged from the dorsal aspect, with labelled cells appearing in the most dorsal telencephalic areas (data not shown). Activations in T5 also resulted in the labelling of fibres within the telencephalon. 6/16 specimens contained fibres in the TAC; two of these specimens also contained labelled fibres in the AC and SOT (see summary Table 5.1).

The third region to show a similar pattern of labelled cells was T6, where 5/6 specimens had some cells clustered around the AC with more dorsal scattered single cells. With activations in this region, cells around the AC appeared posterior and slightly dorsal to the AC (Fig 5.7D), correlating well with the relative positions of T6 and the AC at 1dpf (Fig 5.7A). The scattered single cells were present more dorsally than those around the AC, but not in the most dorsal regions of the telencephalon. However, in all other respects these single distributed cells looked much like those from activations in T4 and T5 (Fig 5.7C). In terms of labelled fibres, 6/6 activations in T6 showed fibres in the TAC, and 2/6 in the AC itself. Again I did not observe any labelled fibres in the SOT, possibly for technical reasons.

### *Cells labelled in T7*

Activations in T7 (Fig 5.7E), a site mid-way along the ventral border of the telencephalon, produced quite different results from either those in T1-T3 or in T4-T6. Cells labelled in this region never contributed to the OB (unlike T1-T3), nor were they found scattered in more dorsal regions at 5dpf (unlike T4-T6). In 6/6 specimens, cells were found clustered in the posterior telencephalon, at mid- and ventral levels (Fig 5.7 F). In general, cells were restricted to a medial posterior quadrant in any telencephalic section; few cells appeared laterally. In the fibre

Figure 5.7: Lateral activations in T6 (A-D) and T7 (E-F).

A-D show one embryo and E-F a second. All scale bars are 50µm

A and B show lateral (A) and anterior (B) views of an activation in T6 at 30hpf (blue arrowheads in A and B). Confocal sections (C and D) at 5dpf at the positions indicated in G reveal isolated cells in the dorsal telencephalon (arrowheads in C) and clustered labelled cells dorso-posterior to the AC (arrowhead in D).

E shows a lateral view of an activation in T7 at 30hpf (blue arrowhead). F shows a single confocal section through the mid-telencephalon at 5dpf (indicated in G) with cells located in the posterior medial telencephalon, posterior to the AC.

AC – anterior commissure  
di – diencephalon  
E – epiphysis  
ey – eye  
OB – olfactory bulb  
OE – olfactory epithelium  
OP – olfactory placode  
SOT – supraoptic tract  
TAC – tract of the anterior commissure  
tel – telencephalon  
v - ventricle

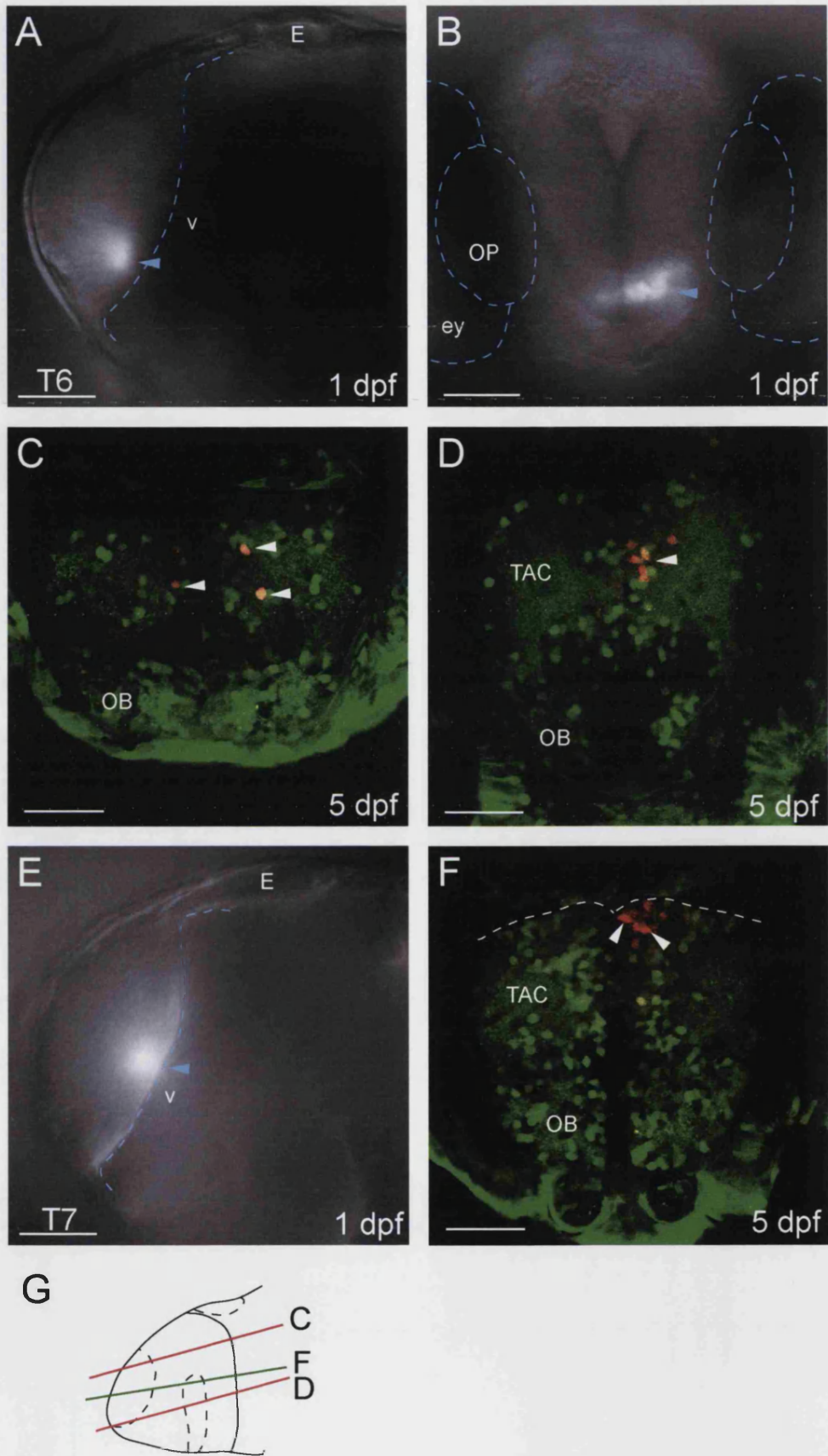


Figure 5.7

tracts, cells labelled in T7 contributed to the TAC in 5/6 specimens, but no labelled fibres were observed in the AC or SOT.

#### *Cells labelled in T8 and T9*

In the final two regions, T8 and T9, cells labelled at 1dpf made contributions to both the 5dpf OB and telencephalon (Fig 5.8). The position of these regions was close to the dorsal regions T1, T2 and T3 that also contributed cells to the OB, but activations in T8 and T9 gave slightly different patterns. Out of 8 specimens labelled in T8, 7 contributed cells to both OB and mid-telencephalic areas and one contributed to the OB alone. Noticeably in these specimens, labelled cells tended to remain relatively close together, even if they became segregated between the telencephalon and OB. In the OB, labelled cells were generally located in posterior regions of the bulb (arrows in Fig 5.8 D), in the area occupied by interneurons (see Figure 3.8 E and F). In fact, in a number of T8 specimens, I saw labelled OB cells with interneuron morphology – a complex and enlarged dendritic arbour (Fig 5.8 E). In accordance with this observation, no labelled axons were seen in the LOT/MOT. In the telencephalon, labelled cells were located anteriorly in mid-telencephalic regions, adjacent to the OB (arrowheads in Fig 5.8 D). This distribution of cells was also visible at 3dpf (Fig 5.8 C). Cells labelled in T8 also contributed fibres to the TAC (3/8), but not visibly to the AC or SOT.

The final region, T9, was located in the middle of the telencephalon, surrounded by the other eight regions (Fig 5.8 G). In terms of cell labelling, this region showed strongest similarity to activations in T8. In 7/7 specimens, labelled cells were found at 5dpf in posterior locations in the OB and in adjacent anterior regions of the telencephalon, at mid- and ventral telencephalic levels (Fig 5.8 H). Contributions to the OB were often quite limited, with a number of specimens containing only a couple of labelled OB neurons. Again like T8 activations, specimens activated in T9 showed no labelling of the LOT/MOT, implying that labelled OB cells might be interneurons. However, distinctive interneuron morphology was not obvious in these specimens. In the telencephalic tracts and commissures, labelled axons were present in 4/7 specimens in the TAC and in 1/7 in the AC.

Figure 5.8: Lateral activations in T8 (A-E) and T9 (G-H).

A-D show the same embryo, G-H a second; all scale bars are 50µm, except where indicated.

A and B show lateral (A) and anterior (B) views of an activation in T8 at 26hpf (blue arrowheads in A and B). C shows a dorsal view of the same embryo with labelled cells in the OB and anterior telencephalon. In a single confocal section (D) at 5dpf, at the level shown in F, labelled cells are present both in the posterior OB (arrows) and anterior mid-telencephalon (arrowheads). E shows a higher power view of the OB in an T8-labelled specimen; white arrowheads indicate local processes of a possible interneuron.

G shows a lateral view of an activation in T9 at 28hpf (blue arrowhead). At 5dpf, a single confocal section (H) at the level shown in F reveals a labelled cell in the posterior OB (arrow) and other labelled cells in the anterior mid-telencephalon (arrowheads in H).

AC – anterior commissure  
di – diencephalon  
E – epiphysis  
ey – eye  
OB – olfactory bulb  
OE – olfactory epithelium  
OP – olfactory placode  
SOT – supraoptic tract  
TAC – tract of the anterior commissure  
tel – telencephalon  
v - ventricle

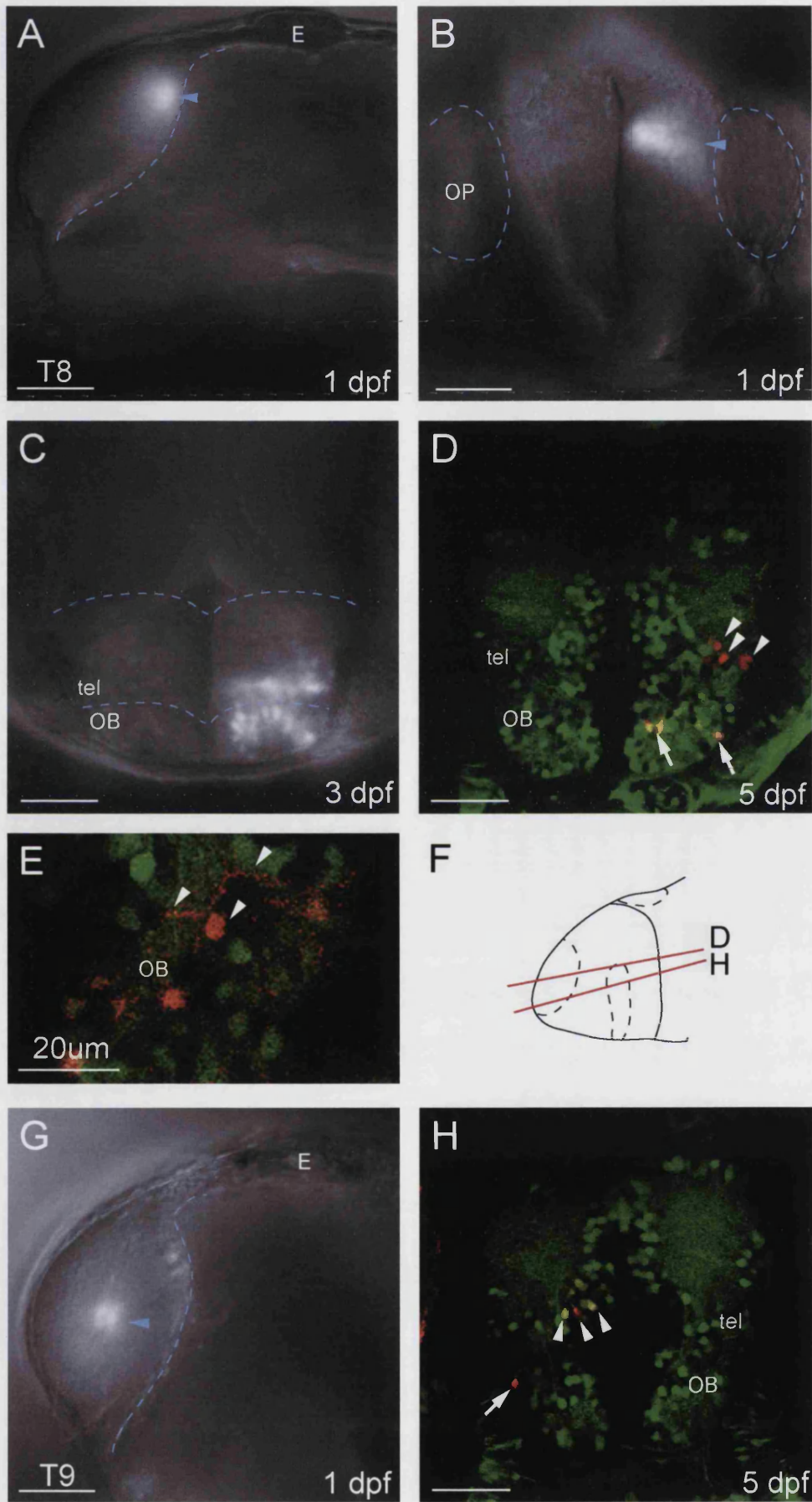


Figure 5.8

### *Timing of T1/roof contribution to the OB*

Having established that the most posterior region of the dorsal telencephalon, designated T1, contributes cells to the OB, I wanted to look more closely at the timing of this contribution. I labelled cells in the single-layered neuroepithelium of the telencephalic roof at 1dpf, analysing the activations immediately afterwards by confocal microscopy (Fig 5.9 A and B). I then re-imaged the same specimens at 2dpf and 3dpf to visualise the movements of labelled cells during this time.

At 1dpf, immediately following the photoconversion, labelled cells were present in a medially-located cluster in the posterior dorsal telencephalon (Fig 5.9 A and B). At 2dpf, these same cells had spread slightly in the medio-lateral axis, but remained adjacent to the posterior border of the telencephalon (Fig 5.9 C). Using the presence of glomeruli to define the limits of the OB, I saw that the labelled cells were directly juxtaposed to but not within the OB at 2dpf (Fig 5.9 D). However at 3dpf, the same labelled cells could be seen within the distinctive morphology of the OB (Fig 5.9 F). Between 2dpf and 3dpf the cohort of labelled cells also continued to spread in a medio-lateral direction, resulting in one labelled cell being at the lateral edge of the OB. However, there was little or no spread in any other axis during this time, with all labelled cells remaining very dorsal in the OB. I repeated this experiment with 5 specimens, and all showed a similar timing of contribution to the OB.

### *Summary*

I have followed the fate of cells from each of nine regions in the telencephalon, designated T1-T9 (Fig 5.10 A). The cells derived from regions labelled at 1dpf fall into two distinct categories – those that make contributions to the OB and those that do not. This data is summarised in Table 5.1 below. The regions that contribute cells to the 5dpf OB are located in more dorsal and posterior regions of the 1dpf telencephalon, namely T1-T3 and T8-T9 (Fig 5.10 A and B). Particularly striking was the result that the most posterior region of the dorsal telencephalon at 1dpf, the telencephalic roof, contributes cells to the OB.

The cells labelled in the OB at 5dpf from activations in T1-T3 and T8-T9 included both projection neurons (as evidenced by the presence of efferent axons in the olfactory tracts) and interneurons (as evidenced by characteristic dendritic arbours). The origins of these two cell types seem to be segregated in the telencephalon, with T1, T2 and T3 contributing more projection neurons and T7 and

Figure 5.9: Following cell movement from T1 into the OB.

All figures show the same embryo; all scale bars are 50µm.

A, C and E are maximum projections of confocal sections, overlaid on transmitted light pictures of the telencephalon; B, D and F are single confocal sections from the same stacks at the levels shown in the schematic diagrams at the end of each panel. Axes within the telencephalon are indicated at the end of each panel.

A and B show all cells (A) and a single confocal section (B) immediately after a dorsal activation in T1 at 28hpf. Labelled cells (arrow in A and arrowhead in B) are located at the midline in the telencephalic "roof". C and D show the same cells at 48hpf in a projection (C; arrows) and single section (D). Arrowheads in D mark labelled cells which lie posterior to the OB territory (marked by dotted lines). In E and F, the same cells are shown at 3dpf in a projection (E; arrows) and single section (F). Labelled cells (arrowheads) are rostrally-located in the telencephalon, within the OB territory (marked in F).

AC – anterior commissure  
di – diencephalon  
E – epiphysis  
ey – eye  
OB – olfactory bulb  
OE – olfactory epithelium  
OP – olfactory placode  
SOT – supraoptic tract  
TAC – tract of the anterior commissure  
tel – telencephalon  
v - ventricle

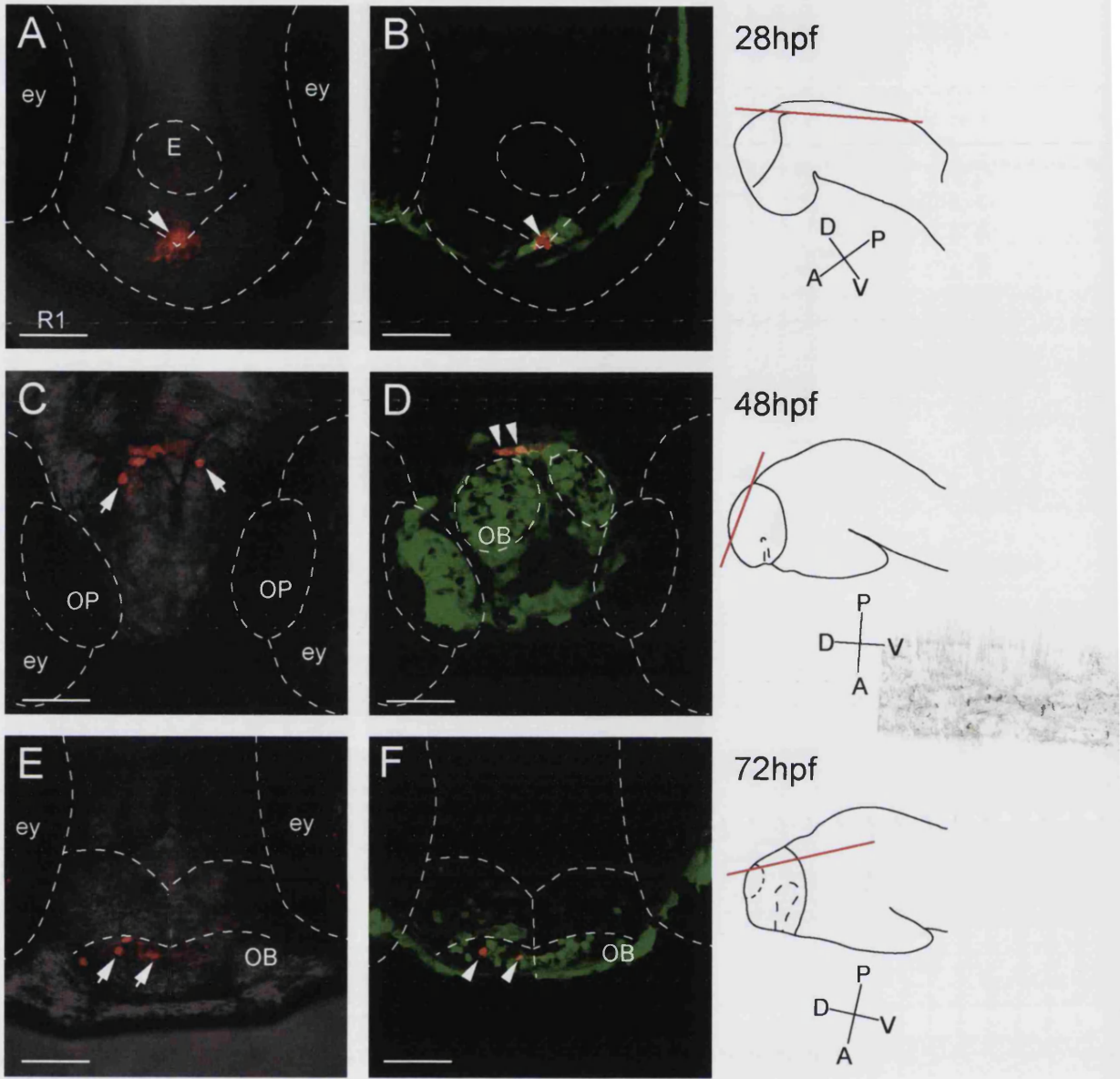


Figure 5.9

**Figure 5.10: Summary diagram showing contributions of regions T1-T9**

A shows a schematic diagram of a 1dpf telencephalon with the regions T1-T9 marked and colour-coded. Regions where 100% of specimens show some OB contribution are highlighted by a red ring; regions where less than 100% show OB contribution are highlighted by a dashed red ring. Regions giving rise to cells which migrate dorsally are highlighted by a green ring.

B shows a schematic diagram of a 5dpf telencephalon, with the distributions of labelled cells resulting from photo-activations in the regions identified and colour-coded in A. The distribution of labelled cells for each region is not intended to exactly replicate the data, but simply to give a general idea of the telencephalic and OB areas to which each region contributes.

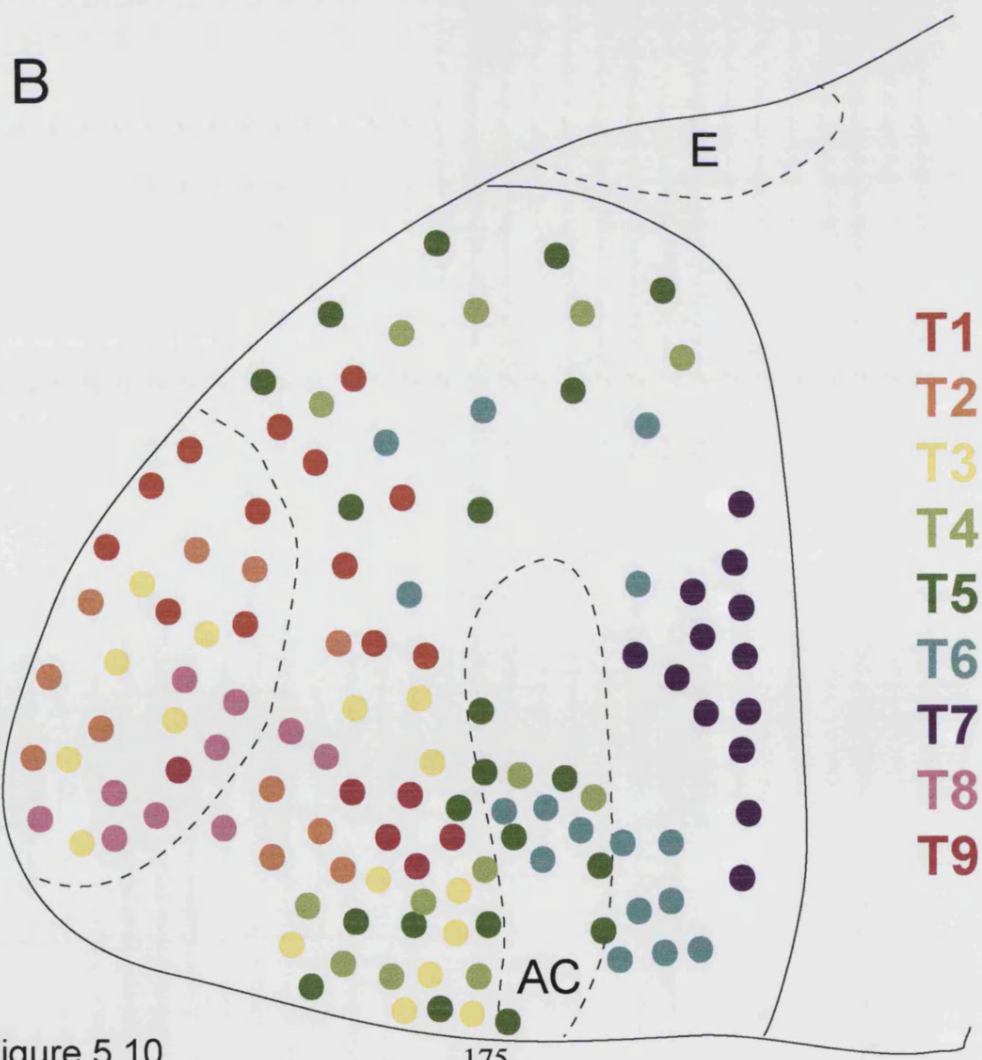
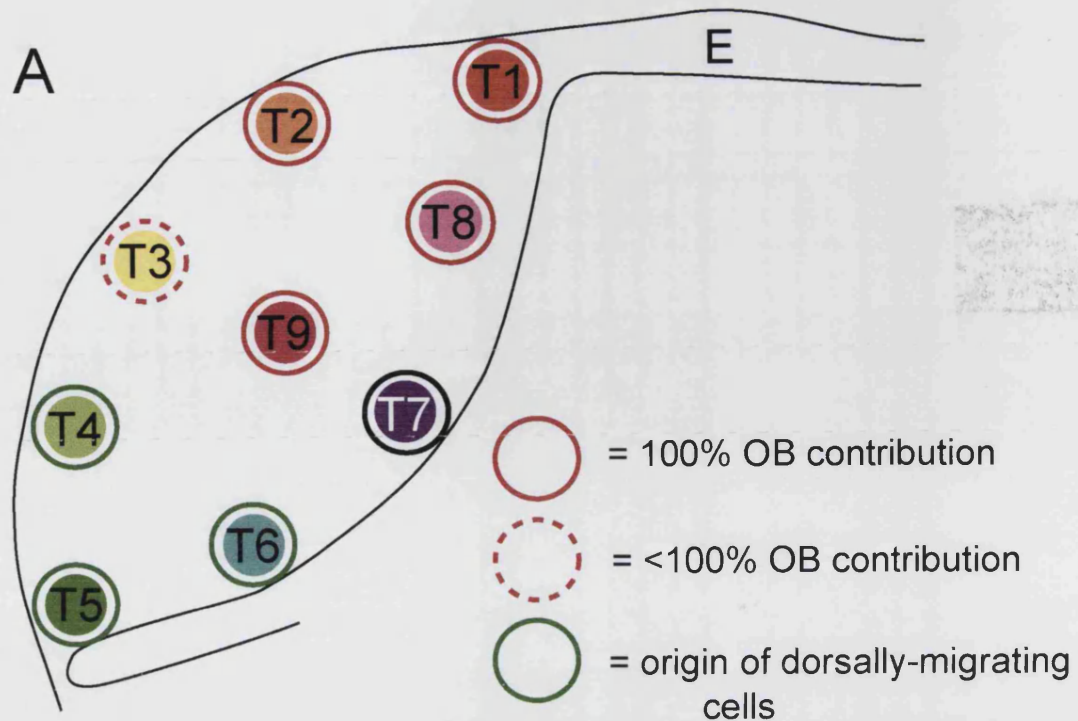


Figure 5.10

T8 more interneurons. This is further suggested by the patterns of labelled fibres in the olfactory tracts (for summary see Table 5.1). However, a precise classification or quantification of these cell types has not been carried out, and some cells with interneuron morphology were also found in T1 specimens.

More ventral regions of the telencephalon, T4-T6, do not contribute any cells to the OB. Rather, they contribute cells to the ventral telencephalon and also single cells to more dorsal telencephalic areas. The positioning and scattered nature of the dorsal cells bears strong similarity to cells seen in the *Tg(dlx4/6:GFP)* line (Fig 3.8).

Table 5.1: Summary of destinations and projections of cells labelled in T1-T9 at 1dpf

Numbers of specimens showing labelling in a particular area, as a proportion of the total number of specimens, is shown in each column; percentages are in red.

Region	Total n=	OB	Tel	LOT/ MOT	TAC	AC	SOT	Positions of labelled cells at 5dpf
T1	31	31/31 100	21/31 68	7/31	27/31	16/31	5/31	OB labelling; mid- and dorsal tel anteriorly
T2	12	12/12 100	7/12 58	4/12	4/12	4/12	0/12	OB labelling; mid- and ventral tel anterior to AC
T3	12	9/12 75	12/12 100	0/12	4/12	0/12	2/12	OB labelling in most specimens; mid- and ventral tel anterior to AC
T4	11	0/11 0	11/11 100	0/11	4/11	5/11	0/11	No OB labelling; ventral tel anterior to AC and mid- and dorsal distribution
T5	16	0/16 0	16/16 100	0/16	6/16	2/16	2/16	No OB labelling; ventral tel around AC and mid- and dorsal distribution
T6	6	0/6 0	6/6 100	0/6	6/6	2/6	0/6	No OB labelling; mid- and ventral tel posterior to AC and mid-tel distribution
T7	6	0/6 0	6/6 100	0/6	5/6	0/6	0/6	No OB labelling; medial, posterior mid- and ventral tel
T8	8	8/8 100	7/8 100	0/8	3/8	0/8	0/8	Posterior OB; anterior mid-tel
T9	7	7/7 100	7/7 100	0/7	4/7	1/7	0/7	Posterior OB; anterior mid-tel

## 5.4 Discussion

I have generated a coarse fate-map of the zebrafish telencephalon between 1dpf and 5dpf, principally to establish the spatial origins of the olfactory bulb (OB). To do this I developed a novel fate-mapping technique based on the naturally fluorescent Kaede protein (Ando et al., 2002). By using a photo-conversion technique to label small groups of cells I sampled a large proportion of the telencephalon, making restricted photo-activations in defined areas (Fig 5.10 A). The strength of this technique is its non-invasiveness, the long-term stability of the tracer and its accessibility to almost all brains areas. In addition, the visualisation of cell morphology remains impressive over the 5-day timescale of the experiment. The fate mapping observations have enabled me to build a picture of the developing telencephalon that fits well with data from other species and gives some novel insights into this brain area.

### *Pallial areas T1, T2 and T3 contribute to the OB – a potential source of projection neurons?*

My findings indicate that the dorsal and posterior telencephalic regions, designated T1, T2 and T3 in this study, contribute cells to the OB. In a subset of labellings performed from the dorsal aspect in the posteriorly-located T1/roof region, the OB was the exclusive destination of labelled cells in the vast majority of specimens (Fig 5.4). This result was particularly striking because it was not predicted for extremely posterior cells in the telencephalic roof to contribute to the rostrally-positioned OB. Furthermore, this result confirmed that at least part of the roof region is neurogenic.

Gene expression analyses suggest that areas T1, T2 and T3 lie within the zebrafish pallium. Genes that mark the pallium in mouse and chick, such as *Emx1* and *Tbr1* (Puelles et al., 2000) are also expressed in the presumptive pallial areas of the zebrafish telencephalon (Kawahara and Dawid, 2002; Mione et al., 2001; Morita et al., 1995; Chapter 4). The pallium extends to the posterior dorsal limit of the telencephalon, although genes such as *emx3* and *tbr1* probably do not show its full extent, being primarily expressed in postmitotic cells (Fig 5.11 B and C). In the telencephalic roof, for example, which is mostly mitotically active (Fig 3.4 A and D), it is not clear whether these genes are expressed. However, a gene that is additionally expressed in proliferating pallial cells, *eomesodermin* (*eom*; Mione et

**Figure 5.11: Comparison of regions T1-T9 with known markers**

A shows the same schematic diagram as in Fig 5.10, a 1 dpf telencephalon with the regions T1-T9 marked and colour-coded, and their contributions to the OB indicated.

B-H show lateral views of pallial (*emx3*, B; *tbr1*, C), subpallial (*dlx4/6*, D; *nk2.1b*, E, taken from Rohr et al., 2001) and Lhx genes (*lhx1a*, F; *lhx1b*, G and *lhx5*, H). Stages are indicated in the lower left corner of each panel.

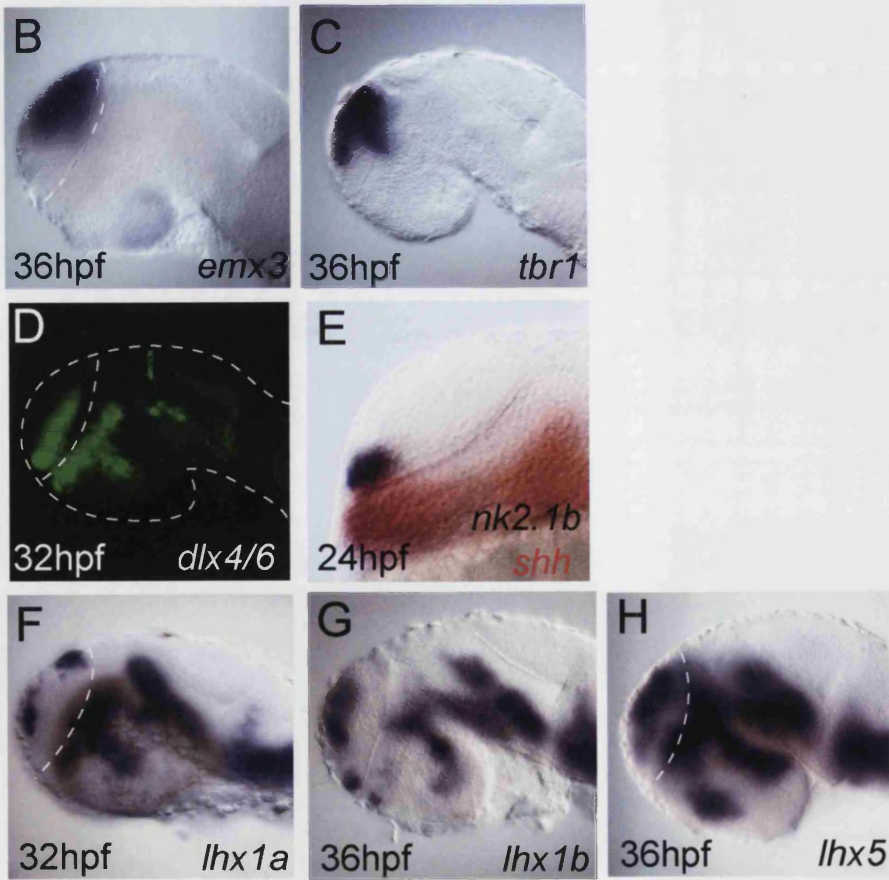
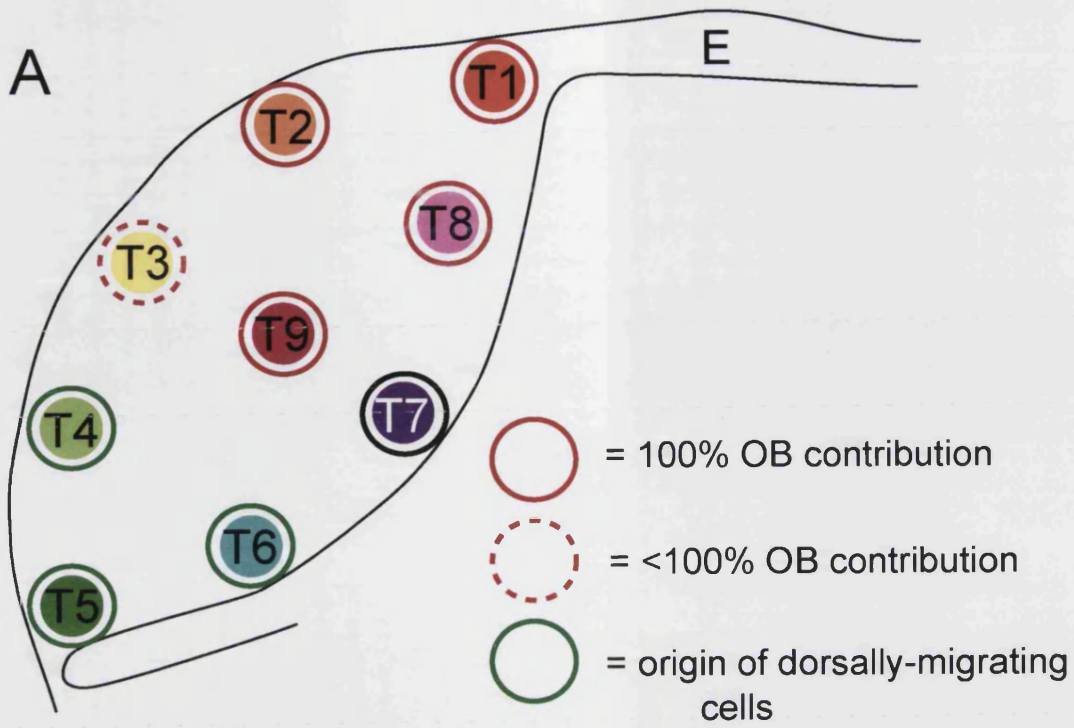


Figure 5.11

al., 2001), suggests a pallial nature for the roof; a more detailed analysis would be required to confirm this. The critical feature of the roof for my experiments was that its thin nature enabled the unambiguous labelling of very small numbers of posterior dorsal cells and revealed their OB contribution.

My data suggests that OB projection neurons have their origins in the pallium. I have not attempted a detailed characterisation of the OB cells labelled by activations in T1, T2 and T3, due to the difficulties of combining the Kaede technique with other cell markers. However, the presence of red Kaede-labelled fibres in the olfactory tracts in 11/43 T1 and T2 specimens (although not in T3 specimens) indicates that some of these cells become OB projection neurons (Fig 5.3 F). A pallial origin of mitral cells was actually suggested by a fate map of the 12hpf zebrafish neural plate, where presumptive pallial regions gave rise to labelled cells in the OB with axons that extended into the AC (Whitlock and Westerfield, 2000). Unfortunately, the authors identified these cells as interneurons, whereas their projection outside the OB actually identifies them as projection neurons. These cells originated in a region that would be included in the T1, T2 or T3 sampled here (Whitlock and Westerfield, 2000). My results also indicate that the expression of the pallial genes *eom* and *tbr1* in zebrafish mitral cells (Mione et al., 2001) does reflect a pallial origin for these cells.

Pallial regions are known to be the source of OB projection neurons in a number of other species. In null mouse mutants for the pallial *Tbr1* or *Emx2* genes the entire mitral cell layer is missing from the bulb (Bulfone et al., 1998; Yoshida et al., 1997). Fate mapping with an *Emx1* reporter line also shows extensive labelling in the OB mitral cell layer, with some sparse labelling in other layers of the bulb (Gorski et al., 2002). Furthermore, the expression of pallial markers such as *xLhx5* and *eomesodermin* by OB mitral cells in *Xenopus* has been used as evidence of their pallial origins (Moreno et al., 2003).

One interesting contrast between my data and that from mammals is the difference in the area of the pallium that contributes projection neurons to the bulb. Focal electroporations of lineage tracing constructs in the rat telencephalon found that only the pallial area directly underlying the future evagination point of the OB contributed mitral cells (Nomura and Osumi, 2004). Similarly fate-mapping studies of early stage chick neural plate found only a small domain nested within the presumptive ventral pallium gives rise to OB neurons (Cobos et al., 2001b).

Unfortunately the chick OB cells were not phenotyped in detail, but they are not interneurons as the origins of those cells have been fate-mapped to the subpallial striatum (Cobos et al., 2001a). In contrast, I find a broad area of the presumed pallial telencephalon contributes to the OB (Fig 5.11). The possible reasons for this and the factors that control OB contribution will be discussed later.

The reduced proportion of specimens contributing cells to the OB from T3 (75%) compared with T1 and T2 (100%) may indicate that T3 lies on the border of an OB-contributing region. Comparison with the pallial markers *emx3* and *tbr1* would place T3 at the anterior border of *emx3* expression, probably extending into the *emx3*-negative, *tbr1*-positive region (compare Fig 5.11 A-C). One possibility is that T3 straddles the pallial/subpallial boundary, and only those activations that labelled at least some pallial cells make an OB contribution. A further possibility is that the *Emx*-negative *Tbr1*-positive area highlights the ventral pallium, as it does in chick and mouse (Puelles et al., 2000). This seems somewhat unlikely, because as discussed above the ventral pallium is the OB contributing region in chick (Cobos et al., 2001b) and probably in rodents (Nomura and Osumi, 2004; Puelles et al., 2000). Therefore T3 labellings would be expected to label more OB cells than T1 and T2, which is clearly not the case. A final possibility is that the *tbr1*-positive *emx3*-negative cells are pallial but migrate to a ventral position around the olfactory tracts by 5dpf (M. Mione, personal communication). This is similar to the movements of some T3 cells that contribute to an area just anterior to the AC (see Table 5.1) and also fits well with my observations of *tbr1* expression at both early and later embryonic stages (Fig 3.8 G and H and 4.9 S and T). It is therefore possible that T3 specimens contribute both to the OB and to structures involved with the formation of the secondary olfactory projections from the bulb into the telencephalon.

#### *Subpallial contribution to the OB – a potential source of interneurons?*

Cells labelled in the regions designated T8 and T9 also contributed cells to the OB. In many ways the patterns of labelled cells in these specimens bore strong similarities to those labelled in T1-T3. However, one striking difference was that no labelled axons were ever seen in the olfactory tracts. Although this does not prove an absence of labelled projection neurons (labelled axons were also absent in T3 specimens), it suggests that T8 and T9 may contribute OB interneurons, neurons that

do not project outside the bulb. These neurons can also be identified by their extremely elaborate dendritic arbours, and OB cells with such a morphology originated from T8 (Fig 5.8 E). In fact, cells with an interneuron morphology were also observed in some T1 specimens, especially those in which the initial activation was relatively broad (data not shown). This suggests that the populations of cells giving rise to interneurons and projection neurons of the OB may initially lie adjacent to each other in the developing telencephalon.

This situation closely parallels that seen in mouse, where early-born GABAergic interneurons of the OB are derived from the ventral telencephalic lateral ganglionic eminence (LGE) (Corbin et al., 2000; Stenman et al., 2003; Yun et al., 2001). This region lies adjacent to the cortex and it is the dorsal part of the LGE that directly abuts the cortex that is the primary source of OB interneurons (Stenman et al., 2003). The LGE expresses a number of ventral telencephalic genes, among that are members of the *Dlx* family. *Dlx1* and *Dlx2* have been shown to be critical for OB interneuron specification (Anderson et al., 1997b; Bulfone et al., 1998) and these genes continue to be expressed in both granule cells and juxtglomerular interneurons within the bulb (Anderson et al., 1999). Comparisons with zebrafish indicate a very similar situation; *dlx* gene expression in zebrafish also marks the ventral telencephalon (Akimenko et al., 1994), a feature highlighted particularly well by the *Tg(dlx4/6:GFP)* line (Zerucha et al., 2000; Fig 5.11 D). In addition this line marks dorsally migrating cells (discussed later and Fig 3.8) and OB interneurons (M. Mione, personal communication; Fig 3.8 and Chapter 3 discussion). A ventral telencephalic origin of OB interneurons in the zebrafish therefore seems extremely likely.

Simply comparing the expression domain of *dlx4/6* at 1 dpf with the positions of T8 and T9 indicates that these regions would encompass some ventro-posterior parts of the *dlx4/6* domain and could therefore be potential sources of OB interneurons (Fig 5.11 A and D). I wanted to test this directly and performed Kaede activations in T8 and T9 in the *Tg(dlx4/6:GFP)* line. Confocal analysis immediately post-activation indicated that T8 and T9 are indeed at least partially overlapping with *dlx4/6* expression (data not shown). Activations in T8 also labelled VZ cells that would potentially turn on *dlx4/6* on becoming postmitotic. However, by 5 dpf the disparity between the fluorescence levels of Kaede (low fluorescence levels due to RNA injection) and GFP (extremely high fluorescence from the integrated

transgene) were too great to identify any double-labelled red Kaede/GFP cells. I was therefore unable to confirm that it is specifically the posterior part of the *dlx4/6* expression domain that gives rise to the interneurons labelled in T8 and T9.

More specific location of the zebrafish equivalent of the LGE, and further experiments to establish whether it is indeed the source of OB interneurons are needed. Unfortunately, zebrafish orthologues of *Gsh1* and *Gsh2* (Corbin et al., 2000) are unknown, but other LGE markers such as *Islet1* (Stenman et al., 2003) have been identified and are highlighted in a zebrafish transgenic GFP line (Higashijima et al., 2000). Although *Islet1* cells are a population of LGE cells that do not contribute to the OB (Stenman et al., 2003), the *Tg(islet1:GFP)* line could still be a useful tool for addressing this issue. Furthermore, in the adult zebrafish telencephalon, the ventral telencephalic areas Vd and Vc have been postulated as striatal (the derivative of the LGE) and, as in mouse, they lie adjacent to the pallium (Wullmann and Rink, 2002). However, the expression patterns of the neurotransmitters that mark the adult fish striatum, such as Substance P (Wullmann and Rink, 2002), are completely unknown in the embryonic telencephalon.

#### *Non-OB contributions of T1-T3 and T8-T9*

Contributions of T1-T3 and T8-T9 included not just OB cells but also cells in other telencephalic regions. These are represented in the schematic diagram in Fig 5.10 B. I have not analysed the non-OB contribution in great detail, partly because in the absence of other markers, for the pallium and subpallium for example, it is difficult to draw meaningful conclusions about the locations of labelled cells. However, there is a surprisingly strong contribution at 5dpf to mid- and ventral areas from presumed pallial regions such as T2 and T3.

As discussed above, some cells labelled in T3 may move to positions around the olfactory tracts by 5dpf, in a region highlighted by *tbr1* expression. Labellings in T2 and T3 may also highlight a pallial to subpallial migration of cells, a potentially exciting finding, although not completely without precedent. Cell tracing experiments using a pallium-specific *Emx1* reporter line in mice revealed isolated tagged cells in the ventral pallium (an area that does not normally express *Emx1*) and in a variety of basal ganglia structures (Gorski et al., 2002). However, without more comprehensively defined pallial and subpallial regions in zebrafish it seems premature to draw parallels between these findings and my own.

A major aim for the future would be to analyse telencephalic distributions of labelled cells more closely. I will need to consider the medio-lateral distribution of labelled cells at 5dpf more carefully, and compare this with the expression domains of known and extensively characterised pallial and subpallial markers.

#### *T4, T5 and T6 –subpallial areas with a pallial contribution*

The fate of cells from T4, T5 and T6 suggests these regions lie within the zebrafish equivalent of the ganglionic eminences. The distribution of labelled cells shows that these regions generate a resident population of ventrally located cells and a second population of migratory cells destined for the dorsal telencephalon (Fig 5.6 and 5.7 A-D). Interestingly, labelled cells in the ventral telencephalon were located around the anterior commissure, their position relative to the commissure dependent upon their relative positions at the time of the activation.

Analysis of the zebrafish *Tg(dlx4/6:GFP)* line (Fig 3.8) shows similarly scattered single cells in mid- and dorsal telencephalic areas at 5dpf. These cells are GABAergic and have the complex morphology characteristic of interneurons (M. Mione, personal communication). They are therefore likely to be ventral telencephalic in origin and could well represent the zebrafish equivalent of the ventral-to-dorsal migration observed for mammalian cortical interneurons (Anderson et al., 1999; Marin and Rubenstein, 2001; Parnavelas et al., 2000). One question is whether my observations of ventral-to-dorsal migration of cells labelled in T4, T5 and T6 can be equated with observations from the *Tg(dlx4/6:GFP)* line. In terms of location, T4, T5 and T6 would be expected to overlap considerably with *dlx4/6* expression (Fig 5.11 A and D), although T4 might also overlap somewhat with the most ventral portions of *tbr1* expression (Fig 5.11 A and C). In addition, none of the other potential *dlx*-expressing regions (T7, T8 and T9) contribute single cells to dorsal telencephalic areas.

This raises the possibility that subpallial regions that give rise to interneurons in the OB and dorsal telencephalon are mutually exclusive. There is strong precedent for this in mammals, where OB interneurons originate predominantly in the LGE (reviewed above), while cortical interneurons originate predominantly in the adjacent medial ganglionic eminence (MGE) (Lavdas et al., 1999; Sussel et al., 1999; Wichterle et al., 1999 and 2001). Both the LGE and the MGE express and are dependent upon *Dlx* genes for their correct specification (Anderson et al., 1997a;

Anderson et al., 1997b); the MGE is additionally dependent on the expression of *Nkx2.1* (Sussel et al., 1999). One question is therefore whether the regions T4, T5 and T6 could lie within the zebrafish equivalent of the MGE. In *Xenopus*, the MGE is very ventrally located in the telencephalon, and expresses *x-Lhx7* (Bachy et al., 2001) and *x-Nkx2.1* (Bachy et al., 2002a). *Nkx2.1* has been duplicated in zebrafish, and one of the paralogues, *nk2.1b*, is indeed expressed in the ventral telencephalon in the environs of T4, T5 and T6 (Rohr et al., 2001; Fig 5.11 E). It would certainly be tempting to designate this region of the zebrafish telencephalon as MGE but this requires more detailed examination of both gene expression domains and cell behaviour.

#### *T4, T5 and T6 may contribute striatal interneurons*

The mammalian and avian MGE and preoptic/anterior endopeduncular (POa/AEP) area also give rise to a tangentially migrating population of cells that furnish the adjacent striatum with cholinergic interneurons (Cobos et al., 2001a; Marin et al., 2000). In some specimens from labellings in T4, T5 and T6, isolated cells were not only present in the most dorsal telencephalic areas but also in mid-telencephalic areas (see Table 5.1), presumably outside the pallium (see Fig 3.8 G and H). It is possible that these cells represent a migration within the subpallium from the zebrafish MGE/POa/AEP equivalents to the striatum. Indeed, the adult zebrafish striatum is proposed to directly underlie the pallium, in the position where these mid-telencephalic scattered cells are seen at 5dpf (Wullimann and Rink, 2002). A combination of fate-mapping with acetylcholine esterase immunolabelling would address this possibility.

#### *Morphogenetic movement vs. migration*

My fate map data demonstrates considerable cell rearrangements in the zebrafish telencephalon over the first 5 days of development. These rearrangements could result from morphogenetic movements of whole populations of cells and/or from discrete cell migrations within a stable background. Some evidence points to the predominance of morphogenetic movement over migration, excepting the obviously migratory cells from T4, T5 and T6 (discussed earlier and in the next section).

Firstly, cells labelled in a single region often remained as cohorts being relatively closely associated, if not in direct contact with each other at 5dpf.

Labelled cells obviously segregated between the OB and the telencephalon, but within the telencephalon they were often relatively closely grouped, especially in areas around the AC.

Furthermore, my analysis of the movements of cells labelled in the T1/roof region at 1dpf and followed for two further days show little evidence of a long-distance migration. The cells move little between 1dpf and 2dpf, and between 2dpf and 3dpf move from a position juxtaposed to the bulb to a dorsal position within the bulb. Even though the whole OB undergoes a significant change in position between 2dpf and 3dpf, data from Chapter 3 suggests this is due to a morphogenetic movement as well as considerable expansion of the bulb. Furthermore, the cells shown in Figure 5.9 do not obviously show the characteristic morphology of migrating cells such as a polarised morphology with leading and/or trailing processes (e.g. Alvarez-Buylla, 1997; Anderson et al., 1997a; Nadarajah et al., 2001).

#### *Guiding tangential migration within the telencephalon*

This study has identified at least one population of migrating cells – those that originate in the ventral telencephalon and move to more dorsal areas. There may also be a migration of interneurons from posterior telencephalic regions to the rostrally-located OB, although this has not been directly observed. It is interesting to consider the factors that regulate tangential migration in other systems, which are primarily the cellular substrate for migration and guidance factors (Marin and Rubenstein, 2003).

Preliminary observations of cells migrating from ventral to dorsal areas of the zebrafish telencephalon at 3dpf indicate that these cells move primarily in superficial, subpial regions (data not shown). This suggests they may migrate in the environs of the tract of the anterior commissure. Mouse corticofugal axons, expressing the cell adhesion molecule TAG-1, have been proposed as a substrate for tangentially migrating cells (Denaxa et al., 2001). However, observed migration routes through the proliferative subventricular zone and neuron-dense lower intermediate zone also indicate non-axonal substrates for tangential migration (Marin and Rubenstein, 2003). Zebrafish do not have an identified SVZ, but tangential migration could certainly occur through the neuron-rich mantle layer. Time-lapse

confocal microscopy of Kaede-labelled or *Tg(dlx4/6:GFP)* tangentially migrating cells would help to address this question.

Experiments in mammals have also identified both repulsive and attractive guidance cues in the ventral AEP/POa and cortex respectively, guiding subpallial to pallial migration (Marin et al., 2003; Wichterle et al., 2003). In zebrafish, *slit1b* is expressed around the AC, at the right time and place to act as a putative repulsive signal for tangentially migrating cells (Hutson et al., 2003). Mammalian *Slit1* and *Slit2* are not the ventrally-located repulsive factors for MGE cells migrating to the cortex, but they are involved in tangential migration from the MGE to the striatum (Marin et al., 2003). The potential role of zebrafish *slit1b* in the guidance of cells migrating to the striatum and/or the pallium should be investigated more closely, possibly using the inducible *slit1* knockdown fish (H. Okamoto and M. Redd, personal communication).

Slit-mediated guidance has also been proposed to regulate the path of OB interneuron precursors migrating from the LGE SVZ in the rostral migratory stream (RMS; Nguyen-Ba-Charvet et al., 2004). As described above it is predominantly the septal source of Slit1 and Slit2 that gives directional cue for Robo2/Robo3-expressing RMS cells. Again, it would be interesting to further examine the expression of zebrafish *slits* and *robos* to see what role they might play in OB-directed cell migration.

A further potential guidance cue is the secreted molecule Reelin. Zebrafish *reelin* is widely expressed in the pallium (Costagli et al., 2002), and its intracellular effector *disabled1 (dab1)* is expressed largely in complimentary areas (A. Costagli, unpublished results). Furthermore, abrogation of Reelin signalling using a *dab1* morpholino results in reduced numbers of pallial Dlx-expressing cells at 5dpf (M. Mione, personal communication). It therefore seems very likely that Reelin signalling plays a role in subpallial to pallial migration in fish. In mammals, Reelin is implicated more in lamination than in guidance, affecting the cortical positioning of both projection neurons and interneurons (Marin and Rubenstein, 2003). However, since the zebrafish pallium does not contain a laminar cortex, the role of Reelin signalling in this system may be predominantly guidance rather than lamination.

Reelin signalling also has roles in the migration of OB interneurons from the striatal SVZ where it acts as a detachment signal for cells in the subpallial RMS once

they reach the OB (Hack et al., 2002). I have not directly shown a migration of OB interneurons from subpallial areas, but *reelin* is expressed in the zebrafish OB and *dab1* extensively in the subpallium (A. Costagli and M. Mione, personal communication). It would therefore be interesting to investigate the possibility of an OB interneuron migration using the Reelin/Dab1 system and by looking at the expression of PSA-NCAM, a cell adhesion molecule essential for the migration of cells in the mammalian RMS (Chazal et al., 2000).

#### *Co-ordinating Kaede fate-mapping data with Lhx expression domains*

One of the primary motives behind carrying out a fate map of the 1dpf telencephalon was to establish whether the progressively more rostrally-located expression domains of the *Lhx* genes *lhx1a*, *lhx1b* and *lhx5* reflected real cell movements. In the absence of GFP lines for any of the *Lhx* genes, my only way to address this question was to label groups of cells in the areas where *lhx1a*, *lhx1b* and *lhx5* are expressed and compare the cell movements and observed expression patterns. Unfortunately, because of the nature of the Kaede labelling technique, I had no possibility of combining the fate-mapping with *in situ* hybridisation for *Lhx* genes.

My fate-mapping data concurs very strongly with the observed expression domains for *lhx1a*, *lhx1b* and *lhx5*. The *lhx1a* telencephalic domain 1 (Fig 5.11 F), which by inspection would lie between T1 and T2 at 1dpf is seen in the OB at 5dpf; T1 and T2 cells also contribute to the OB at 5dpf. The *lhx1a* domain 2 (Fig 5.11 F), which would map to somewhere between T3 and T4, lies anterior to the AC at 5dpf. T3 and T4 cells also contribute to this ventral telencephalic region, among other structures. The expression of *lhx1b* (Fig 5.11 G) is slightly more difficult to place, but it overlaps with the anterior *lhx1a* domain. This probably equates *lhx1b* with T4 and T3, possibly reaching a little further dorsally. At 5dpf, *lhx1b* expression is seen in the ventral telencephalon possibly overlapping with the putative olfactory tract *tbr1* domain just anterior to the AC (M. Mione, personal communication). Cells in T3 and T4 contribute to this region, among other structures. Finally, the *lhx5* dorsal domain (Fig 5.11 H) would be expected to cover a broad area of the dorsal telencephalon, probably T1, T2 and T3, maybe including T8 and T9. At 5dpf, *lhx5*-expressing cells are seen covering a broad region of the OB (Fig 4.4 N and O); in agreement with this T1-T3 and T8-T9 all contribute to the OB. The ventral domain of *lhx5* (Fig 5.11 H) is more difficult to place. It is *dlx4/6* -ve (Fig 4.10 H) but

probably maps to T7 at 1dpf. At 5dpf, *lhx5*-expressing cells are found in a broad ventral-posterior region of the telencephalon (Fig 4.4 N); T7 cells also contribute to this region.

The general concordance between *Lhx* expression data and Kaede fate-mapping data is very good. Although it is difficult to precisely align regions of *Lhx* gene expression to Kaede regions, my comparisons indicate that Kaede-labelled cells from regions where particular *Lhx* genes are expressed are found in the same regions as *Lhx* expression at 5dpf. One important point, however, is that the destinations of *Lhx*-expressing cells represent only a subset of the destinations of Kaede-labelled cells. That is to say in general, *Lhx*-expressing cells only form a subset of those labelled in each Kaede region. The obvious explanation for this is that often the Kaede activations label a broad medio-lateral domain of cells, whereas the *Lhx* expression domains, especially of *lhx1a* and *lhx1b* are restricted in the medio-lateral axis.

#### *What specifies the dorsal telencephalic contribution to the OB?*

Having established that dorsal telencephalic areas contribute projection neurons to the OB, it is interesting to speculate what might define this region. My results show that the region contributing neurons to the OB is larger than the *lhx1a* domain 1. It is more likely that *lhx5*, expressed much more broadly than *lhx1a*, is a marker of cells contributing to the OB. In my expression analysis, the sole destination of the *lhx5* dorsal domain is the OB, similar to the situation in *Xenopus* (Moreno et al., 2003; Moreno et al., 2004). However, in general *Lhx* genes are late markers of neuronal phenotype, and there may be genes upstream that regulate *Lhx* expression to instruct the OB fate.

Mouse knockouts may provide some insight into the genes controlling the mammalian pallial contribution to the OB. However, all knockouts analysed to date have multiple phenotypes with both OB and cortical structures being affected, suggesting that these are upstream of genes that specify OB projection neurons (Zaki et al., 2003). For example, the *Tbr1* knockout mouse has both an absence of mitral/tufted cells in the OB, but also defects in cortical organisation and neurogenesis (Bulfone et al., 1998). Similarly *Emx2* knockouts and *Emx1/2* double knockouts show OB and cortical defects among others (Bishop et al., 2003; Yoshida et al., 1997).

The only mouse mutant with a specific OB phenotype is the *FgfR1* conditional knockout (Hebert et al., 2003). However, the defect in this mutant is not one of mitral cell specification but of proliferation within and morphogenesis of the olfactory bulb. A zebrafish *fgf* mutant, *ace/fgf8*, also has severe olfactory bulb defects with reduced and disorganised glomeruli and a marked reduction in *emx1(emx3)*-labelling in the OB at 3dpf (Shanmugalingam et al., 2000). However, *ace/fgf8* has many other telencephalic defects including disrupted midline patterning in dorsal and ventral territories. It is therefore not clear what role *fgf8* plays in OB development, although the study of this mutant in combination with Kaede labelling might help to elucidate this.

It is my hope that the observations I have made of OB development will aid the screening of mutants, mutagenesis screening being a particular strength of zebrafish research. Particularly relevant is a mutagenesis screen taking place in the *Tg(dlx4/6:GFP)* background (M. Mione et al., personal communication), which should be ideally suited to identifying mutations affecting the OB interneuron population.

#### *Post-embryonic development of the OB*

My experiments demonstrate that the OB is a major derivative of the early telencephalon. Out of the nine regions sampled, five contributed at least some cells to the OB. This suggests that the OB is an important structure for zebrafish and merits a large contribution from the telencephalon. However, at the stage where I ended my experiments the OB is only a fraction of the size it will be in the adult. Estimates place the number of glomeruli in the 3.5dpf embryo at 15 (Dynes and Ngai, 1998), whereas the adult has some 100 glomeruli (Baier and Korsching, 1994). Therefore, although I have established the spatial origins of the embryonic OB, it is still largely unknown how new OB neurons are recruited/generated (Byrd and Brunjes, 1998; Byrd and Brunjes, 2001). A further aspect of postembryonic development that requires further work is how the olfactory bulbs come to be completely separated from the telencephalon as they are in the adult (Wullimann, 1996; Fig 3.1 F). The morphogenetic movements and/or migrations that orchestrate this process will be fascinating to discover.

### *Limitations of the method and further work*

The photoconversion method, using Kaede protein, has proved an excellent tool for making a relatively coarse fate-map of the 1dpf zebrafish telencephalon. By labelling multiple cells in the first instance, I have been able to quickly compile data on the major cell movements and migrations of a large proportion of the telencephalic population. Naturally, I have not sampled the entire brain region but the focus of my question was the origins of the OB and this has been addressed.

However, the Kaede method does have limitations, one of which is the out-of-focus activation that results from using a beam of UV light. This problem is compounded by the fact that the light beam is actually a cone, most restricted at the focal point but flaring out on either side. Thus, performing photoactivation from the lateral aspect can result in a medio-lateral column of labelled cells. Nonetheless, the photoconversion is brightest at the focal plane and my confocal analysis immediately post-activation shows that activations consist of a discrete population of labelled cells (Fig 5.1 E-H). Most importantly, the epifluorescence images taken of each specimen at the time of the photoconversion, from two different aspects, meant that the starting population of labelled cells was always known and could be correlated with data acquired at 5dpf.

Further refinements of the Kaede technique are still desirable, to reduce the numbers of cells labelled and their medio-lateral extent. This may be especially important for activations in the regions where pallial and subpallial areas overlap in the medio-lateral axis, subpallial areas lying medial to pallial areas (Fig 3.8 G and H, also compare *dlx4/6* and *emx1* expression in Fig 5.11). Using Kaede, I hope to develop UV-laser and multi-photon methods to reduce or eliminate out-of-focus activation.

Another approach, not involving Kaede, is to use microelectrode techniques to label single cells with fluorescent tracers (Lyons et al., 2003). I hope to do this in the posterior dorsal region, between T1 and T8. The aim of this approach would be to use GFP lines in conjunction with tracer injections to establish more conclusively the boundary between pallium and subpallium. Following on from this I would hope to identify a region of the subpallium which gives rise to OB interneurons that I could confidently designate as the zebrafish equivalent of the LGE.

Experiments using Kaede RNA, as I have done here, may also be affected by the dilution effects of multiple rounds of cell division. This problem can not create

false-positive results, as red-labelled cells have always either been photoconverted themselves or are descendents of cells that were. However, it may lead me to underestimate the destinations of cells labelled in any particular region. To explore this possibility I could do the experiments over a shorter period (from 1 to 3dpf for example) and could actively target proliferating cells in the VZ to see through how many rounds of division the red signal is sustained.

## Chapter 6: General discussion

Over the course of this thesis work I have used a variety of techniques to characterise the zebrafish telencephalon over the entire period of its embryonic development.

The three main findings of my work are:

- the photoconvertible fluorescent Kaede protein can be used as a non-invasive long-term fate mapping tool in the zebrafish embryo
- a combination of gene expression analyses and fate mapping studies has revealed the posterior telencephalic origin of the zebrafish OB
- fate mapping and the 4D analysis of neuronal organisation and proliferative zones demonstrate a major morphogenetic rearrangement of the zebrafish telencephalon that accounts for the rostral movement of the developing OB and may account for telencephalic eversion

In this final discussion I will draw together the main themes outlined above and discuss a model that may underlie the formation of the mature zebrafish telencephalon.

### *Evidence points to a morphogenetic movement between 2 and 3dpf*

The main findings of the three data chapters in this thesis all point towards a similar conclusion, that a morphogenetic movement between 2dpf and 3dpf is an event which both reorganises the telencephalon and may underlie the eversion process.

The main evidence for this can be summarised as:

1. BrdU labelling of proliferating cells reveals a VZ that extends to the posterior dorsal border of the telencephalon at 2dpf, but which by 3dpf is evident on the dorsal surface, underlying the epidermis. At 5dpf, this dorsally-everted VZ covers the full medio-lateral and rostro-caudal axes of the dorsal telencephalic surface, except for the olfactory bulbs (Fig 3.5).
2. Immunolabelling for mature axons reveals that the olfactory bulb occupies a posterior-dorsal position in the telencephalon at 2dpf but by 3dpf is very rostrally located in the brain (Fig 3.6).
3. Domains of expression of *lhx1a* and *lhx5* in the posterior dorsal telencephalon at 2dpf appear in the OB at 3dpf where they remain until at least 1 month post fertilisation (Fig 4.5).

4. The most posterior areas of the dorsal telencephalon at 1dpf contribute cells to the OB at 5dpf (Fig 5.4, 5.9 and table 5.1)

All of these lines of evidence, accumulated using a variety of different techniques, point towards a morphogenetic movement between 2dpf and 3dpf, which serves to bring posterior-dorsal structures to more rostrally-located positions. I have previously described this movement as rotatory, but it is unclear whether changes in the dorsal telencephalon are paralleled by similar movements in the ventral telencephalon. The perdurance of the preoptic area proliferation zone and the relatively static position of the anterior commissure suggest that the movement may be more confined to the dorsal telencephalon.

#### *What drives a morphogenetic movement?*

If there is indeed a morphogenetic movement that significantly rearranges the telencephalon, then an immediate question is what drives this movement?

Presumably forces both intrinsic to the telencephalon and/or extrinsic forces exerted by adjacent tissues could be responsible. Even differential proliferation may be sufficient to account for the perceived morphogenetic movement. For instance, at 48hpf the ventricular space between the posterior telencephalon and the diencephalon is quite large, meaning that these adjacent brain areas are some distance from each other (Fig 4.5 A and B). However, at 3dpf the space seems much reduced (Fig 4.5 D), and it is possible that proliferation in the dorsal telencephalon fills in this gap and brings the VZ to directly underlie the epidermis on the dorsal surface of the brain. Discriminating between these possibilities would not be easy, but lineage or fate mapping cells in the posterior VZ at 2dpf would give some indication of proliferation and cell movement in this area.

#### *The rostral movement may underlie eversion*

It is clear that whatever the precise mechanism underlying the movement within the dorsal telencephalon between 2 and 3dpf, it results in VZ being evident for the first time on the dorsal rather than the posterior surface of the telencephalon. This is the primary feature of an everted rather than an evaginated telencephalon (Butler, 2000; Butler and Hodos, 1996; Wullimann and Knipp, 2000), and raises the possibility that the observed rostral movement does indeed underlie the eversion process.

The model I am proposing here is certainly much less dramatic than the process suggested by schematic models of eversion such as Fig 6.1 A (Butler, 2000). These models have the major difficulty that they predict a massive rearrangement of telencephalic areas in an everted versus an evaginated telencephalon. Although zebrafish telencephalic areas are not well characterised in terms of function, areas receiving secondary olfactory input are identified by the projections of the olfactory tracts. In both everted and non-everted brains, the olfactory pallium is laterally-located (Wullimann and Rink, 2002). I am not disputing that the adult teleost telencephalon is everted, with deep sulci evident in the lateral wall (Butler, 2000), but simply suggesting that this might arise from extensive cell proliferation during postembryonic stages and therefore mask the much simpler embryonic arrangement.

#### *Insights into the origin of the choroid tela*

A further reported consequence of an everted telencephalon is that the dorsal VZ is covered by a thin choroid tela (Wullimann and Puelles, 1999). This epithelium lies juxtaposed to the neural tissue and is almost certainly secretory (producing cerebrospinal fluid), at least in parts. It has been observed in sectioned material at adult stages (Wullimann and Puelles, 1999) but the embryonic origins of this structure remain completely unexplored. The model I have proposed for telencephalic eversion may also have implications for the origins of the choroid tela.

If the choroid tela has any similarities with the secretory epithelium of evaginated brains, the choroid plexus, then it must be a derivative of the roof of the neural tube. I predict this would be the posterior area of the neuroepithelium that joins the telencephalon to the roof of the diencephalon at 48hpf (Fig 6.1 B). The point of attachment of this roof structure would be just caudal to the developing olfactory bulb, and as the bulb moved to a more rostral position the prospective tela would be pulled over the dorsal surface of the telencephalon, in parallel with the VZ. Thus by 5dpf, a tela would cover the entire dorsal surface of the telencephalon except for the olfactory bulbs (Fig 6.1 B).

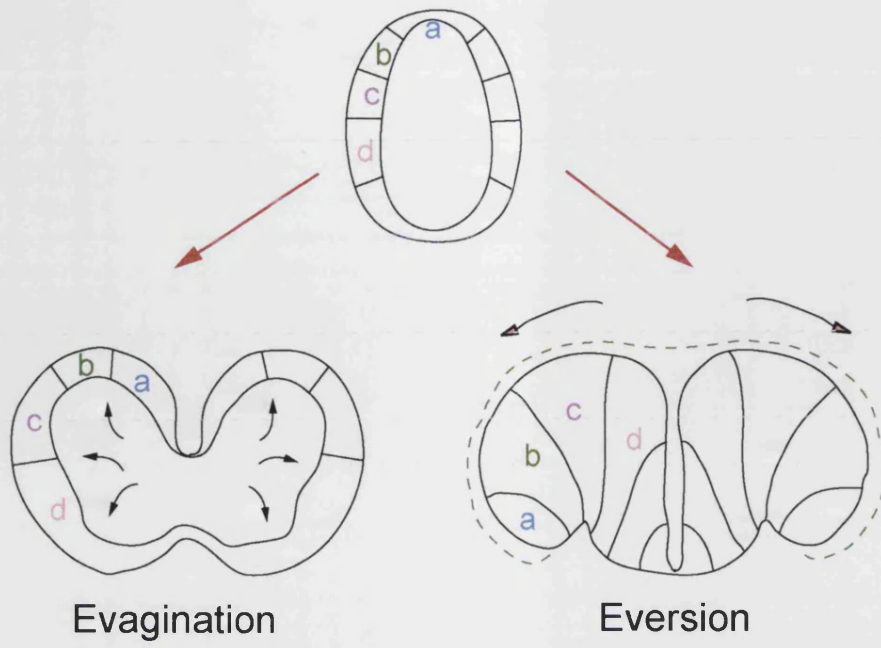
My experiments have not directly addressed the origins of the tela, but some of my observations support the model proposed above. In the 24-36hpf telencephalon, a thin area of neuroepithelium forms a bridge between the posterior telencephalon and the roof of the diencephalon. It is mainly proliferative although a few neurons are evident in the most rostral part of the roof. I suggest that these

**Figure 6.1: Models of eversion and the possible origin of the choroid tela**

A shows the contrasting processes of evagination and eversion, adapted from (Butler 2000). The everted telencephalon is covered by a thin choroid tela, a structure that has its origins in the dorsal neural tube.

B shows my model of eversion from Fig 3.9, modified to include the possible origin and morphogenesis of the choroid tela. The VZ is indicated with red lines, the OB in light blue and the direction of the morphogenetic movement with purple arrows. The choroid tela is indicated by a green line and a green arrowhead. The tela may have its origins in the roof of the 48hpf telencephalon, and following a rostral morphogenetic movement may become spread over the dorsal surface of the telencephalon. Thus the point of attachment of the tela remains just caudal to the OB at all stages.

A



B

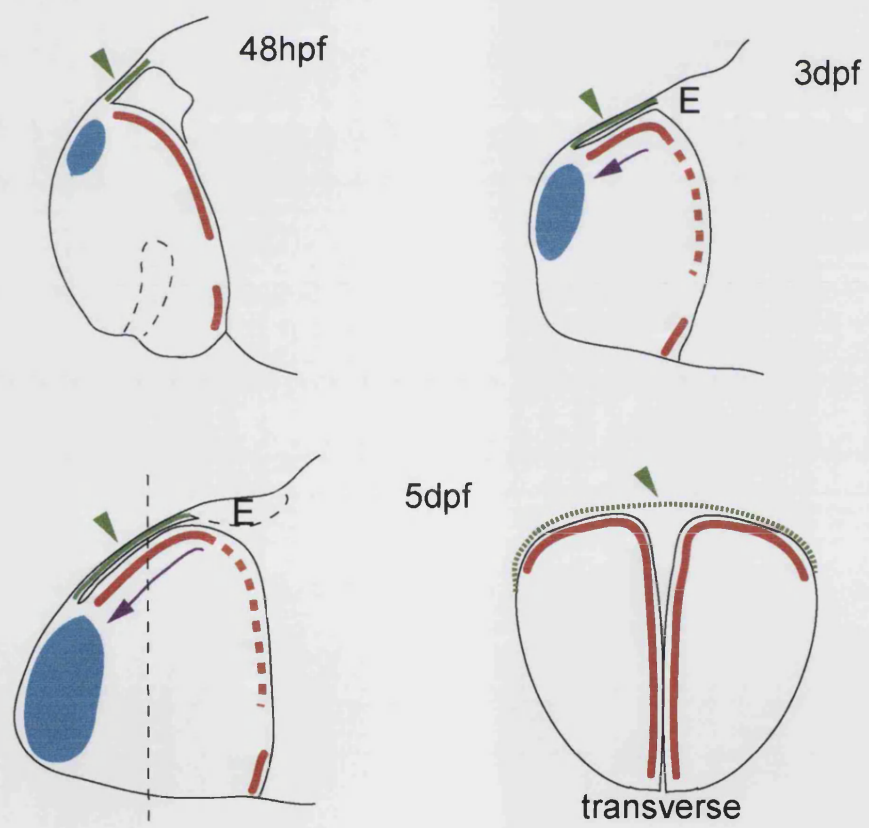


Figure 6.1

neurons would be among the cells we have marked by Kaede labellings in this area and would contribute to the OB. By 48hpf, the epithelial bridge between the telencephalon and diencephalon is much thinner (it is easily removed during dissection) and its point of attachment is just posterior to the OB (Fig 3.1 C and Fig 3.6 C). Cells labelled in the roof at 1dpf are now clearly part of the bulk of telencephalic tissue, suggesting that they have left the roof (Fig 5.9 C and D). At 3dpf, these cells lie within the OB, probably as a result of growth of the OB (Fig 5.9 E and F), and the epithelial tissue is no longer evident (Fig 3.1 D). This of course does not necessarily indicate that it has spread over the dorsal surface of the telencephalon, but it is a possibility.

#### *Testing the predictions of the eversion/choroid tela model*

My model (Figure 6.1) makes a number of predictions relating to the choroid tela that could be directly tested experimentally. Firstly, no structure resembling the tela should be visible over the dorsal surface of the brain at 48hpf. At 3dpf and 5dpf, the point of attachment of the tela should be just caudal/posterior to the OB – the same point at which it attached at 48hpf. There should also therefore be no choroid tela evident over the surface of the OB at any stage. These morphological characteristics would probably be best observed by electron microscopy.

Secondly, markers for the roofplate/tela should expand rapidly between 48hpf and 3dpf and come to cover the dorsal surface of the brain. There are presently no known markers of the choroid tela in zebrafish. Transthyretin, which is a good marker for the choroid plexus in other species is not expressed in fish choroid plexus (Power et al., 2000; Schreiber, 2002). However there are a number of genes involved in the patterning of the mammalian roofplate, choroid plexus and adjacent structures such as members of the Wnt and BMP families. In mammals, *Wnt2b* is expressed in the cortical hem (Monuki et al., 2001) and *Wnt3a* has a role in hippocampal development (Lee et al., 2000). *Bmp2* and *Bmp4* are also expressed in the roofplate and are implicated in choroid plexus specification (Hebert et al., 2002). The roofplate is also beautifully marked by *Gdf7* in mouse (Monuki et al., 2001) and chick (Alexandre and Wassef, 2003) and has been cloned in zebrafish but with little expression analysis (Davidson et al., 1999). In zebrafish, very few members of the Wnt and BMP families have been studied at later stages of embryonic development, but *wnt8b* is expressed in the roof region between the telencephalon and

diencephalon at around 24hpf, and affects development of forebrain structures including the telencephalon (Buckles et al., 2004; Kelly et al., 1995). A future aim would be to assess the expression of this excellent candidate gene between 2 and 5dpf to see whether its expression marks an expanding choroid tela.

Thirdly, the roof of the telencephalon should have dual fates, that is both neurons and choroid tela cells. There is precedent for this in mouse, where tissue labelled with the roofplate marker Gdf7 gives rise to both neurons and choroid plexus (Monuki et al., 2001). My experiments using Kaede labelling indicate that areas of the roof do indeed give rise to neurons. However, without any information about the nature of choroid tela cells I was unable to establish whether any of my experiments also labelled these cells. Future fate tracing experiments and identification of a marker of the choroid tela should establish the neurogenic and non-neurogenic regions of the roof.

#### *Evaluation of the work*

Over the course of this thesis I have explored and described some of the basic processes that underlie the development and morphogenesis of the zebrafish telencephalon. By not confining my work to a single stage, but rather by following processes from early embryonic to postembryonic stages (24hpf to 5dpf), I have been able to monitor the dynamics of proliferation, neurogenesis and morphogenetic movements over the full course of embryonic development. These observations have led me to propose a model that pairs a rostrally-directed morphogenetic movement within the brain with the appearance of a dorsally-everted telencephalon, a characteristic of the actinopterygian fish. A possible, but so far unsubstantiated, extension of the model proposes that the formation of the choroid tela may also result from the previously described morphogenetic movement.

#### *Concluding remarks*

At the moment, much of the research into the development of the zebrafish telencephalon (aside from work on early patterning) is still at a largely observational stage. I see this as being the first phase of necessary groundwork for performing more functional experiments. It is clear from descriptive studies, such as the work presented here, that the commonalities between zebrafish and “higher” vertebrates are probably much more extensive than previously thought. For example, the

identification of populations of migrating cells from subpallial to pallial and OB areas is strongly reminiscent of the migration that populates the chick and mammalian telencephalon and OB with GABAergic interneurons (reviewed in Marin and Rubenstein, 2003).

Much of the literature comparing telencephalic organisation in different species has focussed on tetrapods i.e. mammals, reptiles, birds and amphibians (Marin et al., 1998; Striedter, 1997). Authors have used the term tetrapod to imply that the evolution of tetrapody also saw the evolution of a different kind of brain organisation. Fish have largely been excluded from these analyses, it seems, not because of their lack of land-conquering limbs but because of the everted telencephalon (Striedter, 1997). This is despite the relative wealth of information indicating that the patterning mechanisms at work in the zebrafish telencephalon are similar to those in higher vertebrates (Akimenko et al., 1994; Costagli et al., 2002; Hauptmann et al., 2002; Kawahara and Dawid, 2002; Mione et al., 2001; Morita et al., 1995; Rohr et al., 2001). The lack of a clear model of eversion is clearly hampering much of the potential comparative work that could be done in zebrafish.

It is obviously one of the eventual aims of zebrafish researchers to move beyond comparative studies with mouse and chick, and to use the unique attributes of the zebrafish to their full advantage. For example, the transparency of the early embryo and the ability to follow cells in timelapse without perturbation over extended periods (as shown by Dynes and Ngai, 1998; Koster and Fraser, 2001) are not attributes shared by any other model organism. The ease of mutagenesis screening and the development of transgenic technology are also great incentives for using zebrafish. It is also important, I feel, to encourage non-zebrafish researchers to use zebrafish as part of a question-lead (rather than model-lead) approach to elucidating telencephalic development. Central to such a use of zebrafish is, however, the resolution of some of the outstanding issues such as teleost telencephalic eversion. If the model I propose here is borne out by further experiments, eversion may well turn out to be not such a complicated process after all. But only when this has been rigorously described, with clear identification of telencephalic subdivisions and their homologous structures in the evaginated telencephalons studied by the vast majority of researchers, will the use of the zebrafish model become more widespread.

## References

- Akimenko, M. A., Ekker, M., Wegner, J., Lin, W., and Westerfield, M. (1994). Combinatorial expression of three zebrafish genes related to *distal-less*: part of a homeobox gene code for the head. *J Neurosci* *14*, 3475-3486.
- Alexandre, P., and Wassef, M. (2003). The isthmus organizer links anteroposterior and dorsoventral patterning in the mid/hindbrain by generating roof plate structures. *Development* *130*, 5331-5338.
- Alvarez-Buylla, A. (1997). Mechanism of migration of olfactory bulb interneurons. *Semin Cell Dev Biol* *8*, 207-213.
- Amores, A., Force, A., Yan, Y. L., Joly, L., Amemiya, C., Fritz, A., Ho, R. K., Langeland, J., Prince, V., Wang, Y. L., *et al.* (1998). Zebrafish hox clusters and vertebrate genome evolution. *Science* *282*, 1711-1714.
- Anderson, S., Mione, M., Yun, K., and Rubenstein, J. L. (1999). Differential origins of neocortical projection and local circuit neurons: role of *Dlx* genes in neocortical interneuronogenesis. *Cereb Cortex* *9*, 646-654.
- Anderson, S. A., Eisenstat, D. D., Shi, L., and Rubenstein, J. L. (1997a). Interneuron migration from basal forebrain to neocortex: dependence on *Dlx* genes. *Science* *278*, 474-476.
- Anderson, S. A., Qiu, M., Bulfone, A., Eisenstat, D. D., Meneses, J., Pedersen, R., and Rubenstein, J. L. (1997b). Mutations of the homeobox genes *Dlx-1* and *Dlx-2* disrupt the striatal subventricular zone and differentiation of late born striatal neurons. *Neuron* *19*, 27-37.
- Ando, R., Hama, H., Yamamoto-Hino, M., Mizuno, H., and Miyawaki, A. (2002). An optical marker based on the UV-induced green-to-red photoconversion of a fluorescent protein. *Proc Natl Acad Sci U S A* *99*, 12651-12656.
- Appel, B., Korzh, V., Glasgow, E., Thor, S., Edlund, T., Dawid, I. B., and Eisen, J. S. (1995). Motoneuron fate specification revealed by patterned LIM homeobox gene expression in embryonic zebrafish. *Development* *121*, 4117-4125.
- Bach, I. (2000). The LIM domain: regulation by association. *Mech Dev* *91*, 5-17.

Bach, I., Rodriguez-Esteban, C., Carriere, C., Bhushan, A., Krones, A., Rose, D. W., Glass, C. K., Andersen, B., Izpisua Belmonte, J. C., and Rosenfeld, M. G. (1999). RLIM inhibits functional activity of LIM homeodomain transcription factors via recruitment of the histone deacetylase complex. *Nat Genet* 22, 394-399.

Bachy, I., Berthon, J., and Retaux, S. (2002a). Defining pallial and subpallial divisions in the developing *Xenopus* forebrain. *Mech Dev* 117, 163-172.

Bachy, I., Failli, V., and Retaux, S. (2002b). A LIM-homeodomain code for development and evolution of forebrain connectivity. *Neuroreport* 13, A23-27.

Bachy, I., Vernier, P., and Retaux, S. (2001). The LIM-homeodomain gene family in the developing *Xenopus* brain: conservation and divergences with the mouse related to the evolution of the forebrain. *J Neurosci* 21, 7620-7629.

Baier, H., and Korsching, S. (1994). Olfactory glomeruli in the zebrafish form an invariant pattern and are identifiable across animals. *J Neurosci* 14, 219-230.

Bally-Cuif, L., and Hammerschmidt, M. (2003). Induction and patterning of neuronal development, and its connection to cell cycle control. *Curr Opin Neurobiol* 13, 16-25.

Barth, A. L., Justice, N. J., and Ngai, J. (1996). Asynchronous onset of odorant receptor expression in the developing zebrafish olfactory system. *Neuron* 16, 23-34.

Barth, K. A., and Wilson, S. W. (1995). Expression of zebrafish *nk2.2* is influenced by sonic hedgehog/vertebrate hedgehog-1 and demarcates a zone of neuronal differentiation in the embryonic forebrain. *Development* 121, 1755-1768.

Bishop, K. M., Garel, S., Nakagawa, Y., Rubenstein, J. L., and O'Leary, D. D. (2003). *Emx1* and *Emx2* cooperate to regulate cortical size, lamination, neuronal differentiation, development of cortical efferents, and thalamocortical pathfinding. *J Comp Neurol* 457, 345-360.

Bishop, K. M., Goudreau, G., and O'Leary, D. D. (2000). Regulation of area identity in the mammalian neocortex by *Emx2* and *Pax6*. *Science* 288, 344-349.

Bishop, K. M., Rubenstein, J. L., and O'Leary, D. D. (2002). Distinct actions of *Emx1*, *Emx2*, and *Pax6* in regulating the specification of areas in the developing neocortex. *J Neurosci* 22, 7627-7638.

Briscoe, J., Sussel, L., Serup, P., Hartigan-O'Connor, D., Jessell, T. M., Rubenstein, J. L., and Ericson, J. (1999). Homeobox gene *Nkx2.2* and specification of neuronal identity by graded Sonic hedgehog signalling. *Nature* 398, 622-627.

Buckles, G. R., Thorpe, C. J., Ramel, M. C., and Lekven, A. C. (2004). Combinatorial Wnt control of zebrafish midbrain-hindbrain boundary formation. *Mech Dev* 121, 437-447.

Bulchand, S., Subramanian, L., and Tole, S. (2003). Dynamic spatiotemporal expression of LIM genes and cofactors in the embryonic and postnatal cerebral cortex. *Dev Dyn* 226, 460-469.

Bulfone, A., Martinez, S., Marigo, V., Campanella, M., Basile, A., Quaderi, N., Gattuso, C., Rubenstein, J. L., and Ballabio, A. (1999). Expression pattern of the *Tbr2* (Eomesodermin) gene during mouse and chick brain development. *Mech Dev* 84, 133-138.

Bulfone, A., Smiga, S. M., Shimamura, K., Peterson, A., Puelles, L., and Rubenstein, J. L. (1995). T-brain-1: a homolog of Brachyury whose expression defines molecularly distinct domains within the cerebral cortex. *Neuron* 15, 63-78.

Bulfone, A., Wang, F., Hevner, R., Anderson, S., Cutforth, T., Chen, S., Meneses, J., Pedersen, R., Axel, R., and Rubenstein, J. L. (1998). An olfactory sensory map develops in the absence of normal projection neurons or GABAergic interneurons. *Neuron* 21, 1273-1282.

Butler, A. B. (2000). Topography and topology of the teleost telencephalon: a paradox resolved. *Neurosci Lett* 293, 95-98.

Butler, A. B., and Hodos, W. (1996). *Comparative Vertebrate Neuroanatomy : evolution and adaptation*, Wiley-Liss).

Byrd, C. A., and Brunjes, P. C. (1995). Organization of the olfactory system in the adult zebrafish: histological, immunohistochemical, and quantitative analysis. *J Comp Neurol* 358, 247-259.

Byrd, C. A., and Brunjes, P. C. (1998). Addition of new cells to the olfactory bulb of adult zebrafish. *Ann N Y Acad Sci* 855, 274-276.

Byrd, C. A., and Brunjes, P. C. (2001). Neurogenesis in the olfactory bulb of adult zebrafish. *Neuroscience* 105, 793-801.

- Campbell, K. (2003). Dorsal-ventral patterning in the mammalian telencephalon. *Curr Opin Neurobiol* 13, 50-56.
- Casarosa, S., Fode, C., and Guillemot, F. (1999). Mash1 regulates neurogenesis in the ventral telencephalon. *Development* 126, 525-534.
- Chazal, G., Durbec, P., Jankovski, A., Rougon, G., and Cremer, H. (2000). Consequences of neural cell adhesion molecule deficiency on cell migration in the rostral migratory stream of the mouse. *J Neurosci* 20, 1446-1457.
- Chiang, C., Litingtung, Y., Lee, E., Young, K. E., Corden, J. L., Westphal, H., and Beachy, P. A. (1996). Cyclopia and defective axial patterning in mice lacking Sonic hedgehog gene function. *Nature* 383, 407-413.
- Chitnis, A. B., and Kuwada, J. Y. (1990). Axonogenesis in the brain of zebrafish embryos. *J Neurosci* 10, 1892-1905.
- Cobos, I., Puelles, L., and Martinez, S. (2001a). The avian telencephalic subpallium originates inhibitory neurons that invade tangentially the pallium (dorsal ventricular ridge and cortical areas). *Dev Biol* 239, 30-45.
- Cobos, I., Shimamura, K., Rubenstein, J. L., Martinez, S., and Puelles, L. (2001b). Fate map of the avian anterior forebrain at the four-somite stage, based on the analysis of quail-chick chimeras. *Dev Biol* 239, 46-67.
- Cooper, M. S., D'Amico, L. A., and Henry, C. A. (1999). Confocal microscopic analysis of morphogenetic movements. *Methods Cell Biol* 59, 179-204.
- Corbin, J. G., Gaiano, N., Machold, R. P., Langston, A., and Fishell, G. (2000). The Gsh2 homeodomain gene controls multiple aspects of telencephalic development. *Development* 127, 5007-5020.
- Corbin, J. G., Rutlin, M., Gaiano, N., and Fishell, G. (2003). Combinatorial function of the homeodomain proteins Nkx2.1 and Gsh2 in ventral telencephalic patterning. *Development* 130, 4895-4906.
- Costagli, A., Kapsimali, M., Wilson, S. W., and Mione, M. (2002). Conserved and divergent patterns of Reelin expression in the zebrafish central nervous system. *J Comp Neurol* 450, 73-93.
- Davidson, A. J., Postlethwait, J. H., Yan, Y. L., Beier, D. R., van Doren, C., Foernzler, D., Celeste, A. J., Crosier, K. E., and Crosier, P. S. (1999). Isolation of

zebrafish *gdf7* and comparative genetic mapping of genes belonging to the growth/differentiation factor 5, 6, 7 subgroup of the TGF-beta superfamily. *Genome Res* 9, 121-129.

Dawid, I. B., and Chitnis, A. B. (2001). Lim homeobox genes and the CNS: a close relationship. *Neuron* 30, 301-303.

de Castro, F., Hu, L., Drabkin, H., Sotelo, C., and Chedotal, A. (1999). Chemoattraction and chemorepulsion of olfactory bulb axons by different secreted semaphorins. *J Neurosci* 19, 4428-4436.

Denaxa, M., Chan, C. H., Schachner, M., Parnavelas, J. G., and Karagogeos, D. (2001). The adhesion molecule TAG-1 mediates the migration of cortical interneurons from the ganglionic eminence along the corticofugal fiber system. *Development* 128, 4635-4644.

Denkers, N., Garcia-Villalba, P., Rodesch, C. K., Nielson, K. R., and Mauch, T. J. (2004). FISHing for chick genes: Triple-label whole-mount fluorescence in situ hybridization detects simultaneous and overlapping gene expression in avian embryos. *Dev Dyn* 229, 651-657.

Derobert, Y., Plouhinec, J. L., Sauka-Spengler, T., Le Mentec, C., Baratte, B., Jaillard, D., and Mazan, S. (2002). Structure and expression of three *Emx* genes in the dogfish *Scyliorhinus canicula*: functional and evolutionary implications. *Dev Biol* 247, 390-404.

Dynes, J. L., and Ngai, J. (1998). Pathfinding of olfactory neuron axons to stereotyped glomerular targets revealed by dynamic imaging in living zebrafish embryos. *Neuron* 20, 1081-1091.

Easter, S. S., Jr., Wilson, S. W., Ross, L. S., and Burrill, J. D. (1992). Tract formation in the brain of the zebrafish embryo. *The Nerve Growth Cone ed P C Letourneau*, 337-351.

Edwards, J. G., and Michel, W. C. (2002). Odor-stimulated glutamatergic neurotransmission in the zebrafish olfactory bulb. *J Comp Neurol* 454, 294-309.

Eisen, J. S. (1991). Determination of primary motoneuron identity in developing zebrafish embryos. *Science* 252, 569-572.

Eisenstat, D. D., Liu, J. K., Mione, M., Zhong, W., Yu, G., Anderson, S. A., Ghattas, I., Puelles, L., and Rubenstein, J. L. (1999). DLX-1, DLX-2, and DLX-5 expression define distinct stages of basal forebrain differentiation. *J Comp Neurol* *414*, 217-237.

Ellies, D. L., Stock, D. W., Hatch, G., Giroux, G., Weiss, K. M., and Ekker, M. (1997). Relationship between the genomic organization and the overlapping embryonic expression patterns of the zebrafish *dlx* genes. *Genomics* *45*, 580-590.

Failli, V., Rogard, M., Mattei, M. G., Vernier, P., and Retaux, S. (2000). *Lhx9* and *Lhx9alpha* LIM-homeodomain factors: genomic structure, expression patterns, chromosomal localization, and phylogenetic analysis. *Genomics* *64*, 307-317.

Fernandez, A. S., Pieau, C., Reperant, J., Boncinelli, E., and Wassef, M. (1998). Expression of the *Emx-1* and *Dlx-1* homeobox genes define three molecularly distinct domains in the telencephalon of mouse, chick, turtle and frog embryos: implications for the evolution of telencephalic subdivisions in amniotes. *Development* *125*, 2099-2111.

Force, A., Lynch, M., Pickett, F. B., Amores, A., Yan, Y. L., and Postlethwait, J. (1999). Preservation of duplicate genes by complementary, degenerative mutations. *Genetics* *151*, 1531-1545.

Friedrich, R. W., and Korsching, S. I. (1997). Combinatorial and chemotopic odorant coding in the zebrafish olfactory bulb visualized by optical imaging. *Neuron* *18*, 737-752.

Fukuchi-Shimogori, T., and Grove, E. A. (2003). *Emx2* patterns the neocortex by regulating FGF positional signaling. *Nat Neurosci* *6*, 825-831.

Gimnopoulos, D., Becker, C. G., Ostendorff, H. P., Bach, I., Schachner, M., and Becker, T. (2002). Expression of the zebrafish recognition molecule F3/F11/contactin in a subset of differentiating neurons is regulated by cofactors associated with LIM domains. *Gene Expr Patterns* *2*, 137-143.

Golling, G., Amsterdam, A., Sun, Z., Antonelli, M., Maldonado, E., Chen, W., Burgess, S., Haldi, M., Artzt, K., Farrington, S., *et al.* (2002). Insertional mutagenesis in zebrafish rapidly identifies genes essential for early vertebrate development. *Nat Genet* *31*, 135-140.

Gorski, J. A., Talley, T., Qiu, M., Puellas, L., Rubenstein, J. L., and Jones, K. R. (2002). Cortical excitatory neurons and glia, but not GABAergic neurons, are produced in the *Emx1*-expressing lineage. *J Neurosci* 22, 6309-6314.

Grove, E. A., Tole, S., Limon, J., Yip, L., and Ragsdale, C. W. (1998). The hem of the embryonic cerebral cortex is defined by the expression of multiple *Wnt* genes and is compromised in *Gli3*-deficient mice. *Development* 125, 2315-2325.

Gunhaga, L., Jessell, T. M., and Edlund, T. (2000). Sonic hedgehog signaling at gastrula stages specifies ventral telencephalic cells in the chick embryo. *Development* 127, 3283-3293.

Hack, I., Bancila, M., Loulier, K., Carroll, P., and Cremer, H. (2002). Reelin is a detachment signal in tangential chain-migration during postnatal neurogenesis. *Nat Neurosci* 5, 939-945.

Hauptmann, G., and Gerster, T. (2000). Regulatory gene expression patterns reveal transverse and longitudinal subdivisions of the embryonic zebrafish forebrain. *Mech Dev* 91, 105-118.

Hauptmann, G., Soll, I., and Gerster, T. (2002). The early embryonic zebrafish forebrain is subdivided into molecularly distinct transverse and longitudinal domains. *Brain Res Bull* 57, 371-375.

Heasman, J. (2002). Morpholino oligos: making sense of antisense? *Dev Biol* 243, 209-214.

Hebert, J. M., Lin, M., Partanen, J., Rossant, J., and McConnell, S. K. (2003). FGF signaling through *FGFR1* is required for olfactory bulb morphogenesis. *Development* 130, 1101-1111.

Hebert, J. M., Mishina, Y., and McConnell, S. K. (2002). BMP signaling is required locally to pattern the dorsal telencephalic midline. *Neuron* 35, 1029-1041.

Higashijima, S., Hotta, Y., and Okamoto, H. (2000). Visualization of cranial motor neurons in live transgenic zebrafish expressing green fluorescent protein under the control of the *islet-1* promoter/enhancer. *J Neurosci* 20, 206-218.

Hjorth, J. T., and Key, B. (2001). Are pioneer axons guided by regulatory gene expression domains in the zebrafish forebrain? High-resolution analysis of the patterning of the zebrafish brain during axon tract formation. *Dev Biol* 229, 271-286.

- Hobert, O., and Westphal, H. (2000). Functions of LIM-homeobox genes. *Trends Genet* 16, 75-83.
- Houart, C., Caneparo, L., Heisenberg, C., Barth, K., Take-Uchi, M., and Wilson, S. (2002). Establishment of the telencephalon during gastrulation by local antagonism of Wnt signaling. *Neuron* 35, 255-265.
- Houart, C., Westerfield, M., and Wilson, S. W. (1998). A small population of anterior cells patterns the forebrain during zebrafish gastrulation. *Nature* 391, 788-792.
- Hutson, L. D., and Chien, C. B. (2002). Pathfinding and error correction by retinal axons: the role of *astray/robo2*. *Neuron* 33, 205-217.
- Hutson, L. D., Jurynek, M. J., Yeo, S. Y., Okamoto, H., and Chien, C. B. (2003). Two divergent *slit1* genes in zebrafish. *Dev Dyn* 228, 358-369.
- Jacob, J., and Briscoe, J. (2003). Gli proteins and the control of spinal-cord patterning. *EMBO Rep* 4, 761-765.
- Jessell, T. M. (2000). Neuronal specification in the spinal cord: inductive signals and transcriptional codes. *Nat Rev Genet* 1, 20-29.
- Jessen, J. R., Meng, A., McFarlane, R. J., Paw, B. H., Zon, L. I., Smith, G. R., and Lin, S. (1998). Modification of bacterial artificial chromosomes through chi-stimulated homologous recombination and its application in zebrafish transgenesis. *Proc Natl Acad Sci U S A* 95, 5121-5126.
- Jurata, L. W., and Gill, G. N. (1997). Functional analysis of the nuclear LIM domain interactor NLI. *Mol Cell Biol* 17, 5688-5698.
- Jurata, L. W., Pfaff, S. L., and Gill, G. N. (1998). The nuclear LIM domain interactor NLI mediates homo- and heterodimerization of LIM domain transcription factors. *J Biol Chem* 273, 3152-3157.
- Kania, A., and Jessell, T. M. (2003). Topographic motor projections in the limb imposed by LIM homeodomain protein regulation of ephrin-A:EphA interactions. *Neuron* 38, 581-596.
- Karavanov, A. A., Saint-Jeannet, J. P., Karavanova, I., Taira, M., and Dawid, I. B. (1996). The LIM homeodomain protein *Lim-1* is widely expressed in neural, neural

crest and mesoderm derivatives in vertebrate development. *Int J Dev Biol* 40, 453-461.

Kawahara, A., and Dawid, I. B. (2002). Developmental expression of zebrafish *emx1* during early embryogenesis. *Gene Expr Patterns* 2, 201-206.

Kelly, G. M., Greenstein, P., Erezyilmaz, D. F., and Moon, R. T. (1995). Zebrafish *wnt8* and *wnt8b* share a common activity but are involved in distinct developmental pathways. *Development* 121, 1787-1799.

Kikuchi, Y., Segawa, H., Tokumoto, M., Tsubokawa, T., Hotta, Y., Uyemura, K., and Okamoto, H. (1997). Ocular and cerebellar defects in zebrafish induced by overexpression of the LIM domains of the islet-3 LIM/homeodomain protein. *Neuron* 18, 369-382.

Kimmel, C. B., Ballard, W. W., Kimmel, S. R., Ullmann, B., and Schilling, T. F. (1995). Stages of embryonic development of the zebrafish. *Dev Dyn* 203, 253-310.

Kornack, D. R., and Rakic, P. (2001). The generation, migration, and differentiation of olfactory neurons in the adult primate brain. *Proc Natl Acad Sci U S A* 98, 4752-4757.

Koster, R. W., and Fraser, S. E. (2001). Direct imaging of in vivo neuronal migration in the developing cerebellum. *Curr Biol* 11, 1858-1863.

Krauss, S., Concordet, J. P., and Ingham, P. W. (1993). A functionally conserved homolog of the *Drosophila* segment polarity gene *hh* is expressed in tissues with polarizing activity in zebrafish embryos. *Cell* 75, 1431-1444.

Kuschel, S., Ruther, U., and Theil, T. (2003). A disrupted balance between Bmp/Wnt and Fgf signaling underlies the ventralization of the Gli3 mutant telencephalon. *Dev Biol* 260, 484-495.

Lavdas, A. A., Grigoriou, M., Pachnis, V., and Parnavelas, J. G. (1999). The medial ganglionic eminence gives rise to a population of early neurons in the developing cerebral cortex. *J Neurosci* 19, 7881-7888.

Lee, S. M., Tole, S., Grove, E., and McMahon, A. P. (2000). A local Wnt-3a signal is required for development of the mammalian hippocampus. *Development* 127, 457-467.

- Lister, J. A., Close, J., and Raible, D. W. (2001). Duplicate *mitf* genes in zebrafish: complementary expression and conservation of melanogenic potential. *Dev Biol* 237, 333-344.
- Long, J. E., Garel, S., Depew, M. J., Tobet, S., and Rubenstein, J. L. (2003). *DLX5* regulates development of peripheral and central components of the olfactory system. *J Neurosci* 23, 568-578.
- Lumsden, A., and Keynes, R. (1989). Segmental patterns of neuronal development in the chick hindbrain. *Nature* 337, 424-428.
- Lyons, D. A. (2003) Neurogenesis in the zebrafish hindbrain.
- Lyons, D. A., Guy, A. T., and Clarke, J. D. (2003). Monitoring neural progenitor fate through multiple rounds of division in an intact vertebrate brain. *Development* 130, 3427-3436.
- Macdonald, R., Scholes, J., Strahle, U., Brennan, C., Holder, N., Brand, M., and Wilson, S. W. (1997). The Pax protein *Noi* is required for commissural axon pathway formation in the rostral forebrain. *Development* 124, 2397-2408.
- Macdonald, R., Xu, Q., Barth, K. A., Mikkola, I., Holder, N., Fjose, A., Krauss, S., and Wilson, S. W. (1994). Regulatory gene expression boundaries demarcate sites of neuronal differentiation in the embryonic zebrafish forebrain. *Neuron* 13, 1039-1053.
- Mallamaci, A., Mercurio, S., Muzio, L., Cecchi, C., Pardini, C. L., Gruss, P., and Boncinelli, E. (2000). The lack of *Emx2* causes impairment of Reelin signaling and defects of neuronal migration in the developing cerebral cortex. *J Neurosci* 20, 1109-1118.
- Marin, O., Anderson, S. A., and Rubenstein, J. L. (2000). Origin and molecular specification of striatal interneurons. *J Neurosci* 20, 6063-6076.
- Marin, O., Plump, A. S., Flames, N., Sanchez-Camacho, C., Tessier-Lavigne, M., and Rubenstein, J. L. (2003). Directional guidance of interneuron migration to the cerebral cortex relies on subcortical *Slit1/2*-independent repulsion and cortical attraction. *Development* 130, 1889-1901.
- Marin, O., and Rubenstein, J. L. (2001). A long, remarkable journey: tangential migration in the telencephalon. *Nat Rev Neurosci* 2, 780-790.

- Marin, O., and Rubenstein, J. L. (2003). Cell migration in the forebrain. *Annu Rev Neurosci* 26, 441-483.
- Marin, O., Smeets, W. J., and Gonzalez, A. (1998). Basal ganglia organization in amphibians: evidence for a common pattern in tetrapods. *Prog Neurobiol* 55, 363-397.
- Mione, M., Shanmugalingam, S., Kimelman, D., and Griffin, K. (2001). Overlapping expression of zebrafish T-brain-1 and eomesodermin during forebrain development. *Mech Dev* 100, 93-97.
- Mizuno, H., Mal, T. K., Tong, K. I., Ando, R., Furuta, T., Ikura, M., and Miyawaki, A. (2003). Photo-induced peptide cleavage in the green-to-red conversion of a fluorescent protein. *Mol Cell* 12, 1051-1058.
- Mombaerts, P., Wang, F., Dulac, C., Chao, S. K., Nemes, A., Mendelsohn, M., Edmondson, J., and Axel, R. (1996). Visualizing an olfactory sensory map. *Cell* 87, 675-686.
- Monuki, E. S., Porter, F. D., and Walsh, C. A. (2001). Patterning of the dorsal telencephalon and cerebral cortex by a roof plate-Lhx2 pathway. *Neuron* 32, 591-604.
- Monuki, E. S., and Walsh, C. A. (2001). Mechanisms of cerebral cortical patterning in mice and humans. *Nat Neurosci* 4 *Suppl*, 1199-1206.
- Moreno, N., Bachy, I., Retaux, S., and Gonzalez, A. (2003). Pallial origin of mitral cells in the olfactory bulbs of *Xenopus*. *Neuroreport* 14, 2355-2358.
- Moreno, N., Bachy, I., Retaux, S., and Gonzalez, A. (2004). LIM-homeodomain genes as developmental and adult genetic markers of *Xenopus* forebrain functional subdivisions. *J Comp Neurol* 472, 52-72.
- Morita, T., Nitta, H., Kiyama, Y., Mori, H., and Mishina, M. (1995). Differential expression of two zebrafish *emx* homeoprotein mRNAs in the developing brain. *Neurosci Lett* 198, 131-134.
- Muzio, L., DiBenedetto, B., Stoykova, A., Boncinelli, E., Gruss, P., and Mallamaci, A. (2002). Conversion of cerebral cortex into basal ganglia in *Emx2*(-/-) *Pax6*(*Sey/Sey*) double-mutant mice. *Nat Neurosci* 5, 737-745.

- Muzio, L., and Mallamaci, A. (2003). *Emx1, emx2 and pax6 in specification, regionalization and arealization of the cerebral cortex. Cereb Cortex 13, 641-647.*
- Nadarajah, B., Brunstrom, J. E., Grutzendler, J., Wong, R. O., and Pearlman, A. L. (2001). Two modes of radial migration in early development of the cerebral cortex. *Nat Neurosci 4, 143-150.*
- Nakagawa, Y., and O'Leary, D. D. (2001). Combinatorial expression patterns of LIM-homeodomain and other regulatory genes parcellate developing thalamus. *J Neurosci 21, 2711-2725.*
- Nery, S., Wichterle, H., and Fishell, G. (2001). Sonic hedgehog contributes to oligodendrocyte specification in the mammalian forebrain. *Development 128, 527-540.*
- Ngai, J., Dowling, M. M., Buck, L., Axel, R., and Chess, A. (1993). The family of genes encoding odorant receptors in the channel catfish. *Cell 72, 657-666.*
- Nguyen Ba-Charvet, K. T., Brose, K., Marillat, V., Kidd, T., Goodman, C. S., Tessier-Lavigne, M., Sotelo, C., and Chedotal, A. (1999). Slit2-Mediated chemorepulsion and collapse of developing forebrain axons. *Neuron 22, 463-473.*
- Nguyen-Ba-Charvet, K. T., Picard-Riera, N., Tessier-Lavigne, M., Baron-Van Evercooren, A., Sotelo, C., and Chedotal, A. (2004). Multiple roles for slits in the control of cell migration in the rostral migratory stream. *J Neurosci 24, 1497-1506.*
- Nguyen-Ba-Charvet, K. T., Plump, A. S., Tessier-Lavigne, M., and Chedotal, A. (2002). Slit1 and slit2 proteins control the development of the lateral olfactory tract. *J Neurosci 22, 5473-5480.*
- Nomura, T., and Osumi, N. (2004). Misrouting of mitral cell progenitors in the Pax6/small eye rat telencephalon. *Development 131, 787-796.*
- Park, H. C., Kim, C. H., Bae, Y. K., Yeo, S. Y., Kim, S. H., Hong, S. K., Shin, J., Yoo, K. W., Hibi, M., Hirano, T., *et al.* (2000). Analysis of upstream elements in the HuC promoter leads to the establishment of transgenic zebrafish with fluorescent neurons. *Dev Biol 227, 279-293.*
- Park, H. C., Mehta, A., Richardson, J. S., and Appel, B. (2002). *olig2* is required for zebrafish primary motor neuron and oligodendrocyte development. *Dev Biol 248, 356-368.*

Parnavelas, J. G., Anderson, S. A., Lavdas, A. A., Grigoriou, M., Pachnis, V., and Rubenstein, J. L. (2000). The contribution of the ganglionic eminence to the neuronal cell types of the cerebral cortex. *Novartis Found Symp* 228, 129-139; discussion 139-147.

Pencea, V., Bingaman, K. D., Freedman, L. J., and Luskin, M. B. (2001). Neurogenesis in the subventricular zone and rostral migratory stream of the neonatal and adult primate forebrain. *Exp Neurol* 172, 1-16.

Pencea, V., and Luskin, M. B. (2003). Prenatal development of the rodent rostral migratory stream. *J Comp Neurol* 463, 402-418.

Portavella, M., Vargas, J. P., Torres, B., and Salas, C. (2002). The effects of telencephalic pallial lesions on spatial, temporal, and emotional learning in goldfish. *Brain Res Bull* 57, 397-399.

Postlethwait, J. H., Yan, Y. L., Gates, M. A., Horne, S., Amores, A., Brownlie, A., Donovan, A., Egan, E. S., Force, A., Gong, Z., *et al.* (1998). Vertebrate genome evolution and the zebrafish gene map. *Nat Genet* 18, 345-349.

Power, D. M., Elias, N. P., Richardson, S. J., Mendes, J., Soares, C. M., and Santos, C. R. (2000). Evolution of the thyroid hormone-binding protein, transthyretin. *Gen Comp Endocrinol* 119, 241-255.

Puelles, L., Kuwana, E., Puelles, E., Bulfone, A., Shimamura, K., Keleher, J., Smiga, S., and Rubenstein, J. L. (2000). Pallial and subpallial derivatives in the embryonic chick and mouse telencephalon, traced by the expression of the genes *Dlx-2*, *Emx-1*, *Nkx-2.1*, *Pax-6*, and *Tbr-1*. *J Comp Neurol* 424, 409-438.

Puelles, L., and Rubenstein, J. L. (1993). Expression patterns of homeobox and other putative regulatory genes in the embryonic mouse forebrain suggest a neuromeric organization. *Trends Neurosci* 16, 472-479.

Puelles, L., and Rubenstein, J. L. (2003). Forebrain gene expression domains and the evolving prosomeric model. *Trends Neurosci* 26, 469-476.

Rallu, M., Machold, R., Gaiano, N., Corbin, J. G., McMahon, A. P., and Fishell, G. (2002). Dorsoventral patterning is established in the telencephalon of mutants lacking both *Gli3* and Hedgehog signaling. *Development* 129, 4963-4974.

- Reed, R. R. (2004). After the holy grail: establishing a molecular basis for Mammalian olfaction. *Cell* 116, 329-336.
- Riedel, G., and Krug, L. (1997). The forebrain of the blind cave fish *Astyanax hubbsi* (Characidae). II. Projections of the olfactory bulb. *Brain Behav Evol* 49, 39-52.
- Rink, E., and Wullimann, M. F. (2001). The teleostean (zebrafish) dopaminergic system ascending to the subpallium (striatum) is located in the basal diencephalon (posterior tuberculum). *Brain Res* 889, 316-330.
- Rohr, K. B., Barth, K. A., Varga, Z. M., and Wilson, S. W. (2001). The nodal pathway acts upstream of hedgehog signaling to specify ventral telencephalic identity. *Neuron* 29, 341-351.
- Ross, L. S., Parrett, T., and Easter, S. S., Jr. (1992). Axonogenesis and morphogenesis in the embryonic zebrafish brain. *J Neurosci* 12, 467-482.
- Salas, C., Broglio, C., and Rodriguez, F. (2003). Evolution of forebrain and spatial cognition in vertebrates: conservation across diversity. *Brain Behav Evol* 62, 72-82.
- Schreiber, G. (2002). The evolutionary and integrative roles of transthyretin in thyroid hormone homeostasis. *J Endocrinol* 175, 61-73.
- Segawa, H., Miyashita, T., Hirate, Y., Higashijima, S., Chino, N., Uyemura, K., Kikuchi, Y., and Okamoto, H. (2001). Functional repression of *Islet-2* by disruption of complex with *Ldb* impairs peripheral axonal outgrowth in embryonic zebrafish. *Neuron* 30, 423-436.
- Shanmugalingam, S. (1999) Mechanisms of patterning and neurogenesis in the zebrafish forebrain.
- Shanmugalingam, S., Houart, C., Picker, A., Reifers, F., Macdonald, R., Barth, A., Griffin, K., Brand, M., and Wilson, S. W. (2000). *Ace/Fgf8* is required for forebrain commissure formation and patterning of the telencephalon. *Development* 127, 2549-2561.
- Shawlot, W., and Behringer, R. R. (1995). Requirement for *Lim1* in head-organizer function. *Nature* 374, 425-430.

- Shawlot, W., Wakamiya, M., Kwan, K. M., Kania, A., Jessell, T. M., and Behringer, R. R. (1999). *Lim1* is required in both primitive streak-derived tissues and visceral endoderm for head formation in the mouse. *Development* *126*, 4925-4932.
- Sheng, H. Z., Bertuzzi, S., Chiang, C., Shawlot, W., Taira, M., Dawid, I., and Westphal, H. (1997). Expression of murine *Lhx5* suggests a role in specifying the forebrain. *Dev Dyn* *208*, 266-277.
- Shimamura, K., and Rubenstein, J. L. (1997). Inductive interactions direct early regionalization of the mouse forebrain. *Development* *124*, 2709-2718.
- Shinozaki, K., Yoshida, M., Nakamura, M., Aizawa, S., and Suda, Y. (2004). *Emx1* and *Emx2* cooperate in initial phase of archipallium development. *Mech Dev* *121*, 475-489.
- Shirasaki, R., and Pfaff, S. L. (2002). Transcriptional codes and the control of neuronal identity. *Annu Rev Neurosci* *25*, 251-281.
- Stenman, J., Toresson, H., and Campbell, K. (2003). Identification of two distinct progenitor populations in the lateral ganglionic eminence: implications for striatal and olfactory bulb neurogenesis. *J Neurosci* *23*, 167-174.
- Stern, C. D. (2002). Induction and initial patterning of the nervous system - the chick embryo enters the scene. *Curr Opin Genet Dev* *12*, 447-451.
- Stoykova, A., Treichel, D., Hallonet, M., and Gruss, P. (2000). *Pax6* modulates the dorsoventral patterning of the mammalian telencephalon. *J Neurosci* *20*, 8042-8050.
- Striedter, G. F. (1997). The telencephalon of tetrapods in evolution. *Brain Behav Evol* *49*, 179-213.
- Stuhmer, T., Anderson, S. A., Ekker, M., and Rubenstein, J. L. (2002). Ectopic expression of the *Dlx* genes induces glutamic acid decarboxylase and *Dlx* expression. *Development* *129*, 245-252.
- Sussel, L., Marin, O., Kimura, S., and Rubenstein, J. L. (1999). Loss of *Nkx2.1* homeobox gene function results in a ventral to dorsal molecular respecification within the basal telencephalon: evidence for a transformation of the pallidum into the striatum. *Development* *126*, 3359-3370.

- Taira, M., Otani, H., Saint-Jeannet, J. P., and Dawid, I. B. (1994). Role of the LIM class homeodomain protein Xlim-1 in neural and muscle induction by the Spemann organizer in *Xenopus*. *Nature* *372*, 677-679.
- Talbot, W. S., and Hopkins, N. (2000). Zebrafish mutations and functional analysis of the vertebrate genome. *Genes Dev* *14*, 755-762.
- Thaler, J. P., Lee, S. K., Jurata, L. W., Gill, G. N., and Pfaff, S. L. (2002). LIM factor Lhx3 contributes to the specification of motor neuron and interneuron identity through cell-type-specific protein-protein interactions. *Cell* *110*, 237-249.
- Theil, T., Alvarez-Bolado, G., Walter, A., and Ruther, U. (1999). Gli3 is required for Emx gene expression during dorsal telencephalon development. *Development* *126*, 3561-3571.
- Tole, S., Ragsdale, C. W., and Grove, E. A. (2000). Dorsoventral patterning of the telencephalon is disrupted in the mouse mutant extra-toes(J). *Dev Biol* *217*, 254-265.
- Tomioka, N., Osumi, N., Sato, Y., Inoue, T., Nakamura, S., Fujisawa, H., and Hirata, T. (2000). Neocortical origin and tangential migration of guidepost neurons in the lateral olfactory tract. *J Neurosci* *20*, 5802-5812.
- Toresson, H., Potter, S. S., and Campbell, K. (2000). Genetic control of dorsal-ventral identity in the telencephalon: opposing roles for Pax6 and Gsh2. *Development* *127*, 4361-4371.
- Toyama, R., Curtiss, P. E., Otani, H., Kimura, M., Dawid, I. B., and Taira, M. (1995). The LIM class homeobox gene lim5: implied role in CNS patterning in *Xenopus* and zebrafish. *Dev Biol* *170*, 583-593.
- Toyama, R., and Dawid, I. B. (1997). lim6, a novel LIM homeobox gene in the zebrafish: comparison of its expression pattern with lim1. *Dev Dyn* *209*, 406-417.
- Toyama, R., Kobayashi, M., Tomita, T., and Dawid, I. B. (1998). Expression of LIM-domain binding protein (ldb) genes during zebrafish embryogenesis. *Mech Dev* *71*, 197-200.
- Varga, Z. M., Amores, A., Lewis, K. E., Yan, Y. L., Postlethwait, J. H., Eisen, J. S., and Westerfield, M. (2001). Zebrafish smoothed functions in ventral neural tube specification and axon tract formation. *Development* *128*, 3497-3509.

Varga, Z. M., Wegner, J., and Westerfield, M. (1999). Anterior movement of ventral diencephalic precursors separates the primordial eye field in the neural plate and requires cyclops. *Development* *126*, 5533-5546.

Walshe, J., and Mason, I. (2003). Unique and combinatorial functions of Fgf3 and Fgf8 during zebrafish forebrain development. *Development* *130*, 4337-4349.

Watanabe, M., Rebert, M. L., Andreazzoli, M., Takahashi, N., Toyama, R., Zimmerman, S., Whitman, M., and Dawid, I. B. (2002). Regulation of the Lim-1 gene is mediated through conserved FAST-1/FoxH1 sites in the first intron. *Dev Dyn* *225*, 448-456.

Weiss, J. B., Von Ohlen, T., Mellerick, D. M., Dressler, G., Doe, C. Q., and Scott, M. P. (1998). Dorsoventral patterning in the Drosophila central nervous system: the intermediate neuroblasts defective homeobox gene specifies intermediate column identity. *Genes Dev* *12*, 3591-3602.

Westerfield, M. (2000). *The zebrafish book. A guide for the laboratory use of zebrafish (Danio rerio)*. 4th edition edn, University of Oregon Press, Eugene).

Whitlock, K. E., and Westerfield, M. (1998). A transient population of neurons pioneers the olfactory pathway in the zebrafish. *J Neurosci* *18*, 8919-8927.

Whitlock, K. E., and Westerfield, M. (2000). The olfactory placodes of the zebrafish form by convergence of cellular fields at the edge of the neural plate. *Development* *127*, 3645-3653.

Wichterle, H., Alvarez-Dolado, M., Erskine, L., and Alvarez-Buylla, A. (2003). Permissive corridor and diffusible gradients direct medial ganglionic eminence cell migration to the neocortex. *Proc Natl Acad Sci U S A* *100*, 727-732.

Wichterle, H., Garcia-Verdugo, J. M., Herrera, D. G., and Alvarez-Buylla, A. (1999). Young neurons from medial ganglionic eminence disperse in adult and embryonic brain. *Nat Neurosci* *2*, 461-466.

Wichterle, H., Turnbull, D. H., Nery, S., Fishell, G., and Alvarez-Buylla, A. (2001). In utero fate mapping reveals distinct migratory pathways and fates of neurons born in the mammalian basal forebrain. *Development* *128*, 3759-3771.

Wienholds, E., van Eeden, F., Kusters, M., Mudde, J., Plasterk, R. H., and Cuppen, E. (2003). Efficient target-selected mutagenesis in zebrafish. *Genome Res* *13*, 2700-2707.

Wilson, S. W., Brennan, C., Macdonald, R., Brand, M., and Holder, N. (1997). Analysis of axon tract formation in the zebrafish brain: the role of territories of gene expression and their boundaries. *Cell Tissue Res* *290*, 189-196.

Wilson, S. W., and Houart, C. (2004). Early steps in the development of the forebrain. *Dev Cell* *6*, 167-181.

Wilson, S. W., Ross, L. S., Parrett, T., and Easter, S. S., Jr. (1990). The development of a simple scaffold of axon tracts in the brain of the embryonic zebrafish, *Brachydanio rerio*. *Development* *108*, 121-145.

Wilson, S. W., and Rubenstein, J. L. (2000). Induction and dorsoventral patterning of the telencephalon. *Neuron* *28*, 641-651.

Wullimann, M. F., and Knipp, S. (2000). Proliferation pattern changes in the zebrafish brain from embryonic through early postembryonic stages. *Anat Embryol (Berl)* *202*, 385-400.

Wullimann, M. F., and Mueller, T. (2002). Expression of *Zash-1a* in the postembryonic zebrafish brain allows comparison to mouse *Mash1* domains. *Brain Res Gene Expr Patterns* *1*, 187-192.

Wullimann, M. F., and Mueller, T. (2004). Identification and morphogenesis of the eminentia thalami in the zebrafish. *J Comp Neurol* *471*, 37-48.

Wullimann, M. F., and Puelles, L. (1999). Postembryonic neural proliferation in the zebrafish forebrain and its relationship to prosomeric domains. *Anat Embryol (Berl)* *199*, 329-348.

Wullimann, M. F., and Rink, E. (2002). The teleostean forebrain: a comparative and developmental view based on early proliferation, *Pax6* activity and catecholaminergic organization. *Brain Res Bull* *57*, 363-370.

Wullimann, M. F., and Rupp, B. (1996). *Neuroanatomy of the Zebrafish Brain: a Topological Atlas*, (Birkhauser Boston).

Yanez, J., and Anadon, R. (1994). Afferent and efferent connections of the habenula in the larval sea lamprey (*Petromyzon marinus* L.): an experimental study. *J Comp Neurol* 345, 148-160.

Yonei-Tamura, S., Tamura, K., Tsukui, T., and Izpisua Belmonte, J. C. (1999). Spatially and temporally-restricted expression of two T-box genes during zebrafish embryogenesis. *Mech Dev* 80, 219-221.

Yoshida, M., Suda, Y., Matsuo, I., Miyamoto, N., Takeda, N., Kuratani, S., and Aizawa, S. (1997). *Emx1* and *Emx2* functions in development of dorsal telencephalon. *Development* 124, 101-111.

Yun, K., Fischman, S., Johnson, J., Hrabe de Angelis, M., Weinmaster, G., and Rubenstein, J. L. (2002). Modulation of the notch signaling by *Mash1* and *Dlx1/2* regulates sequential specification and differentiation of progenitor cell types in the subcortical telencephalon. *Development* 129, 5029-5040.

Yun, K., Potter, S., and Rubenstein, J. L. (2001). *Gsh2* and *Pax6* play complementary roles in dorsoventral patterning of the mammalian telencephalon. *Development* 128, 193-205.

Zaki, P. A., Quinn, J. C., and Price, D. J. (2003). Mouse models of telencephalic development. *Curr Opin Genet Dev* 13, 423-437.

Zerucha, T., Stuhmer, T., Hatch, G., Park, B. K., Long, Q., Yu, G., Gambarotta, A., Schultz, J. R., Rubenstein, J. L., and Ekker, M. (2000). A highly conserved enhancer in the *Dlx5/Dlx6* intergenic region is the site of cross-regulatory interactions between *Dlx* genes in the embryonic forebrain. *J Neurosci* 20, 709-721.

Zhao, Y., Sheng, H. Z., Amini, R., Grinberg, A., Lee, E., Huang, S., Taira, M., and Westphal, H. (1999). Control of hippocampal morphogenesis and neuronal differentiation by the LIM homeobox gene *Lhx5*. *Science* 284, 1155-1158.